



UNIVERSIDAD NACIONAL AUTÓNOMA DE MÉXICO
DOCTORADO EN CIENCIAS BIOMÉDICAS
FACULTAD DE ESTUDIOS SUPERIORES IZTACALA

**IDENTIFICACIÓN DE UN GRUPO DE MIRNAS ASOCIADOS A LA
PROGRESIÓN CLÍNICA EN CÁNCER DE MAMA**

TESIS
QUE PARA OPTAR POR EL GRADO DE:
DOCTOR EN CIENCIAS BIOMÉDICAS

PRESENTA:
ANTONIO DANIEL MARTÍNEZ GUTÉRREZ

DIRECTOR DE TESIS
DR. CARLOS G. PÉREZ PLASENCIA
FACULTAD DE ESTUDIOS SUPERIORES IZTACALA
COMITÉ TUTOR
DR. ENRIQUE LEMUS HERNANDEZ
INSTITUTO DE ECOLOGIA
DR. ALEJANDRO GARCÍA CARRANCÁ
INSTITUTO DE INVESTIGACIONES BIOMEDICAS

CIUDAD DE MÉXICO, JULIO DEL 2021



Universidad Nacional
Autónoma de México



UNAM – Dirección General de Bibliotecas
Tesis Digitales
Restricciones de uso

DERECHOS RESERVADOS ©
PROHIBIDA SU REPRODUCCIÓN TOTAL O PARCIAL

Todo el material contenido en esta tesis esta protegido por la Ley Federal del Derecho de Autor (LFDA) de los Estados Unidos Mexicanos (México).

El uso de imágenes, fragmentos de videos, y demás material que sea objeto de protección de los derechos de autor, será exclusivamente para fines educativos e informativos y deberá citar la fuente donde la obtuvo mencionando el autor o autores. Cualquier uso distinto como el lucro, reproducción, edición o modificación, será perseguido y sancionado por el respectivo titular de los Derechos de Autor.

*A mis padres, **Antonio** y **Carina**, pilares fundamentales en mi vida, por motivarme y ayudarme a ser siempre el mejor y por su infinito apoyo incondicional.*

*A mi hermano **Bruno**, por las enriquecedoras e interesantes conversaciones que tenemos en el área de Computación/Matemáticas y por ayudarme siempre en esta última.*

*A la **Dra. Veliah Hernández Solano**, por su sabiduría y por estar siempre conmigo cuando tuve emergencias médicas, gracias a usted pude desarrollarme como una persona normal y llegar hasta donde estoy.*

*A mis mejores amigos **Luis Brain (Chaniz)** y miembros de la P.D y GDS: **Osman (DuendiCerdo Iscariote)**, **Enrique (Mounstrique Trollibio)**, **Adrián (Cuyo lesbiano)** y **Javier (Hit & Run Jemima)** por todas las risas, viajes y excelentes momentos que hemos tenido en los 10 años de conocernos.*

Agradecimientos

Al **Dr. Carlos Pérez Plasencia** por todas sus enseñanzas y la formación que me dio durante mi estancia en su laboratorio, y por siempre apoyarme a lograr mis metas profesionales al permitirme estudiar una segunda carrera mientras hacia el Doctorado.

A la **Dra. Alma Delia Campos Parra** por considerarme y permitirme colaborar en sus proyectos.

Al **Dr. Jossimar Coronel Hernandez** y el **Dr. Oliver Millan Catalán** por ayudarme y esclarecer mis dudas en la parte experimental.

A **Alexandra Elbakyan** y el proyecto **Sci-Hub** por facilitar el acceso gratuito a artículos científicos altamente costosos y por quitar todas las barreras en el camino de la ciencia.

“All we have to decide is what to do with the time that is given us”
— **J.R.R. Tolkien, The Fellowship of the Ring**

Resumen

El cáncer de mama es la neoplasia con el mayor número de incidencia y mortalidad en mujeres. Aunque los mecanismos moleculares asociados con el desarrollo de este tumor se han descrito ampliamente, la etapa metastásica de esta enfermedad sigue teniendo una alta mortalidad. En años recientes, múltiples estudios han mostrado que los microRNAs o miRNAs regulan múltiples procesos biológicos en sistemas complejos como el cáncer. En el presente trabajo describimos un grupo de 61 miRNAs consistentemente sobre-expresados en muestras de cáncer de mama, los cuales regulan el 39% del transcriptoma tumoral. Mediante herramientas de minería de datos en la base de datos del TCGA, se obtuvieron las lecturas provenientes de RNA-seq de miRNA y mRNA provenientes de 1091 muestras tumorales y 110 tejidos adyacentes y se infirió la red de regulación miRNA-mRNA. Se evaluó la actividad oncogénica de cada miRNA y se demostró que estas moléculas se encuentran regulando vías de señalización comúnmente alteradas en cáncer como ciclo celular, PI3K-AKT, reparación de daño al DNA y k-Ras. Usando análisis univariados y multivariados, encontramos que cinco de estos miRNAs podrían ser empleados como biomarcadores del pronóstico de supervivencia global. Posteriormente, confirmamos la sobre-expresión de dos miRNAs en 56 muestras de tumores de mama localmente avanzados obtenidas del archivo histopatológico del Instituto Nacional de Cancerología de México, mostrando concordancia con el análisis bioinformático previo.

Abstract

Breast cancer is the neoplasm with the highest number of deaths in women. Although the molecular mechanisms associated with the development of this tumor have been widely described, metastatic disease has a high mortality rate. In recent years, several studies demonstrated that microRNAs or miRNAs regulate complex processes in different biological systems including cancer. In the present work, we describe a group of 61 miRNAs consistently over-expressed in breast cancer (BC) samples that regulate the breast cancer transcriptome. By means of data mining from TCGA, miRNA and mRNA sequencing data corresponding to 1091 BC patients and 110 normal adjacent tissues were downloaded and a miRNA–mRNA network was inferred. Evaluation of their oncogenic activity demonstrated that they were involved in the regulation of classical cancer pathways such as cell cycle, PI3K–AKT, DNA repair, and k-Ras signaling. Using univariate and multivariate analysis, we found that five of these miRNAs could be used as biomarkers for the prognosis of overall survival. Furthermore, we confirmed the over-expression of two of them in 56 locally advanced BC samples obtained from the histopathological archive of the National Cancer Institute of Mexico, showing concordance with our previous bioinformatic analysis.

Índice general

Índice de figuras	XI
Índice de tablas	XII
1. Introducción	1
1.1. El cáncer	1
1.2. El cáncer de mama	2
1.2.1. Clasificación molecular	3
1.2.2. Estadificación del cáncer de mama	4
1.2.3. La progresión tumoral	5
1.3. Los miRNAs	7
1.3.1. Biogénesis y función de los miRNAs	7
1.3.2. Los miRNAs como reguladores positivos de la expresión génica	8
1.3.3. La participación de los miRNAs en cáncer	10
1.4. El estudio del cáncer y los miRNAs desde una perspectiva de biología de sistemas	12
1.4.1. Los miRNAs como reguladores maestros del fenotipo tumoral	13
1.4.2. Inferencia de redes de regulación transcripcional mediante algoritmos de información mutua	14
1.4.3. Trabajos previos en la identificación de miRNAs reguladores maestros	16
2. Justificación	18
3. Hipótesis	19
4. Objetivos	20
4.1. Objetivos generales	20
4.2. Objetivos particulares	20
5. Metodología	22
5.1. Identificación de miRNAs sobre-expresados en todos los estadios clínicos	22
5.2. Identificación de miRNAs reguladores maestros	23

ÍNDICE GENERAL

5.3. Determinación de la actividad Oncogénica de los MMRs	23
5.4. Análisis de vías de señalización	25
5.5. Clasificación y expresión diferencial de los miRNAs entre los subtipos intrínsecos de cáncer de mama	25
5.6. Análisis de supervivencia	25
5.7. Obtención de muestras de pacientes del Instituto Nacional de Cancerología	26
5.8. Extracción de RNA y PCR en tiempo real	26
5.9. Meta-análisis en el Human Protein Atlas	27
6. Resultados	28
6.1. Identificación de los miRNAs sobre-expresados durante todos los estadios clínicos	28
6.2. Identificación de los miRNAs reguladores maestros	29
6.3. Análisis de las vías de señalización	32
6.4. Predicción de la actividad oncogénica de los MMRs	35
6.5. Participación de los OncoMMRs con actividad oncogénica en el fenotipo tumoral	37
6.6. Identificación de los MMRs con relevancia clínica	42
6.7. Impacto de los MMRs en los subtipos intrínsecos	43
6.8. Validación en tejidos tumorales localmente avanzados del Instituto Nacional de Cancerología	47
7. Discusión y conclusiones	48
8. Producción científica	54
8.1. Martinez-Gutierrez, Antonio-D. , et al. Identification of miRNA Master Regulators in Breast Cancer. Cells. 2020	54
8.2. Martinez-Gutierrez, Antonio-D. , et al. miRNA profile obtained by next-generation sequencing in metastatic breast cancer patients is able to predict the response to systemic treatments. International Journal of Molecular Medicine. 2019	75
8.3. Martinez-Rivera V., Cardenas-Monroy, M.,..... Martinez-Gutierrez, Antonio-D. , et al. Dysregulation of miR-381-3p and miR- 23b-3p in skeletal muscle could be a possible estimator of early post-mortem interval in rats. PeerJ. 2021	90
8.4. Figueroa-Gonzalez G., Carrillo-Hernandez, J.,..... Martinez-Gutierrez, Antonio-D. , et al. Negative regulation of serine threonine kinase 11 (Stk11) through mir-100 in head and neck cancer. Genes. 2020	110
8.5. Coronel-Hernandez J., Lopez-Urrutia, E.,..... Martinez-Gutierrez, Antonio-D. , et al. Cell migration and proliferation are regulated by miR-26a in colorectal cancer via the PTEN–AKT axis. Cancer Cell International. 2019	128

8.6. Lopez-Urrutia, E., Coronel-Hernandez J.,..., Martinez-Gutierrez, Antonio-D. , et al. MiR-26a downregulates retinoblastoma in colorectal cancer. Tumor Biology. 2017	143
9. Figuras suplementarias	153
9.1. Figura suplementaria 1	153
Bibliografía	159

Índice de figuras

1.1. Los Hallmarks del Cáncer	2
1.2. Incidencia y mortalidad por cáncer de mama en México	3
1.3. Clasificación surrogada del cáncer de mama.	4
1.4. Progresión del cáncer de mama.	5
1.5. Biogenesis de los miRNAs	8
1.6. Los miRNAs en cáncer	11
1.7. Reguladores maestros en glioblastoma	14
1.8. Representación de la entropía y la información mutua	16
6.1. miRNAs sobre-expresados en todos los estadios clínicos	29
6.2. miRNAs reguladores maestros en cáncer de mama	32
6.3. Analisis de las vías de señalización usando la plataforma WebGestalt	34
6.4. Actividad Oncogénica de los 61 MMRs	36
6.5. Los 14 OncoMMRs y los genes driver que regulan	39
6.6. Correlación entre los principales OncoMMRs y la expresión de los genes driver ARHGEF10 y SRSF2.	41
6.7. Curvas Kaplan-Meier para la sobrevida global con los 5 MMRs con significancia clínica	43
6.8. Expresión diferencial de los 5 MMRs con relevancia clínica en los subtipos intrínsecos basados en la clasificación PAM50.	46
6.9. Validación de tres MMRs en 56 muestras de pacientes localmente avanzados usando qPCR en tiempo real.	48

Índice de tablas

1.1. Clasificación TNM	4
6.1. MMRs y genes con el mayor grado en la red	31
6.2. Los 14 OncoMMRs y su actividad oncogénica	38
6.3. Principales genes drivers regulados por los OncoMMRs.	38
6.4. Regresiones de Cox para la supervivencia global en pacientes con cáncer de mama del TCGA	44

Introducción

1.1. El cáncer

El cáncer es una enfermedad compleja y multifactorial; molecularmente caracterizada por la desregulación de múltiples vías de señalización y procesos biológicos como producto de alteraciones genéticas y epigenéticas que llevarán a las células afectadas a proliferar sin control. Desde hace más de dos décadas se sabe que para lograr este objetivo, las células tumorales adquieren ciertos rasgos distintivos de forma paulatina y por etapas [1], lo que finalmente les permitirá proliferar sin control y adquirir características más agresivas, conocidas como *hallmarks del cáncer* (Figura 1.1) [2].

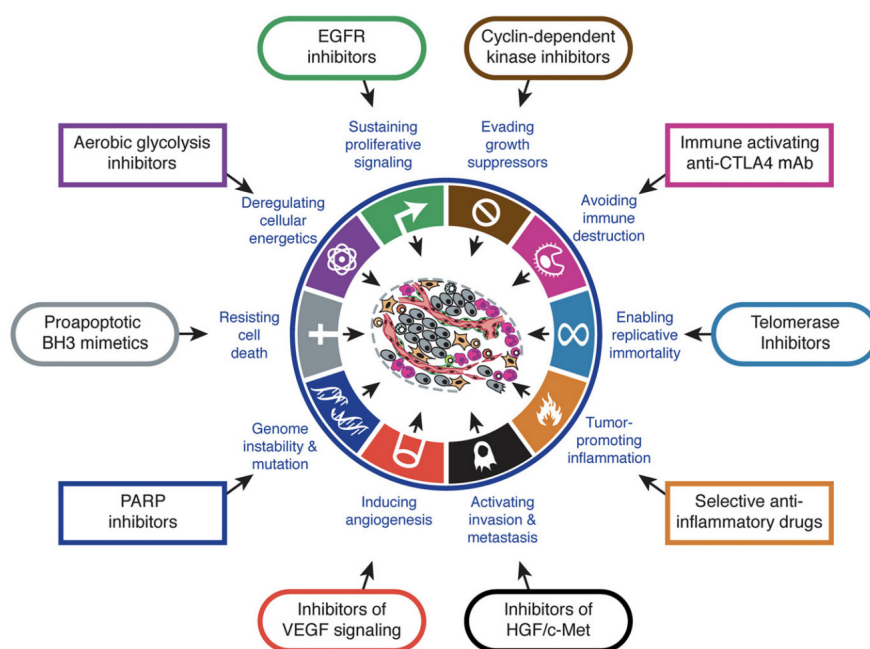


Figura 1.1: Los Hallmarks del Cáncer. Tomado de [2]

1.2. El cáncer de mama

Se denomina cáncer de mama a las neoplasias que se originan a partir de las células del tejido mamario. Este tipo de tumores ocupa el primer lugar tanto a nivel mundial como en nuestro país por incidencia y mortalidad en mujeres, provocando cerca de 7000 muertes y 27000 casos nuevos al año en México (Figura 1.2) [3], convirtiéndolo en uno de los principales problemas de salud a nivel nacional.

Estas neoplasias pueden clasificarse en carcinomas ductales in situ (CDIS), si se originan en las células epiteliales ductales, o bien en carcinomas lobulillares in situ (CLIS) si provienen de las células lobulillares. Cabe destacar que el CDIS es la forma más común de cáncer no invasor de la mama [4].

1.2. EL CÁNCER DE MAMA

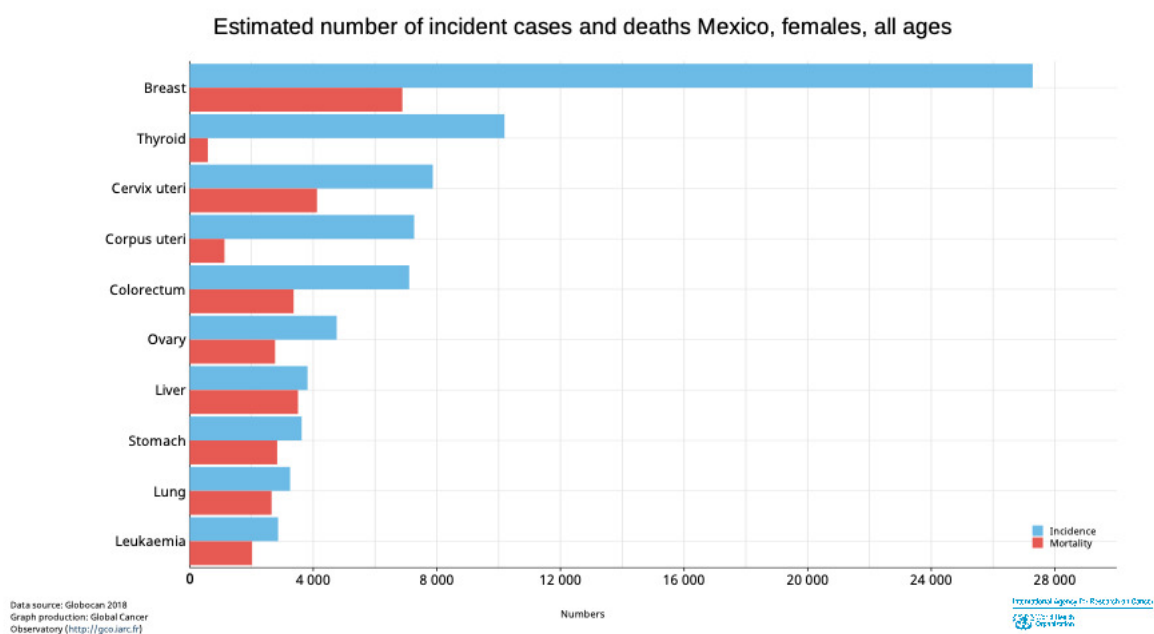


Figura 1.2: Incidencia y mortalidad por cáncer de mama en México.

1.2.1. Clasificación molecular

Por otro lado, se ha observado que esta enfermedad es altamente heterogénea, tanto clínica como molecularmente [5]. Esta complejidad a nivel molecular se observó por primera vez usando la tecnología de microarreglos en tumores mamarios, donde se encontró que esta enfermedad podía ser agrupada en subtipos moleculares dependiendo de una lista intrínseca de genes [6]. En la actualidad se reconocen al menos 5 subtipos moleculares basados en la expresión de 58 genes de la firma PAM50 [7]. Esta clasificación se usa en conjunto con la clasificación histopatológica, separando a los tumores en dos grupos: receptores de estrógeno positivo y receptores de estrógeno negativo. La determinación del subtipo molecular de los tumores es de vital importancia ya que cada uno tiene un comportamiento biológico y pronóstico diferente para los pacientes [5] (Figura 1.3)

CAPÍTULO 1. INTRODUCCIÓN

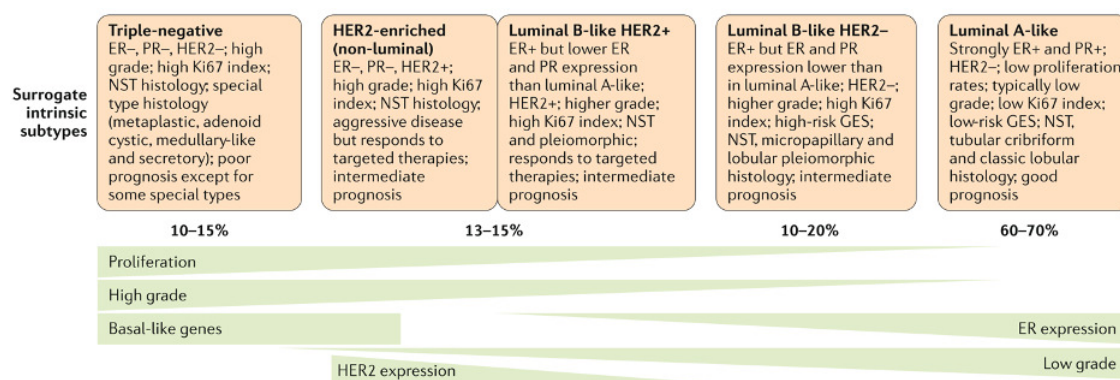


Figura 1.3: Clasificación surrogada del cáncer de mama. Tomado de [5]

1.2.2. Estadificación del cáncer de mama

Los tumores mamarios son estadificados de acuerdo a la clasificación TNM [8] donde se toman en cuenta características como el tamaño del tumor, la presencia de nodos linfáticos invadidos y metástasis (Tabla 1.1). Esta estadificación es de suma importancia ya que proporciona información respecto al pronóstico de los pacientes, ya que en gran medida su probable supervivencia depende del estadio clínico inicial en el que fueron diagnosticados [4]. Esta clasificación puede verse como un reflejo del proceso conocido como progresión tumoral.

Clasificación TNM			
Estadio	T	N	M
0	Tis	N0	M0
IA	T1a	N0	M0
IB	T0, T1a	N1mi	M0
IIA	T0, T1a, T2	N1b	M0
IIB	T2, T3	N1, N0	M0
IIIA	T0, T1a, T2, T3	N1, N2	M0
IIIB	T4	N1, N2	M0
IIIC	Cualquier T	N3	M0
IV	Cualquier T	Cualquier N	M1

Tabla 1.1

1.2.3. La progresión tumoral

La carcinogénesis puede ser dividida en 4 etapas: iniciación, promoción, conversión maligna y progresión tumoral [1]. Durante las tres primeras etapas, las células se verán sometidas y acumularán aberraciones genómicas, lo que tendrá como consecuencia la selección y expansión de células que expresarán un fenotipo maligno.

Finalmente, durante la progresión tumoral, estas células ya transformadas comenzarán a adquirir de forma paulatina otros hallmarks del cáncer que les permitirán adquirir un fenotipo más agresivo [9]. En el caso del cáncer de mama, este proceso puede ser observado durante la transformación de un carcinoma ductal in situ a (DCIS) a un carcinoma ductal invasivo, el cual tendrá la tendencia a hacer metástasis (Figura 1.4).

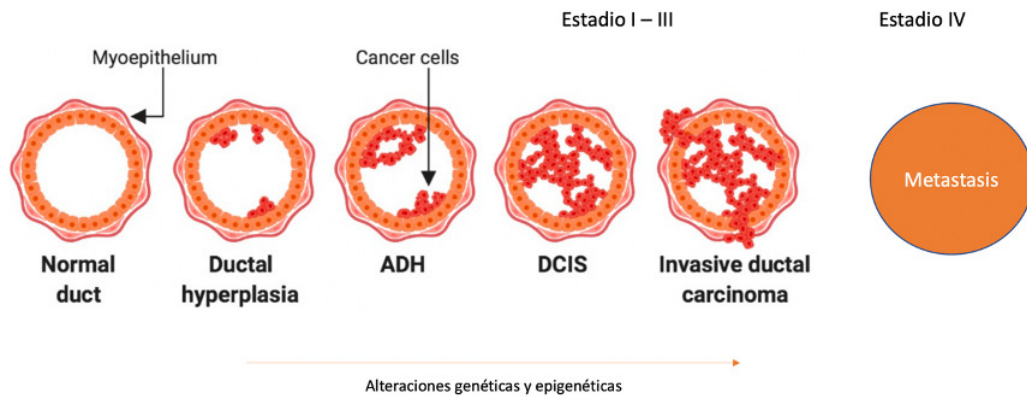


Figura 1.4: Progresión del cáncer de mama. ADH: Hiperplasia ductal atípica. DCIS : Carcinoma ductal in situ.

Como se mencionó anteriormente, desde el punto de vista clínico, la progresión tumoral puede verse reflejada en la estadificación TNM. Así, un tumor de la mama en estadio I será un carcinoma ductal invasivo, mientras que un tumor en estadio IV ya habrá conseguido hacer metástasis (Figura 1.4). Además, la evidencia muestra que, durante la evolución del tumor, la mayoría de las aberraciones genómicas son adqui-

CAPÍTULO 1. INTRODUCCIÓN

ridas en etapas tempranas del desarrollo del tumor [1], por lo tanto, identificar estas alteraciones que son mantenidas durante la progresión tumoral es de gran importancia

1.3. Los miRNAs

Uno de los grandes hallazgos modernos que se obtuvieron gracias a las tecnologías de secuenciación de nueva generación fue el descubrimiento de que solo cerca del 1.5 % del genoma estaba compuesto de genes que codificaban a proteínas [10], mientras que el resto estaba compuesto de secuencias que solo se transcriben a RNA, entre las que se encuentran los RNAs no codificantes como los miRNAs.

Estos resultados hicieron evidente el papel fundamental de estas secuencias en la regulación de la minúscula parte codificante del genoma.

1.3.1. Biogénesis y función de los miRNAs

Los miRNAs son una clase de RNAs no codificantes pequeños, de 21 a 23 nucleótidos de longitud cuya principal función es la regulación postranscripcional de cientos o miles de genes blanco. Además, estos son agrupados en familias basadas en la similitud entre sus secuencias semilla, la cual esta compuesta por sus nucleótidos 2-8 y que determina la complementariedad con sus genes blanco [11].

Estas moléculas son transcritas por la polimerasa 2 en el núcleo, lo que generará un pri-miRNA, el cual será procesado por un complejo compuesto por DGCR8 y DROSHA y exportado al citoplasma por XPO5. Ahí, la gran mayoría de miRNAs serán procesados por segunda vez por DICER 1, generando los miRNAs maduros.

El miRNA maduro será parte de un complejo proteico junto con las moléculas Argonauta 1-4, llamado complejo de silenciamiento (RISC), el cual será guiado por complementariedad del miRNA a la región 3'UTR de sus genes blanco. Si existe una complementariedad perfecta entre el miRNA y el blanco, se producirá una degradación del mRNA blanco por acción de Argonauta 2, sin embargo, este mecanismo es poco común en mamíferos. Por otra parte, una complementariedad parcial entre el miRNA-

CAPÍTULO 1. INTRODUCCIÓN

mRNA resultará en una deadenilación [12] o un bloqueo en la traducción del mRNA blanco [13] (Figura 1.5).

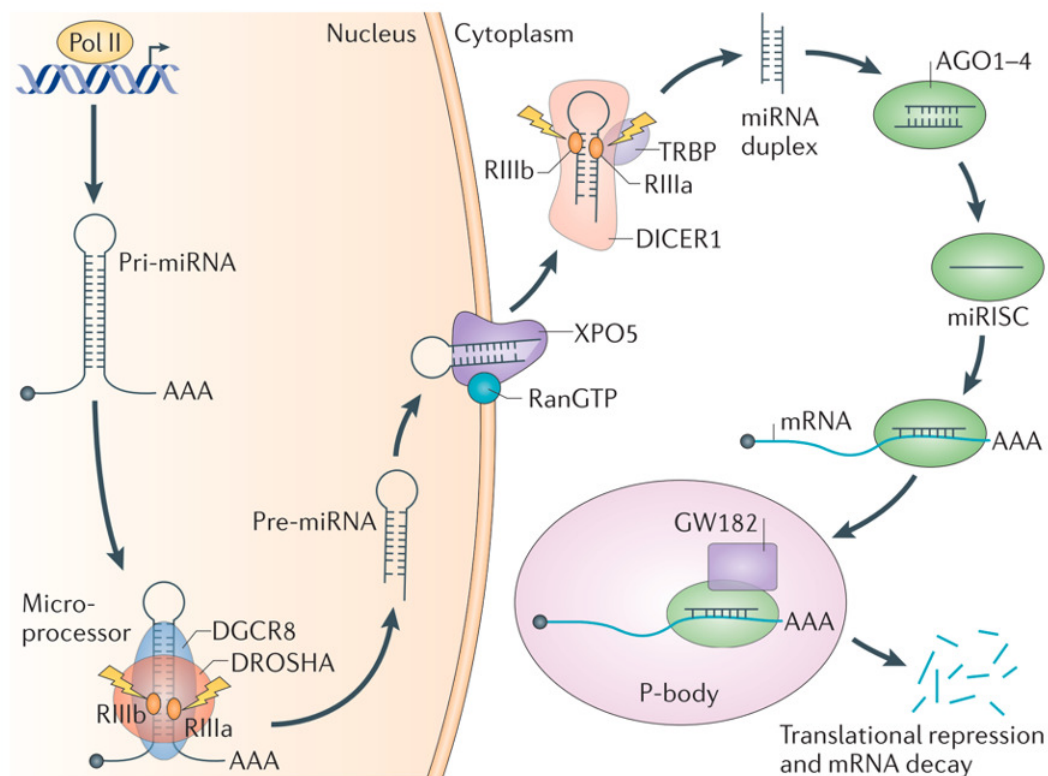


Figura 1.5: Biogénesis de los miRNAs. Tomado de [13]

1.3.2. Los miRNAs como reguladores positivos de la expresión génica

Si bien la actividad canónica de los miRNAs es reprimir la expresión de sus posibles mRNAs blancos, también se han reportado al menos cuatro mecanismos mediante los cuales son capaces de activar la expresión de sus blancos [14, 15].

El primer mecanismo involucra la capacidad de unirse a los elementos ricos en AU (AREs) presentes en la región 3' UTR de los genes [14], estas regiones están estrechamente involucradas en la estabilidad del mRNA y en su traducción. Esta unión se logra gracias a las dos proteínas asociadas a AREs que contiene el complejo RISC :

PAI-RBP1 y FXR1 [16]. Por otra parte, Argonauta 2 (AGO2) es un importante efector de RISC que puede asociarse con FXR1 [17], los cuales al hacer interacción aumentan la traducción del mRNA [18]. Se han reportado múltiples miRNAs que utilizan este mecanismo para regular positivamente la expresión de sus blancos: El complejo compuesto por AGO2 y miR-3693 se une al ARE de TNF α para reclutar a FXR1 y estimular la traducción de TNF α [19]. Por otra parte, miR-125b aumenta la estabilidad y la expresión del mRNA de KB-Ras2 al reducir la degradación de las AREs [20]. Este mecanismo también se ha visto utilizado por miR-346, let-7, miR-4661, miR-34, miR-145 y miR-1 [19, 14, 21, 22, 23, 24, 25].

También se ha observado a varios miRNAs que interactúan con la región 5' UTR de sus blancos: miR-10a favorece la traducción de sus mRNAs blancos mediante la interacción con la región 5' UTR [15], mientras que miR-346 aumenta la expresión de mRNA de su blanco RIP140 [26]. Otros ejemplos incluyen a miR-483-5p el cual se une a la región 5' UTR de IGF2 favoreciendo su transcripción [27] y a miR-122 el cual aumenta la traducción del virus de la hepatitis C mediante la unión con dos regiones 5' UTR de su genoma [28].

Un tercer mecanismo mediante el cual los miRNAs regulan positivamente a sus blancos involucra la interacción directa con las secuencias promotoras de sus mRNA blancos [29, 30]. Finalmente se ha observado un cuarto mecanismo mediante el cual miR-24-1 activa la transcripción de sus blancos al actuar sobre los enhancers de sus blancos [31].

Si bien hasta el momento se han descrito más interacciones miRNA-mRNA negativas que positivas, considerando las pocas interacciones que se han validado experimentalmente y dada la naturaleza multi-blanco de los miRNAs es probable que la actividad reguladora positiva de los miRNAs sea más común de lo que se ha descrito hasta el momento.

1.3.3. La participación de los miRNAs en cáncer

Durante la última década se ha caracterizado ampliamente la participación de los miRNAs en cáncer, donde se ha encontrado que en tejidos tumorales existe un patrón de subexpresión global de estas moléculas [32]. Por otra parte, se ha encontrado que estas moléculas se encuentran estrechamente involucradas en la regulación de procesos como apoptosis, proliferación celular y metástasis, eventos cruciales de la carcinogénesis [33] y con la adquisición de los diferentes hallmarks del cáncer [34, 35].

Además, se ha visto que pueden ser usadas de forma eficiente como biomarcadores no solo de la presencia de tumores [36] sino de características clínicas de importancia como la supervivencia global [33] y la respuesta al tratamiento [37]. Además se les ha relacionado con estadios clínicos avanzados, metástasis a los nodos linfáticos y con un peor pronóstico [38].

En el contexto tumoral, se ha demostrado la existencia de miRNAs que actúan tanto como oncogenes –inhibiendo la expresión de genes supresores de tumores- y como supresores de tumores [39, 40] (Figura 1.6), sin embargo su actividad específica en un tipo tumoral será contexto-dependiente del estado transcripcional en el que se encuentren las células.

En cáncer de mama se ha observado que la expresión diferencial de los miRNAs es dependiente del subtipo molecular [41] y que están desregulados durante la progresión de tejido sano a carcinomas in situ a carcinomas ductales invasivos [42]. Durante este último proceso se ha visto que hay una correlación entre el incremento en la expresión de oncomiRNAs, como miR-21 -el cual tiene como blancos a diversos supresores de tumores como p53 y TPM1- con la progresión. Por lo que se ha sugerido que tienen un rol patológico en esta enfermedad [43].

Sin embargo, y dada la naturaleza de estas moléculas, es necesaria una aproximación de biología de sistemas para entender de forma más específica su participación durante

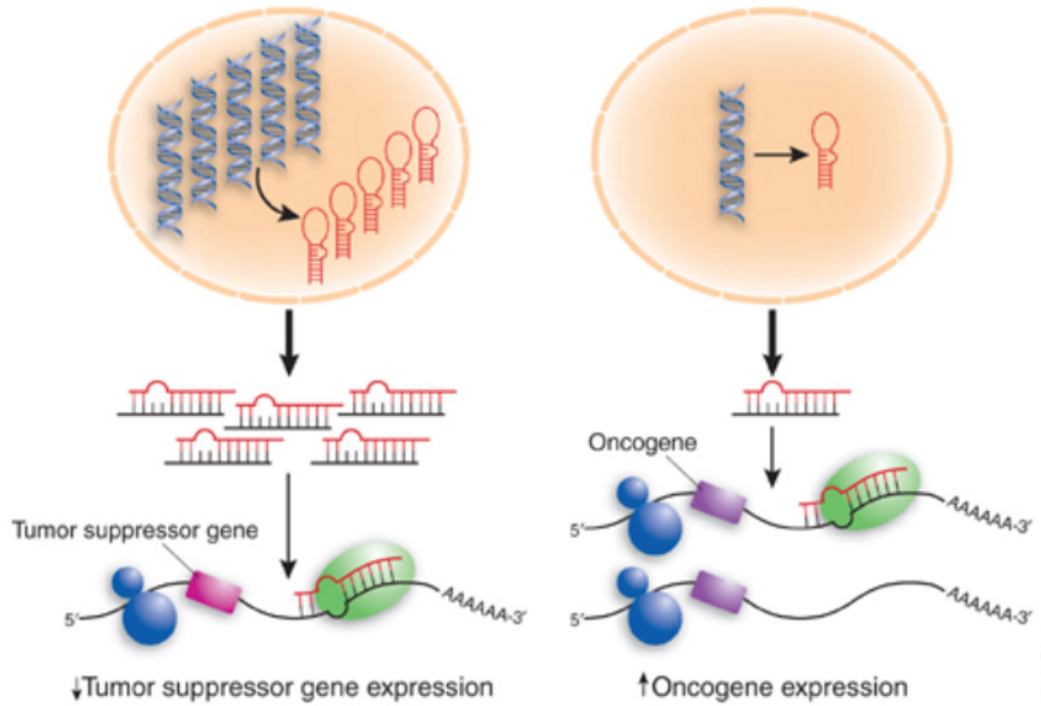


Figura 1.6: Los miRNAs en cáncer. Un miRNA es llamado OncomiR si este regula negativamente a un supresor de tumor y será llamado un miRNA supresor de tumores si regula a un Oncogen

el proceso de carcinogenesis.

1.4. El estudio del cáncer y los miRNAs desde una perspectiva de biología de sistemas

En la actualidad y gracias a los avances en las tecnologías de secuenciación de nueva generación y en genómica, se ha podido observar y caracterizar la complejidad transcriptómica del cáncer. En este punto, y debido a la gran cantidad de datos e hipótesis generadas por estas tecnologías, se ha hecho evidente la necesidad de migrar el estudio de esta enfermedad desde una perspectiva reduccionista a una integral para poder entender su funcionamiento.

Esta perspectiva es lograda mediante aproximaciones basadas en biología de sistemas, cuya principal premisa es que un sistema complejo consiste en múltiples componentes que interactúan entre sí de forma no lineal, los cuales no pueden ser completamente descritos al observar solo sus componentes [44]. De esta manera, un sistema biológico complejo como el cáncer no puede ser completamente descrito al observar solamente la expresión de algunos oncogenes o vías de señalización alteradas de forma puntual, sino al modelar las complejas redes de interacción entre estas y todo su transcriptoma.

En el caso específico de cáncer, es posible desarrollar este tipo de aproximaciones gracias a las bases de datos públicas donde se almacenan los resultados de experimentos de secuenciación. De estos, el proyecto más completo y ambicioso es The cancer genome atlas (TCGA) [45], una iniciativa del National Cancer Institute (NCI) y el National Human Genome Research Institute (NHGRI) donde se caracterizaron y secuenciaron 33 tipos de tumores, incluyendo el de mama. Usando estos datos es posible integrar los perfiles de expresión de miRNAs y los de mRNA con la finalidad de correlacionar la expresión de ambos y de esta manera poder reconstruir la compleja red de regulación en tumores, infiriendo la actividad global que tienen los miRNAs en el transcriptoma [46]

1.4. EL ESTUDIO DEL CÁNCER Y LOS MIRNAS DESDE UNA PERSPECTIVA DE BIOLOGÍA DE SISTEMAS

1.4.1. Los miRNAs como reguladores maestros del fenotipo tumoral

La regulación de procesos biológicos como el crecimiento o muerte celular es llevada a cabo no por simples cascadas de señalización, si no por redes complejas e intrínsecamente estables de genes, las cuales están compuestas por nodos alta y débilmente conectados [47]. Estos genes altamente conectados son esenciales para mantener la estabilidad fenotípica en condiciones de aberraciones internas y externas, lo que es conocido como robustez celular [48].

Una característica del cáncer es que mantiene un alto grado de robustez celular [49], esto a pesar de las múltiples aberraciones externas e internas a las que están sometidos. Si bien durante las últimas décadas se ha descrito ampliamente la alta heterogeneidad de los tumores [50], la evidencia ha mostrado que a nivel transcripcional se mantiene un perfil alterado, pero estable [49], como lo muestran múltiples estudios de Single cell RNA-seq donde se ha observado que los perfiles transcripcionales de las células tumorales a pesar de tener una gran heterogeneidad pueden ser agrupadas en clústers al seleccionar genes de vías de señalización con una alta relevancia biológica [51, 52, 53], lo cual permite que los tumores se mantengan viables y por consiguiente, progresando.

En este contexto, se define conceptualmente a los reguladores maestros en cáncer como aquellas moléculas drivers o conductoras cuya actividad aberrante es suficiente -aunque no estrictamente necesarias de forma individual- para inducir y mantener la transformación celular, mediante la regulación del estado transcripcional de una célula tumoral tanto de forma directa e indirecta de genes clave ó conductores en el fenotipo tumoral(Figura 1.7) [49].

Por sus características, como la capacidad de poder regular múltiples genes a la vez, se ha propuesto la existencia de miRNAs que actúan como reguladores maestros del fenotipo tumoral [54], los cuales estarían actuando como nodos centrales en la red tumoral al ayudar a la estabilización de esta red y por consiguiente, manteniendo el

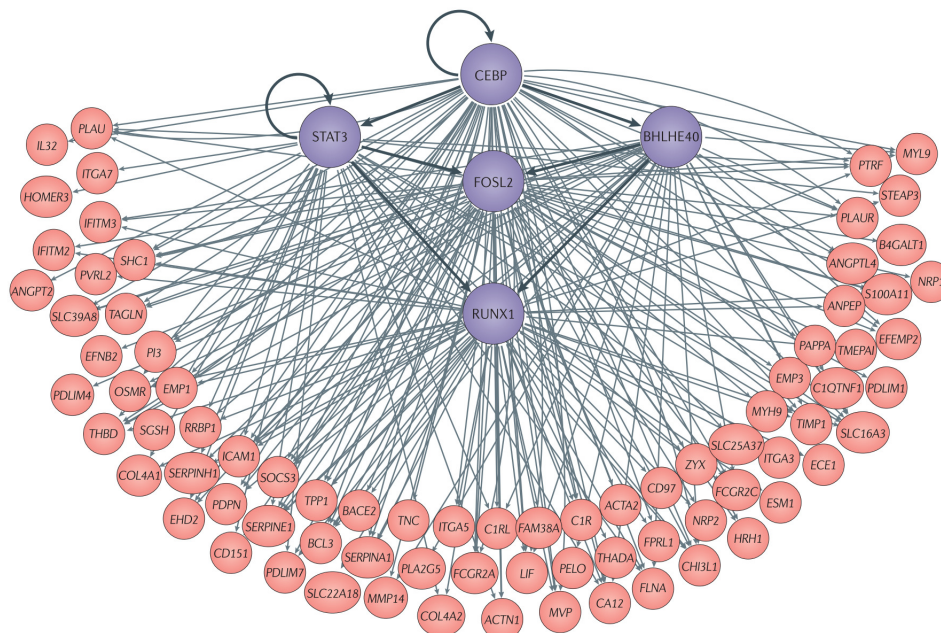


Figura 1.7: Reguladores maestros en glioblastoma. Se observa como los factores de transcripción en color morado actúan como reguladores maestros en glioblastoma al regular el 74% de los genes del subtipo mesenquimal. Tomado de [49]

fenotipo tumoral e influenciando la progresión.

1.4.2. Inferencia de redes de regulación transcripcional mediante algoritmos de información mutua

La inferencia de redes hace referencia a la reconstrucción mediante ingeniería inversa de redes de regulación transcripcional mediante datos obtenidos por experimentos de secuenciación [55]. En biología de sistemas, la reconstrucción de estas redes es clasificada en dos grupos: bottom up y top down. En la aproximación "bottom up" hace referencia a aquellas técnicas donde inhiben las moléculas y sus posibles blancos de forma específica mediante experimentos de biología molecular, para posteriormente integrar la información y reconstruir la red. Por otra parte, en la aproximación top down se hacen inferencias y correlaciones entre las moléculas a partir de datos genómicos obtenidos

1.4. EL ESTUDIO DEL CÁNCER Y LOS MIRNAS DESDE UNA PERSPECTIVA DE BIOLOGÍA DE SISTEMAS

mediante herramientas de alto rendimiento para poder inferir las redes de regulación [56]. Este proceso de inferencia de redes es llamado como un proceso de ingeniería inversa, ya que se infieren los patrones de regulación a partir de datos observacionales.

Una de las aproximaciones para hacer esta inferencia es la utilización de métodos que correlacionan la expresión entre las moléculas, entre ellas una de las más robustas y utilizadas es la inferencia mediante la medición de la información mutua. Esta medición está basada en la teoría de la información de Shannon y es empleada para medir la asociación no lineal entre dos genes [56], ya que mide la dependencia entre dos variables. Para dos genes X y Y se define la información mutua como:

$$I(X; Y) = H(Y) - H(Y|X) = H(X) - H(X|Y) = \sum_{x_i \in X, y_j \in Y} p(x_i, y_j) \log \frac{p(X_i, Y_j)}{p(X_i)p(Y_j)} \quad (1.1)$$

Donde: $X_i (i = 1, 2, \dots, m)$, $Y_j (j = 1, 2, \dots, n)$ representan los valores de expresión en diferentes muestras, $p(X_i)$ y $p(Y_j)$ las probabilidades marginales para cada valor discreto $X_i \in X$ y $Y_j \in Y$ respectivamente. Por otra parte, $p(X_i, Y_j)$ es la probabilidad conjunta de X_i y Y_j .

Donde un valor alto de información mutua podría indicar que hay una relación muy estrecha entre dos genes, por contraparte un valor bajo representa independencia entre ambos genes [57]. De esta manera, la información mutua $I(X; Y)$ puede ser descrita como la diferencia en la entropía y la entropía condicional $H(X|Y)$ es la cantidad de información de X cuando Y es conocida. Por consiguiente, es interpretada como la información que es residuo X o Y omitiendo la información cuando X o Y es conocida [55] (Figura 1.8).

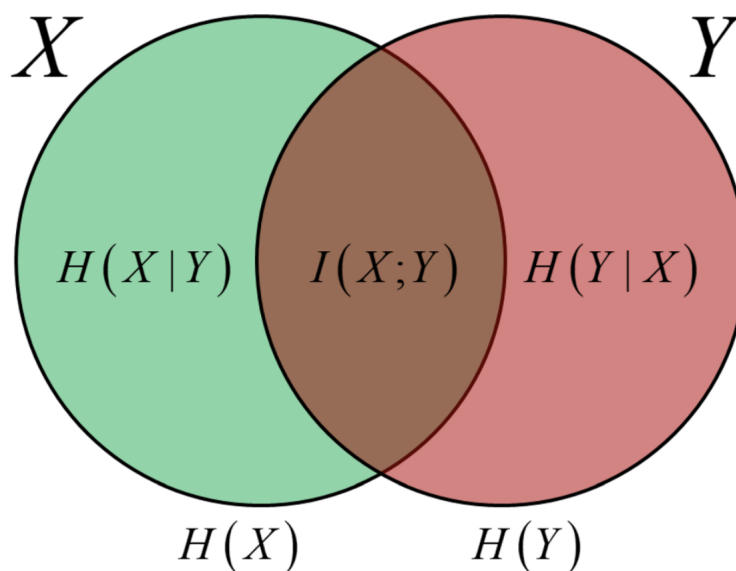


Figura 1.8: Representación de la entropía y la información mutua

Una propiedad observada en las redes de regulación transcripcional es la de escala libre ó "scale free" [58], esto implica que la distribución del grado de los nodos sigue una ley potencial, es decir la fracción de $P(k)$ nodos que tienen k conexiones es: $P(k) \sim k^{-\gamma}$, con $2 < \gamma < 3$. Esto implica que la gran mayoría de la red es dominada por un pequeño grupo de nodos altamente conectados, los cuales son denominados reguladores maestros al estar involucrados en la regulación de la mayoría de genes que definen y mantienen un fenotipo [47].

1.4.3. Trabajos previos en la identificación de miRNAs reguladores maestros

Algoritmos basados en la inferencia de información mutua como ARACNE [59] han sido ampliamente usados para inferir redes de regulación transcripcional y de reguladores maestros [60]. Por ejemplo, en cáncer de Ovario, el grupo de Yang et al., predijeron que 8 miRNAs que incluían a miR-506, miR-141 y miR-200a podrían estar regulando al

1.4. EL ESTUDIO DEL CÁNCER Y LOS MIRNAS DESDE UNA PERSPECTIVA DE BIOLOGÍA DE SISTEMAS

89 % del transcriptoma tumoral, validando experimentalmente en un modelo ortotópico de ratón que miR-506 inhibía la migración e invasión [61].

Por otro lado, en cáncer colorectal, Cantini et al., describen un grupo de 24 miRNAs reguladores maestros que se encontraban sub-expresados en el subtipo stem/mesenquimal/serrado (SSM), los cuales al ser validados en líneas celulares mostraron regular las mismas vías de señalización, sugiriendo que estos reguladores maestros conducían el fenotipo SSM [62].

En otro estudio, utilizando datos del proyecto de cáncer de mama de la iniciativa The Cancer Genome Atlas [45], Cantini et al., desarrollaron un algoritmo para identificar miRNAs que actúan co-expresándose en clústers como reguladores maestros, identificando 5 posibles grupos de miRNAs reguladores maestros dependientes del subtipo molecular y encontrando que miR-199a/214 se encontraba sub-expresado en tumores triple negativos y asociado a la regulación de la transición epitelio-mesénquima [63].

Justificación

Si bien existe una desregulación de miRNAs en cáncer de mama, no todos ellos tienen la misma importancia para el tumor. Además, dado que el tumor se encuentra en un constante proceso de selección, es plausible suponer la existencia de miRNAs reguladores maestros cuya expresión sea sobre-activada desde estadios clínicos tempranos (I), y mantenida e incluso incrementada en estadios clínicos avanzados (IV), los cuales posiblemente le confieren una ventaja evolutiva que favorezca la progresión del tumor. El objetivo de este proyecto es correlacionar la expresión de miRNAs cuyo nivel de expresión se incremente con relación al estadio clínico y evaluar su posible participación como reguladores maestros del fenotipo tumoral. La identificación de estos miRNAs así como sus principales genes blanco permitirá ampliar nuestro conocimiento del complejo mecanismo de la progresión tumoral.

Hipótesis

Existen miRNAs reguladores maestros cuya sobreexpresión es persistente en los distintos estadios clínicos en cáncer de mama, regulando procesos y genes clave en la progresión del fenotipo tumoral

Objetivos

4.1. Objetivos generales

- Identificar los miRNAs sobre-expresados persistentes durante la progresión en cáncer de mama en pacientes del TCGA.
- Determinar la participación de los miRNAs en el fenotipo tumoral.
- Determinar la relevancia clínica de este grupo de miRNAs

4.2. Objetivos particulares

- Identificar los miRNAs sobre-expresados en todos los estadios clínicos de tumores mamarios del proyecto TCGA
- Inferir la red de regulación miRNA-mRNA e identificar los miRNAs reguladores maestros (MMRs)
- Determinar las principales vías de señalización reguladas
- Determinar la actividad oncogénica de cada MMR

4.2. OBJETIVOS PARTICULARES

- Evaluar la asociación entre la expresión de los miRNAs y la sobrevida global de los pacientes
- Validar la expresión de 4 miRNAs en muestras de tumores mamarios del Instituto Nacional de Cancerología

5.1. Identificación de miRNAs sobre-expresados en todos los estadios clínicos

Para identificar los miRNAs consistentemente sobre-expresados en cáncer de mama, primero se obtuvieron los counts de RNA-seq del proyecto de cáncer de mama del TCGA [45], correspondientes a 1091 pacientes con datos de RNA-seq y de miRNA-seq con estadios clínicos I-IV y 110 tejidos adyacentes sanos usando el paquete de Bioconductor TCGAbiolinks [64]. El análisis de expresión diferencial fue realizado con el paquete DESeq2 [65]. Se seleccionaron solo aquellos miRNAs que tuvieran un False Discovery Rate ≤ 0.05 y un $\log_2\text{FoldChange}$ de al menos $+0.5$.

La correlación entre la expresión de los miRNAs y los estadios TNM definidos por la American Joint Committee on Cancer (AJCC) fue realizada utilizando la correlación de Spearman, incluida en el paquete de R Hmisc. Solo consideramos aquellos miRNAs con un p-value ≤ 0.05 y un coeficiente de correlación positivo.

5.2. Identificación de miRNAs reguladores maestros

Para identificar aquellos miRNAs que pudieran estar actuando como reguladores maestros, primero se obtuvieron los mRNAs diferencialmente expresados en los tejidos tumorales de las muestras de cáncer de mama del TCGA utilizando los paquetes TCGABiolinks y DESeq2. Se consideraron solo aquellos mRNAs que tuvieron un False Discovery Rate ≤ 0.05 . Posteriormente, ambos datasets de miRNAs y mRNAs fueron normalizados utilizando el método de Variance Stabilizing Transformation (VST) implementado en el paquete DESeq2.

Después, se reconstruyó la red de regulación miRNA-mRNA utilizando ambos datasets de miRNAs sobre-expresados y mRNAs diferencialmente expresados con el algoritmo de ARACNe-AP [59] utilizando un bootstrap de 100. Las interacciones miRNA-mRNA obtenidas por esta reconstrucción fueron filtradas en función de su presencia en al menos una base de datos de predicción (DIANA-microT-CDS, ElMMo, MicroCosm, miRanda, miRDB, PicTar, PITA and TargetScan) y/ó en una base de datos con evidencia experimental de la interacción (miRecords, miRTarBase, TarBase) utilizando el paquete de Bioconductor multiMir [66]. Finalmente, utilizamos el algoritmo de inferencia de reguladores maestros (MARINA)[67] incluido en el paquete de Bioconductor VIPER [60] y seleccionando solo a aquellos miRNAs reguladores maestros (MMRs) que tuvieran un False Discovery Rate ≤ 0.05 . Las características topológicas de la red fueron analizadas utilizando Cytoscape v3.7.1.

5.3. Determinación de la actividad Oncogénica de los MMRs

Cualquier miRNA tiene la capacidad de regular tanto los oncogenes como los genes supresores de tumores (TSG), por lo que determinamos como Actividad Oncogénica (OA) como la relación y dirección de la regulación (sobre-expresar o reprimir) entre

CAPÍTULO 5. METODOLOGÍA

oncogenes y TSG que un miRNA dado puede regular a la vez. Para calcular la Actividad Oncogénica de cada miRNA, primero se obtuvieron los datos manualmente curados de oncogenes y TSG validados como genes drivers ó conductores de la carcinogenesis del catálogo de mutaciones somáticas en cáncer (COSMIC)[68]. Después, definimos y calculamos el Efecto Oncogénico (Oe) como la suma de oncogenes posiblemente sobre-expresados por el miRNA y los posibles TSG regulados a la baja por el miRNA, con la siguiente fórmula:

$$Oe = (U_{ONC} + D_{TSG}) - ONC_{TSG} \quad (5.1)$$

Con: Oe = Efecto Oncogénico; U_{ONC} = Oncogenes sobre-expresados; D_{TSG} = Genes supresores de tumores regulados a la baja; ONC_{TSG} = Genes con función dual como oncogenes y supresores de tumores.

Por lo tanto, definimos el Efecto Anti-oncogénico (Ae) como la suma de TSG sobre-expresados y oncogenes regulados a la baja por el miRNA:

$$Ae = (D_{ONC} + U_{TSG}) - ONC_{TSG} \quad (5.2)$$

Con: Ae = Efecto Anti-oncogénico; D_{ONC} = Oncogenes regulados a la baja; U_{TSG} = Genes supresores de tumores sobre-expresados; ONC_{TSG} = Genes con función dual como oncogenes y supresores de tumores.

Finalmente, definimos la Actividad Oncogénica (OA) como la relación entre el Efecto Oncogénico menos el Efecto Anti-Oncogénico y el número total de posibles genes drivers de cada miRNA:

$$OA = \frac{Oe - Ae}{T} \quad (5.3)$$

Con: OA = Actividad Oncogénica; Oe = Efecto Oncogénico; Ae = Efecto Anti-

oncogénico; T= Número total de posibles genes driver blancos (oncogenes, supresores de tumores y genes con actividad dual)

5.4. Análisis de vías de señalización

El análisis de vías de señalización se realizó utilizando la plataforma WebGestalt [69](<http://www.webgestalt.org>); empleando la lista de mRNAs diferencialmente expresados y su log2FoldChange. Se consideraron significativas a aquellas vías de señalización con un False Discovery Rate ≤ 0.05 .

5.5. Clasificación y expresión diferencial de los miRNAs entre los subtipos intrínsecos de cáncer de mama

La clasificación de las muestras del TCGA en los subtipos basados en la clasificación PAM50 fue realizada utilizando el paquete de Bioconductor Genefu[70]. La expresión diferencial de los miRNAs entre los subtipos se llevó a cabo con el paquete DESeq2 [65], considerando aquellas moléculas con un False Discovery Rate ≤ 0.05 como significativas.

5.6. Análisis de supervivencia

Para realizar el análisis de supervivencia primero se obtuvieron los datos clínicos de los 1091 pacientes del TCGA utilizando el paquete TCGABiolinks. Después, dividimos a los pacientes en dos grupos: Alta y baja expresión, basado en la mediana de la expresión de cada MMR. Las curvas Kaplan-Meier y las regresiones de Cox fueron calculadas usando el paquete Survival de R. Las regresiones multivariadas de Cox fueron ajustadas utilizando la edad y el estadio clínico de los pacientes. La significancia estadística se determino con una prueba de log-rank < 0.01 .

5.7. Obtención de muestras de pacientes del Instituto Nacional de Cancerología

Se utilizó un grupo prospectivo de 56 pacientes diagnosticados con cáncer de mama localmente Avanzados. Se obtuvieron bloques embebidos en parafina (FFPE) del departamento de patología del Instituto Nacional de Cancerología. Todos los pacientes incluidos en este estudio firmaron un formulario de consentimiento informado, con el número de protocolo (015/03/019/ICI).

5.8. Extracción de RNA y PCR en tiempo real

El RNA total fue extraído de los bloques de parafina usando el kit miRNeasyFFPE (Cat. No. 217504 Qiagen. Hilden, Germany). El RNA fue cuantificado en el fluorometro Qubit 3.0 con el kit Qubit RNA HS Assay (Cat. No. Q32852. Thermo Fisher Scientific. Waltham, MA, USA). El control de calidad del RNA obtenido se realizó mediante el ratio 260/280 y se considero un valor ≥ 1.9 como aceptable. La reacción de transcripción reversa fue realizada utilizando 10 ng de RNA con el kit TaqMan Advanced miRNA cDNA Synthesis (Cat. No. A28007. Thermo Fisher Scientific) siguiendo las recomendaciones del fabricante. La PCR cuantitativa en tiempo real fue realizada con sondas TaqMan Advanced miRNA para los miRNAs: hsa-miR-940, hsa-miR-1307-3p y hsa-miR-340-3p usando a hsa-miR-16 como control endógeno (Cat. No. 4331182, Thermo Fisher Scientific). El tamaño de los fragmentos de amplificación de cada miRNA fue de 60 nt.

La reacción de q-PCR se realizó con 40 ciclos de 95 °C por 20 segundos y 90°C por 1 segundo con el kit Taqman Fast Advanced Master Mix (Cat. No. 4444557, Thermo Fisher Scientific) en un sistema Step One (Thermo Fisher Scientific). Todas la reacciones fueron realizadas por triplicado y los fold changes fueron calculados usando el

5.9. META-ANÁLISIS EN EL HUMAN PROTEIN ATLAS

método $2^{-\Delta\Delta CT}$. La prueba U de Mann-Whitney fue usada para identificar a los miRNAs con una expresión significativa, considerando una $p \leq 0.05$ como estadísticamente significativa.

5.9. Meta-análisis en el Human Protein Atlas

Sé obtuvieron los datos de proteómica basados en anticuerpos constituidos por 2 muestras de tejido sano de la mama y 11 muestras de cáncer de mama del The Human Protein Atlas [71], donde se comparó la tinción entre los dos grupos.

Resultados

6.1. Identificación de los miRNAs sobre-expresados durante todos los estadios clínicos

Nuestro primer objetivo fue obtener una lista de aquellos miRNAs que estuvieran sobre-expresados durante todos los estadios clínicos (Estadio I - IV) en los datos obtenidos del proyecto de cáncer de mama del TCGA. Como se observa en la Figura 6.1, encontramos 217 miRNAs que se encontraban sobre-expresados en todos los estadios clínicos. Posteriormente, correlacionamos la expresión de los miRNAs con los estadios clínicos usando la correlación de spearman, esto con la finalidad de obtener solo aquellas moléculas que tuvieran una asociación positiva con los estadios clínicos. De este último análisis obtuvimos 204 miRNAs que mostraron una correlación positiva y significativa (Tabla suplementaria 1).

6.2. IDENTIFICACIÓN DE LOS MIRNAS REGULADORES MAESTROS

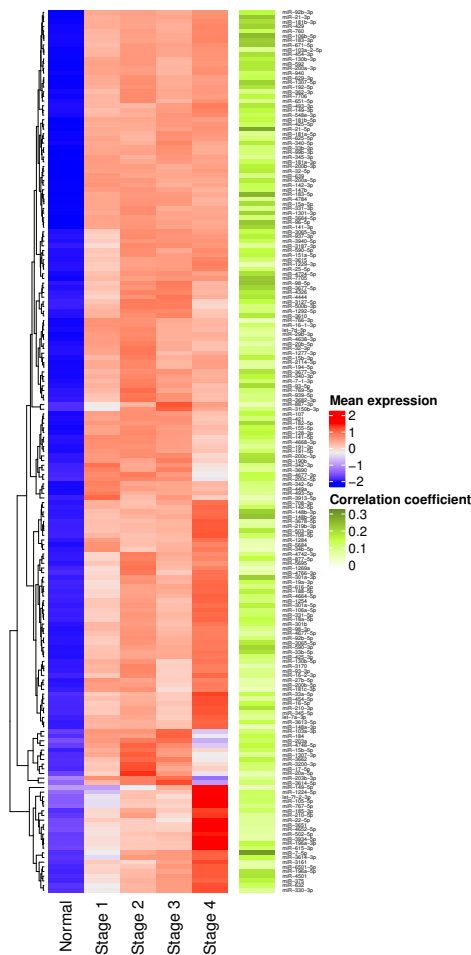


Figura 6.1: miRNAs sobre-expresados en todos los estadios clínicos. El heatmap de la izquierda muestra la expresión de 217 miRNAs sobre-expresados (representado en color rojo) en tumores y regulados a la baja (representado en color azul) en tejidos adyacentes sanos. Como se observa en el heatmap de la derecha, la mayoría de los miRNAs muestran una correlación positiva (representada en color verde) entre su expresión y el estadio clínico

6.2. Identificación de los miRNAs reguladores maestros

Empleando los 204 miRNAs significativamente sobre-expresados, se procedió a analizar su posible rol en el desarrollo del fenotipo tumoral. Para lograr este objetivo, primero se infirió la red de regulación miRNA-mRNA usando el algoritmo de información mutua ARACNe [59] y los genes diferencialmente expresados. Dada la existencia

CAPÍTULO 6. RESULTADOS

de reportes previos que demuestran la habilidad de los miRNAs de sobre-expresar sus blancos [15, 14], se consideraron ambos posibles tipos de blancos (sobre-expresados y sub-expresados) en tejidos tumorales para la reconstrucción de la red. La red de regulación resultante se compuso de 676,784 interacciones miRNA-mRNA (Tabla suplementaria 2).

Posteriormente, se filtró esta red con base en la predicción de la interacción miRNA-mRNA mediante los algoritmos más utilizados en el área (DIANA-microT-CDS, EIM-Mo, MicroCosm, miRanda, miRDB, PicTar, PITA and TargetScan) y en la presencia de la interacción ya validada en bases de datos experimentales (miRecords, miRTarBase, TarBase). Se consideraron aquellas interacciones miRNA-mRNA presentes en al menos una base de datos, dado que en la literatura se ha demostrado que la union de diferentes algoritmos de predicción tiene una mayor sensibilidad y precision que la intersección [72]. Este filtro permitió reducir la red a 32,205 interacciones (Tabla suplementaria 3).

Por último, utilizamos esta red filtrada para inferir los miRNAs reguladores maestros (MMRs) usando el algoritmo de inferencia de reguladores maestros (MARINa) [67] incluido en el paquete de Bioconductor Viper [60], considerando solo a aquellos MMRs que tuvieran un p-value ajustado < 0.05 . Los resultados mostraron que el transcriptoma tumoral podría ser regulado por un conjunto de 61 MMRs (Figura 6.2), involucrados en 16,444 interacciones constituidas por 6530 (39%) del total de los 14,449 genes diferencialmente expresados en el transcriptoma de los tumores. Aunque cada MMR se encontraba regulando un conjunto de ambos genes sobre y sub-expresados, la principal actividad global y su score de enriquecimiento normalizado inferidos por MARINa mostraban que todos los MMRs presentaban una actividad global de regulación negativa de sus blancos (Figura 6.2).

Posteriormente, fue de interés identificar que genes blancos y miRNAs presentaban el mayor número de interacciones, por lo que se procedió a analizar la topología de la red con el objetivo de obtener el grado de los nodos; la métrica que refleja el numero de

6.2. IDENTIFICACIÓN DE LOS MIRNAS REGULADORES MAESTROS

miRNAs		Genes		
Nombre	Grado	Nombre	Grado	Gen log2FoldChange
hsa-miR-106b-5p	1179	RUNX1T1	24	-1.715126046
hsa-miR-590-3p	996	BNC2	20	-0.440592219
hsa-miR-93-5p	970	TNS1	20	-3.104826764
hsa-miR-671-5p	921	DLC1	18	-1.789077079
hsa-miR-939-5p	711	FOXP2	18	-1.963889919
hsa-miR-877-5p	670	IGF1	17	-2.494558934
hsa-miR-130b-3p	585	ZEB2	17	-1.552276689
hsa-miR-16-5p	547	ANK2	16	-2.347077977
hsa-miR-301a-3p	546	BACH2	16	-1.35469313
hsa-miR-15b-5p	529	TCF4	16	-0.872983915
hsa-miR-940	483	ZCCHC24	16	-1.552147667
hsa-miR-301b	469	ZFHX4	16	-1.12229256
hsa-miR-106a-5p	451	NOVA1	15	-0.712825148
hsa-miR-1254	398	TSHZ3	15	-0.478344046
hsa-miR-93-3p	373	BHLHE41	14	-1.138290499
hsa-miR-141-3p	355	CCND2	14	-0.965637676
hsa-miR-96-5p	338	CREBRF	14	-0.973637932
hsa-miR-454-3p	329	PRICKLE2	14	-1.12294618
hsa-miR-200c-3p	329	QKI	14	-1.25158266
hsa-miR-429	327	RACGAP1	14	1.909634723

Tabla 6.1: MMRs y genes con el mayor grado en la red

aristas por vértice en la red. Observamos que miR-106b-5p era el MMR con el mayor número de blancos, seguido por miR-590-3p, miR-93-5p, miR-671-5P y miR-939-5p (Tabla 6.1). Por otro lado, los genes con el mayor número de MMRs regulándolos fueron RUNX1T1, BNC2, TNS1, DLC1 y FOXP2. Como se observa en la Tabla 6.1, de los 20 genes más regulados, solo RACGAP1 presentaba una sobre-expresión en los tumores, mientras que los restantes genes mostraban una patrón de sub-expresión.

CAPÍTULO 6. RESULTADOS

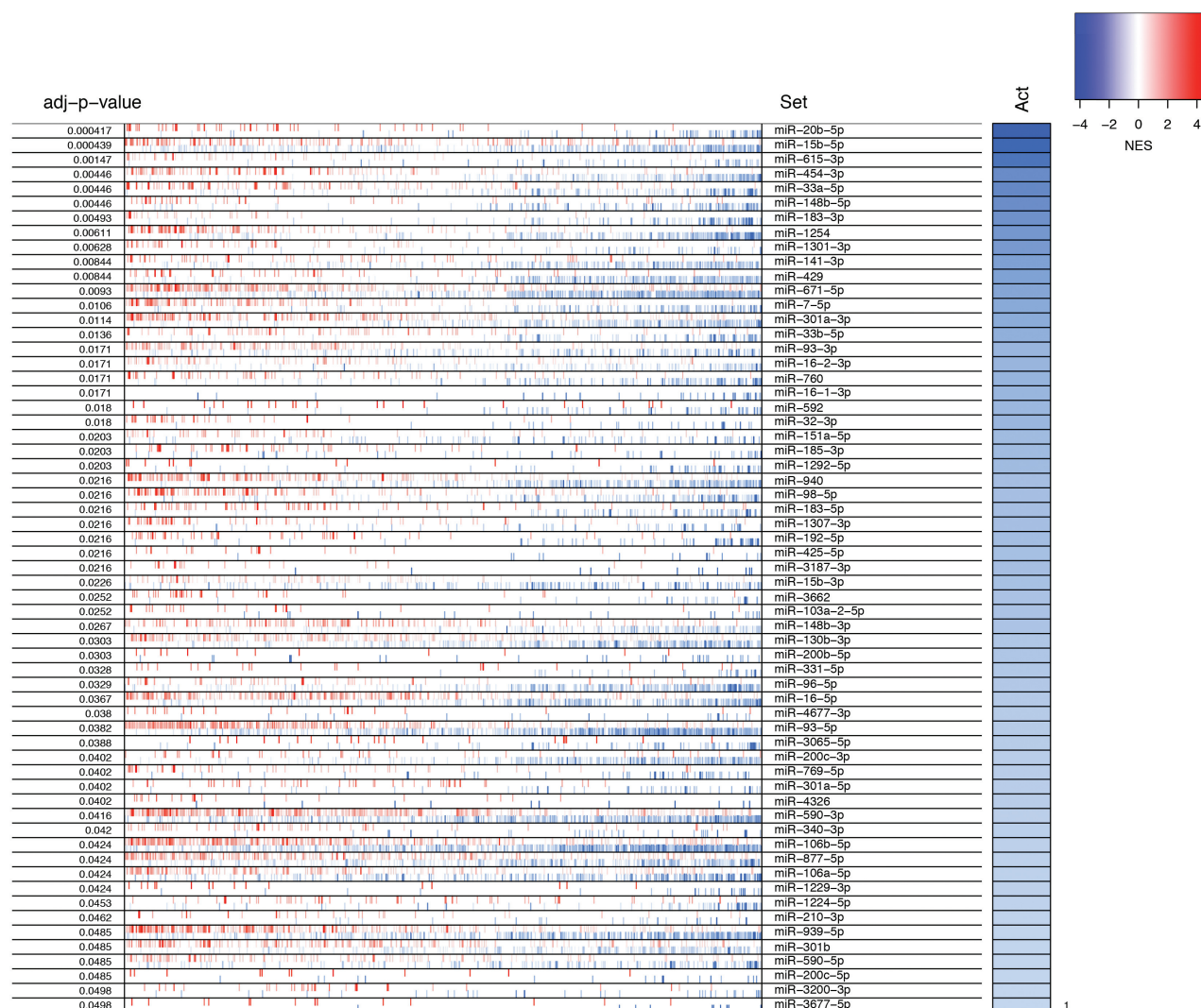


Figura 6.2: miRNAs reguladores maestros en cáncer de mama. El heatmap representa la expresión en $\log_2\text{FoldChange}$ de cada blanco regulado por cada miRNA, donde el color rojo representa una sobre-expresión y en azul una sub-expresión. La barra de la derecha muestra la actividad de regulación global de cada miRNA en relación a todos sus blancos, representado como un score de enriquecimiento normalizado (NES), donde el color azul representa un NES negativo y el color rojo un NES positivo

6.3. Análisis de las vías de señalización

Para conocer los procesos biológicos que podrían verse alterados por los MMRs, se procedió a realizar el análisis de las vías de señalización utilizando dos de las bases de

6.3. ANÁLISIS DE LAS VÍAS DE SEÑALIZACIÓN

datos más usadas: KEGG y Wikipathways cancer, empleando los 6530 genes únicos regulados por los MMRs. En la Figura 6.3 A y B se muestran las principales vías de señalización alteradas por los MMRs, las cuales se encuentran involucradas en la regulación de múltiples vías oncogénicas como el ciclo celular, la señalización de RAS, la vía de PI3K-AKT-mTOR, la vía de respuesta al daño a DNA y la vía de p53. Asimismo encontramos una concordancia en tres vías de señalización en ambas bases de datos: ciclo celular, señalización de Ras y las vías de respuesta al daño a DNA. Cabe destacar que de los 6530 genes empleados, solo 2542 y 862 se encontraban anotados en las bases de datos KEGG y Wikipathways cancer respectivamente. Esto representa el 38.9% y el 13% de los genes empleados, por lo que los procesos biológicos en los que pudieran estar participando el resto de los genes son desconocidos.

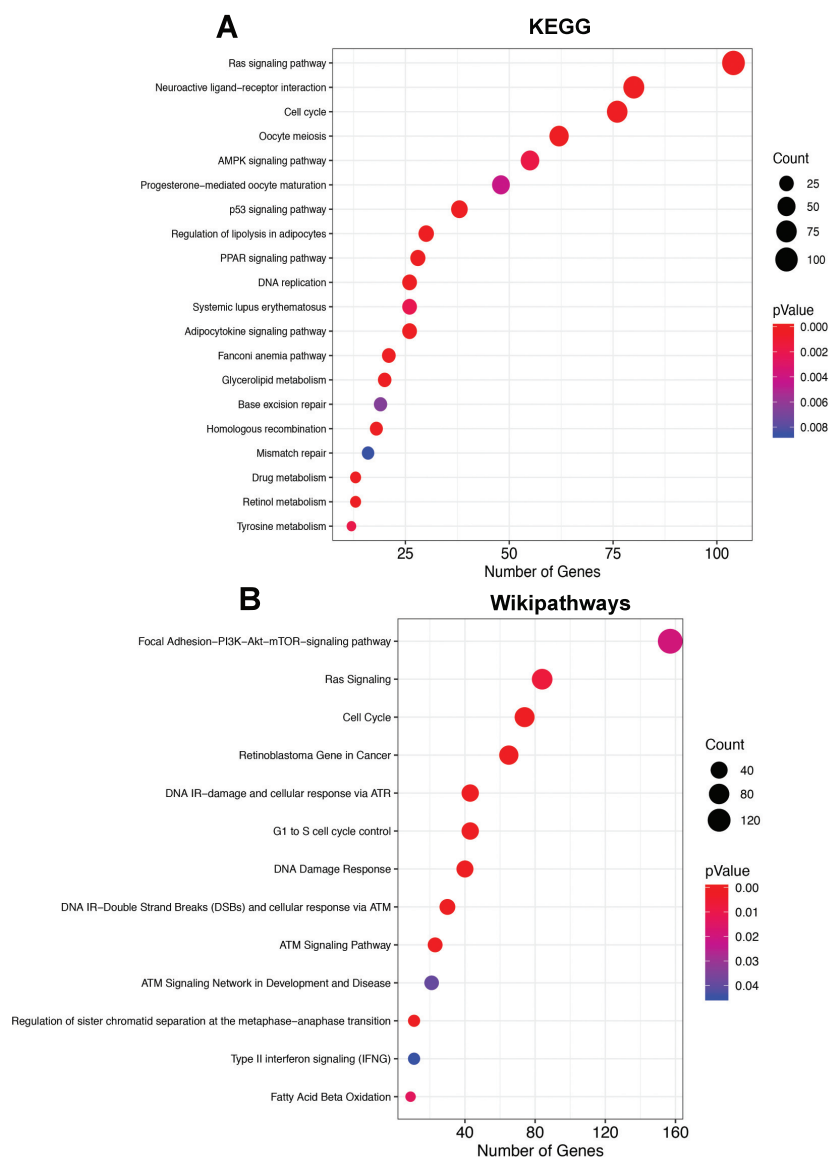


Figura 6.3: Analisis de las vías de señalización usando la plataforma WebGestalt]. (A) Muestra las vías enriquecidas en la base de datos de KEGG. El tamaño de los puntos representa el número de genes implicados en la vía de señalización, mientras que el color de los puntos representa la significancia del análisis, donde el color rojo representa una mayor significancia. (B) Muestra las vías de señalización enriquecidas en la base de datos de Wikipathways

6.4. Predicción de la actividad oncogénica de los MMRs

Razonamos que la contribución oncogénica de cada MMRA a la célula tumoral podría medirse como el balance entre los genes drivers validados como oncogenes o supresores de tumores que cada MMRA podría estar regulando en un momento dado. Definimos este balance como Actividad Oncogénica, la cual es calculada para cada MMRA como se mencionó en la sección de metodología. Cabe destacar que *per se* la medida de la información mutua entre un miRNA y su posible blanco mRNA no indica la direccionalidad de la regulación (sobre-expresión del blanco o represión), por lo que usamos el log2FoldChange como medida de la direccionalidad entre cada MMRA y sus posibles blancos. La base de datos COSMIC empleada para calcular la Actividad Oncogénica de cada MMR contenía 723 oncogenes y genes supresores de tumores driver manualmente curados de la literatura, de los cuales 336 se encontraban en la red miRNA-mRNA inferida.

Como se observa en la Figura 6.4, encontramos que de los 61 MMRs, 14 mostraban una actividad oncogénica (OncoMMRs), 35 una actividad supresora de tumores y 12 una actividad oncogénica neutra. Los MMRs que tuvieron la actividad oncogénica más alta fueron: miR-3200-3p, miR-185-3p, miR-3187-3p y miR-210-3p, mientras que los MMRs que presentaban una actividad supresora de tumores más alta fueron: miR-4677-3p, miR-4326, miR-769-5p, miR-103a-2-5p y miR-3677-5p. Estos resultados sugieren que cada MMR contribuye de manera positiva o negativa al fenotipo tumoral, donde la mayor parte lo hace actuando predominantemente como miRNAs supresores de tumores.

CAPÍTULO 6. RESULTADOS

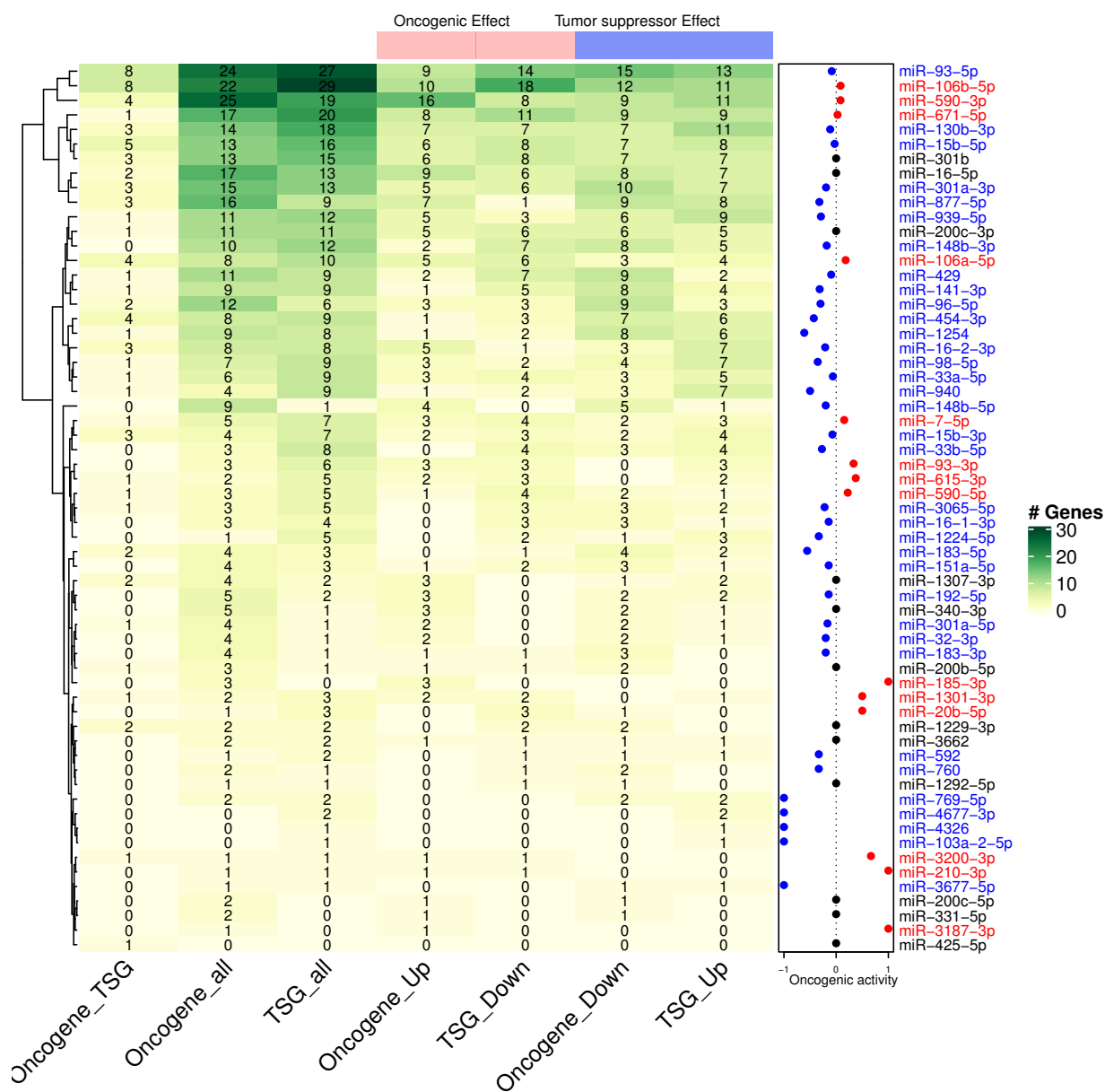


Figura 6.4: Actividad Oncogénica de los 61 MMRs. El heatmap muestra el número de oncogenes y genes supresores de tumores anotados en la base de datos COSMIC, donde el color verde representa un mayor número de genes. La gráfica de puntos a la derecha representa la actividad oncogénica de cada MMR, donde el color azul representa una actividad supresora de tumores, el color negro una actividad oncogénica neutra y el color rojo una actividad oncogénica.

6.5. Participación de los OncoMMRs con actividad oncogénica en el fenotipo tumoral

Posteriormente, fue de interés elucidar los mecanismos y los genes driver regulados por los 14 OncoMMRs con actividad oncogénica en el fenotipo tumoral. Como se muestra en la Figura 6.5A,, los 14 OncoMMRs regulaban en conjunto a 144 genes drivers. Además, los 4 OncoMMRs que regulan el mayor número de genes drivers están involucrados de forma común en los hallmarks de invasión y metástasis y en la evasión del crecimiento celular, aunque de forma individual cada OncoMMR regulaba hallmarks específicos Figura 6.5B.

Los 4 principales OncoMMRs con el mayor número de genes drivers regulados fueron: miR-106b-5p, seguido por miR-590-3p, miR-671-5p, y miR-106a-5p con 51, 44, 37, and 18 genes, respectivamente (Tabla 6.2)

Respecto a los principales genes drivers que presentaban una mayor regulación por los OncoMMRs, estos fueron el supresor de tumores FAT homolog 4 (FAT4), Kruppel like factor 6 (KLF6), Rho guanine nucleotide exchange factor 10 (ARHGEF10) y RB transcriptional corepressor 1 (RB1); cabe destacar que todos ellos se encontraban sub-expresados en los tumores. Por otra parte, los oncogenes High mobility groupAT-Hook 1 (HMGA1), Forkhead box A1 (FOXA1), y Serine and arginine rich splicing factor 2 (SRSF2) se encontraban (como era esperado) sobre-expresados en los tumores (Tabla 6.3).

Interesantemente, encontramos un grupo de genes driver coregulados por los 4 principales OncoMMRs. De estos, el supresor de tumores ARHGEF10 [73] y el oncogen SRSF2[74] mostraron estar comúnmente regulados por tres (miR-106b-5p, miR-590-3p, y miR-671-5p) y cuatro (miR-106b-5p, miR-590-3p, miR-671-5p, and miR-106a-5p) OncoMMRs respectivamente. Como se muestra en la figura 6.6A, los tres OncoMMRs exhibían una correlación negativa con el supresor de tumor ARHGEF10. Por otra par-

CAPÍTULO 6. RESULTADOS

OncoMMRs		
Nombre	Grado	Actividad Oncogénica
hsa-miR-106b-5p	51	0.08
hsa-miR-590-3p	44	0.08
hsa-miR-671-5p	37	0.02
hsa-miR-106a-5p	18	0.18
hsa-miR-7-5p	12	0.15
hsa-miR-93-3p	9	0.33
hsa-miR-590-5p	8	0.22
hsa-miR-615-3p	7	0.37
hsa-miR-1301-3p	5	0.5
hsa-miR-20b-5p	4	0.5
hsa-miR-185-3p	3	1
hsa-miR-3200-3p	2	0.66
hsa-miR-210-3p	2	1
hsa-miR-3187-3p	1	1

Tabla 6.2: Los 14 OncoMMRs y su actividad oncogénica

Genes Driver			
Nombre	Grado	log2FoldChange	Tipo de Gen
FAT4	4	-1.730874783	TSG
KLF6	4	-1.328673644	TSG
HMGA1	4	1.565787561	ONCOGEN
FOXA1	3	1.821835781	ONCOGEN
SRSF2	3	0.364903752	ONCOGEN
ARHGEF10	3	-0.996701079	TSG
RB1	3	-0.218520176	TSG
TAL1	3	-1.94737771	ONCOGEN
SET	3	0.514086719	ONCOGEN
PHF6	3	0.481518774	TSG
TGFBR2	3	-2.210252149	TSG
EBF1	3	-3.058271914	TSG
CPEB3	3	-0.49523291	TSG
PIK3R1	3	-1.39435573	TSG
MALT1	2	-0.234938295	ONCOGEN
WWTR1	2	-0.582536021	ONCOGEN
AR	2	0.508141889	ONCOGEN
KNSTRN	2	1.180623437	ONCOGEN
XPO1	2	0.327813155	ONCOGEN
ERBB2	2	2.020220978	ONCOGEN

Tabla 6.3: Principales genes drivers regulados por los OncoMMRs.

6.5. PARTICIPACIÓN DE LOS ONCOMMRS CON ACTIVIDAD ONCOGÉNICA EN EL FENOTIPO TUMORAL

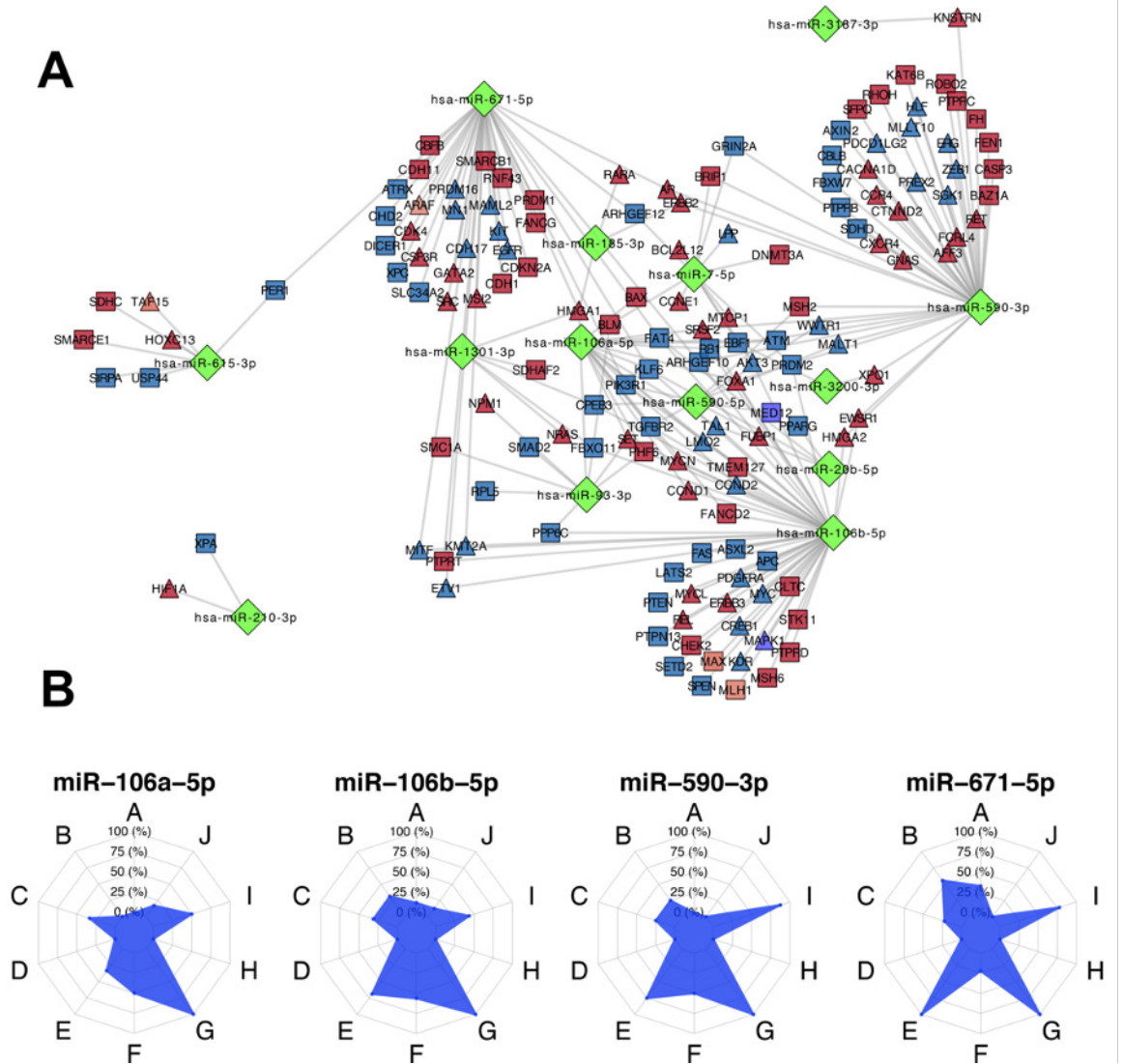


Figura 6.5: Los 14 OncoMMRs y los genes driver que regulan. (A) La red de los OncoMMRs donde los miRNAs son representados con forma de diamante en color verde, los oncogenes como triángulos y los genes supresores como rectángulos; el color azul y rojo representan la sub-expresión y la sobre-expresión de los genes respectivamente. (B) Los gráficos de radar muestran el enriquecimiento de genes por hallmark para los 4 OncoMMRs con el mayor número de genes blanco, donde se muestran los hallmarks que son promovidos: A: Angiogénesis, B: Inmortalidad replicativa celular, C: Cambio en el metabolismo celular, D: Evasión del sistema inmune, E: Evasión de la muerte celular programada, F: Inestabilidad genómica, G: Invasión y metástasis, H: Aumento en las señales de proliferación, I: Supresión del crecimiento, J: Promoción de la inflamación por el tumor

CAPÍTULO 6. RESULTADOS

te, los 4 OncoMMRs mostraron una correlación positiva con el oncogen SRSF2, donde la mayor correlación fue observada con miR-106b-5p, con una correlación de 0.419. Además, ambos ARHGEF10 y SRSF2 presentaron el mismo patrón de expresión a nivel de proteína en muestras sanas y de cáncer de mama del The Human Protein Atlas (Figura 6.6C,D)

6.5. PARTICIPACIÓN DE LOS ONCOMMRS CON ACTIVIDAD ONCOGÉNICA EN EL FENOTIPO TUMORAL

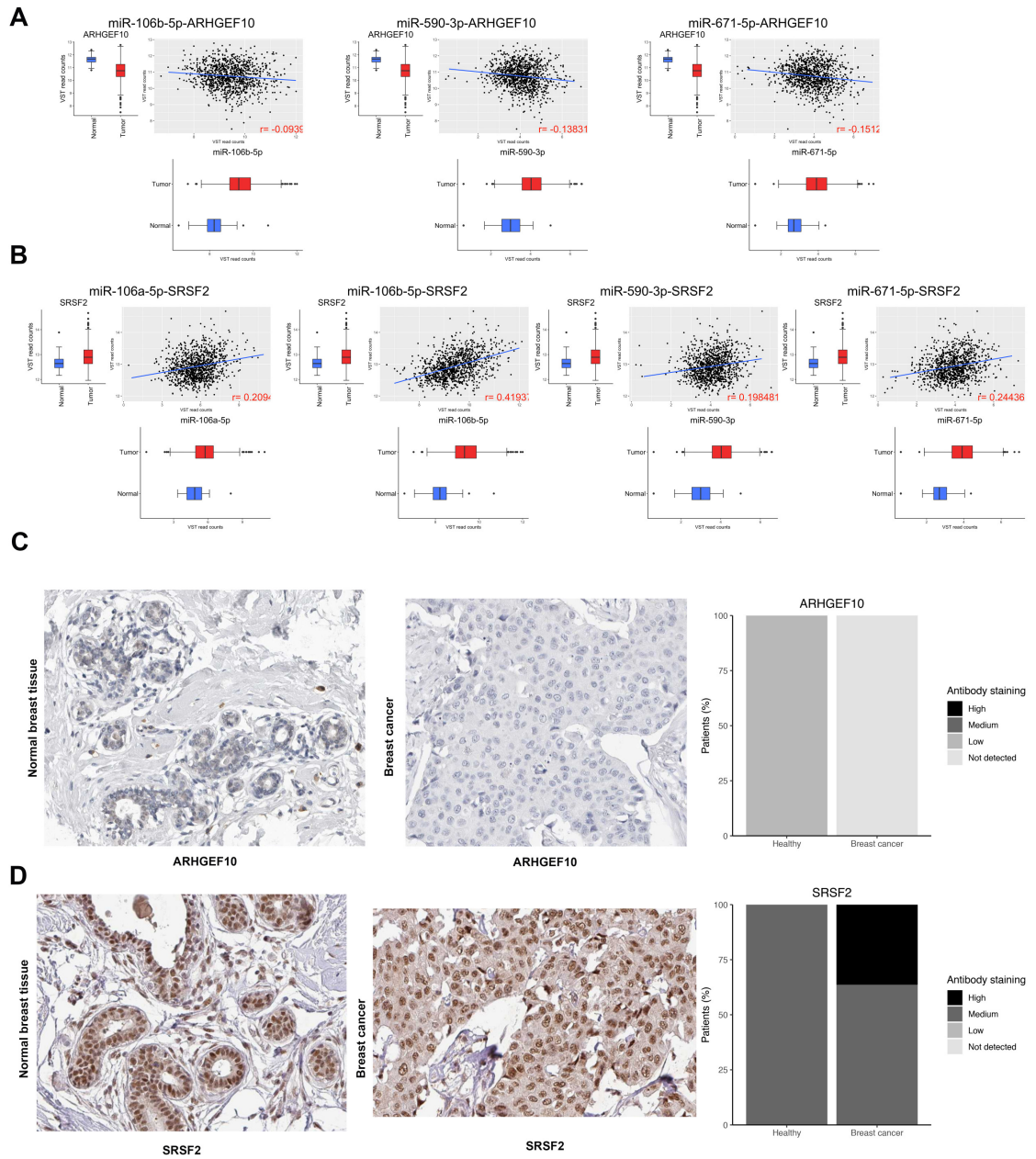


Figura 6.6: Correlación entre los principales OncoMMRs y la expresión de los genes driver ARHGEF10 y SRSF2. (A) La correlación entre los OncoMMRs y ARHGEF10. (B) La correlación entre los OncoMMRs y SRSF2. Los boxplots en color rojo representan la expresión de las moléculas en tejidos tumorales mientras que el color azul en muestras adyacentes sanas. (C,D) Muestran la expresión a nivel proteína de ARHGEF10 y SRSF2 en muestras de tejido mamario obtenidas del The Human Protein Atlas.

6.6. Identificación de los MMRs con relevancia clínica

Como los 61 MMRs se encontraban sobre-expresados en todos los estadios clínicos, razonamos que podrían ser utilizados como biomarcadores de la supervivencia en las pacientes con cáncer de mama. Para evaluar esto, agrupamos a las pacientes del TCGA en dos grupos: alta y baja expresión para cada MMR. Las curvas Kaplan-Meier con la prueba de log-rank mostraron que 5 MMRs (miR-151a-5p, miR-340-3p, miR-877-5p, miR-940, y miR-1307-3p) presentaban diferencias significativas en la supervivencia de ambos grupos de pacientes. Los resultados también mostraron que para estos 5 MMRs, los pacientes con una expresión alta presentaban una peor supervivencia global (Figura 6.7), aunque el impacto de estos MMRs en la supervivencia variaba dependiendo del subtipo intrínseco analizado; donde miR-151a-5p mostró diferencias significativas en el subtipo Normal-like ($p = 0.0024$), miR-877-5p en el subtipo Luminal A ($p = 0.043$), miR-940 en el subtipo Normal-like ($p = 0.0014$) y miR-1307-3p en el subtipo Luminal A subtype ($p = 0.048$) y el subtipo Normal like ($p = 0.0001$), mientras que miR-340-3p no mostró diferencias significativas (Figura suplementaria 1).

Por otra parte, las regresiones de COX univariadas y multivariadas utilizando la edad, el estadio clínico, los receptores de estrógeno (ER) y de progesterona (PR) como covariables sugirieron además que miR-1307-3p podría ser usado como un factor pronóstico de la supervivencia global de las pacientes con cáncer de mama (Tabla 6.4).

6.7. IMPACTO DE LOS MMRs EN LOS SUBTIPOS INTRÍNSECOS

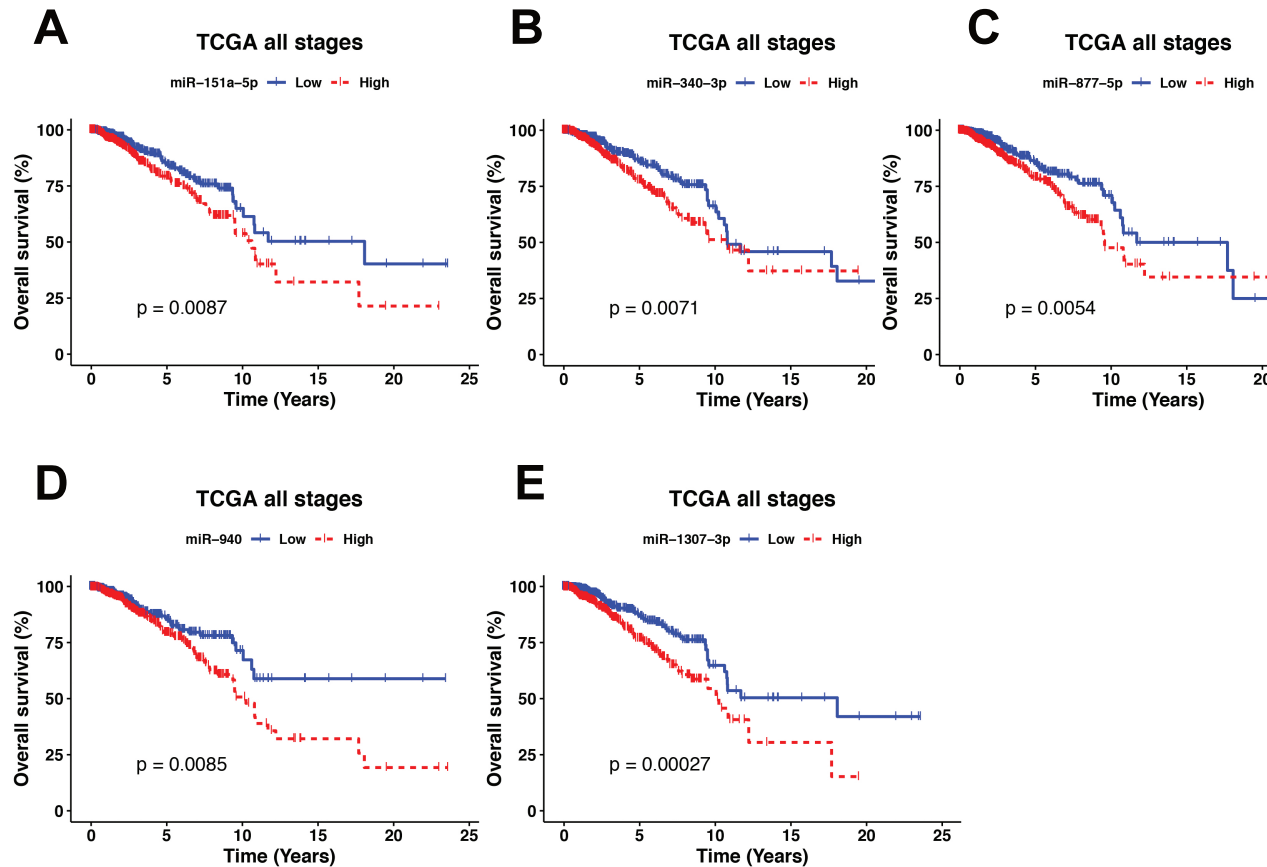


Figura 6.7: Curvas Kaplan-Meier para la supervivencia global con los 5 MMRs con significancia clínica. (A) Muestra las diferencias en la supervivencia de las pacientes con una alta y baja expresión para miR-151a-5p. Las líneas azules representan a las pacientes con una baja expresión del miRNA y la roja a las pacientes con una alta expresión. (B) Supervivencia para miR-340-3p. (C) Supervivencia para miR-877-5p. (D) Supervivencia para miR-940 y (E) Supervivencia para miR-1307-3p.

6.7. Impacto de los MMRs en los subtipos intrínsecos

Posteriormente se evaluó la expresión de los 5 MMRs con relevancia clínica en los subtipos intrínsecos de cáncer de mama basados en la clasificación PAM-50, ya que observamos diferencias en la supervivencia de los pacientes dependiendo del subtipo y considerando que los subtipos intrínsecos presentan diferentes perfiles moleculares que impactan en múltiples características clínicas como el desenlace de los pacientes [75].

CAPÍTULO 6. RESULTADOS

	Supervivencia global	Univariado		Multivariado	
		HR (95 % CI)	p-value	HR (95 % CI)	p-value
miR-151a-5p	Alta vs. baja expresión	0.64 (0.46-0.9)	0.0093	0.76 (0.50-1.16)	0.2172
miR-940		0.63 (0.44-0.89)	0.0091	0.77 (0.53-1.14)	0.2026
miR-1307-3p		0.53 (0.38-0.75)	0.00033	0.63 (0.42-0.97)	0.0357
miR-340-3p		0.63 (0.45-0.89)	0.0076	0.91 (0.61-1.34)	0.6429
miR-877-5p		0.62 (0.44-0.87)	0.0059	0.98 (0.66-1.45)	0.9272
Edad	<58 vs. 58	1.9 (1.3-2.6)	0.00038	2.12 (1.49-3.01)	2.78E-05
ER	Negativo vs. positivo	0.57 (0.4-0.81)	0.0017	0.68 (0.39-1.19)	0.1802
PR	Negativo vs. positivo	0.65 (0.47-0.91)	0.013	0.88 (0.51-1.50)	0.6473
Estadío clínico		2.3 (1.8-2.8)	2.6E-12	2.48 (1.96-3.14)	3.51E-14

Tabla 6.4: Regresiones de Cox para la supervivencia global en pacientes con cáncer de mama del TCGA.

Este análisis mostró dos principales resultados: primero, que los 5 MMRs se encuentran sobre-expresados en todos los subtipos cuando se comparan contra los tejidos adyacentes sanos (Figura 6.8 A-E), lo que concuerda con la hipótesis principal. Segundo, existen diferencias en la expresión de los MMRs entre los subtipos. En el caso de miR-151a-5p, no observamos diferencias significativas entre los subtipos Her2 vs. normal-like y entre Her2. vs Luminal B, donde la expresión de este MMR es menor y significativa en el subtipo basal cuando es comparado contra los demás subtipos (Figura 6.8 A).

En el caso de miR-340-3p, no encontramos diferencias entre los subtipos basal vs. Her2 y Luminal B vs. normal-like; por otro lado, este miRNA se encontraba sobre-expresado en las comparaciones entre Luminal A vs. normal-like y Luminal A vs. Luminal B (Figura 6.8 B). Este patrón también fue observado para los MMRs miR-877-5p, miR-940 y miR-1307-3p, donde las comparaciones entre Luminal A vs normal-like y Luminal A vs. Luminal B mostraron una sobre-expresión de los MMRs, mientras que la comparación entre Luminal B vs. normal-like no presentó diferencias significativas (Figura 6.8 C-E).

Además, observamos que miR-940 presentaba el mayor número de diferencias no significativas entre los subtipos, lo que sugiere que su expresión es homogénea en estos subtipos (Figura 6.8 D). Por otra parte, miR-877-5p presentó el mayor número de diferencias significativas, lo que indica una alta heterogeneidad en su expresión depen-

6.7. IMPACTO DE LOS MMRS EN LOS SUBTIPOS INTRÍNSECOS

diendo del subtipo (Figura 6.8 C). Interesantemente, los resultados mostraron que a parte del tejido sano, los 5 MMRS presentaban una mayor expresión exclusivamente en el subtipo Luminal A cuando era comparado con los demás subtipos (Figura 6.8 A-E).

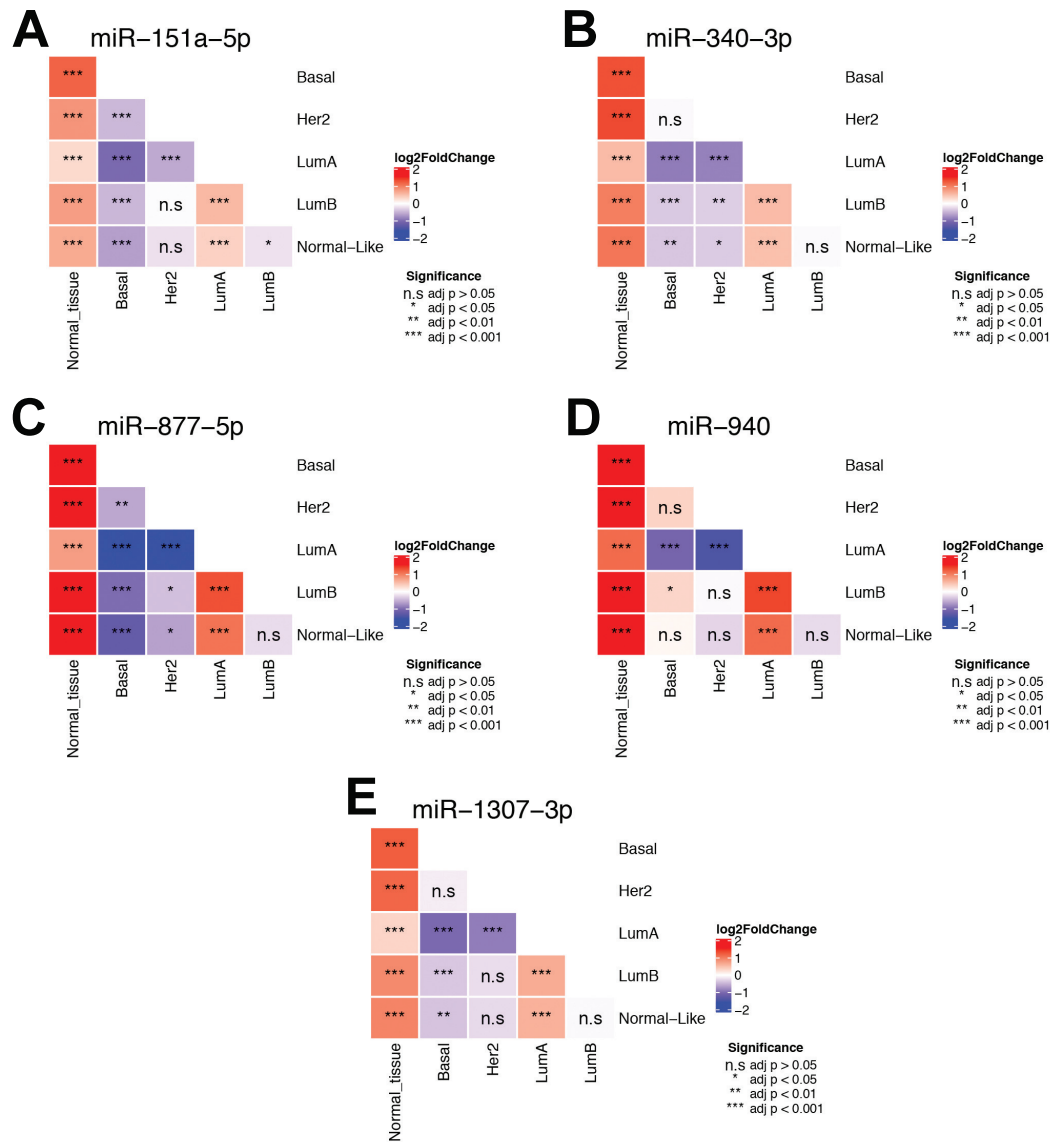


Figura 6.8: Expresión diferencial de los 5 MMRs con relevancia clínica en los subtipos intrínsecos basados en la clasificación PAM50. (A) Muestra la expresión diferencial de miR-151a-5p. El heatmap representa el log2FoldChange por cada comparación, donde en color rojo se muestra un foldchange positivo y en azul uno negativo. La significancia estadística se muestra dentro de cada celda, donde * = adj.p < 0.05, ** = adj.p < 0.01, *** = adj.p < 0.001 y n.s = adj.p > 0.05. (B) Representa a miR-340. (C) Muestra a miR-877-5p. (D) Representa a miR-940. (E) Muestra a miR-1307-3p.

6.8. Validación en tejidos tumorales localmente avanzados del Instituto Nacional de Cancerología

Para este estudio, validamos la expresión de tres de los MMRs que mostraron significancia estadística en las regresiones de cox univariadas y multivariadas en una cohorte independiente de pacientes. Por lo tanto, validamos a miR-340-3p, miR-940, y miR-1307-3p en muestras tumorales embebidas en parafina de pacientes diagnosticados con tumores localmente avanzados. Se colectaron muestras de 56 pacientes del Instituto Nacional de Cancerología, compuestas por 8 Her2, 20 Luminal A, 14 Luminal B, y 13 muestras triple negativas. Como se muestra en la Figura 6.9, en la comparación entre tejidos sanos vs. tumorales, miR-940 y miR-1307-3p se encontraron significativamente sobre-expresados en muestras tumorales, mostrando el mismo patrón de expresión que el análisis bioinformático previo.

Posteriormente, nos interesamos en evaluar si el patrón de sobre-expresión de los MMRs era similar en los subtipos intrínsecos. En el caso de miR-1307-3p, no observamos diferencias significativas entre los subtipos moleculares, lo que significa que se sobre-expresó de forma constante entre los subtipos (Figura 6.9 A). Por otra parte, observamos que miR-940 presentaba una mayor expresión en el subtipo triple negativo en comparación con los subtipos Luminal A y B (Figura 6.9 B), mientras que miR-340-3p no mostró diferencias significativas en muestras sanas vs. tumores ni entre los subtipos intrínsecos (Figura 6.9 C). Estos resultados sugieren la alta posibilidad de usar miR-1307-3p y miR-940 como posibles biomarcadores, independientemente del subtipo molecular en cáncer de mama.

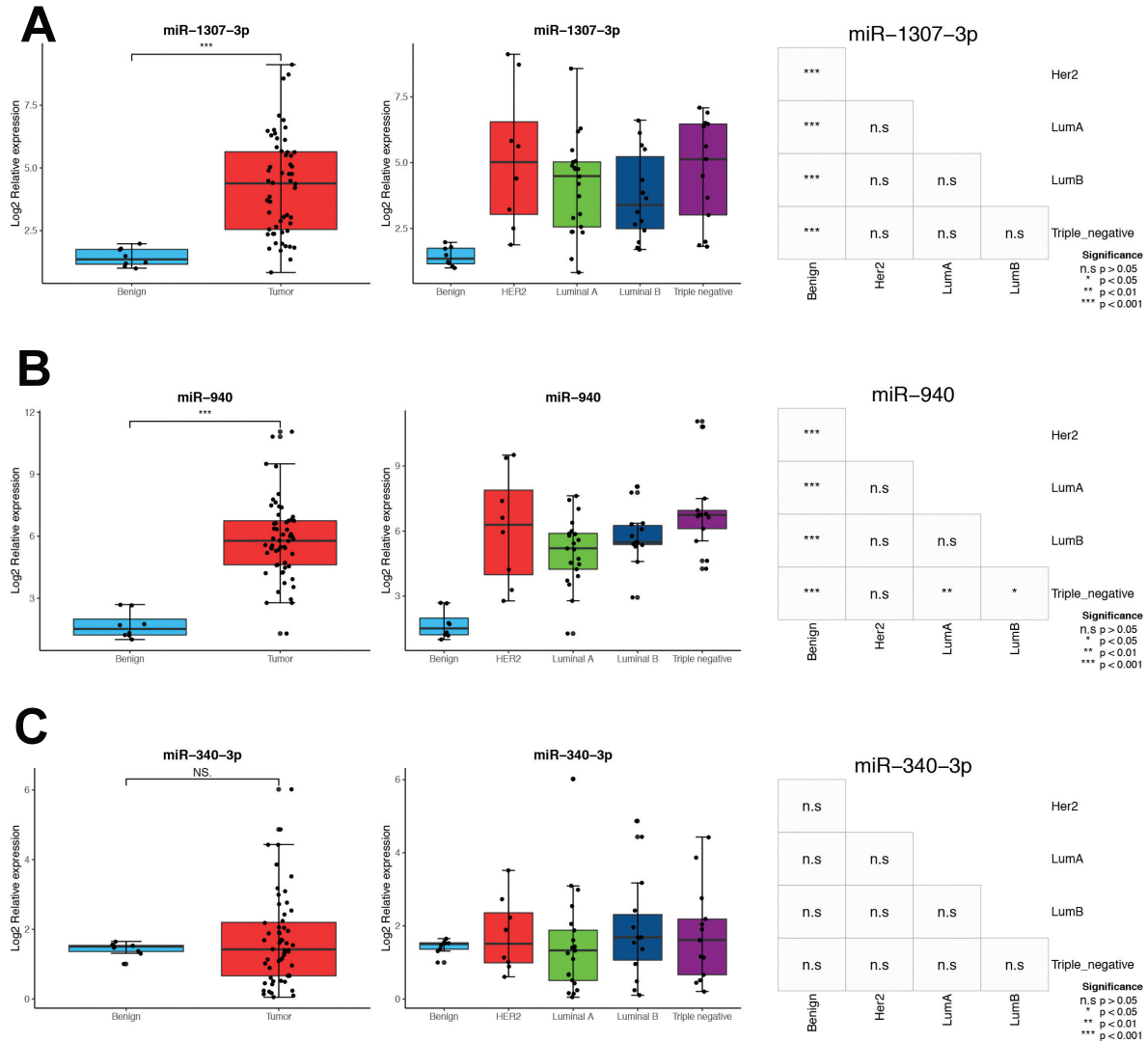


Figura 6.9: Validación de tres MMRs en 56 muestras de pacientes localmente avanzados usando qPCR en tiempo real. (A) Muestra la expresión de miR-1307-3p en tejidos sanos vs. tumorales y entre los subtipos intrínsecos. Los boxplots representan la expresión relativa en log2 mientras que el heatmap muestra la significancia de las comparaciones entre los subtipos, donde la significancia se encuentra anotada como: * = $p < 0.05$, ** = $p < 0.01$, *** = $p < 0.001$ y n.s = $p > 0.05$. (B) Expresión de miR-940. (C) Expresión de miR-340-3p.

Discusión y conclusiones

Desde una perspectiva de biología de sistemas, el cáncer es el resultado de un incremento en la entropía, por ejemplo, un incremento en el desorden celular que llevará a aberraciones a nivel genético y epigenético que afectarán el perfil transcripcional y proteómico de las células tumorales [76]. En este contexto caótico, las células tumorales deben de mantener sus funciones celulares a pesar de las aberraciones a las que están sujetas, preservando la robustez celular mediante múltiples mecanismos como la regulación post-transcripcional ejercida por los miRNAs [77]. La evidencia previa ha demostrado que, a pesar de que los tumores presentan diferentes perfiles de mutaciones somáticas, estos presentan transcriptomas desregulados similares [78], lo que implica la presencia de moléculas estabilizadoras que permiten el mantenimiento de las funciones celulares que dependen del transcriptoma. Se ha propuesto que estas moléculas reguladoras maestras podrían ser los miRNAs, moléculas capaces de mantener el transcriptoma celular independientemente de los eventos que llevaron al desarrollo del tumor y de las aberraciones a las que la célula tumoral está sujeta. Esto confiere robustez a los procesos biológicos mediante el reforzamiento de los perfiles transcripcionales y la estabilización de los niveles de expresión de los transcritos aberrantes.

Este trabajo representa un esfuerzo para elucidar un grupo de miRNAs reguladores maestros (MMRs) constantemente sobre-expresados en cada estadio clínico en cáncer

CAPÍTULO 7. DISCUSIÓN Y CONCLUSIONES

de mama y la evaluación de su actividad oncogénica con relación a los oncogenes/supresores de tumores que regulan.

En este trabajo nos enfocamos en encontrar los MMRs constantemente sobreexpresados en la carcinogénesis de los tumores mamarios y su participación con la transformación oncogénica. Para hacerlo, integramos los datos de miRNAs y mRNA de la base de datos pública del proyecto de cáncer de mama del TCGA, y utilizamos el algoritmo de inferencia de reguladores maestros (MARINA)[60], el cual ha sido exitosamente usado para inferir proteínas aberrantes [60] y otros reguladores maestros transcripcionales [79].

Nuestros resultados muestran la existencia de 61 MMRs presentes de forma consistente en todos los estadios clínicos de tumores mamarios, los cuales en conjunto están asociados con la regulación del 39% de los genes diferencialmente expresados en el transcriptoma tumoral. Como esperábamos, las principales vías de señalización alteradas por este grupo de MMRs son hallmarks del cáncer como el ciclo celular, la vía de PI3K-AKT-mTOR y la reparación del daño a DNA entre otras, como se ha reportado en otros estudios. Aunque el cáncer de mama es una enfermedad altamente heterogénea, este resultado refuerza el concepto y participación de MMRs que pudieran estar regulando un grupo de genes diferencialmente expresados y compartidos por todos los subtipos intrínsecos del cáncer de mama y cuya principal función es mantener los mecanismos y vías de señalización centrales que un tumor necesita en cada etapa de la tumorigénesis y que los diferencia de un tejido sano, como los hallmarks de la resistencia a la muerte celular, el mantenimiento de las señales de proliferación y la evasión de supresores del crecimiento.

Uno de los principales retos al analizar la participación de los miRNAs en cáncer es su clasificación en oncomiRNAs o en supresores de tumores, debido a su naturaleza multi-blanco [80]. En este trabajo abordamos este problema mediante el cálculo de la actividad oncogénica de cada miRNA, una medida propuesta por Svoronos et al.

[80]. Esto lo resolvimos al tomar en cuenta solamente a aquellos genes blanco que han sido documentados como drivers o causales de la tumorigenesis mediante múltiples experimentos. Cuando nos enfocamos en la regulación de este tipo de genes nuestros resultados mostraron que la mayoría de los miRNAs se encontraban participando como supresores de tumores, lo que es consistente con otras publicaciones [81]. Este resultado podría indicar que a pesar de que la célula tumoral se encuentra en una tendencia descontrolada a proliferar, aun hay mecanismos de regulación muy fina -incluyendo a los miRNAs- que están involucrados en este balance proliferativo. Sin embargo, más estudios in vivo e in vitro son requeridos para validar esta hipótesis.

Nuestros resultados revelaron un grupo de MMRs que se encontraban actuando principalmente como OncoMMRs, los cuales posiblemente estén involucrados en el mantenimiento del fenotipo tumoral. En este análisis, nos enfocamos en los cuatro principales OncoMMRs que tuvieron el mayor número de posibles blancos (miR-106b-5p, miR-106a-5p, miR-671-5p y miR-590-3p). La sobreexpresión de estos miRNAs ya ha sido asociada anteriormente con un incremento en la proliferación, migración, invasión y en la radio-resistencia [82, 83, 84, 85, 86, 87], lo que concuerda con nuestros resultados. Además, estos cuatro OncoMMRs se encontraban altamente enriquecidos en genes involucrados en la invasión y metástasis, lo que sugiere que podrían estar participando de manera conjunta en estos hallmarks.

Al respecto de los genes regulados por los MMRs, encontramos una regulación redundante de los genes supresores de tumores FAT4 y KLF6, entre otros, cuya expresión ha sido asociada con un fenotipo más agresivo en cáncer de mama [88, 89, 90]. Además, encontramos que el gen supresor de tumores ARHGEF10 y el oncogen SRSF1 se encontraban negativa y positivamente regulados por miR-106b-5p, miR-106a-5p, miR-671-5p y miR-590-3p, con un patrón de expresión similar a nivel de proteínas en tejidos de cáncer de mama, lo que valida nuestros resultados. Aunque nuestros resultados de validación fueron obtenidos en un número limitado de muestras, se requiere un análisis más profundo para corroborar la correlación entre la expresión de ARHGEF10 y SRSF2 en

CAPÍTULO 7. DISCUSIÓN Y CONCLUSIONES

una cohorte mayor de muestras tumorales mamarias. Estudios recientes sugieren que ARHGEF10 participa como un supresor de tumores involucrado en la activación de la apoptosis durante el daño al DNA [73]. Por lo tanto, nuestros resultados sugieren que este supresor de tumores también se encuentra sujeto a una co-regulación por los OncoMMRS miR-106b-5p, miR-671-5p y miR-590-3p.

Por otra parte, el factor de splicing SRSF1 ha sido reportado como sobreexpresado en tumores mamarios y actuando como un oncogen al producir isoformas aberrantes de los genes pro-apoptóticos BCL2 Like 11 (BIM) y BIN1, los cuales están involucrados en el fenotipo tumoral. Sin embargo, es importante recalcar que estas posibles interacciones entre MMRs y genes drivers debe de ser confirmada en experimentos *in vitro*.

Los miRNAs han sido propuestos como biomarcadores moleculares en múltiples investigaciones [91, 92, 93, 94], debido a su expresión específica y estabilidad para su medición en muestras de sangre periféricas. Por lo tanto, nos enfocamos en buscar aquellos MMRs asociados con el pronóstico clínico. Nuestros resultados mostraron que aquellos pacientes con una mayor expresión de miR-1307-3p, miR-940 Y miR-340-3p tuvieron una peor supervivencia global, sugiriendo que podrían ser usados como posibles biomarcadores al ser evaluados en tumores de todos los subtipos moleculares, mientras que la sobreexpresión de miR-1307-3p y miR-940 solo pudo ser validada en una cohorte independiente de tumores de mama compuesta por una población mexicana-mestiza. De ellos, solo miR-1307-3p ha sido previamente asociado con quimio-resistencia [95] y resistencia al cisplatino [96].

Respecto a miR-940, otros reportes señalan una sub-expresión de esta molécula en una cohorte China [97, 98]. Estos reportes controversiales resaltan la importancia de la participación de los miRNAs como posibles biomarcadores en cáncer de mama.

En resumen, estos resultados sugieren la existencia y participación de un grupo de 61 MMRs que pudieran tener una gran importancia para el mantenimiento del fenotipo tumoral, ya que se encuentran presentes en todos los estadios de esta enfermedad y al






estar regulando un conjunto de genes que han sido validados como conductores de la tumorigenesis. Sin embargo, se requieren de experimentos in vitro e in vivo para poder validar la participación de estas moléculas en la tumorigenesis y como probables biomarcadores.

Producción científica

- 8.1. Martinez-Gutierrez, Antonio-D., et al. Identification of miRNA Master Regulators in Breast Cancer. Cells. 2020**

Article

Identification of miRNA Master Regulators in Breast Cancer

Antonio Daniel Martínez-Gutierrez ¹, David Cantú de León ¹, Oliver Millan-Catalan ¹, Jossimar Coronel-Hernandez ¹, Alma D. Campos-Parra ¹, Fany Porras-Reyes ², Angelica Exayana-Alderete ³, César López-Camarillo ⁴, Nadia J Jacobo-Herrera ⁵, Rosalio Ramos-Payan ⁶ and Carlos Pérez-Plasencia ^{1,7,*}

¹ Laboratorio de Genómica, Instituto Nacional de Cancerología, Tlalpan, CDMX 14080, Mexico; maga94@comunidad.unam.mx (A.D.M.-G.); dfcantu@gmail.com (D.C.d.L.); oliver.millan.sg@gmail.com (O.M.-C.); jossithunders@gmail.com (J.C.-H.); adcamposparra@gmail.com (A.D.C.-P.)

² Servicio de Anatomía Patológica, Instituto Nacional de Cancerología, Tlalpan, CDMX 14080, Mexico; car_plas@yahoo.com

³ Decanato, Ciencias de la Salud, Universidad Autónoma de Guadalajara, Jal Zapopan 45129, Mexico; drako098@hotmail.com

⁴ Posgrado en Ciencias Biomédicas, Universidad Autónoma de la Ciudad de México, CDMX 03100, Mexico; genomicas@yahoo.com.mx

⁵ INCMNSZ, Unidad de Bioquímica, Tlalpan, CDMX 14080, Mexico; nadia.jacobo@gmail.com

⁶ Faculty of Biology, Autonomous University of Sinaloa, Culiacán 80007, Sin, Mexico; rosaliorp@uas.edu.mx

⁷ Laboratorio de Genómica, Unidad de Biomedicina, FES-IZTACALA, UNAM, Tlalnepantla 54090, Mexico

* Correspondence: carlos.pplas@gmail.com; Tel.: +52-(55)-5623-1333 (ext. 39807)

Received: 19 May 2020; Accepted: 25 June 2020; Published: 3 July 2020



Abstract: Breast cancer is the neoplasm with the highest number of deaths in women. Although the molecular mechanisms associated with the development of this tumor have been widely described, metastatic disease has a high mortality rate. In recent years, several studies show that microRNAs or miRNAs regulate complex processes in different biological systems including cancer. In the present work, we describe a group of 61 miRNAs consistently over-expressed in breast cancer (BC) samples that regulate the breast cancer transcriptome. By means of data mining from TCGA, miRNA and mRNA sequencing data corresponding to 1091 BC patients and 110 normal adjacent tissues were downloaded and a miRNA–mRNA network was inferred. Calculations of their oncogenic activity demonstrated that they were involved in the regulation of classical cancer pathways such as cell cycle, PI3K–AKT, DNA repair, and k-Ras signaling. Using univariate and multivariate analysis, we found that five of these miRNAs could be used as biomarkers for the prognosis of overall survival. Furthermore, we confirmed the over-expression of two of them in 56 locally advanced BC samples obtained from the histopathological archive of the National Cancer Institute of Mexico, showing concordance with our previous bioinformatic analysis.

Keywords: miRNA; breast cancer; master regulator; integrative analysis; TCGA data analysis

1. Introduction

Breast cancer (BC) is the leading type of neoplasia in the female population, with two million new cases diagnosed worldwide each year [1]. Advanced clinical stages are related to higher mortality rates due to their metastatic behavior [2]; therefore, it is necessary to investigate and understand the molecular mechanisms underlying the metastatic cancer phenotype.

Tumor progression is the tendency of tumoral cells to acquire traits—usually known as hallmarks—such as the loss of cellular differentiation, an increased cell cycle, invasion, and metastases that lead to a more aggressive phenotype [3]. One class of molecules known to be involved in tumor progression are the microRNAs or miRNAs. These molecules are small non-coding RNAs of 21 to 23 nucleotides, whose main function is the post-transcriptional regulation of a whole range of genes and are key regulators of oncogenic pathways [4]. In BC, their pathogenic participation has been extensively investigated, showing that these molecules display an aberrant expression pattern that can distinguish between normal and BC tumor tissues [5]; they can also successfully identify different subtypes of BC [6], and are involved in the transition of specific key events during the progression of the disease [7]. Likewise, they have been successfully used as prognostic biomarkers in invasive ductal carcinoma tumors [8] and in specific subtypes such as the triple negative [9]. Due to their multitarget nature miRNAs can maintain the major characteristics of cancer phenotype; such kind of miRNAs are known as master regulators (MMR) [10].

The use of high-throughput data and the inference of miRNA–mRNA networks is a bioinformatic tool that allows us to understand the complex participation of miRNAs in cancer (reviewed in [11]). For instance, in serous ovarian cancer, it was found that eight miRNAs were able to regulate 89% of genes associated with the mesenchymal phenotype [8]. Meanwhile, in BC, it was found that miRNAs act as co-transcriptional modules that could be both positively and negatively associated to their target mRNAs [12]. Another study by Cantini et al., showed that the miR-199/miR-214 cluster of polycistronic miRNAs was acting as an MMR by regulating the epithelial to mesenchymal transition [13]. Another example of an integrated analysis of miRNAs and expression profiles reported a set of miRNA master regulators in colorectal cancer, which were responsible for the regulation of this cancer subtype [10]. In the present work, our major aim was the identification of miRNAs acting as master regulators that were consistently upregulated along the clinical stages of BC. To achieve this, we downloaded from TCGA miRNA and mRNA sequencing data corresponding to 1091 BC patients and 110 normal adjacent tissues. The expression data were compared between tumors and normal tissues. We obtained 209 consistently over-expressed miRNAs along the different cancer stages. Of them, 61 miRNA were considered master regulators in the BC transcriptome through inferring their miRNA–mRNA network using the ARACNe algorithm [14]. Next, we calculated the oncogenic activity of each (61) miRNA to the breast tumor by considering the number and expression profile of validated oncogenes and tumor suppressors genes they regulate. This group of miRNAs was involved in the regulation of pathways such as cell cycle, PI3K–AKT, DNA repair, k-ras signaling, among others. Using univariate and multivariate analysis, we found that five of these miRNAs could be used as biomarkers related to the overall survival rate. Furthermore, we validated the overexpression of three of them in locally advanced BC samples obtained from the histopathological archives of the National Cancer Institute of Mexico, showing concordance with our previous bioinformatic analysis.

2. Materials and Methods

2.1. Analysis of Upregulated miRNAs in Clinical Stages

The general workflow is shown in Figure 1. To identify the consistently upregulated miRNAs in breast cancer, we first obtained the hiseq read counts from the TCGA BC project [15] corresponding to 1091 BC patients (Stages I–IV) and 110 normal adjacent tissues using the Bioconductor package TCGABIOLINKS [16]. Differential expression analysis was carried out using DESeq2 [17]. Only miRNAs with an FDR ≤ 0.05 and a log2FoldChange of at least +0.5 were considered. The correlation between miRNA expression and TNM stages defined by the American Joint Committee on Cancer (AJCC) was done using Spearman correlation, included in the R package Hmisc. We only considered miRNAs with a *p*-value of ≤ 0.05 and a positive correlation coefficient.

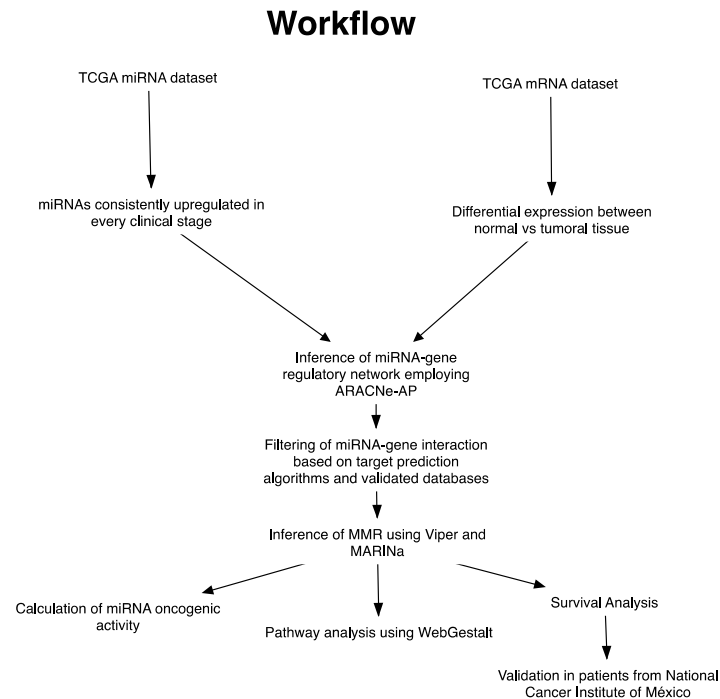


Figure 1. General workflow.

2.2. Identification of miRNA Master Regulators

To determine the number of miRNAs acting as master regulators in BC, we obtained mRNAs differentially expressed in tumor tissues employing TCGABIOLINKS and DESeq2. Only mRNAs with an $FDR \leq 0.05$ were considered for this analysis. Subsequently, mRNA and miRNA datasets were normalized using the VST method implemented in the DESeq2 package. Next, we reconstructed the miRNA–mRNA network with ARACNe-AP [14] employing our previously filtered data consisting of the overexpressed miRNAs and the differentially expressed mRNAs, using 100 bootstrap replications. The miRNA–mRNA interactions in the resulting network were filtered based on their presence in at least one predicted (DIANA-microT-CDS, EIMMo, MicroCosm, miRanda, miRDB, PicTar, PITA and TargetScan) and/or experimentally validated databases (miRecords, miRTarBase, TarBase) using the Bioconductor package multiMir [18]. With this approach, we ensured that the resulting network contained both inferred and experimentally validated data. Next, we employed the master regulator inference algorithm [19] included in the Bioconductor package [20]. miRNAs were assigned as MMR if they had an $FDR \leq 0.05$. Finally, the network analysis was carried out with Cytoscape v3.7.1 (National Institute of General Medical Sciences (NIGMS), Bethesda, MD, USA) [21].

2.3. Oncogenic Activity of miRNAs MMR

Any miRNA has the ability to regulate both oncogenes and tumor suppressor genes. Hence its oncogenic activity (OA) is the likelihood that a given miRNA will regulate an oncogene and a tumor suppressor gene in both ways i.e., upregulate an Oncogene, down-regulate a tumor suppressor gene or vice versa. To obtain the oncogenic activity for each miRNA, we first downloaded the manually curated oncogene/tumor suppressor data from the Catalogue of somatic mutations in cancer (COSMIC [22]).

Therefore, we first calculated its Oncogenic Effect (OE) as the sum of upregulated oncogenes and down-regulated TSG, which is represented with the following formula:

$$O_e = (U_{ONC} + D_{TSG}) - ONC_{TSG} \quad (1)$$

where: O_e = Oncogenic effect; U_{ONC} = Upregulated oncogenes; D_{TSG} = Downregulated tumor suppressor genes; ONC_{TSG} = Genes with dual function as oncogenes and tumor suppressors.

Then, the Anti-oncogenic Effect (AE) as the sum of up-regulated TSG and down-regulated oncogenes:

$$A_e = (D_{ONC} + U_{TSG}) - ONC_{TSG} \quad (2)$$

where: A_e = Antioncogenic effect; D_{ONC} = Downregulated oncogenes; U_{TSG} = Upregulated tumor suppressor genes; ONC_{TSG} = Genes with dual function as oncogenes and tumor suppressors.

Finally, the OA is the relation between AO-OE and the total number of possible driver targets for each miRNA:

$$O_A = \frac{O_e - A_e}{T} \quad (3)$$

where: O_A = Oncogenic activity; O_e = Oncogenic effect; A_e = Antioncogenic effect; T = Total number of targets (oncogenes, tumor suppressor genes and genes with dual function).

2.4. Pathway Analysis

The pathway analysis was done using the WebGestalt platform [23] (<http://www.webgestalt.org>); we uploaded the differentially expressed mRNA gene symbols and their log2FoldChange. Statistically significant pathways were considered with an FDR ≤ 0.05 .

2.5. Intrinsic Subtype Classification and Differential Expression

The PAM50 subtype classification of the TCGA samples was assessed using the Bioconductor package Genefu [24]. Differential expression between subtypes was carried out using the Bioconductor package DESeq2 [17], where miRNAs with an FDR ≤ 0.05 were considered as significant.

2.6. Survival Analysis

Clinical data was obtained from the 1091 BC patients analyzed from the TCGA. Next, we divided the patients into two groups, high and low expression based on the median expression of each MMRs. Kaplan–Meier curves and Cox regressions were obtained in the R environment using the survival package, the multivariate Cox regressions were adjusted using the age and clinical stages of the patients. Statistical significance was assessed using log-rank test < 0.01 .

2.7. Patient Samples

A prospective group of 56 patients diagnosed with locally advanced BC were enrolled. Formalin-fixed paraffin-embedded (FFPE) tissue blocks were obtained from the Pathology department at the Instituto Nacional de Cancerología. All patients included in the present study signed an informed consent form; protocol number (015/03/019/ICI).

2.8. RNA Isolation and Real-Time qPCR

Total RNA was extracted from the FFPE tissue blocks using the miRNeasy FFPE Kit (Cat. No. 217504 Qiagen. Hilden, Germany). RNA was quantified in Qubit 3.0 Fluorometer with Qubit RNA HS Assay Kit (Cat. No. Q32852. Thermo Fisher Scientific. Waltham, MA, USA). Reverse transcription was performed using 10 ng of RNA with TaqMan Advanced miRNA cDNA Synthesis Kit (Cat. No. A28007. Thermo Fisher Scientific) following the manufacturer's recommendations. Quantitative real time PCR was performed with TaqMan Advanced miRNA Assays for: hsa-miR-940, hsa-miR-1307-3p,

hsa-miR-340-3p using hsa-miR-16 as an endogenous control (Cat. No. 4331182, Thermo Fisher Scientific). q-PCR reaction was performed at 95 °C for 20 s and at 95 °C for 1 s (40 cycles) with Taqman Fast Advanced Master Mix (Cat. No. 4444557, Thermo Fisher Scientific) on Step One System (Thermo Fisher Scientific). All reactions were performed in triplicate and fold changes were calculated using the $2^{-\Delta\Delta CT}$ method. The Mann–Whitney U test was used to identify significant miRNAs, considering $p < 0.05$ as statistically significant.

2.9. Tissue Expression Meta-Analysis

Antibody-based proteomic data of 2 normal breast tissues and 11 BC samples were obtained from The Human Protein atlas [25], where the staining activity was compared between the two groups.

3. Results

3.1. Identification of miRNAs Consistently Upregulated in Breast Tumor Tissues

Our aim was to get a list of miRNAs consistently upregulated in BC (Stages I–IV) obtained from the TCGA breast cancer project. We selected only those miRNAs that had an FDR < 0.05 . In total, 217 miRNAs constantly upregulated in all clinical stages (Figure 2) were found. To verify the upregulation of these miRNAs, expression levels were correlated to the clinical stages using the Spearman correlation. From the last analysis, 204 miRNAs had a significantly positive correlation (Table S1).

3.2. Identification of MMRs

Employing the 204 significantly upregulated BC miRNAs, we analyzed their role in the development of the tumor phenotype, so we proceeded to investigate their possible targets and pathways. To do that, we first inferred the tumor miRNA–gene network with an information theory approach, using the mutual information algorithm ARACNe [14] and the differentially expressed genes. Given previous reports demonstrating the ability of miRNAs to upregulate their targets [26,27], we considered both downregulated and upregulated genes in tumoral tissues. The resulting regulatory network consisted of 676,784 miRNA–gene interactions (Table S2). Next, we filtered the network based on the presence of the miRNA–gene interaction inferred by prediction algorithms. We considered interactions present in at least one database (DIANA-microT-CDS, EIMMo, MicroCosm, miRanda, miRDB, PicTar, PITA and TargetScan) and/or experimentally validated databases (miRecords, miRTarBase, TarBase), since it has been observed that the union of different prediction algorithms have a higher sensitivity and precision than the intersection [28]. This step permitted us to reduce the network to 36,205 miRNA–gene interactions (Table S3).

Finally, we used the filtered network to infer the MMR using the master regulatory inference algorithm (MARINa) [19] included in the VIPER R package [20]; only those miRNAs with an adj-p value < 0.05 were considered. The results revealed that the tumoral transcriptome could be regulated by 61 putative MMRs (Figure 3), involved in 16,444 interactions, consisting of 6530 (39%) out of 14,449 total genes found to be differentially expressed in the transcriptome of breast tumors (Figure S1, Tables S4 and S8). Although each miRNA had both up- and downregulated targets, the main activity and normalized enrichment score (NES) of all MMRs was the downregulation pattern of their targets, as shown in Figure 3 (Table S5).

Subsequently, we were interested in identifying which targets and miRNAs had the largest number of interactions, so we topologically analyzed the network to further obtain the node degree, a metric that reflects the number of links per node involved in the network. We observed that miR-106b-5p was a MMR with the highest number of total targets present in tumors, followed by miR-590-3p, miR-93-5p, miR-671-5p, and miR-939-5p (Table 1). On the other hand, the genes with the higher number of miRNAs regulating them were RUNX1T1, BNC2, TNS1, DLC1, and FOXP2. As shown in Table 1, of the 20 most regulated genes, only RACGAP1 had a positive fold change in tumors, while the remaining genes showed a downregulation pattern.

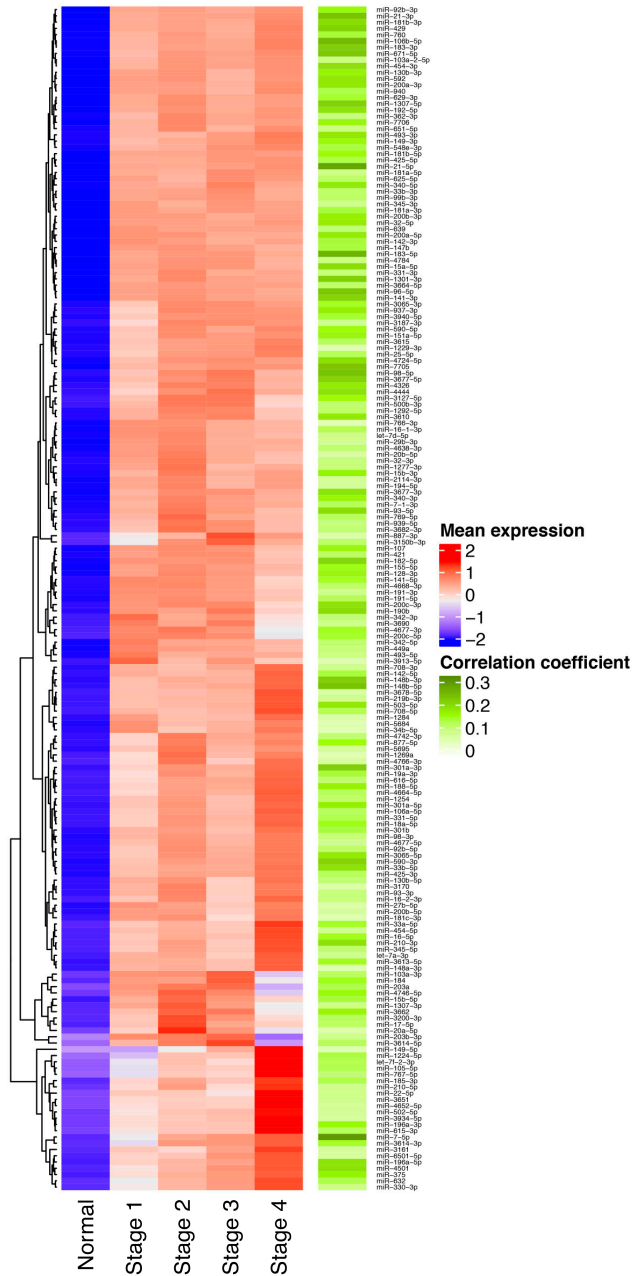


Figure 2. Overexpressed miRNAs across all clinical stages. The left heatmap shows the expression of 217 miRNAs over-expressed in breast cancer (BC) tissues (depicted in red) and downregulated in normal tissues (blue). As shown the majority of miRNAs had a positive correlation (green) between expression level and clinical stage.

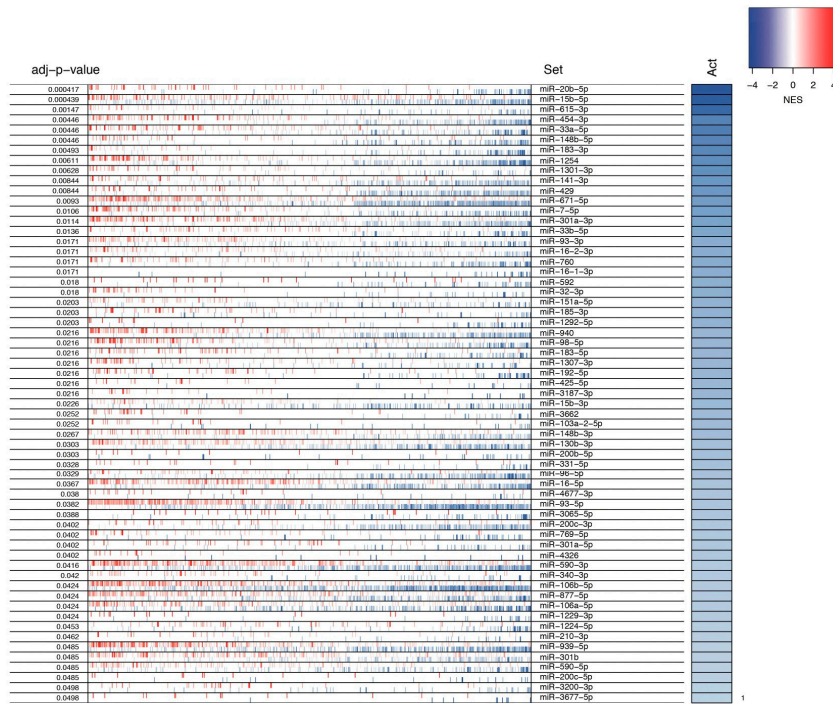


Figure 3. miRNA master regulators in breast cancer. The heatmap represents the log₂ fold change expression of each miRNA target, where red shows an overexpression and blue a downregulation in BC tissues. The right bar shows the global regulation activity of each miRNA related to its multiple targets, represented as the normalized enrichment score (NES), where blue represents a negative NES and red a positive. As shown, all of the miRNAs exhibit a negative NES.

Table 1. Top degree miRNAs and genes in the network.

miRNAs.		Genes		
Name	Degree	Name	Degree	Gene log ₂ FoldChange
hsa-miR-106b-5p	1179	RUNX1T1	24	-1.715126046
hsa-miR-590-3p	996	BNC2	20	-0.440592219
hsa-miR-93-5p	970	TNS1	20	-3.104826764
hsa-miR-671-5p	921	DLC1	18	-1.789077079
hsa-miR-939-5p	711	FOXP2	18	-1.963889919
hsa-miR-877-5p	670	IGF1	17	-2.494558934
hsa-miR-130b-3p	585	ZEB2	17	-1.552276689
hsa-miR-16-5p	547	ANK2	16	-2.347077977
hsa-miR-301a-3p	546	BACH2	16	-1.35469313
hsa-miR-15b-5p	529	TCF4	16	-0.872983915
hsa-miR-940	483	ZCCHC24	16	-1.552147667
hsa-miR-301b	469	ZFHX4	16	-1.12229256
hsa-miR-106a-5p	451	NOVA1	15	-0.712825148
hsa-miR-1254	398	TSHZ3	15	-0.478344046
hsa-miR-93-3p	373	BHLHE41	14	-1.138290499
hsa-miR-141-3p	355	CCND2	14	-0.965637676
hsa-miR-96-5p	338	CREBRF	14	-0.973637932
hsa-miR-454-3p	329	PRICKLE2	14	-1.12294618
hsa-miR-200c-3p	329	QKI	14	-1.25158266
hsa-miR-429	327	RACGAP1	14	1.909634723

3.3. Pathway Analysis

For the sake of knowing the biological processes that could be altered by the MMRs, we did a pathway analysis using two of the most-used pathway databases, KEGG and Wikipathways cancer database. Therefore, we uploaded the 6530 unique genes regulated by the MMRs. In Figure 4A,B, we show the activity of the MMRs predicted to be involved in the regulation of multiple oncogenic associated pathways such as cell cycle, Ras signaling, PI3K–AKT–mTOR, DNA damage response, and p53 pathway. A concordance between both gene annotation databases was found in three pathways, cell cycle, Ras signaling, and pathways involved in DNA damage response. It should be noted that of the 6530 unique genes, only 2542 and 862 genes were annotated in the KEGG and Wikipathways databases, respectively. Such numbers represent 38.9% and 13% of the total uploaded genes; thus, the biological processes in which the remaining genes that are not currently annotated could be participating in remain unknown.

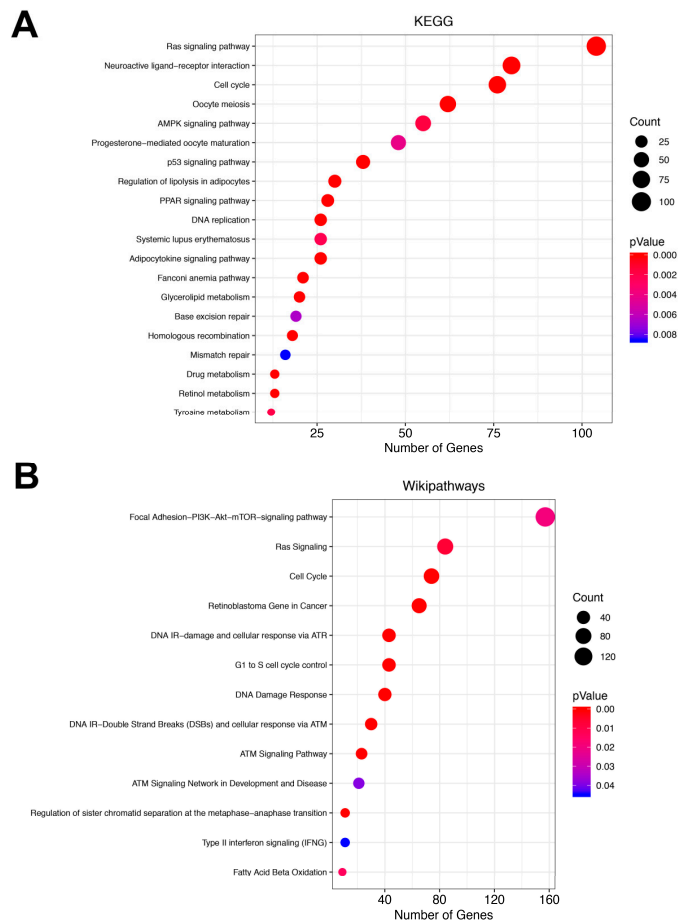


Figure 4. Pathway analysis in the WebGestalt platform. (A) Shows the enriched pathways in the KEGG database. The size of the dots depicts the number of genes in the pathway, while the dot color represents the significance of the analysis, where red shows a more significantly enriched pathway. (B) Shows the pathway enrichment in the Wikipathways database.

3.4. Prediction of miRNAs Oncogenic Activity

We reasoned that each MMRA oncogenic contribution to the tumor cell could be measured as the balance of validated driver oncogenes and tumor suppressor genes they could regulate. We termed this balance as the oncogenic activity, which was calculated for each miRNA as mentioned in the Methods section. It should be noted that per se the mutual information measure between miRNA and mRNA does not give the directionality of the regulation (positive or negative); thus, we used the log2FoldChange as a measure of directionality between each miRNA and their targets. The COSMIC database contained 723 manually curated oncogenes and tumor suppressor genes, of which 336 of them were present in our inferred miRNA–mRNA network.

As shown in Figure 5, we found that, of the 61 MMR, 14 had a positive oncogenic activity, 35 had a negative oncogenic activity, and 12 of them had a neutral oncogenic activity. We noticed that the miRNAs with the highest oncogenic activity were miR-3200-3p, miR-185-3p, miR-3187-3p, and miR-210-3p, while the miRNAs with the lowest net oncogenic activity were miR-4677-3p, miR-4326, miR-769-5p, miR-103a-2-5p, and miR-3677-5p. This result suggests that each MMR has negative or positive participation in the tumoral phenotype, whereas a high proportion of them act predominantly as tumor suppressor miRNAs.

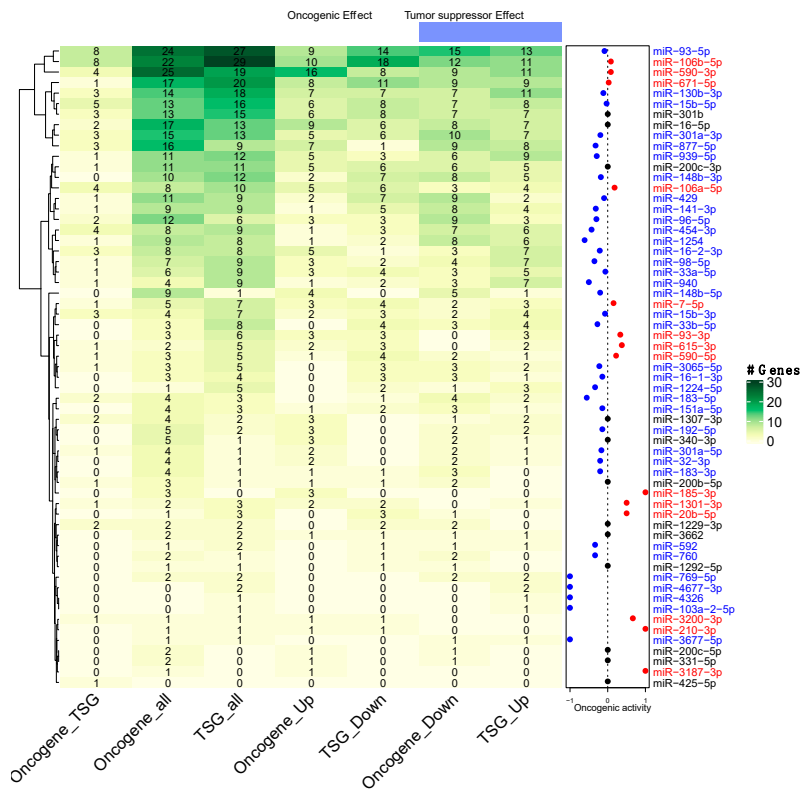


Figure 5. Oncogenic net activity of the 61 miRNAs The heatmap shows the number of annotated oncogenes and tumor suppressors in the COSMIC database, where green represents a higher number of genes. The right dot plot represents each miRNA oncogenic activity, where blue shows a tumor suppressor activity, black a neutral activity, and red an oncogenic activity.

3.5. Participation of miRNAs Acting as Oncogenic Drivers

Next, we wanted to know the tumor mechanisms and the driver genes regulated by the 14 MMRs that had a positive contribution to the tumoral phenotype. As shown in Figure 6A, the 14 MMRs regulate 144 gene drivers. Moreover, the top four most highly connected MMRs were commonly involved in invasion and metastasis and resisting cell death, although there were specific hallmarks regulated by each OncoMMRs (Figure 6B).

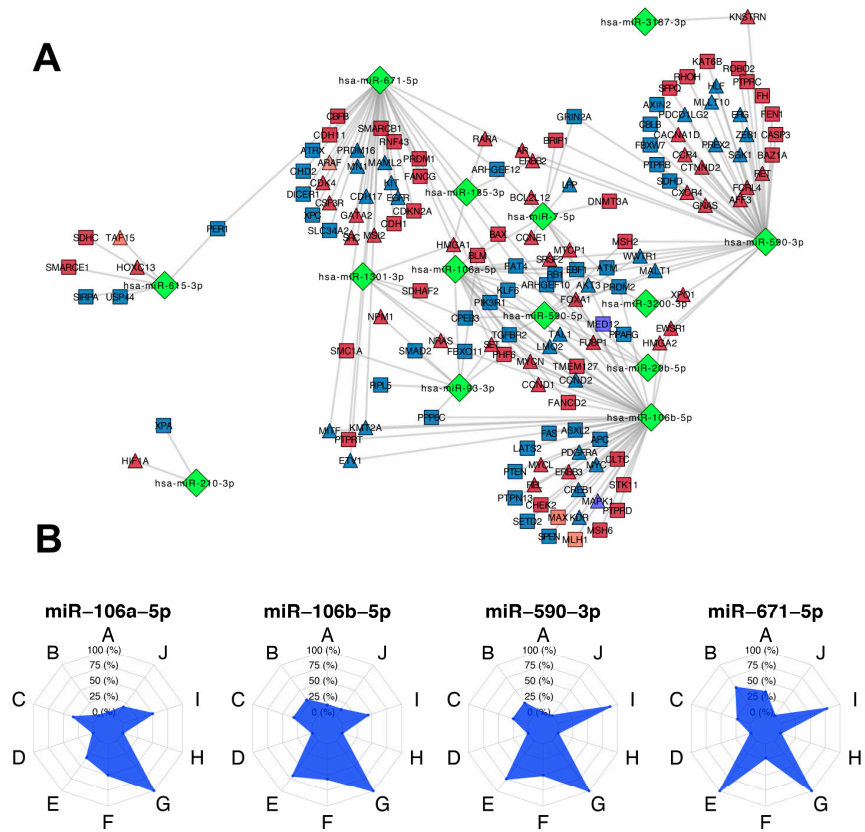


Figure 6. The 14 oncogenic miRNA master regulators (OncoMMRs) with a positive contribution to the tumoral phenotype and their driver targets. (A) The OncoMMR network where miRNAs are depicted as green diamonds, oncogenes as triangles and tumor suppressor genes as rectangles; blue and red represent downregulated and overexpressed genes, respectively. (B) Radar plots show the enrichment of genes as per the hallmark for the top four most highly connected OncoMMRs, where A: Angiogenesis, B: Cell replicative immortality, C: Change of cellular energetics, D: Evading immune response, E: Evading programmed cell death, F: Genome instability, G: Invasion and metastasis, H: Proliferative signaling, I: Suppression of growth, J: Tumor promoting inflammation.

The top four most highly connected OncoMMR were miR-106b-5p, followed by miR-590-3p, miR-671-5p, and miR-106a-5p with 51, 44, 37, and 18 genes, respectively (Table 2). We observed that OncoMMRs with the higher oncogenic activity had the smallest number of regulated targets.

Table 2. OncoMMRs and their oncogenic activity.

OncoMMRs		
Name	Degree	Oncogenic Activity
miR-106b-5p	51	0.08
miR-590-3p	44	0.08
miR-671-5p	37	0.02
miR-106a-5p	18	0.18
miR-7-5p	12	0.15
miR-93-3p	9	0.33
miR-590-5p	8	0.22
miR-615-3p	7	0.37
miR-1301-3p	5	0.5
miR-20b-5p	4	0.5
miR-185-3p	3	1
miR-3200-3p	2	0.66
miR-210-3p	2	1
miR-3187-3p	1	1

With respect to the top tumor driver genes that were more regulated by OncoMMRs, these were the tumor suppressor genes FAT homolog 4 (FAT4), Kruppel like factor 6 (KLF6), Rho guanine nucleotide exchange factor 10 (ARHGEF10), and the RB transcriptional corepressor 1 (RB1); all of them were downregulated in tumoral tissues. Moreover, the oncogenes High mobility group AT-Hook 1 (HMGA1), Forkhead box A1 (FOXA1), and the Serine and arginine rich splicing factor 2 (SRSF2) were (as expected) over-expressed (Table S6).

Interestingly, there was a group of genes co-regulated by all four OncoMMRs. Of these, the tumor suppressor ARHGEF10 [29] and the oncogene SRSF2 [30] were commonly regulated by three (miR-106b-5p, miR-590-3p, and miR-671-5p) and four (miR-106b-5p, miR-590-3p, miR-671-5p, and miR-106a-5p) OncoMMRs, respectively, in the network (Table S7). As shown in Figure 7A, all three OncoMMR exhibited a negative correlation with the tumor suppressor ARHGEF10. Moreover, all of the four OncoMMRs showed a positive correlation with the oncogene SRSF2, where the largest correlation coefficient was observed for miR-106b-5p with 0.419. Moreover, both ARHGEF10 and SRSF2 showed the same trend of expression at the protein level in breast cancer tissues, as shown in Figure 7C,D.

3.6. Identification of miRNA Master Regulators with Clinical Relevance

As all MMR were upregulated in all clinical stages, we reasoned that they could be used as survival biomarkers in breast cancer patients. To achieve this, TCGA patients were grouped in high and low expression for each MMR. Kaplan-Meier curves with log-rank p showed that 5 MMR (miR-151a-5p, miR-340-3p, miR-877-5p, miR-940, and miR-1307-3p) had significant differences between the two groups. The results showed that for all five MMR, patients with a higher expression had a worse overall survival (Figure 8), although the impact of the MMRs in the survival varied depending of the intrinsic subtypes analyzed, where miR-151a-5p showed significant differences in the Normal-like subtype ($p = 0.0024$), miR-877-5p in the Luminal A subtype ($p = 0.043$), miR-940 in the Normal-like subtype ($p = 0.0014$) and miR-1307-3p in the Luminal A subtype ($p = 0.048$) and the Normal like subtype ($p = 0.0001$), whereas miR-340-3p showed no significant differences (Figure S2).

Univariate and Multivariate cox regressions using age, clinical stages, estrogen receptors (ER), and progesterone receptors (PR) status as covariates further suggested that miR-1307-3p could be used as prognostic factor of the overall survival for patients with breast cancer (Table 3).

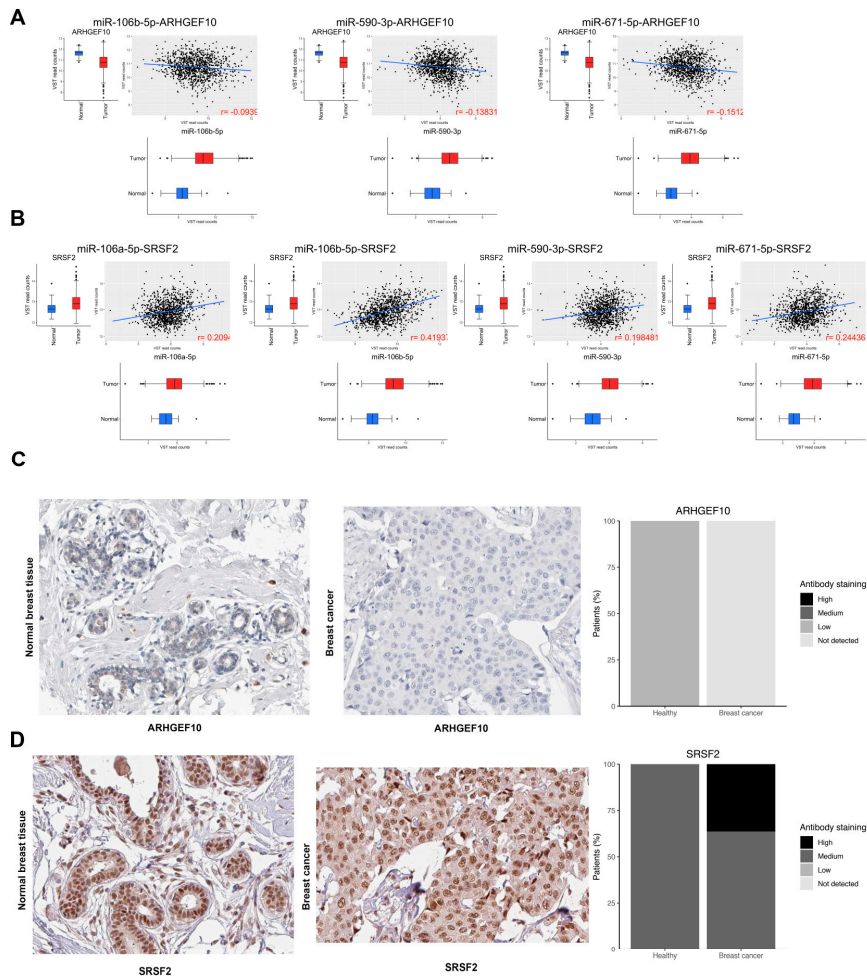


Figure 7. Correlation between the top OncoMMRs and the expression of the driver genes ARHGEF10 and SRSF2. (A) The correlation between the OncoMMRs and ARHGEF10. (B) The correlation between the OncoMMRs and SRSF2. Red boxplots represent the expression of the molecules in tumor tissues and blue in normal tissues. (C,D) protein expression of ARHGEF10 and SRSF2 from breast tissues of the human protein atlas.

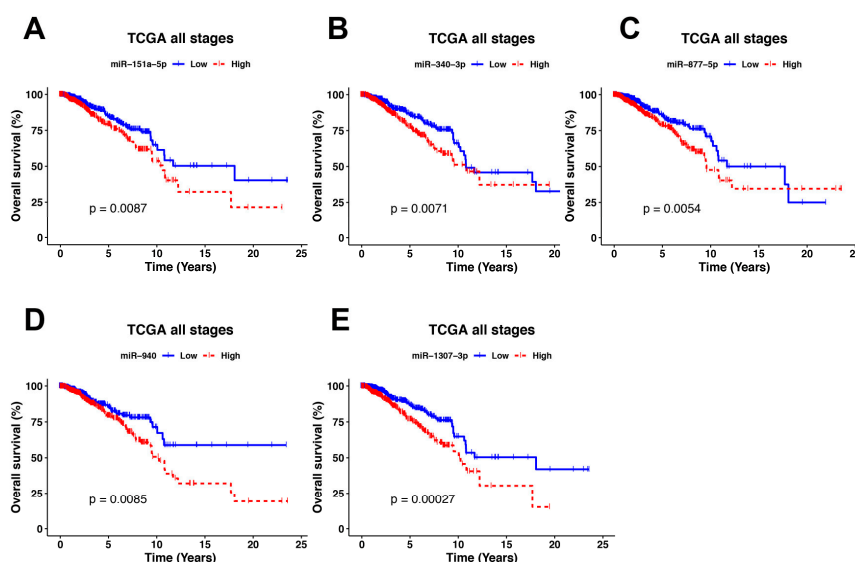


Figure 8. Kaplan–Meier overall survival analysis based on five clinically significant MMRs. (A) Shows the differences in the survival of patients with a high and low expression of miR-151a-5p. Blue lines represent patients with a low miRNA expression and red patients with a high expression. (B) Survival for miR-340-3p. (C) Survival for miR-877-5p. (D) Survival for miR-940 and (E) Survival for miR-1307-3p.

Table 3. Cox regression analysis of the overall survival of the breast cancer patients.

	Overall Survival	Univariate Analysis		Multivariate Analysis	
		HR (95% CI)	p-Value	HR (95% CI)	p-Value
miR-151a-5p		0.64 (0.46–0.9)	0.0093	0.76 (0.50–1.16)	0.2172
miR-940		0.63 (0.44–0.89)	0.0091	0.77 (0.53–1.14)	0.2026
miR-1307-3p		0.53 (0.38–0.75)	0.00033	0.63 (0.42–0.97)	0.0357
miR-340-3p		0.63 (0.45–0.89)	0.0076	0.91 (0.61–1.34)	0.6429
miR-877-5p		0.62 (0.44–0.87)	0.0059	0.98 (0.66–1.45)	0.9272
Age at diagnosis	<58 vs. ≥58	1.9 (1.3–2.6)	0.00038	2.12 (1.49–3.01)	2.78×10^{-5}
ER	Negative vs. positive	0.57 (0.4–0.81)	0.0017	0.68 (0.39–1.19)	0.1802
PR		0.65 (0.47–0.91)	0.013	0.88 (0.51–1.50)	0.6473
Clinical stage		2.3 (1.8–2.8)	2.6×10^{-12}	2.48 (1.96–3.14)	3.51×10^{-14}

3.7. Impact of MMRs in the BC Intrinsic Subtypes

Next we evaluated the expression of the five MMRs in the intrinsic subtypes of BC based in the PAM-50 classification, as we observed differences in the survival of patients depending on the subtype and considering that the intrinsic subtypes show different molecular profiles that impact on clinical characteristics such as the patient outcome [31]. This analysis showed two main results: first, all of the five MMRs are overexpressed in the subtypes when compared with normal adjacent tissue (Figure 9A–E), which is in accordance with our main hypothesis. Second, there are differences in the expression of the MMRs between subtypes. In the case of miR-151a-5p, we observed no significant differences between the Her2 vs. normal-like and Her2 vs. Luminal B subtypes, where the expression of this MMR is lower and significant in the basal subtype when compared with the other subtypes (Figure 9A).

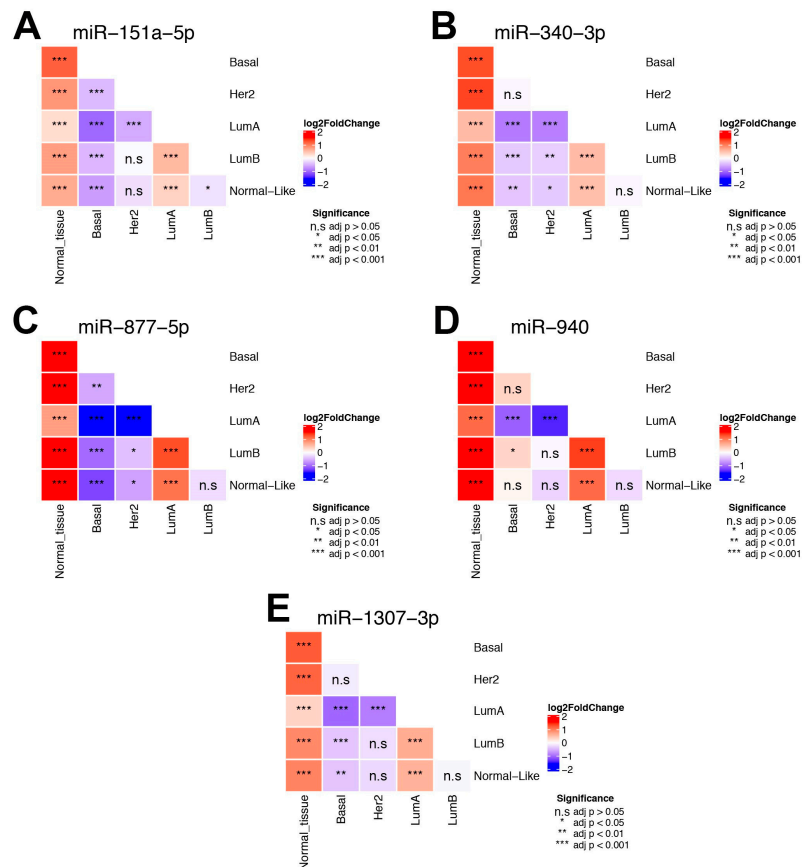


Figure 9. Differential expression of the five MMRs between PAM50 intrinsic subtypes. (A) Shows the differential expression of miR-151a-5p. The heatmap represents the log₂FoldChange between each subtype comparison, where red shows a positive foldchange and blue a negative one. Significance is shown inside each cell, where * = adj *p* < 0.05, ** = adj *p* < 0.01, *** = adj *p* < 0.001 and n.s. = adj *p* > 0.05. (B) Represents miR-340, (C) Depicts miR-877 5p, (D) Shows miR-940 and (E) Represents the differential expression between subtypes of miR-1307-3p.

For miR-340-3p, there were no significant differences in the basal vs. Her2 and Luminal B vs. normal-like subtype; moreover, this miRNA was overexpressed in the Luminal A vs. normal-like and Luminal A vs. Luminal B comparisons (Figure 9B). This pattern was also observed for miR-877-5p, miR-940 and miR-1307, where the comparisons between Luminal A vs. normal-like, Luminal A vs. Luminal B showed an overexpression of the miRNAs, whereas Luminal B vs. normal-like was not significant (Figure 9C–E).

We observed that miR-940 had the largest number of non-significant differences between the subtypes, thus making the expression homogeneous between certain subtypes (Figure 9D). On the other hand, miR-877-5p had the largest number of significant differences, which shows a heterogeneous expression between the subtypes (Figure 9C). Interestingly, the results show that aside from the normal tissue, all five MMRs had a higher expression exclusively in the Luminal A when compared to the other subtypes (Figure 9A–E and Figure S1).

3.8. Validation in Locally Advanced Tumoral Tissues

For this study, we wanted to validate the expression profile of three of the univariate and multivariate significant MMRs in an independent cohort. Therefore, we verified the expression level of miR-340-3p, miR-940, and miR-1307-3p in the paraffin-embedded breast tumoral tissue of locally advanced samples. Samples were collected from 56 patients from the National Cancer Institute of Mexico, composed of 8 Her2, 20 Luminal A, 14 Luminal B, and 13 triple negative. As shown in Figure 10, in the comparison between normal vs. tumoral tissue, miR-940, and miR-1307-3p were significantly overexpressed in tumoral tissues, showing the same trend as our previous bioinformatic analysis. Next, we were interested if the trend of MMR overexpression was constant in the molecular subtypes. In the case of miR-1307-3p, we observed no significant differences between the molecular subtypes, meaning that it was constantly overexpressed (Figure 10A), Moreover, we observed that miR-940 had a higher expression in the triple-negative subtype compared to the Luminal A and B (Figure 10B), whereas miR-340-3p showed no significant differences in tumors or in the intrinsic subtypes (Figure 10C). This result makes it feasible to use miR-1307-3p and miR-940 as biomarkers, independent of the molecular subtype.

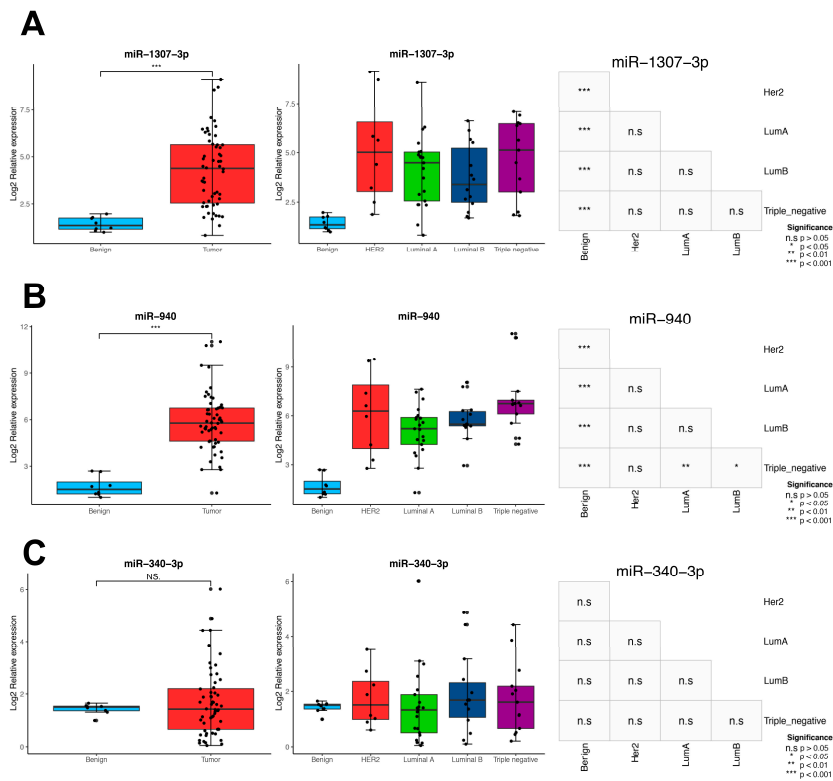


Figure 10. Validation in 56 locally advanced breast cancer samples using real-time qPCR. (A) Expression of miR-1307-3p in normal vs tumoral tissues and between the tumor subtypes. The boxplots represent the log2 relative expression and the heatmap shows the significance of the comparisons between each subtype, where the significance is annotated as * = $p < 0.05$, ** = $p < 0.01$, *** = $p < 0.001$ and n.s = $p > 0.05$. (B) Expression of miR-940 and (C) Expression of miR-340-3p.

4. Discussion

The system's biological perspective of cancer is the result of increased entropy, e.g., an increase in cell disorder, leading to aberrations at the genetic and epigenetic level affecting the transcriptional and proteomic profiles of tumor cells [32]. In this chaotic context, the cancer cells must maintain their cellular functions despite the multiple aberrations and insults they are subjected to, preserving the cell robustness by multiple mechanisms such as the post-transcriptional regulation exerted by miRNAs [33]. Previous evidence has demonstrated that, although tumors could have different somatic mutational profiles, they present similar dysregulated transcriptomes [34], implying the presence of stabilizers that allow the maintenance of the cellular functions reliant on the transcriptome. It has been proposed that these master regulators are miRNAs, molecules capable of maintaining the cell transcriptome independent of the events that led to tumor development and the aberrations that the tumor cell is constantly subjected to. All of this confers robustness to biological processes by reinforcing transcriptional profiles and stabilizing expression levels of aberrant transcripts, mainly in copy numbers [35].

Previous studies have hypothesized the presence of miRNAs acting as master regulators in cancer [10], with further studies reinforcing this hypothesis by showing their involvement in co-transcriptional modules in breast tumors [12]. Later, several theoretical and experimental studies confirmed a hypothesis in ovarian [36], colorectal [37], and breast cancers [13]. However, the main pitfalls for studies involving similar computational pipelines are first that they disregard biological information present miRNA–mRNA validated databases. Secondly, they do not take into account the interaction with validated driver oncogenes/tumor suppressors due to its prominent role in carcinogenesis. To our knowledge, this work represents the first effort to elucidate a set of MMRs constantly upregulated in every clinical stage in breast cancer and its relation to the oncogenes/tumor suppressors they regulate.

In this research, we aimed to find the MMRs consistently upregulated in the carcinogenesis of breast tumors and correlate their participation to the oncogenic transformation. To do so, we integrated miRNAs and mRNA data from the TCGA breast project through adaptation of the Master Regulator Inference algorithm (MARINA), an algorithm that was formerly approved inferring aberrant proteins [20] and transcriptional master regulators. [38].

We observed 61 MMRs present consistently in all stages of breast cancer, which were associated with the regulation of 39% of the differentially expressed genes in the breast cancer transcriptome. As expected, the major pathways regulated by the MMR panel are hallmarks of cancer such as the cell cycle and PI3K–AKT–mTOR pathway and DNA repair, among others, as previously reported in several studies (Figure 4). Although BC is a heterogeneous disease, this result reinforces the concept and participation of MMRs that could be regulating a common “core” of genes shared by every intrinsic subtype of BC and whose main function is maintaining the core mechanisms and pathways that a tumor needs in every step of the tumorigenesis and that differentiates them from normal healthy tissue, such as the hallmarks of resisting cell death, sustaining proliferative signaling, enabling replicative immortality and evading growth suppressors.

One of the current challenges when analyzing miRNAs is their classification as oncomiRNAs or tumor suppressor miRNAs due to their diverse nature [39]. In this work, we addressed this problem by calculating the individual miRNA oncogenic activity, a measure proposed by Svoronos et al. [39]. To solve it, we exclusively took those identified driver genes proved to be causal of the development of cancer. When we focused on the regulation of just this class of genes our results showed that most of the miRNAs were acting as a tumor suppressors, which is consistent with other publications (reviewed in [40]). This outcome could suggest that although the tumoral cell has an uncontrolled proliferation tendency, there are fine-regulating mechanisms—including miRNAs—that are involved in the balance of proliferation (Figure 5). However, proving this in vivo and in vitro validation is still necessary.

Our findings revealed a group of MMRs that were acting predominantly as OncoMMRs involved in the maintenance of tumoral phenotype. In this analysis, we focused on the top four OncoMMRs that had the largest number of targets (miR-106b-5p, miR-106a-5p, miR-671-5p, and miR-590-3p) (Figure 6). The expression levels of this OncoMMRs have been widely associated with increased cell proliferation, migration, invasion, and radioresistance [41–46] showing concordance with our results. Moreover, the top-four OncoMMRs mentioned before were highly enriched in genes involved in invasion and metastasis, suggesting a co-participation in this hallmark.

Regarding genes regulated by MMRs, we discovered a redundant regulation of the tumor suppressors FAT4 and KLF6, among others, whose loss of expression has been associated with a more aggressive phenotype in breast cancer (Table 2) [47–49]. Moreover, we found that the tumor suppressor ARHGEF10 and the oncogene SRSF1 were negatively and positively co-regulated by miR-106b-5p, miR-106a-5p, miR-671-5p, and miR-590-3p, whereas this pattern was observed at the protein level in breast cancer tissues (Figure 7), validating our results. Even though these results were obtained with a limited number of samples, it deserves future analysis to corroborate the correlation between the expression of ARHGEF10 and SRSF2 in a large number of tumor tissues. Recent reports suggest that ARHGEF10 participates as a tumor suppressor involved in the activation of apoptosis during DNA damage [29]. Thus, our outcomes propose that this TSG is subjected to co-regulation by the Onco-MMMRs miR-106b-5p, miR-671-5p, and miR-590-3p. On the other hand, the splicing factor SRSF1 has been observed to be upregulated in breast tumors acting as an oncogene by producing impaired splicing isoforms of the pro-apoptotic genes BCL2 Like 11 (BIM) and the Bridging integrator 1 (BIN1) which are involved in the tumoral phenotype. However, it should be noted that these possible interactions between MMRs and driver genes need to be further confirmed by *in vitro* experiments.

miRNAs have been proposed as molecular biomarkers in numerous investigations [7–9,50], due to their specific expression, stability, and suitability for measurements in peripheral blood. Therefore, we searched for MMRs associated with patient prognosis. We observed that patients with a higher expression of miR-1307-3p, miR-940, and miR-340-3p had a worse overall survival, suggesting their potential use as biomarkers when evaluated on all tumors (Figure 8), whereas miR-1307-3p and miR-940 also showed an over-expression in an independent breast cancer cohort composed of Mexican–Mestizo BC patients only (Figure 9). Of them, only miR-1307-3p has been previously associated with chemoresistance [51] and resistance to cisplatin [52]. Other reports highlighted a downregulated activity of miR-940 in a Chinese cohort [53,54]. Such controversial studies highlight the importance of the participation of miRNAs as possible biomarkers in BC.

In summary, these results suggest the participation of a group of 61 MMRs that could be of high importance for the maintenance of tumor phenotype, as they are present in all the stages of the disease, and regulate a set of proved TSGs. Nevertheless, *in vitro* and *in vivo* experiments are required to prove their participation in BC carcinogenesis and as putative biomarkers.

Supplementary Materials: The following are available online at <http://www.mdpi.com/2073-4409/9/7/1610/s1>, Figure S1: MMR regulatory network, Table S1: Differential expression of miRNAs between stages, Table S2: Regulatory network of all miRNA-gene interactions, Table S3: Filtered miRNA-gene network, Table S4: mRNA DE expression between normal tissue and tumoral tissues, Table S5: Master regulator analysis, Table S6: Top driver genes regulated by the OncoMMRs, Table S7: OncoMMR regulatory network, Table S8: Differentially expressed protein-coding genes between normal vs. tumour samples.

Author Contributions: Conceptualization C.P.-P.; methodology and software A.D.M.-G.; validation, O.M.-C., J.C.-H., F.P.-R.; formal analysis, C.P.-P., A.D.M.-G., A.E.-A.; resources, D.C.d.L., C.L.-C. and N.J.J.-H.; writing—original draft preparation, C.P.P., A.D.M.-G. and A.D.C.-P.; writing—review and editing, C.P.-P.; visualization, R.R.-P.; project administration, A.D.C.-P. Funding C.P.-P. All authors have read and agreed to the published version of the manuscript.

Funding: This research was funded by Instituto Nacional de Cancerología, grant number 2019-015-22.

Acknowledgments: Antonio Daniel Martínez Gutierrez is a doctoral student from Programa de Doctorado en Ciencias Biomedicas, Universidad Nacional Autónoma de México (UNAM) and received fellowship 628988 from CONACYT.

Conflicts of Interest: The authors declare no conflict of interest.

References

1. Bray, F.; Ferlay, J.; Soerjomataram, I.; Siegel, R.L.; Torre, L.A.; Jemal, A. Global cancer statistics 2018: GLOBOCAN estimates of incidence and mortality worldwide for 36 cancers in 185 countries. *CA Cancer J. Clin.* **2018**, *68*, 394–424. [[CrossRef](#)] [[PubMed](#)]
2. DeSantis, C.E.; Ma, J.; Gaudet, M.M.; Newman, L.A.; Miller, K.D.; Goding Sauer, A.; Jemal, A.; Siegel, R.L. Breast cancer statistics, 2019. *CA Cancer J. Clin.* **2019**, *69*, 438–451. [[CrossRef](#)]
3. Conti, C.J. Mechanisms of Tumor Progression. *Compr. Toxicol.* **2010**, 335–347. [[CrossRef](#)]
4. Williams, M.; Cheng, Y.Y.; Blenkinsop, C.; Reid, G. Exploring Mechanisms of MicroRNA Downregulation in Cancer. *MicroRNA* **2017**, *6*, 2–16. [[CrossRef](#)] [[PubMed](#)]
5. Iorio, M.V.; Ferracin, M.; Liu, C.G.; Veronese, A.; Spizzo, R.; Sabbioni, S.; Magri, E.; Pedriali, M.; Fabbri, M.; Campiglio, M.; et al. MicroRNA gene expression deregulation in human breast cancer. *Cancer Res.* **2005**, *65*, 7065–7070. [[CrossRef](#)] [[PubMed](#)]
6. Iorio, M.V.; Casalini, P.; Tagliabue, E.; Ménard, S.; Croce, C.M. MicroRNA profiling as a tool to understand prognosis, therapy response and resistance in breast cancer. *Eur. J. Cancer* **2008**, *44*, 2753–2759. [[CrossRef](#)]
7. Volinia, S.; Galasso, M.; Sana, M.E.; Wise, T.F.; Palatini, J.; Huebner, K.; Croce, C.M. Breast cancer signatures for invasiveness and prognosis defined by deep sequencing of microRNA. *Proc. Natl. Acad. Sci. USA* **2012**, *109*, 3024–3029. [[CrossRef](#)] [[PubMed](#)]
8. Volinia, S.; Croce, C.M. Prognostic microRNA/mRNA signature from the integrated analysis of patients with invasive breast cancer. *Proc. Natl. Acad. Sci. USA* **2013**, *110*, 7413–7417. [[CrossRef](#)]
9. Cascione, L.; Gasparini, P.; Lovat, F.; Carasi, S.; Pulvirenti, A.; Ferro, A.; Alder, H.; He, G.; Vecchione, A.; Croce, C.M.; et al. Integrated MicroRNA and mRNA Signatures Associated with Survival in Triple Negative Breast Cancer. *PLoS ONE* **2013**, *8*, e55910. [[CrossRef](#)] [[PubMed](#)]
10. Voorhoeve, P.M. MicroRNAs: Oncogenes, tumor suppressors or master regulators of cancer heterogeneity? *Biochim. Biophys. Acta* **2010**, *1805*, 72–86. [[CrossRef](#)]
11. Dragomir, M.; Mafra, A.C.P.; Dias, S.M.G.; Vasilescu, C.; Calin, G.A. Using microRNA Networks to Understand Cancer. *Int. J. Mol. Sci.* **2018**, *19*, 1871. [[CrossRef](#)] [[PubMed](#)]
12. Dvinge, H.; Git, A.; Gräf, S.; Salmon-Divon, M.; Curtis, C.; Sottoriva, A.; Zhao, Y.; Hirst, M.; Armitage, J.; Miska, E.A.; et al. The shaping and functional consequences of the microRNA landscape in breast cancer. *Nature* **2013**, *497*, 378–382. [[CrossRef](#)]
13. Cantini, L.; Bertoli, G.; Cava, C.; Dubois, T.; Zinovyev, A.; Caselle, M.; Castiglioni, I.; Barillot, E.; Martignetti, L. Identification of microRNA clusters cooperatively acting on epithelial to mesenchymal transition in triple negative breast cancer. *Nucleic Acids Res.* **2019**, *47*, 2205–2215. [[CrossRef](#)]
14. Lachmann, A.; Giorgi, F.M.; Lopez, G.; Califano, A. ARACNe-AP: Gene network reverse engineering through adaptive partitioning inference of mutual information. *Bioinformatics* **2016**, *32*, 2233–2235. [[CrossRef](#)]
15. Koboldt, D.C.; Fulton, R.S.; McLellan, M.D.; Schmidt, H.; Kalicki-Veizer, J.; McMichael, J.F.; Fulton, L.L.; Dooling, D.J.; Ding, L.; Mardis, E.R.; et al. Comprehensive molecular portraits of human breast tumours. *Nature* **2012**, *490*, 61–70. [[CrossRef](#)]
16. Colaprico, A.; Silva, T.C.; Olsen, C.; Garofano, L.; Cava, C.; Garolini, D.; Sabetot, T.S.; Malta, T.M.; Pagnotta, S.M.; Castiglioni, I.; et al. TCGAbiolinks: An R/Bioconductor package for integrative analysis of TCGA data. *Nucleic Acids Res.* **2016**, *44*, e71. [[CrossRef](#)]
17. Love, M.I.; Huber, W.; Anders, S. Moderated estimation of fold change and dispersion for RNA-seq data with DESeq2. *Genome Biol.* **2014**, *15*, 550. [[CrossRef](#)]
18. Ru, Y.; Kechris, K.J.; Tabakoff, B.; Hoffman, P.; Radcliffe, R.A.; Bowler, R.; Mahaffey, S.; Rossi, S.; Calin, G.A.; Bemis, L.; et al. The multiMiR R package and database: Integration of microRNA-target interactions along with their disease and drug associations. *Nucleic Acids Res.* **2014**, *42*, e133. [[CrossRef](#)] [[PubMed](#)]
19. Lefebvre, C.; Rajbhandari, P.; Alvarez, M.J.; Bandaru, P.; Lim, W.K.; Sato, M.; Wang, K.; Sumazin, P.; Kustagi, M.; Bisikirska, B.C.; et al. A human B-cell interactome identifies MYB and FOXM1 as master regulators of proliferation in germinal centers. *Mol. Syst. Biol.* **2010**, *6*, 377. [[CrossRef](#)]
20. Alvarez, M.J.; Shen, Y.; Giorgi, F.M.; Lachmann, A.; Ding, B.B.; Ye, B.H.; Califano, A. Functional characterization of somatic mutations in cancer using network-based inference of protein activity. *Nat. Genet.* **2016**, *48*, 838–847. [[CrossRef](#)]

21. Shannon, P.; Markiel, A.; Ozier, O.; Baliga, N.S.; Wang, J.T.; Ramage, D.; Amin, N.; Schwikowski, B.; Ideker, T. Cytoscape: A software Environment for integrated models of biomolecular interaction networks. *Genome Res.* **2003**, *13*, 2498–2504. [[CrossRef](#)]
22. Tate, J.G.; Bamford, S.; Jubb, H.C.; Sondka, Z.; Beare, D.M.; Bindal, N.; Boutselakis, H.; Cole, C.G.; Creatore, C.; Dawson, E.; et al. COSMIC: The Catalogue Of Somatic Mutations In Cancer. *Nucleic Acids Res.* **2019**, *47*, D941–D947. [[CrossRef](#)] [[PubMed](#)]
23. Liao, Y.; Wang, J.; Jaehnig, E.J.; Shi, Z.; Zhang, B. WebGestalt 2019: Gene set analysis toolkit with revamped UIs and APIs. *Nucleic Acids Res.* **2019**, *47*, W199–W205. [[CrossRef](#)] [[PubMed](#)]
24. Gendoo, D.M.A.; Ratanasirigulchai, N.; Schröder, M.S.; Paré, L.; Parker, J.S.; Prat, A.; Haibe-Kains, B. Genefu: An R/Bioconductor package for computation of gene expression-based signatures in breast cancer. *Bioinformatics* **2016**, *32*, 1097–1099. [[CrossRef](#)] [[PubMed](#)]
25. Uhlen, M.; Fagerberg, L.; Hallstrom, B.M.; Lindskog, C.; Oksvold, P.; Mardinoglu, A.; Sivertsson, A.; Kampf, C.; Sjostedt, E.; Asplund, A.; et al. Tissue-based map of the human proteome. *Science* **2015**, *347*, 1260419. [[CrossRef](#)]
26. Ørom, U.A.; Nielsen, F.C.; Lund, A.H. MicroRNA-10a binds the 5'UTR of ribosomal protein mRNAs and enhances their translation. *Mol. Cell* **2008**, *30*, 460–471. [[CrossRef](#)]
27. Vasudevan, S. Posttranscriptional Upregulation by MicroRNAs. *Wiley Interdiscip. Rev. RNA* **2012**, *3*, 311–330. [[CrossRef](#)]
28. Oliveira, A.C.; Bovolenta, L.A.; Nachtigall, P.G.; Herkenhoff, M.E.; Lemke, N.; Pinhal, D. Combining Results from Distinct MicroRNA Target Prediction Tools Enhances the Performance of Analyses. *Front. Genet.* **2017**, *8*, 59. [[CrossRef](#)]
29. Cooke, S.L.; Pole, J.C.M.; Chin, S.F.; Ellis, I.O.; Caldas, C.; Edwards, P.A.W. High-resolution array CGH clarifies events occurring on 8p in carcinogenesis. *BMC Cancer* **2008**, *8*, 288. [[CrossRef](#)]
30. Anczuków, O.; Rosenberg, A.Z.; Akerman, M.; Das, S.; Zhan, L.; Karni, R.; Muthuswamy, S.K.; Krainer, A.R. The splicing factor SRSF1 regulates apoptosis and proliferation to promote mammary epithelial cell transformation. *Nat. Struct. Mol. Biol.* **2012**, *19*, 220–228. [[CrossRef](#)]
31. Eroles, P.; Bosch, A.; Alejandro Pérez-Fidalgo, J.; Lluch, A. Molecular biology in breast cancer: Intrinsic subtypes and signaling pathways. *Cancer Treat. Rev.* **2012**, *38*, 698–707. [[CrossRef](#)] [[PubMed](#)]
32. Tarabichi, M.; Antoniou, A.; Saiselet, M.; Pita, J.M.; Andry, G.; Dumont, J.E.; Detours, V.; Maenhaut, C. Systems biology of cancer: Entropy, disorder, and selection-driven evolution to independence, invasion and “swarm intelligence”. *Cancer Metastasis Rev.* **2013**, *32*, 403–421. [[CrossRef](#)] [[PubMed](#)]
33. Ebert, M.S.; Sharp, P.A. Roles for microRNAs in conferring robustness to biological processes. *Cell* **2012**, *149*, 515–524. [[CrossRef](#)] [[PubMed](#)]
34. Chen, J.C.; Alvarez, M.J.; Talos, F.; Dhruv, H.; Rieckhof, G.E.; Iyer, A.; Diefes, K.L.; Aldape, K.; Berens, M.; Shen, M.M.; et al. Identification of causal genetic drivers of human disease through systems-level analysis of regulatory networks. *Cell* **2014**, *159*, 402–414. [[CrossRef](#)] [[PubMed](#)]
35. Califano, A.; Alvarez, M.J. The recurrent architecture of tumour initiation, progression and drug sensitivity. *Nat. Rev. Cancer* **2017**, *17*, 116–130. [[CrossRef](#)] [[PubMed](#)]
36. Yang, D.; Sun, Y.; Hu, L.; Zheng, H.; Ji, P.; Pecot, C.V.; Zhao, Y.; Reynolds, S.; Cheng, H.; Rupaimoole, R.; et al. Integrated Analyses Identify a Master MicroRNA Regulatory Network for the Mesenchymal Subtype in Serous Ovarian Cancer. *Cancer Cell* **2013**, *23*, 186–199. [[CrossRef](#)] [[PubMed](#)]
37. Cantini, L.; Isella, C.; Petti, C.; Picco, G.; Chiola, S.; Ficarra, E.; Caselle, M.; Medico, E. MicroRNA–mRNA interactions underlying colorectal cancer molecular subtypes. *Nat. Commun.* **2015**, *6*, 1–12. [[CrossRef](#)]
38. Tovar, H.; García-Herrera, R.; Espinal-Enríquez, J. Transcriptional master regulator analysis in breast cancer genetic networks. *Comput. Biol. Chem.* **2015**, *59*, 67–77. [[CrossRef](#)]
39. Svoronos, A.A.; Engelman, D.M.; Slack, F.J. OncomiR or Tumor Suppressor? The Duplicity of MicroRNAs in Cancer. *Cancer Res.* **2016**, *76*, 3666–3670. [[CrossRef](#)]
40. Oliveto, S.; Mancino, M.; Manfrini, N.; Biffo, S. Role of microRNAs in translation regulation and cancer. *World J. Biol. Chem.* **2017**, *8*, 45–56. [[CrossRef](#)]
41. Lee, J.; Kim, H.E.; Song, Y.-S.; Cho, E.Y.; Lee, A. miR-106b-5p and miR-17-5p could predict recurrence and progression in breast ductal carcinoma in situ based on the transforming growth factor-beta pathway. *Breast Cancer Res. Treat.* **2019**. [[CrossRef](#)] [[PubMed](#)]
42. Xiang, W.; He, J.; Huang, C.; Chen, L.; Tao, D.; Wu, X.; Wang, M.; Luo, G.; Xiao, X.; Zeng, F.; et al. miR-106b-5p targets tumor suppressor gene SETD2 to inactivate its function in clear cell renal cell carcinoma. *Oncotarget* **2015**, *6*, 4066–4079. [[CrossRef](#)] [[PubMed](#)]

43. Gu, H.; Gu, S.; Zhang, X.; Zhang, S.; Zhang, D.; Lin, J.; Hasengbayi, S.; Han, W. miR-106b-5p promotes aggressive progression of hepatocellular carcinoma via targeting RUNX3. *Cancer Med.* **2019**. [[CrossRef](#)]
44. You, F.; Luan, H.; Sun, D.; Cui, T.; Ding, P.; Tang, H.; Sun, D. MiRNA-106a Promotes Breast Cancer Cell Proliferation, Clonogenicity, Migration, and Invasion Through Inhibiting Apoptosis and Chemosensitivity. *DNA Cell Biol.* **2019**, *38*, 198–207. [[CrossRef](#)]
45. Salem, M.; Shan, Y.; Bernaudo, S.; Peng, C. miR-590-3p Targets Cyclin G2 and FOXO3 to Promote Ovarian Cancer Cell Proliferation, Invasion, and Spheroid Formation. *Int. J. Mol. Sci.* **2019**, *20*, 1810. [[CrossRef](#)] [[PubMed](#)]
46. Sun, Z.-Q.; Shi, K.; Zhou, Q.-B.; Zeng, X.-Y.; Liu, J.; Yang, S.-X.; Wang, Q.-S.; Li, Z.; Wang, G.-X.; Song, J.-M.; et al. MiR-590-3p promotes proliferation and metastasis of colorectal cancer via Hippo pathway. *Oncotarget* **2017**, *8*, 58061–58071. [[CrossRef](#)] [[PubMed](#)]
47. Hou, L.; Chen, M.; Zhao, X.; Li, J.; Deng, S.; Hu, J.; Yang, H.; Jiang, J. FAT4 functions as a tumor suppressor in triple-negative breast cancer. *Tumor Biol.* **2016**, *37*, 16337–16343. [[CrossRef](#)] [[PubMed](#)]
48. Ozdemir, F.; Koksall, M.; Ozmen, V.; Aydin, I.; Buyru, N. Mutations and Krüppel-like factor 6 (KLF6) expression levels in breast cancer. *Tumor Biol.* **2014**, *35*, 5219–5225. [[CrossRef](#)]
49. Gao, Y.; Li, H.; Ma, X.; Fan, Y.; Ni, D.; Zhang, Y.; Huang, Q.; Liu, K.; Li, X.; Wang, L.; et al. KLF6 suppresses metastasis of clear cell renal cell carcinoma via transcriptional repression of E2F1. *Cancer Res.* **2017**, *77*, 330–342. [[CrossRef](#)]
50. Gasparini, P.; Cascione, L.; Fassan, M.; Lovat, F.; Guler, G.; Balci, S.; Irkkan, C.; Morrison, C.; Croce, C.M.; Shapiro, C.L.; et al. microRNA expression profiling identifies a four microRNA signature as a novel diagnostic and prognostic biomarker in triple negative breast cancers. *Oncotarget* **2014**, *5*, 1174–1184. [[CrossRef](#)]
51. Chen, W.-T.; Yang, Y.-J.; Zhang, Z.-D.; An, Q.; Li, N.; Liu, W.; Yang, B. MiR-1307 promotes ovarian cancer cell chemoresistance by targeting the ING5 expression. *J. Ovar. Res.* **2017**, *10*, 1. [[CrossRef](#)]
52. Wang, X.; Zhu, J. Mir-1307 regulates cisplatin resistance by targeting Mdm4 in breast cancer expressing wild type P53. *Thorac. Cancer* **2018**, *9*, 676–683. [[CrossRef](#)] [[PubMed](#)]
53. Liu, W.; Xu, Y.; Guan, H.; Meng, H. Clinical potential of miR-940 as a diagnostic and prognostic biomarker in breast cancer patients. *Cancer Biomark.* **2018**, *22*, 487–493. [[CrossRef](#)] [[PubMed](#)]
54. Hou, L.; Chen, M.; Yang, H.; Xing, T.; Li, J.; Li, G.; Zhang, L.; Deng, S.; Hu, J.; Zhao, X.; et al. MiR-940 Inhibited Cell Growth and Migration in Triple-Negative Breast Cancer. *Med. Sci. Monit.* **2016**, *22*, 3666–3672. [[CrossRef](#)] [[PubMed](#)]



8.2. MARTINEZ-GUTIERREZ, ANTONIO-D., ET AL. MIRNA PROFILE OBTAINED BY NEXT-GENERATION SEQUENCING IN METASTATIC BREAST CANCER PATIENTS IS ABLE TO PREDICT THE RESPONSE TO SYSTEMIC TREATMENTS. INTERNATIONAL JOURNAL OF MOLECULAR MEDICINE. 2019

8.2. Martinez-Gutierrez, Antonio-D., et al. miRNA profile obtained by next-generation sequencing in metastatic breast cancer patients is able to predict the response to systemic treatments. International Journal of Molecular Medicine. 2019

miRNA profile obtained by next-generation sequencing in metastatic breast cancer patients is able to predict the response to systemic treatments

ANTONIO DANIEL MARTINEZ-GUTIERREZ^{1*}, OLIVER MILLAN CATALAN^{1*}, RAFAEL VÁZQUEZ-ROMO², FANY IRIS PORRAS REYES³, ALBERTO ALVARADO-MIRANDA⁴, FERNANDO LARA MEDINA⁴, JUAN E. BARGALLO-ROCHA⁴, LUZ TONATZIN OROZCO MORENO¹, DAVID CANTÚ DE LEÓN⁵, LUIS ALONSO HERRERA⁵, CÉSAR LÓPEZ-CAMARILLO⁶, CARLOS PÉREZ-PLASENCIA^{1,7} and ALMA D. CAMPOS-PARRA¹

¹Laboratorio de Genómica, ²Departamento de Cirugía de Tumores Mamaros, ³Servicio de Anatomía Patológica, and ⁴Unidad de Cáncer de Mama, Instituto Nacional de Cancerología (INCan); ⁵Unidad de Investigación Biomédica en Cáncer, Instituto Nacional de Cancerología (INCan)-Instituto de Investigaciones Biomédicas, UNAM, Mexico City 14080; ⁶Posgrado en Ciencias Genómicas, Universidad Autónoma de la Ciudad de México, CDMX, Mexico City 03100; ⁷Unidad de Biomedicina, FES-IZTACALA, Universidad Nacional Autónoma de México (UNAM), Tlalnepantla 54090, Mexico

Received March 21, 2019; Accepted July 3, 2019

DOI: 10.3892/ijmm.2019.4292

Abstract. Metastatic breast cancer (MBC) is a challenge for oncologists, and public efforts should focus on identifying additional molecular markers and therapeutic management to improve clinical outcomes. Among all diagnosed cases of breast cancer (BC; approximately 10%) involve metastatic disease; notably, approximately 40% of patients with early-stage BC develop metastasis within 5 years. The management of MBC consists of systemic therapy. Despite different treatment options, the 5-year survival rate is <20%, which may be due to a lack of response with *de novo* or acquired resistance. MicroRNAs (miRNAs or miRs) are promising biomarkers as they are readily detectable and have a broad spectrum and potential clinical applications. The aim of this study was to identify a miRNA profile for distinguishing patients with MBC who respond to systemic treatment. Patients with MBC were treated according to the National Comprehensive Cancer Network guidelines. We performed miRNA-Seq on 9 primary tumors using the Thermo Fisher Scientific Ion S5 system. To obtain global miRNA profiles, we

carried out differentially expressed gene elimination strategy (DEGES) analysis between the responsive and non-responsive patients. The results identified a profile of 12 miRNAs associated with the response to systemic treatment. The data were validated in an independent cohort (TCGA database). Based on the results, the upregulation of miR-342-3p and miR-187-3p was associated with the response to systemic treatment, and with an increased progression-free survival (PFS) and overall survival (OS); by contrast, the downregulation of miR-301a-3p was associated with a higher PFS and OS. On the whole, the findings of this study indicate that these miRNAs may serve as biomarkers for the response to systemic treatment or the prognosis of patients with MBC. However, these data should be validated experimentally in other robust cohorts and using different specimens before implementing these miRNAs as biomarkers in clinical practice to benefit this group of patients.

Introduction

Breast cancer (BC) is the most prevalent type of cancer among women worldwide, with an estimated 1.7 million newly diagnosed cases in 2015. Although metastatic BC (MBC) is present in only 10% of all diagnosed patients, approximately 30-40% of early-stage BC cases will develop metastasis within 5 years (1,2). The management of MBC is not curative, and treatment consists of systemic therapy involving chemotherapy, hormonal agents and targeted therapy (3). Despite various treatment options, the 5-year survival ratio remains <20% [SEER Stat Fact Sheets: Breast Cancer. National Cancer Institute (4)]. This poor prognosis may be due to the fact that more than one-third of patients with MBC do not respond to chemotherapy (anthracyclines and taxanes), with a response rate to first-line treatment of only 20% [95% confidence index (CI) 11-28%]. Therefore, the progression of the disease

Correspondence to: Dr Carlos Pérez-Plasencia or Dr Alma D. Campos-Parra, Laboratorio de Genómica, Instituto Nacional de Cancerología (INCan), 22 Av. San Fernando, Col. Sección XVI, Tlalpan, Mexico City 14080, Mexico
E-mail: car.pplas@gmail.com
E-mail: adcamposparra@gmail.com

*Contributed equally

Key words: microRNAs, metastatic breast cancer, next-generation sequencing

occurs in <1 year. *De novo* or acquired resistance is the main reason for tumor relapse, contributing to a poor prognosis, a lack of therapeutic response and a fatal clinical outcome (5,6).

MicroRNAs (miRNAs or miRs) are small non-coding RNAs ~22 nt in length that negatively regulate gene expression through base pairing at 3' or 5'-untranslated regions of messenger RNAs (mRNAs) (7). miRNAs are readily detected in formalin-fixed paraffin-embedded sections and in body fluids (e.g., blood, plasma, serum and saliva), and accordingly, these molecules have the potential to be used in clinical practice (8,9). A number of miRNAs play substantial roles in drug sensitivity/resistance in BC, and yet the majority of them have only been explored in early-stage disease (10).

Although MBC is not curable, the extent of survival with the quality of life is an important aspect for patients. In this regard, the aim of this study was to identify, through miRNA sequencing, a miRNA profile for patients with MBC who respond to systemic treatment. The results identified 12 miRNAs involved in response to systemic treatment (hormonotherapy and chemotherapy). In particular, the upregulation of miR-342-3p and miR-187-3p was associated with the response to systemic treatment, and with an improved progression-free survival (PFS) and overall survival (OS). Conversely, the downregulation of miR-301a-3p was associated with an increased PFS and OS. A further gene set enrichment analysis of putative targets of the identified miRNAs revealed their involvement in cancer, cytokine-cytokine receptor interaction, glioma, endocytosis and the mitogen-activated protein kinase (MAPK) signaling pathways. On the whole, we identified miRNAs associated with the response to systemic treatment, PFS and OS in patients with MBC. The results of this study confirm the importance of miRNAs as potential biomarkers of the response to treatment in patients with metastatic disease.

Patients and methods

Patient selection and treatment regimen. This prospective cohort study was approved by the Central Ethics and Scientific Committee at the National Cancer Institute in Mexico City (approval no. CEI/1001/16; 016/010/IBI). Informed consent was obtained for each patient enrolled. A total of 9 patients were enrolled diagnosed with MBC confirmed by positron emission tomography (PET) and computed tomography (CT) scans. All patients were treated according to the National Comprehensive Cancer Network (NCCN) guidelines (11). As first-line treatment, 44.4% of the patients received hormonal therapy and 55.5% platinum-based chemotherapy.

Outcome measurement. As mentioned above, all patients underwent PET or CT and were evaluated by The Response Evaluation Criteria in Solid Tumors (RECIST) at baseline and at 6 months (12). PFS was defined as the time from the commencement of treatment until disease progression or the last visit. OS was defined as the time from diagnosis until death or the last visit.

Preparation of tissue samples. A total of 9 MBC biopsies were collected from February, 2018 to November, 2018 at the time of diagnosis prior to any therapeutic procedures. Total RNA

was extracted from the tumor samples using TRIzol reagent (cat. no. 15596-026, Invitrogen; Thermo Fisher Scientific) and subsequently purified with the miRNeasy Mini kit (cat. no. 217004; Qiagen) according to the manufacturer's instructions. The RNA concentration was determined by Qubit 2.0 fluorometry using the Qubit RNA HS Assay kit (Thermo Fisher Scientific). After biopsies were obtained, pathological confirmation of at least 80% tumor cells was obtained. To construct a small RNA library, small RNAs ranging from 10 to 40 nt were assessed for quality and quantity using an Agilent 2100 bioanalyzer (Agilent Technologies).

Library preparation. Small RNA libraries were prepared using Ion Total RNA-Seq V2 (Life Technologies; Thermo Fisher Scientific; cat. nos. 4475936 and 44797789) according to the manufacturer's instructions. Following adapter ligation, first-strand cDNA synthesis and amplification were performed as follows: 94° for 2 min and 14 cycles at 94° 30 sec, 62° 30 sec and 68° 30 sec. Briefly, adapters were ligated to small RNAs (25 ng/sample), and libraries from 9 samples were pooled together in equimolar ratios (100 pM) for template preparation and chip loading using the Ion Chef System. The libraries were sequenced with Ion S5 using S530 chips, as recommended by the manufacturer (Life Technologies; Thermo Fisher Scientific; cat. nos. 4475936 and 44797789).

Data analysis. Raw reads were processed using the small RNA sequencing plugin provided in the Ion Torrent Suite (Thermo Fisher Scientific), and options were set to only retain reads between 17 and 35 nt. The trimmed reads were analyzed with Chimera using the default settings and aligned using the latest version of miRBase (13). The resulting miRNA counts were filtered, and only miRNAs with at least 1 count in every sample were retained. Normalization and differential expression analysis were carried out with the Bioconductor package DESeq2 (14), and miRNAs with a P-value <0.05 were selected for further analysis.

Identification of putative miRNA targets. To identify possible targets of each miRNA, we first downloaded the TCGA Breast transcriptome dataset using Bioconductor package TCGA biolinks (15). Subsequently, we assessed differentially expressed (DE) genes between normal and stage IV primary tumor tissue with DESeq2, only selecting those mRNAs with P-adj <0.01 and a log₂ Fold change ≤ -1. As this would mean that the expression is at least 0.5-fold lower in the tumor samples, in this manner, we ensured that the putative mRNA targets of the miRNAs were downregulated in the tumor samples. Subsequently, we used these downregulated mRNAs with the Bioconductor package miRNetap to predict targets in 5 databases (PicTar (pictar.mdc-berlin.de), TargetScan (targetscan.org), miRanda (microrna.org), DIANA (diana.imis.athena-innovation.gr) and miRDB (mirdb.org); we only considered predicted targets identified by at least 2 databases. Pearson's correlation coefficients were calculated between the predicted targets and miRNAs using the TCGA data.

Statistical analysis. For descriptive purposes, continuous variables are summarized as arithmetic means, medians and standard deviations. The Fisher-Pitman permutation test from

the coin R package was employed using the normalized rlog counts ($P < 0.05$). The Mann-Whitney U-test (non-parametric test) was used for inferential comparisons. Statistically significant and borderline significant variables ($P < 0.1$) were included in multivariate logistic regression analysis. Survival results were analyzed using the Kaplan-Meier technique, and the log-rank test was employed for comparisons between subgroups. All variables were dichotomized for analyzing survival curves. Hazard ratios (HRs) were calculated along with their corresponding 95% CIs as a measure of association. Statistical significance was defined as $P < 0.05$ using Student's t-test. Statistical analysis was conducted using R/Bioconductor.

Results

Clinical characteristics of patients with MBC and response rates to systemic treatment. Samples from 9 patients were sequenced. All patients were females and had stage IV disease. The mean of age of the patients was 53 years. All patients had an Eastern Cooperative Oncology Group (ECOG) performance status of 0 or 1. The most frequent metastasis sites were the cervical ganglia, mediastinum and lungs. The most frequent molecular subtype was luminal A. Four patients received hormone therapy (letrozol) and five patients received chemotherapy (docetaxel, paclitaxel, paclitaxel/trastuzumab or cyclophosphamide/adriamycin). According to RECIST, the overall response rate (ORR) was 44.44% (22.2% complete response and 22.2% partial response), stable disease was observed in 44.4%, and the disease progressed in 11.1% of patients (Table I).

Identification of DE miRNAs in patients with MBC. To reveal putative miRNA biomarkers for the response to systemic treatment, we first assessed DE miRNAs between the responders and non-responder's groups. In total 12 miRNAs were found with P -values < 0.05 . It has been estimated that a sample size of > 60 is needed to achieve an FDR of 10% (16); however, due to the nature of patients with MBC it is unlikely, that this number of samples will be obtained. Due to the small sample size in this study, the lowest FDR that was obtained was 0.25; thus, we opted for a P -value filtering and validation of our results in an independent and larger cohort to reduce the disadvantages of using a P -value.

This analysis revealed a panel of 12 miRNAs that separated the patients in these 2 groups. This panel included miRNAs with a P -value < 0.05 , among which 8 were upregulated (miR-7-5p, miR-141-3p, miR-187-3p, miR-200b-3p, miR-200c-3p, miR-301a-3p, miR-342-3p and miR-3182) and 4 were downregulated (miR-361-3p, miR-1273a, miR-4459 and miR-4485-3p) in the responders vs. the non-responders (Fig. 1). We then performed unsupervised hierarchical clustering of the 12 DE miRNAs using the Euclidian distance. As shown in Fig. 2, the tumors were clustered according to the respective response to treatment. It is important to mention that, in order to obtain the DE miRNAs, we employed DESeq2, an algorithm that assumes a negative binomial distribution (17,18), which is one of the best methods with which to analyze RNA-seq data due to its stringency, good control of false-positives, and improved sensitivity and specificity. Moreover, in addition

Table I. Clinicopathologic characteristics of the patients.

Clinical parameters	Patients n=9 (100%)
Sex	
Female	9 (100)
Age	
>50	6 (66.6)
≤50	3 (33.3)
ECOG status	
0-2	9 (100)
3-4	0 (0)
Histopathology	
Infiltrating ductal carcinoma	5 (55.5)
Classic lobular carcinoma	1 (11.1)
Non-specific infiltrative	2 (22.2)
Canalicular carcinoma	1 (11.1)
Molecular subtype	
Luminal A	5 (55.5)
Luminal B	2 (22.2)
Triple negative	2 (22.2)
Treatment	
Hormonotherapy	4 (44.4)
Chemotherapy	5 (55.5)
Metastatic	
Liver	2 (22.2)
Lung	3 (33.3)
Bones	2 (22.2)
Cervical Ganglia	5 (55.5)
Axillary Ganglia	1 (11.1)
Mediastinum	4 (44.4)
Response to systemic treatments	
Complete response	2 (22.2)
Partial response	2 (22.2)
Stable disease	4 (44.4)
Progression	1 (11.1)

to this, we employed the Fisher-Pitman permutation test on the 12 miRNAs. The results revealed that 6 miRNAs exhibited significant differences between the 2 groups ($P < 0.05$) (miR-4485-3p, miR-1273a, miR-342-3p, miR-200c-3p, miR-200b-3p and miR-187-3p) and 1 miRNA was close to being significant (miR-301a-3p, $P = 0.055$) (Table SI).

miRNAs with clinical significance. To assess the clinical significance of the miRNA panel, we applied the non-parametric Mann-Whitney U test using clinical variables (Table II). The results revealed significant differences in the expression levels of some miRNAs according to the site of metastasis. For example, miR-4459 was overexpressed in patients with lung metastasis ($P = 0.02$); this same miRNA was overexpressed in those with mediastinum metastasis ($P = 0.03$). Patients without lung metastasis exhibited an upregulation of miR-342-3p and miR-200b-3p ($P = 0.02$ and $P = 0.04$, respectively), and miR-4485-3p, miR-1273a and miR-361-3p were overexpressed

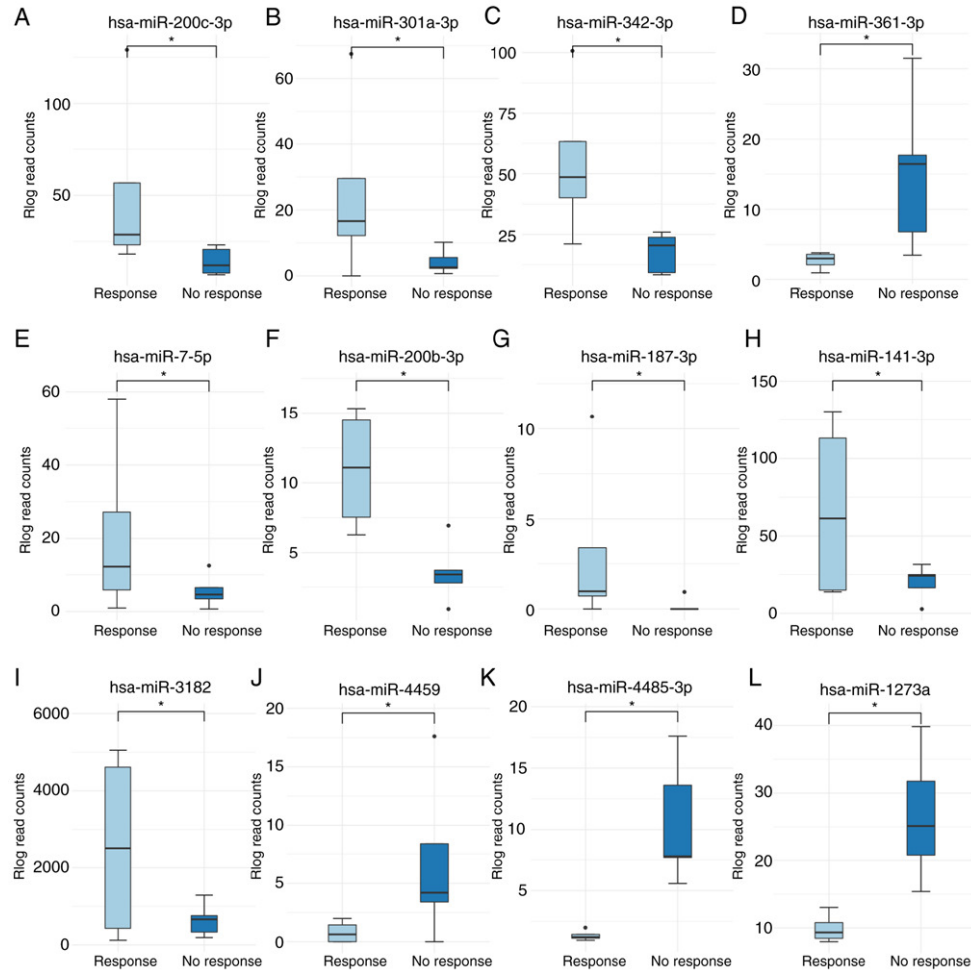


Figure 1. (A-L) MicroRNAs associated with the response to systemic treatment in BC. Each bar plot shows the number of reads for each miRNA according to response (R) vs. no response (NR) to systemic treatment. * $P < 0.05$. BC, breast cancer.

in those without cervical ganglia metastasis ($P=0.03$, $P=0.01$ and $P=0.01$, respectively). Notably, we found no significant differences in the expression levels of the 12 miRNAs in patients with liver or bone metastasis (Table II).

Validation of the panel of miRNAs in TCGA in patients with stage IV disease. We further evaluated this miRNA panel in an independent cohort using TCGA. All the clinical data of the patients with MBC included in the database were obtained using the clinical variable 'Person neoplasm cancer status', and only those patients with complete information of their clinical outcome were selected (follow-up median, 2.6 years). Through this analysis, we identified 17 patients with MBC from the 1,060 patients with BC included in this cohort. A patient was excluded due to the unavailability of clinical response data.

We then classified these patients into 2 groups according to their response to systemic treatment: Response vs. no response (in terms of TCGA: Tumor-free and with tumor, respectively). Only 2 patients of 14 presented a response to systemic treatment (Table SII).

The validation of the miRNA panel obtained from our cohort in these 2 TCGA groups (responders vs. no responders), revealed that TCGA patients expressed 8 of the 12 miRNAs (miR-200c-3p, miR-301a-3p, miR-342-3p, miR-361-3p, miR-7-5p, miR-200b-3p, miR-187-3p and miR-141-3p) (Fig. 3). A trend of the upregulation of miR-200c-3p, miR-342-3p, miR-200b-3p, miR-187-3p and miR-141-3p was evident in the response group (Fig. 3A, C, F and G), which was in accordance with the results from our cohort (Fig. 1A, C, F and G).

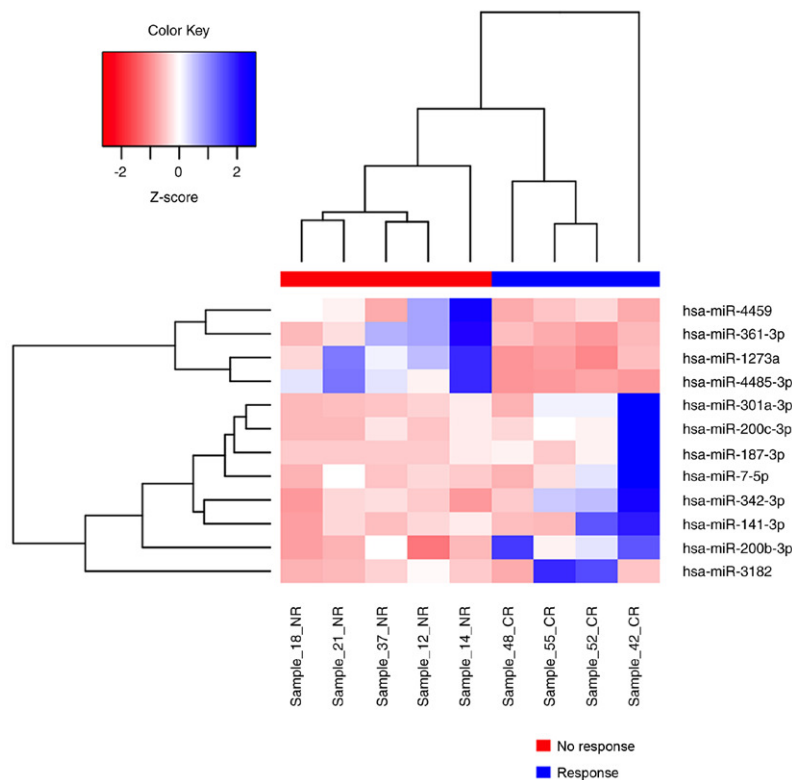


Figure 2. Hierarchical clustering of miRNA expression. The BC samples were classified into 2 different groups (response vs. no response to systemic treatments) based on expression levels. Each column represents a patient with MBC, and each row represents a single miRNA. The expression of miRNAs is represented in blue (upregulated), red (downregulated) and white (no significant change or absence of data). BC, breast cancer; MBC, metastatic breast cancer.

miRNAs associated with the survival of patients in TCGA with stage IV disease. Using the available TCGA clinical data, we determined the impact of the 8 validated miRNAs on survival by associating miRNA expression (high or low) with PFS and OS (Figs. 4 and 5). Kaplan-Meier analysis revealed that patients with a better PFS had a high expression of miR-342-3p and miR-187-3p (median survival: miR-342-3p, 1.79 vs. 2.58 years, $P=0.12$; miR-187-3p, 2.17 vs. 2.47; $P=0.11$; Fig. 4C and G), but a low expression of miR-301a-3p (2.63 vs. 0.9; $P=0.13$; Fig. 4B). Moreover, this trend was also observed for OS: A high expression of miR-342-3p and miR-187-3p was found in the patients with a better OS (miR-342-3p, 2.26 vs. 3.16 years, $P=0.04$; miR-187-3p, 3.74 vs. 2.22, $P=0.047$; Fig. 5C and G), with a low expression of miR-301a-3p (3.45 vs. 1.68, $P=0.03$; Fig. 5B). According to univariate analysis of these 3 miRNAs, only miR-342-3p was associated with OS (HR, 0.25; 95% CI, 0.006-1.2; $P>0.056$), although borderline in multivariate regression Cox analyses (HR, 0.08; 95% CI, 0.006-1.2; $P=0.068$). According to univariate analysis, miR-187-3p was associated with PFS (HR, 0.25; 95% CI, 0.062-0.98; $P>0.046$) and none miRNA was associated with PFS in multivariate regression Cox analyses (Tables III and SIII).

Identification of mRNA targets of miRNAs and their participation in pathways of cancer. We focused in the identification of the mRNA targets for miR-342-3p, miR-187-3p and miR-301a-3p as we observed that their expression was associated with the response to systemic treatment and with PFS, both in our data and in the TCGA data. Patients with a higher expression of miR-342-3p and miR-187-3p exhibited a trend for a longer PFS, although none of the survival curves were statistically significant due to the small size of the cohort (Fig. 4C and G). To achieve this goal, we analyzed the TCGA breast transcriptome dataset, as described in the Patients and methods section. We reasoned that, since these 3 miRNAs were overexpressed in patients with response to systemic treatment, they may thus act as tumor-suppressor miRNAs, probably inhibiting key oncogenes. Thus, to obtain their putative targets, we only focused on the downregulated mRNAs.

We found 8,116 downregulated mRNAs in the tumor samples. Using 5 databases (PicTar, TargetScan, miRanda, DIANA and miRDB), we identified 416 mRNAs predicted to be potential targets of the 3 miRNAs (Table SIV). To achieve further insight into the biological functions of these

Table II. Clinicopathologic characteristics related to miRNA expression in patients with metastatic breast cancer.

Variables	Patients n=9	miR-4485-3p Mean ± SD	miR-1273a Mean ± SD	miR-361-3p Mean ± SD	miR-342-3p Mean ± SD	miR-200c-3p Mean ± SD	miR-301a-3p Mean ± SD
Age							
≤53	6	7.94±6.51	22.28±12.20	10.67±11.77	35.55±35.39	34.025±47.18	17.93±25.33
>53	3	3.33±3.85	13.13±6.63	7.59±7.68	31.14±13.43	23.85±7.68	6.29±8.76
P-value		0.38	0.39	0.9	0.71	0.71	0.54
Smoking							
Positive	3	10.32±6.39	28.57±9.99	21.86±8.35	18.56±8.50	18.67±5.81	6.12±3.82
Negative	6	4.44±5.16	14.46±8.92	3.53±1.91	41.84±32.97	36.61±46.36	17.28±25.78
P-value		0.16	0.09	0.02	0.38	0.9	1
Treatment							
Hormone therapy	4	7.56±5.077	20.23±8.33	7.57±6.105	39.70±41.39	41.19±58.93	18.26±32.83
Chemotherapy	5	5.47±7.02	18.31±13.95	6.105±11.30	29.58±18.01	22.18±7.65	9.79±7.18
P-value		0.55	0.55	1	0.9	0.55	0.73
HER2							
Positive	2	9.79±11.03	23.89±22.54	16.24±21.56	29.99±29.31	24.01±1.20	13.54±4.74
Negative	7	5.43±4.70	17.815±8.47	7.75±6.49	35.25±30.99	32.52±43.48	13.56±24.42
P-value		0.5	1	1	1	0.5	0.33
Menarche							
>12 years	4	11.14±5.47	29.36±8.31	18.10±10.16	19.87±7.42	15.98±7.16	5.15±3.67
≤12 years	5	2.61±2.86	11.00±3.12	2.87±1.16	45.45±35.51	42.35±49.39	20.28±27.62
P-value		0.03	0.01	0.01	0.41	0.41	0.7
Site of metastasis							
Liver							
Positive	2	11.59±8.49	32.48±10.39	24.58±9.76	17.62±7.81	7.88±3.25	7.88±3.25
Negative	7	5.54±5.03	15.75±9.22	5.67±5.60	18.56±9.88	6.46±7.91	6.46±7.91
P-value		0.42	0.14	0.7	1	0.64	0.64
Lung							
Positive	2	10.29±6.41	26.78±12.30	17.55±14.00	12.70±6.74	14.08±8.26	5.49±4.74
Negative	7	4.46±5.18	15.35±9.29	5.68±5.59	44.77±30.05	38.91±44.91	17.59±25.54
P-value		0.26	0.16	0.26	0.02	0.26	0.71
Mediastinum							
Positive	2	2.97±3.23	12.59±5.88	6.20±6.93	49.60±36.43	48.23±53.98	21.75±31.39
Negative	7	9.14±6.49	24.42±12.04	12.39±12.25	21.67±15.39	16.55±11.03	7.00±6.34
P-value		0.19	0.11	0.55	0.11	0.28	0.73
Bone							
Positive	1	7.39±8.78	22.39±13.24	5.17±2.29	62.24±54.34	68.51±85.67	34.88±46.13
Negative	8	6.12±5.84	18.24±11.50	10.92±11.35	26.03±16.69	19.81±8.44	7.46±7.11
P-value		1	0.66	1	0.33	0.88	0.66
Cervical ganglia							
Positive	3	2.61±2.86	11.00±3.12	2.87±1.16	45.45±35.51	42.35±49.39	20.28±27.62
Negative	4	11.14±5.47	29.36±8.31	18.10±10.16	19.87±7.42	15.98±7.16	5.15±3.67
P-value		0.03	0.01	0.01	0.41	0.41	0.73
miRNA expression in other miRNAs							
Variables	miR-4459 Mean ± SD	miR-200b-3p Mean ± SD	miR-3182 Mean ± SD	miR-141-3p Mean ± SD	miR-7-5p Mean ± SD	miR-187-3p Mean ± SD	
Age							
≤53	5.92±6.36	5.50±4.85	1,245.80±1,623.86	53.52±52.01	16.54±21.12	2.09±4.22	
>53	0.41±0.72	9.50±5.05	1,976.99±2,681.96	15.85±1.32	3.98±3.31	0.31±0.55	
P-value	0.08	0.26	0.9	0.16	0.38	0.67	

Table II. Continued.

Variables	miR-4459 Mean ± SD	miR-200b-3p Mean ± SD	miR-3182 Mean ± SD	miR-141-3p Mean ± SD	miR-7-5p Mean ± SD	miR-187-3p Mean ± SD
Smoking						
Positive	8.65±8.80	3.85±2.99	903.56±338.08	24.04±7.53	4.86±1.54	0.30±0.53
Negative	1.80±1.73	8.32±5.34	1,782.52±2,318	49.09±54.96	16.10±21.50	2.10±4.21
P-value	0.35	0.38	0.54	0.9	0.54	0.47
Treatment						
Hormone therapy	1.89±2.21	6.83±5.24	453.168±247.04	43.61±58.49	18.66±26.72	2.66±5.32
Chemotherapy	5.84±7.32	6.83±5.44	2,318.62±2,276.15	38.44±39.20	7.30±5.92	0.57±0.52
P-value	0.53	0.9	0.28	1	1	0.68
HER2						
Positive	9.79±11.03	5.83±3.00	2,565.25±2,691.15	69.44±53.67	10.76±8.67	0.96±0.04
Negative	2.46±3.12	7.12±5.61	1,182.18±1,752.23	32.54±43.72	12.80±20.36	1.65±3.98
P-value	0.29	0.88	0.5	0.22	0.66	0.26
Menarche						
>12 years	7.34±7.65	3.73±2.45	760.75±397.20	24.26±6.16	6.77±4.00	0.23±0.46
≤12 years	1.48±1.73	9.31±5.33	2,072.55±2,466.90	53.92±60.00	16.82±23.96	2.52±4.57
P-value	0.26	0.19	0.9	0.73	0.9	0.22
Site of metastasis						
Liver						
Positive	12.98±6.52	2.31±1.96	976.16±443.83	27.84±5.15	5.57±1.33	0.46±0.65
Negative	1.80±1.73	7.11±4.50	1,820.28±2,295.30	30.11±38.51	7.00±6.59	0.32±0.50
P-value	0.06	0.28	0.85	0.42	1	1
Lung						
Positive	10.05±6.85	2.47±1.41	714.16±551.74	19.49±14.91	3.94±2.96	0.30±0.53
Negative	1.10±1.39	9.01±4.72	1,877.22±2,250.58	51.36±52.90	16.56±21.13	2.10±4.21
P-value	0.02	0.04	0.9	0.71	0.26	0.47
Mediastinum						
Positive	0.49±0.99	11.10±4.28	1,469.77±2,016.29	67.36±60.17	19.83±26.40	3.15±5.02
Negative	6.96±6.48	3.42±1.92	1,505±2,027.359	19.44±11.26	6.36±4.29	0.18±0.41
P-value	0.03	0.01	0.9	0.41	0.73	0.08
Bone						
Positive	1.70±2.40	8.80±7.64	432.07±141.03	77.61±74.47	35.25±32.21	5.32±7.53
Negative	4.77±6.37	6.27±4.69	1,791.66±2,071.41	30.20±35.18	5.81±5.52	0.41±0.51
P-value	0.65	0.88	0.5	0.22	0.11	0.63
Cervical ganglia						
Positive	1.48±1.73	9.31±5.33	2,072.55±2,466.90	53.92±60.00	16.82±23.96	2.52±4.57
Negative	7.34±7.65	3.73±2.45	760.75±397.20	24.26±6.16	6.77±4.00	0.23±0.46
P-value	0.26	0.19	0.9	0.73	0.9	0.22

Values in bold font indicate statistically significant differences (P<0.05).

miRNAs, we performed KEGG pathway analysis of the 416 predicted targets in WEB-based Gene SET Analysis Toolkit. We only selected the top altered pathways per miRNA, considering those that had a P-value <0.05 and ranked them by their P-value, and identified 16 dysregulated signaling pathways related to miR-342-3p, miR-187-3p and miR-301a-3p (Fig. 6). Moreover, the results revealed miR-301a-3p and miR-342-3p affected the same pathways in cancer, cytokine-cytokine receptor interaction, glioma

and endocytosis. We also observed this effect between miR-342-3p and miR-187-3p, which affect the MAPK signaling pathway (Fig. 6).

Identification of main miR-342-3p targets. To investigate the main predicted targets, we focused on miR-342-3p as it was associated with a lack of lung metastasis and response to treatment and was a prognostic factor for OS in both the Kaplan-Meier and Cox multivariate analyses. Pearson's

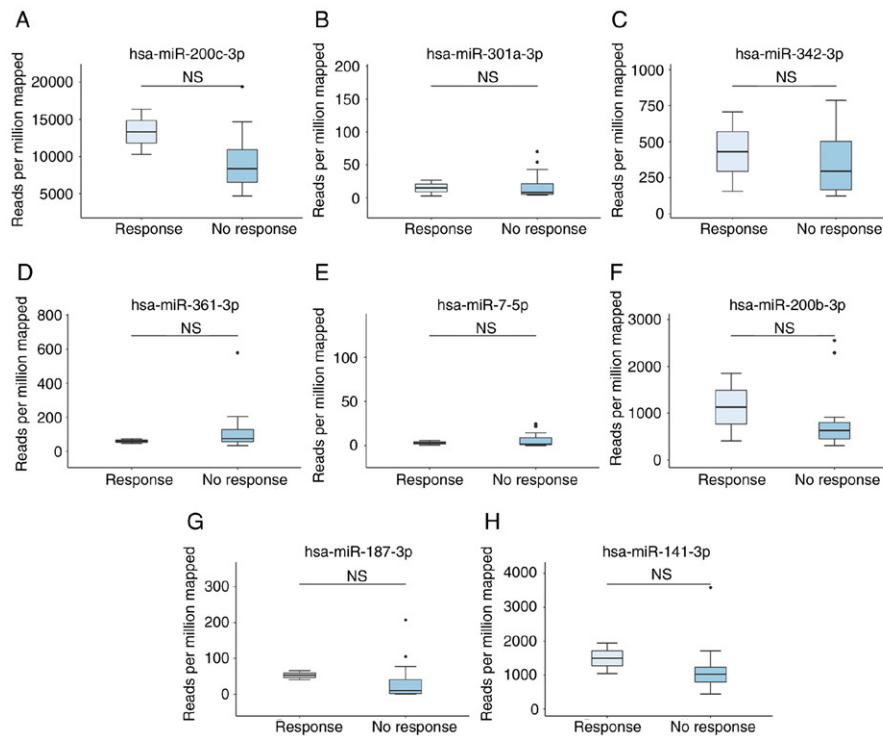


Figure 3. (A-H) MicroRNAs associated with the response to systemic treatment in BC in the TCGA cohort. The bar plot shows the numbers of reads for each miRNA according to response (R) vs. no response (NR) to systemic treatment.

correlation analysis was performed between miR-342-3p and the predicted targets, only considering interactions with a negative coefficient and with a P-value <0.05. Based on these criteria, the number of mRNAs targets was reduced from 56 to 15 (Table SV), and the predicted targets were ranked according their correlation coefficient. In total 8 mRNAs were found to be the main targets of miR-342-3p (Fig. 7). The most negatively correlated target was the nucleic transcription factor early B cell factor1 (EBF1) (Fig. 7A). Other transcription factors were also determined as targets, such as mesenchyme homeobox 2 (MEOX2), zinc finger E-box binding homeobox 1 and 2 (ZEB1/ZEB2) (Fig. 7C, E and F). In addition, tumor suppressors were related to this miRNA, including transmembrane protein 170B (TMEM170B), SRY-box 6 (SOX6) and large tumor suppressor kinase 2 (LATS2). Acetyl-CoA synthetase long chain family member 4 (ACSL4) is another identified target involved in arachidonic acid metabolism (Fig. 7G).

Discussion

In the era of personalized therapy, it has been reported that more than one-third of patients with MBC do not respond to systemic treatment (1,6). However, there is a permanent effort on the part of the scientific community to identify biomarkers

that can help patients with MCB who will benefit from systemic therapy (5,6,10). This study is a pioneer in this regard, and our findings highlight the important role of miRNAs as predictors of response to systemic treatment in MBC.

It is well known that chemotherapy and hormone therapy act through different mechanisms; this is the reason why systemic treatment for patients with BC is decided according to the molecular subtype (3). In spite of this, it has been reported that the detection of a single miRNA or group of these can predict resistance to multiple therapeutic strategies; however, the majority of studies are still preclinical (10). In this regard, we focused on identifying miRNAs associated with response to systemic treatments in patients with MBC that could be considered biomarkers of response to systemic treatments in the near future, irrespective of the molecular subtype.

Through a comprehensive sequencing approach, we obtained a panel of 12 miRNAs that separated patients with MBC into 2 groups: Responders vs. non-responders (Figs. 1 and 2). In an effort to provide information about biomarkers for the response to treatment in patients with MBC, we validated our results in a large clinical cohort using TCGA. Previous studies have confirmed that TCGA cohorts represent a robust and external independent means of validating genomic data (19,20). Indeed, this genomic database symbolizes a revolution in the acquisition of information about

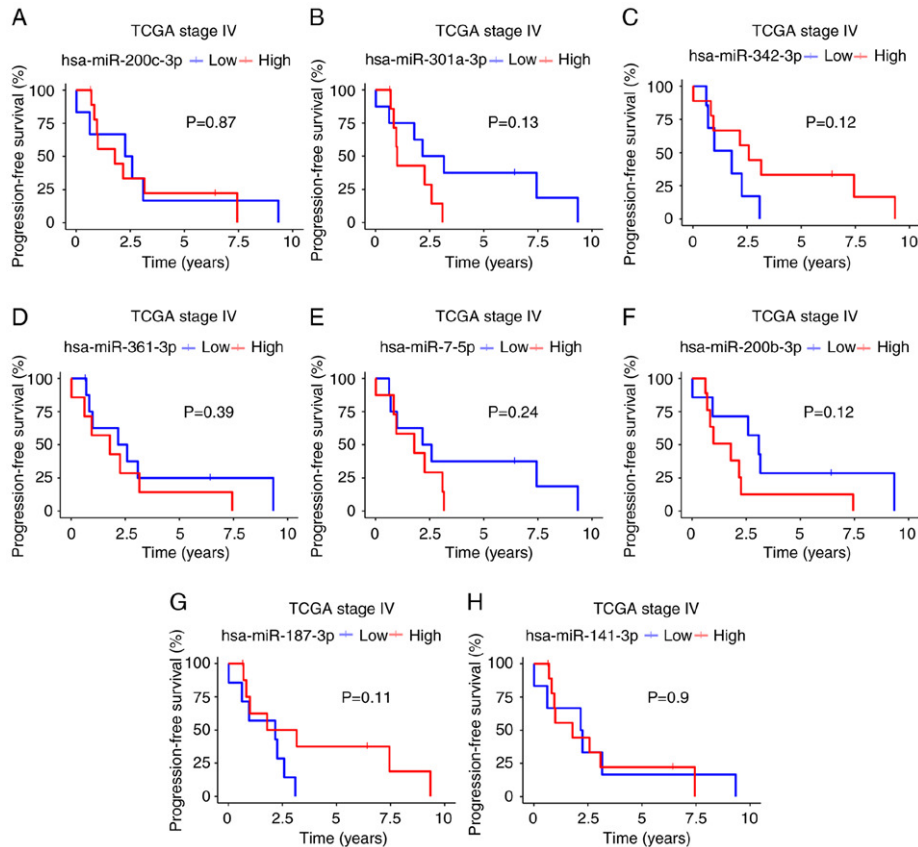


Figure 4. (A-H) Progression-free survival of patients with stage IV disease in TCGA based on 8 validated miRNAs. The high expression of miRNAs is shown by a red line. A blue line denotes miRNA downregulation.

tumors. The TCGA dataset has established validated quality standards ensuring homogeneity across data generated by multiple research groups; a precise strict set of criteria to be used for advanced genomic analysis and sequencing technologies of tissue samples exist. Moreover, TCGA includes data from a treatment-naïve cohort of 1,060 patients with BC (19). For our analysis, we retrieved genomic data for 16 patients with stage IV disease, 2 of whom presented a response to systemic treatment.

We validated our miRNA dataset in these patients with stage IV disease from TCGA and found that the upregulation of miR-342-3p and miR-187-3p was associated with a response to systemic treatment. Moreover, miR-342-3p, miR-187-3p and miR-301a-3p were associated with PFS and OS. Although we found clinical relevance for miR-187-3p and miR-301a-3p, there is little information about the roles and clinical relevance of these molecules in BC. A study published in 2012 reported that miR-187 expression was associated with an aggressive, invasive phenotype and a poor outcome in BC, which is contrary to the results of the present study; however, the cohort

consisted of patients with early and locally advanced stages, and the authors did not validate their data using TCGA (21). Nonetheless, miR-187 expression has been shown to inhibit the proliferation, migration and invasion of osteosarcoma by targeting ZEB2 (22). Similarly, two other studies reported that miR-187-3p expression induces apoptosis and inhibits cellular migration, invasion and metastasis in non-small cell lung cancer and hepatocellular carcinoma (23,24).

In this study, we found miR-301a-3p downregulation to be associated with an improved PFS and OS; similarly, a recent study demonstrated that this miRNA plays an oncogenic role and that its expression is associated with metastasis and a poor prognosis of patients with estrogen receptor-positive BC. Furthermore, the expression of miR-301a-3p contributes to the development of estrogen independence and a highly invasive phenotype of BC (25). In hepatocellular carcinoma, higher levels of miR-301a-3p expression have been associated with a poor prognosis and chemoresistance, as demonstrated by an *in vitro* analysis (26). Overall, these findings provide us with an opportunity to enhance our knowledge about the

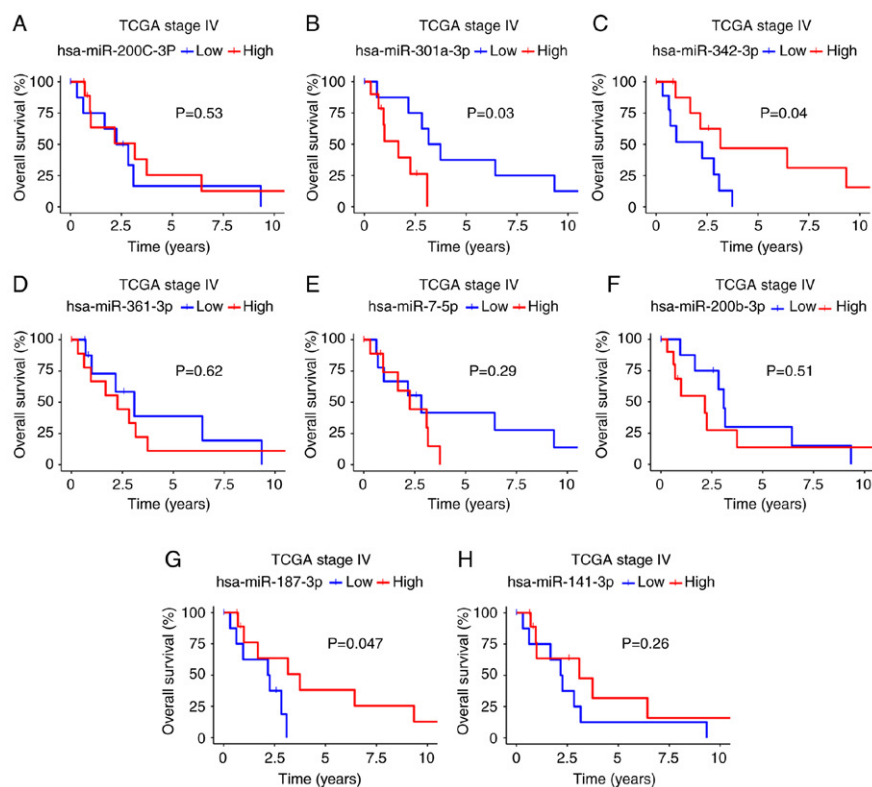


Figure 5. (A-H) Overall survival of patients with stage IV disease in TCGA based on 8 validated miRNAs. A high expression of miRNAs is shown by a red line. A blue line denotes miRNA downregulation.

roles of miR-187-3p and miR-301a-3p as treatment response or prognosis biomarkers for MBC and other neoplasia.

In this study, the upregulation of miR-342-3p was associated with the absence of lung metastasis and the response to systemic therapy, and was found to be a prognostic factor for OS. It has also been reported that high levels of miR-342-expression may act as a biomarker for tamoxifen sensitivity in estrogen receptor-alpha-positive BC (27). Similarly, miR-342 downregulation has been reported to be related to recurrence as it contributes to tamoxifen resistance by regulating genes involved in apoptosis and cell cycle progression, both processes that influence breast tumorigenesis and tumor response to therapeutic intervention (28). These findings are supported by the results in the study by Young *et al.*, who reported that a high expression of miR-342 was related to tamoxifen sensitivity and a better survival in a TCGA cohort (29).

In this study, we identified the main targets of miR-342-3p, and by integrating this information, we found that some of these targets have been implicated in treatment resistance mechanisms. For instance, EBF1 is involved in drug resistance and may be a potential prognostic marker in leukemia (30). The overexpression of different transcription factors, such as

MEOX2 and ZEB1 contributes to chemoresistance in lung and breast cancers, respectively (31,32) and the overexpression of ZEB2 appears to be involved in resistance to cisplatin and epidermal growth factor inhibitors in gastric and bladder cancers, respectively (33,34). Another target identified was ACSL4, which was recently associated with drug resistance in BC through the involvement of ABC transporters (35). Further characterization of miR-342-3p targets revealed a negative correlation with the tumor suppressor TMEM170B; although it has been reported that its overexpression in BC promotes inhibition of the WNT/ β -catenin pathway, its association with resistance to treatment has not been evaluated (36). Taken together, the results highlight the importance and participation of miR-342-3p in regulating several traits involved in tumor progression and resistance to treatment.

The results of this study indicate that miR-342-3p in coordination with miR-301a-3p participates in cytokine-cytokine receptor interaction, glioma and endocytosis pathways, which are involved in drug resistance and associated with a poor prognosis (Fig. 6). Recent RNA-Seq data demonstrate that the cytokine-cytokine receptor interaction pathway is a key factor in treatment resistance of triple-negative BC (37), concordant with studies describing that cytokines secreted via cancer

Table III. Overall survival in patients expressing the miRNA panel.

	Overall survival			
	Univariate analysis		Multivariate analysis	
	HR (95% CI)	P-value	HR (95% CI)	P-value
Age				
<60 vs. >60 years	0.36 (0.084-1.5)	0.17	0.10 (0.004-2.46)	0.162
Progesterone status				
Positive vs. negative	0.51 (0.13-1.9)	0.32	3.73 (0.277-50.34)	0.32
hsa-miR-187-3p				
High vs. low	0.22 (0.042-1.2)	0.082	1.19 (0.08-17.89)	0.89
hsa-miR-301a-3p				
High vs. low	4.1 (0.75-23)	0.1	0.72 (0.07-6.82)	0.77
hsa-miR-342-3p				
High vs. low	0.25 (0.062-1)	0.056	0.08 (0.006-1.200)	0.068

Values in bold font indicate statistically significant differences (P<0.05).

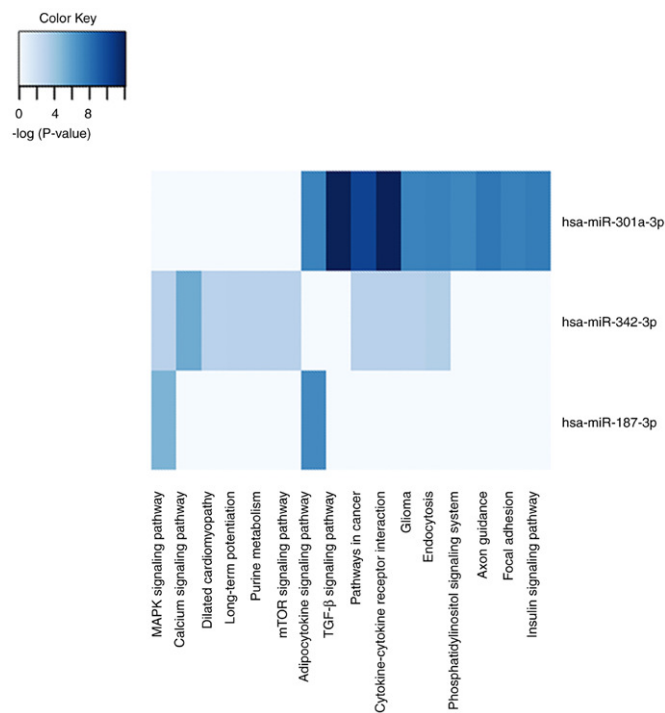


Figure 6. KEGG pathway heatmap. Functional annotation of 3 miRNAs using the KEGG pathway database with adjusted P-values showed the top altered pathways dysregulated by miR-342-3p, miR-187-3p and miR-301a-3p.

stroma cells are crucial for conferring resistance to chemotherapy (38,39). Endocytosis is another process that when

altered, is involved in resistance to trastuzumab in BC through Src-mediated phosphorylation of CAV1 (40). Finally, we found

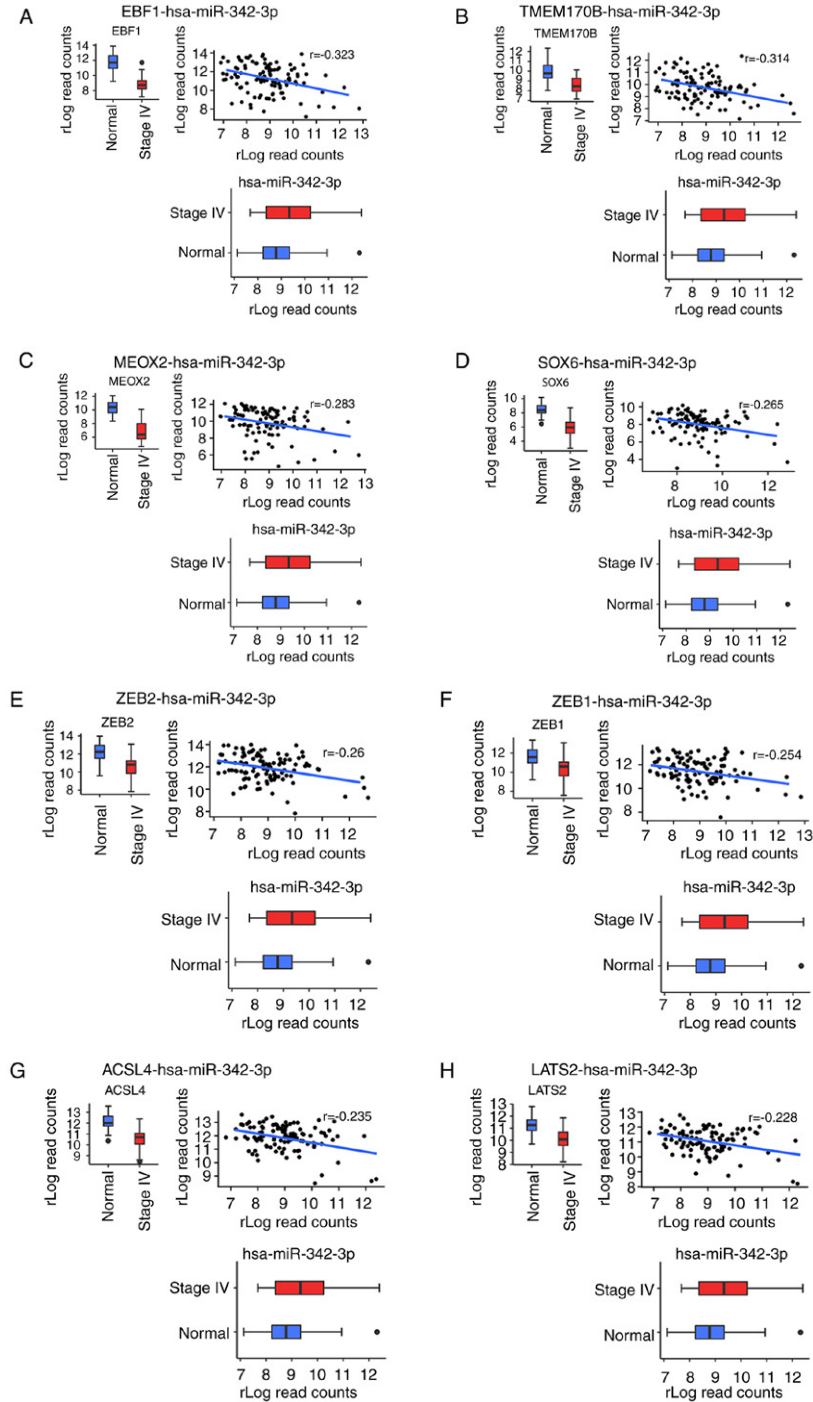


Figure 7. (A-H) Correlation analysis between miR-342-3p and the main predicted targets. Eight mRNAs were found to be the main targets of miR-342-3p.

that miR-342-3p and miR-187-3p regulate the MAPK cascade, which is involved in several important physiological functions such as proliferation, survival and chemoresistance, as well as a poor outcome of patients with BC (41,42).

The limitations of this study were the following: i) The small number of patients with MBC (only 2 of whom in the TCGA cohort presented a response to treatment) and; ii) from the patients in TCGA, only one was Hispanic and the remainder Caucasian; thus, considering ethnicity, it could be considered that BC is a disease with similar transcriptomic and genomic alterations. Nonetheless, on the whole, our results suggest that miRNA-342-3p and miRNA-187-3p may serve as good biomarkers for a response to systemic treatment in patients with MBC and that miR-301-3p may constitute a prognosis biomarker. However, these data should be validated experimentally in other robust cohorts and using different specimens before implementing these miRNAs as biomarkers in clinical practice to benefit this group of patients.

Acknowledgements

The authors would like to thank Tumor Bank of the Instituto Nacional de Cancerología (INCan) of México City for providing some biological samples. The authors would also like to thank Dr Alfonso Méndez Tenorio from Escuela Nacional de Ciencias Biológicas, Instituto Politécnico Nacional for the support with ThermoFisher Scientific Ion S5 equipment. In addition, the authors would like to thank Histotechnology Eduardo Bautista Nava for its support in the performance of immunohistochemistry and the interns Gerardo Cuamani Mitznahuatl and Jaime Jesús Ordóñez Adán, for their support in the collection of clinical data. Antonio Daniel Martínez Gutierrez is a doctoral student from Programa de Doctorado en Ciencias Biomedicas, Universidad Nacional Autónoma de México (UNAM) and was supported by CONACYT (628988).

Funding

This study was supported by the Council for Science and Technology (CONACYT) (SALUD-2015-1-262044, PN-249020).

Availability of data and materials

All data generated or analyzed during this study are included in this published article or are available from the corresponding author on reasonable request.

Authors' contributions

ADCP and CPP were the principal investigators and contributed to the conception and design of the study. ADMG contributed to all bioinformatics analyses. OMC CLC, LTOM and ADCP were involved in the sequencing. FIPR contributed to the pathological analysis of the samples. RVR, AAM, FLM, JEBR, LAH and DCDL recollected samples and were responsible for all clinical data of the patients. ADCP, ADMG and CPP wrote, drafted, revised the manuscript. All authors contributed to the conception of the article; all authors

revised the final manuscript and agreed to its submission to this journal.

Ethics approval and consent to participate

This study complies with ethical standards. The study was approved by Instituto Nacional de Cancerología of México City ethics committees. The participants provided consent, including patient information, after they received verbal and written explanation. Individual consent was signed by each individual.

Patient consent for publication

Not applicable.

Competing interests

The authors declare that they have no competing interests.

References

- Gonzalez-Angulo AM, Morales-Vasquez F and Hortobagyi GN: Overview of resistance to systemic therapy in patients with breast cancer. *Adv Exp Med Biol* 608: 1-22, 2007.
- Visovsky C: Treatment considerations for the management of patients with hormone receptor-positive metastatic breast cancer. *J Adv Pract Oncol* 5: 321-330, 2014.
- Berthold D: Third consensus on medical treatment of metastatic breast cancer. *Ann Oncol* 21: 665; author reply 655-656, 2010.
- Cancer Stat Facts: Female Breast Cancer. <https://seer.cancer.gov/statfacts/html/breast.html>. Accessed January 31, 2019.
- Haynes B, Sarma A, Nangia-Makker P and Shekhar MP: Breast cancer complexity: Implications of intratumoral heterogeneity in clinical management. *Cancer Metastasis Rev* 36: 547-555, 2017.
- Bakker JL, Wever K, van Waesberghe JH, Beeker A, Meijers-Heijboer H, Konings IR and Verheul HMW: What is the benefit of treatment with multiple lines of chemotherapy for patients with metastatic breast cancer? A retrospective cohort study. *Cancer Epidemiol* 39: 848-853, 2015.
- Lee Y, Jeon K, Lee JT, Kim S and Kim VN: MicroRNA maturation: Stepwise processing and subcellular localization. *EMBO J* 21: 4663-4670, 2002.
- Bovell L, Shanmugam C, Katkooori VR, Zhang B, Vogtmann E, Grizzle WE and Manne U: miRNAs are stable in colorectal cancer archival tissue blocks. *Front Biosci (Elite Ed)* 4: 1937-1940, 2012.
- Occhipinti G, Giulietti M, Principato G and Piva F: The choice of endogenous controls in exosomal microRNA assessments from biofluids. *Tumour Biol* 37: 11657-11665, 2016.
- Campos-Parra AD, Mitznahuatl GC, Pedroza-Torres A, Romo RV, Reyes FIP, López-Urrutia E and Pérez-Plasencia C: Micro-RNAs as potential predictors of response to breast cancer systemic therapy: Future clinical implications. *Int J Mol Sci* 18, 2017.
- Gradishar WJ, Anderson BO, Balassanian R, Blair SL, Burstein HJ, Cyr A, Elias AD, Farrar WB, Forero A, Giordano SH, et al: NCCN guidelines insights: Breast cancer, version 1.2017. *J Natl Compr Cancer Netw* 15: 433-451, 2017.
- Watanabe H, Okada M, Kaji Y, Satouchi M, Sato Y, Yamabe Y, Onaya H, Endo M, Sone M and Arai Y: New response evaluation criteria in solid tumours-revised RECIST guideline (version 1.1). *Gan To Kagaku Ryoho* 36: 2495-2501, 2009 (In Japanese).
- Vitsios DM and Enright AJ: Chimira: Analysis of small RNA sequencing data and microRNA modifications. *Bioinformatics* 31: 3365-3367, 2015.
- Love MI, Huber W and Anders S: Moderated estimation of fold change and dispersion for RNA-seq data with DESeq2. *Genome Biol* 15: 550, 2014.
- Colaprico A, Silva TC, Olsen C, Garofano L, Cava C, Carolini D, Sabedot TS, Malta TM, Pagnotta SM, Castiglioni I, et al: TCGAAbiolinks: An R/Bioconductor package for integrative analysis of TCGA data. *Nucleic Acids Res* 44: e71, 2016.
- Tibshirani R: A simple method for assessing sample sizes in microarray experiments. *BMC Bioinformatics* 7: 106, 2006.

17. Rapaport F, Khanin R, Liang Y, Pirun M, Krek A, Zumbo P, Mason CE, Socci ND and Betel D: Erratum to: Comprehensive evaluation of differential gene expression analysis methods for RNA-seq data. *Genome Biol* 16: 261, 2015.
18. Costa-Silva J, Domingues D and Lopes FM: RNA-Seq differential expression analysis: An extended review and a software tool. *PLoS One* 12: e0190152, 2017.
19. Chin L, Andersen JN and Futreal PA: Cancer genomics: From discovery science to personalized medicine. *Nat Med* 17: 297-303, 2011.
20. Mulrane L, Madden SF, Brennan DJ, Gremel G, McGee SF, McNally S, Martin F, Crown JP, Jirstrom K, Higgins DG, *et al.*: miR-187 is an independent prognostic factor in breast cancer and confers increased invasive potential in vitro. *Clin Cancer Res* 18: 6702-6713, 2012.
21. Liu J, Lichtenberg T, Hoadley KA, Poisson LM, Lazar AJ, Cherniack AD, Kovatich AJ, Benz CC, Levine DA, Lee AV, *et al.*: An integrated TCGA pan-cancer clinical data resource to drive high-quality survival outcome analytics. *Cell* 173: 400.e11-416.e11, 2018.
22. Fei D, Zhao K, Yuan H, Xing J and Zhao D: MicroRNA-187 exerts tumor-suppressing functions in osteosarcoma by targeting ZEB2. *Am J Cancer Res* 6: 2859-2868, 2016.
23. Sun C, Li S, Yang C, Xi Y, Wang L, Zhang F and Li D: MicroRNA-187-3p mitigates non-small cell lung cancer (NSCLC) development through down-regulation of BCL6. *Biochem Biophys Res Commun* 471: 82-88, 2016.
24. Dou C, Liu Z, Xu M, Jia Y, Wang Y, Li Q, Yang W, Zheng X, Tu K and Liu Q: MiR-187-3p inhibits the metastasis and epithelial-mesenchymal transition of hepatocellular carcinoma by targeting S100A4. *Cancer Lett* 381: 380-390, 2016.
25. Lettlova S, Brynychova V, Blecha J, Vrana D, Vondrusova M, Soucek P and Truksa J: MiR-301a-3p suppresses estrogen signaling by directly inhibiting ESR1 in ER α positive breast cancer. *Cell Physiol Biochem* 46: 2601-2615, 2018.
26. Hu J, Ruan J, Liu X, Xiao C and Xiong J: MicroRNA-301a-3p suppressed the progression of hepatocellular carcinoma via targeting VGLL4. *Pathol Res Pract* 214: 2039-2045, 2018.
27. He YJ, Wu JZ, Ji MH, Ma T, Qiao EQ, Ma R and Tang JH: MiR-342 is associated with estrogen receptor- α expression and response to tamoxifen in breast cancer. *Exp Ther Med* 5: 813-818, 2013.
28. Cittelly DM, Das PM, Spoelstra NS, Edgerton SM, Richer JK, Thor AD and Jones FE: Downregulation of miR-342 is associated with tamoxifen resistant breast tumors. *Mol Cancer* 9: 317, 2010.
29. Young J, Kawaguchi T, Yan L, Qi Q, Liu S and Takabe K: Tamoxifen sensitivity-related microRNA-342 is a useful biomarker for breast cancer survival. *Oncotarget* 8: 99978-99989, 2017.
30. Liao D: Emerging roles of the EBF family of transcription factors in tumor suppression. *Mol Cancer Res* 7: 1893-1901, 2009.
31. Ávila-Moreno F, Armas-López L, Álvarez-Moran AM, López-Bujanda Z, Ortiz-Quintero B, Hidalgo-Miranda A, Urrea-Ramírez F, Rivera-Rosales RM, Vázquez-Manríquez E, Peña-Mirabal E, *et al.*: Overexpression of MEOX2 and TWIST1 is associated with H3K27me3 levels and determines lung cancer chemoresistance and prognosis. *PLoS One* 9: e114104, 2014.
32. Zhang X, Zhang Z, Zhang Q, Zhang Q, Sun P, Xiang R, Ren G and Yang S: ZEB1 confers chemotherapeutic resistance to breast cancer by activating ATM. *Cell Death Dis* 9: 57, 2018.
33. Jiang T, Dong P, Li L, Ma X, Xu P, Zhu H, Wang Y, Yang B, Liu K, Liu J, *et al.*: MicroRNA-200c regulates cisplatin resistance by targeting ZEB2 in human gastric cancer cells. *Oncol Rep* 38: 151-158, 2017.
34. Adam L, Zhong M, Choi W, Qi W, Nicoloso M, Arora A, Calin G, Wang H, Siefker-Radtke A, McConkey D, *et al.*: MiR-200 expression regulates epithelial-to-mesenchymal transition in bladder cancer cells and reverses resistance to epidermal growth factor receptor therapy. *Clin Cancer Res* 15: 5060-5072, 2009.
35. Orlando UD, Castillo AF, Medrano MAR, Solano AR, Maloberti PM and Podesta EJ: Acyl-CoA synthetase-4 is implicated in drug resistance in breast cancer cell lines involving the regulation of energy-dependent transporter expression. *Biochem Pharmacol* 159: 52-63, 2019.
36. Li M, Han Y, Zhou H, Li X, Lin C, Zhang E, Chi X, Hu J and Xu H: Transmembrane protein 170B is a novel breast tumorigenesis suppressor gene that inhibits the Wnt/ β -catenin pathway. *Cell Death Dis* 9: 91, 2018.
37. Shaheen S, Fawaz F, Shah S and Büsselberg D: Differential expression and pathway analysis in drug-resistant triple-negative breast cancer cell lines using RNASeq analysis. *Int J Mol Sci* 19, 2018.
38. Jones VS, Huang RY, Chen LP, Chen ZS, Fu L and Huang RP: Cytokines in cancer drug resistance: Cues to new therapeutic strategies. *Biochim Biophys Acta* 1865: 255-265, 2016.
39. Senthilane DA, Rowe A, Thomford NE, Shipanga H, Munro D, Mazeedi MA, Almazaydi HA, Kallmeyer K, Dandara C, Pepper MS, *et al.*: The role of tumor microenvironment in chemoresistance: To survive, keep your enemies closer. *Int J Mol Sci* 18, 2017.
40. Sung M, Tan X, Lu B, Golas J, Hosselet C, Wang F, Tylaska L, King L, Zhou D, Dushin R, *et al.*: Caveolae-mediated endocytosis as a novel mechanism of resistance to trastuzumab emtansine (T-DM1). *Mol Cancer Ther* 17: 243-253, 2018.
41. De Luca A, Maiello MR, D'Alessio A, Pergameno M and Normanno N: The RAS/RAF/MEK/ERK and the PI3K/AKT signalling pathways: Role in cancer pathogenesis and implications for therapeutic approaches. *Expert Opin Ther Targets* 16 (Suppl 2): S17-S27, 2012.
42. Generali D, Buffa FM, Berruti A, Brizzi MP, Campo L, Bonardi S, Bersiga A, Allevi G, Milani M, Aguggini S, *et al.*: Phosphorylated ER α , HIF-1 α , and MAPK signaling as predictors of primary endocrine treatment response and resistance in patients with breast cancer. *J Clin Oncol* 27: 227-234, 2009.



This work is licensed under a Creative Commons Attribution-NonCommercial-NoDerivatives 4.0 International (CC BY-NC-ND 4.0) License.

- 8.3. Martinez-Rivera V., Cardenas-Monroy, ,M.,.....,Martinez-Gutierrez, Antonio-D., et al. Dysregulation of miR-381-3p and miR- 23b-3p in skeletal muscle could be a possible estimator of early post-mortem interval in rats. PeerJ. 2021

Dysregulation of miR-381-3p and miR-23b-3p in skeletal muscle could be a possible estimator of early post-mortem interval in rats

Vanessa Martínez-Rivera¹, Christian A. Cárdenas-Monroy¹, Oliver Millan-Catalan^{2,3}, Jessica González-Corona¹, N. Sofia Huerta-Pacheco⁴, Antonio Martínez-Gutiérrez², Alexa Villavicencio-Queijeiro¹, Carlos Pedraza-Lara⁵, Alfredo Hidalgo-Miranda⁶, María Elena Bravo-Gómez⁷, Carlos Pérez-Plasencia^{2,3} and Mariano Guardado-Estrada¹

¹Laboratorio de Genética, Ciencia Forense, Facultad de Medicina, Universidad Nacional Autónoma de México, Ciudad de México, México

²Unidad de Investigación Biomédica en Cáncer, Laboratorio de Genómica, Instituto Nacional de Cancerología, Ciudad de México, México

³Unidad de Investigación Biomédica en Cáncer, Laboratorio de Genómica, Facultad de Estudios Superiores Iztacala, Universidad Nacional Autónoma de México, Ciudad de México, México

⁴Cátedras CONACYT—Ciencia Forense, Facultad de Medicina, Universidad Nacional Autónoma de México, Ciudad de México, México

⁵Laboratorio de Entomología, Ciencia Forense, Facultad de Medicina, Universidad Nacional Autónoma de México, Ciudad de México, México

⁶Laboratorio de Genómica del Cáncer, Instituto Nacional de Medicina Genómica (INMEGEN), Nacional de Medicina Genómica, Ciudad de México, México

⁷Laboratorio de Toxicología, Ciencia Forense, Facultad de Medicina, Universidad Nacional Autónoma de México, Ciudad de México, México

ABSTRACT

Background. The post-mortem interval (PMI) is the time elapsed since the death of an individual until the body is found, which is relevant for forensic purposes. The miRNAs regulate the expression of some genes; and due to their small size, they can better support degradation, which makes them suitable for forensic analysis. In the present work, we evaluated the gene expression of miR-381-3p, miR-23b-3p, and miR-144-3p in skeletal muscle in a murine model at the early PMI.

Methods. We designed a rat model to evaluate the early PMI under controlled conditions. This model consisted in 25 rats divided into five groups of rats, that correspond to the 0, 3, 6, 12 and 24 hours of PMI. The 0 h-PMI was considered as the control group. Muscle samples were taken from each rat to analyze the expression of miR-381-3p, miR-23b-3p, and miR-144-3p by quantitative RT-PCR. The gene expression of each miRNA was expressed as *Fold Change* (FC) and compared among groups. To find the targets of these miRNAs and the pathways where they participate, we performed an in-silico analysis. From the gene targets of miR-381-3p identified in the silico analysis, the *EPC1* gene was selected for gene expression analysis by quantitative RT-PCR in these samples. Also, to evaluate if miR-381-3p could predict the early PMI, a mixed effects model was calculated using its gene expression.

Results. An upregulation of miR-381-3p was found at 24 h-PMI compared with the control group of 0 h-PMI and (FC = 1.02 vs. FC = 1.96; $p = 0.0079$). This was the

Submitted 14 August 2020
Accepted 22 February 2021
Published 27 April 2021

Corresponding author
Mariano Guardado-Estrada,
mguardado@cienciaforense.facmed.
unam.mx

Academic editor
Gwyn Gould

Additional Information and
Declarations can be found on
page 14

DOI 10.7717/peerj.11102

© Copyright
2021 Martínez-Rivera et al.

Distributed under
Creative Commons CC-BY 4.0

OPEN ACCESS

How to cite this article Martínez-Rivera V, Cárdenas-Monroy CA, Millan-Catalan O, González-Corona J, Huerta-Pacheco NS, Martínez-Gutiérrez A, Villavicencio-Queijeiro A, Pedraza-Lara C, Hidalgo-Miranda A, Bravo-Gómez ME, Pérez-Plasencia C, Guardado-Estrada M. 2021. Dysregulation of miR-381-3p and miR-23b-3p in skeletal muscle could be a possible estimator of early post-mortem interval in rats. *PeerJ* 9:e11102 <http://doi.org/10.7717/peerj.11102>

opposite for miR-23b-3p, which had a down-regulation at 24 h-PMI compared to 0 h-PMI (FC = 1.22 vs. FC = 0.13; $p = 0.0079$). Moreover, the gene expression of miR-381-3p increased throughout the first 24 h of PMI, contrary to miR-23b-3p. The targets of these two miRNAs, participate in biological pathways related to hypoxia, apoptosis, and RNA metabolism. The gene expression of *EPC1* was found downregulated at 3 and 12 h of PMI, whereas it remained unchanged at 6 h and 24 h of PMI. Using a multivariate analysis, it was possible to predict the FC of miR-381-3p of all but 6 h-PMI analyzed PMIs.

Discussion. The present results suggest that miR-23b-3p and miR-381-3p participate at the early PMI, probably regulating the expression of some genes related to the autolysis process as *EPC1* gene. Although the miR-381-3p gene expression is a potential estimator of PMI, further studies will be required to obtain better estimates.

Subjects Cell Biology, Genetics, Molecular Biology

Keywords miRNA, Gene-expression, Post-mortem interval, Forensics

INTRODUCTION

The post-mortem interval (PMI) is defined as the time elapsed between the death of an individual and the time the body is found; it being relevant for forensic purposes (Maile *et al.*, 2017). At early PMI (3–72 h after death), morphological changes appear, such as decay of temperature (*algor mortis*), cadaveric stiffness (*rigors mortis*), and changes in body coloration (*livor mortis*) (Lee Goff, 2009; Maile *et al.*, 2017). The identification of these morphological changes is helpful to estimate the PMI. In the meantime, a process called autolysis occurs in the cells of a dead body, characterized by an absence of inflammatory response and cell destruction due to liberation of the enzymes of some organelles (Tomita *et al.*, 2004).

However, the occurrence of these external morphological changes could vary due to different factors such as the environment, cause of the death, among others; this can make it difficult to estimate PMI (Madea, 2016). Thus, other methods have been developed where some components in vitreous humor or synovial fluid are quantified for PMI estimation (Madea *et al.*, 1994; Madea, Kreuzer & Banaschak, 2001; Zilg *et al.*, 2015; Madea, 2016; Ansari & Menon, 2017). Nevertheless, as with physical changes, variations in the quantifications of these elements reduce the confidence in the calculation of PMI (Muñoz Barús *et al.*, 2002; Madea, 2016).

Other molecules that have been studied for PMI estimation are nucleic acids (Koppelkamm *et al.*, 2011; Itani *et al.*, 2011). For instance, RNA degradation has been studied in different tissues throughout the PMIs (Koppelkamm *et al.*, 2011). Although it is expected that after the death of an individual the RNA transcription halts, there are many studies that analyzed the expression of some genes at different PMIs (Pozhitkov *et al.*, 2017). After death, transcriptional activity has been found in several tissues analyzed in humans and other organisms (Vishnoi & Rani, 2017; Pozhitkov *et al.*, 2017; Ferreira *et al.*, 2018). For instance, a study performed in mice and zebra fish found an upregulation of genes that

participate in several biological processes such as stress, immune response and apoptosis, among others (Pozhitkov et al., 2017). In humans, the changes of transcriptional activity at early PMI depend on the analyzed tissue, as well as the rate of RNA degradation in them (Ferreira et al., 2018). Although there is not a complete understanding of the underlying mechanism of this transcriptional activity at PMI, it is suggested that epigenetic regulation could be involved (Pozhitkov et al., 2017).

The miRNAs are small 22 nucleotide-length non-coding RNAs which can post-transcriptionally regulate the expression of genes implicated in several pathways (Vishnoi & Rani, 2017). Due to their small size, the miRNAs endure extreme conditions without degradation, making them suitable for forensic purposes (Wang et al., 2013; Lv et al., 2014). In fact, it has been reported that miRNAs regulate several processes such as apoptosis and inflammation, which are implicated in the process of body decomposition (Chen et al., 2018b; Zhou et al., 2019; Jiang et al., 2020). On the other hand, a continuous expression of some miRNAs at different PMI has been found in the spleen, heart muscle, brain, and bone on both rats and humans (Li et al., 2014; Lv et al., 2014; Nagy et al., 2015; Na, 2020).

For this work we analyzed the expression of miR-144-3p, miR-23b-3p, and miR-381-3p, which participate in apoptosis and inflammation, in rat skeletal muscle at early PMI. In fact, it has been reported that miR-144-3p, miR-23b-3p and miR-381-3p regulate the gene expression of BCL6, PROK2, and IL15RA, respectively, which were found to be altered at the PMI (Pozhitkov et al., 2017; Kozomara, Birgaoanu & Griffiths-Jones, 2019). First, we established a PMI rat model to analyze the expression of these three miRNAs in rat skeletal muscle at different post-mortem intervals. On the other hand, we performed an in-silico analysis to identify the gene targets of these miRNAs to quantify one of them in these samples. Finally, the expression of *EPC1*, which is target of miR-381-3p in these samples, was analyzed.

MATERIALS & METHODS

PMI rat model

A total of 25 adult male Wistar rats was selected for the study; all with an average weight of 200 \pm 20 gr. These rats were sorted into five groups, which correspond to the 0, 3, 6, 12 and 24 h of post-mortem interval (h-PMI). The 0 h-PMI was considered the control group. The rats from 3, 6, 12 and 24 h-PMI groups, were euthanized by cervical dislocation and placed in a Binder KBW 240TM climatic chamber with a constant temperature of 25 °C. After the PMI time elapsed in each group, the presence of internal and external morphological changes was evaluated on every rat. Every rat was physically explored, in a cephalocaudal fashion, to evaluate the presence or absence of *algor mortis* (AM), *livor mortis* (LM), *rigor mortis* upper body (RMU), *rigor mortis* lower body (RML), drying (DR), generalized edema (ED), hair loss (HL), abdomen green discoloration (AGD), and abdominal distention (AD), which are physical signs present at early post-mortem interval (Dix, 1999; Brooks, 2016). Also, each animal was dissected to evaluate the presence of brain liquefaction (BL), brain edema (BE), discoloration of liver (DL), loss of liver consistency (LLC), muscle *livor mortis* (MML), bowel swelling (BS), ascites (AS), and loss

of muscle consistency (LMC). Once the evaluation was performed, 200 mg of femoral muscle sample was obtained and stored at -80°C until analysis. The rats from the control group were euthanized by cervical dislocation, and muscle samples were taken immediately and stored at -80°C until analysis. As in the other PMI-groups, control group rats were externally and physically evaluated for the presence of cadaveric signs. All procedures were evaluated and approved by the local ethic and scientific committee and the committee for the care and use of laboratory animals (CICUAL) of the Faculty of Medicine from the National Autonomous University of Mexico (UNAM) with approval number 102-2018, and 027-CIC-201, respectively; the procedures were also performed in strict accordance to local (NOM-062-ZOO-1999) and international norms of laboratory animals handling.

RNA extraction

For miRNAs analysis, total RNA was extracted from the rat skeletal muscle samples using glass beads for rupture and Trizol™ Reagent. In brief, a fraction between 50 and 100 mg of frozen tissue was collected in a 2 mL tube with 2 mm glass beads (ZR BashingBead Lysis Tubes, Zymo Research) and 1 mL of Trizol™ Reagent. Then, 200 μl of chloroform was added and mixed to be centrifuged at 12,000 g for 15 min at 4°C . After this step, total RNA extraction was performed according to manufacturer's recommendations. The obtained RNA was quantified with an UV-spectrophotometer NanoDrop™ 2000 (Thermo Scientific), and the integrity was evaluated qualitatively in agarose gels.

miRNAs quantification by RT-PCR

From the total RNA of muscle samples, miRNA cDNA was synthesized using the kit TaqMan Advanced miRNA cDNA Synthesis kit (Applied Biosystems). This kit performs the poly(A) tailing reaction via adaptor ligation previous to the miRNA cDNA synthesis. All reactions were performed according to the manufacturer's protocol. Gene expression of miR-144-3p, miR-23b-3p, and miR-381-3p was evaluated by qRT-PCR using the TaqMan® probes rno481325_mir, rno478602_mir, and rno481460_mir, respectively. The miR-361-5p (rno481127_mir) was used as internal control, since it has been seen that its expression is stable under extreme conditions, such as cancer (*Della Bella & Stoddart, 2019*). The miRNAs quantification was performed in a StepOne™ Real-Time PCR System (Thermo Fisher Scientific, Waltham, Massachusetts, U.S.A) using 10 ng of total cDNA, 0.5 μl of the TaqMan® Advanced miRNA Assay (20X), and 5 μl of TaqMan® Fast Advanced Master Mix (2X) in a total volume of 7.5 μl . Each quantitative RT-PCR was incubated at 95°C for 20 s, then at 95°C for 3 min with 40 cycles of denaturation and annealing/extension at 60°C for 30 s. Each miRNA was analyzed separately, and each sample was run by triplicate. Each miRNA was relatively quantified with the $2^{-\Delta\Delta\text{CT}}$ method, and data is presented as fold change (FC), which is the gene expression normalized to miR-361-5p and relative to the 0 h-PMI group (*Livak & Schmittgen, 2001*).

mRNA quantification by RT-PCR

From the total RNA extracted from the rat's muscle samples, cDNA was synthesized using High-Capacity cDNA Reverse Transcription Kit (Thermo Fisher Scientific, Waltham, Massachusetts, U.S.A). The reaction was performed in a total volume of 20 μl , which

included 1 µg of RNA, 2 µl of 10X RT Buffer, 0.8 µl of 25X dNTP Mix, 2 µl of 10X RT Random Primers, and 1 µl of MultiScribe Reverse Transcriptase. Reactions were incubated at 25 °C for 10 min, at 37 °C for 120 min, and at 85 °C for 5 min; then they were stored at –20 °C for further analyses. Gene expression of *EPC1* (Rn01538512_m1) was evaluated with RT-PCR using TaqMan® probes. To normalize the expression of *EPC1*, the *ACTB* gene (Rn00667869_m1) was used in the analysis as a housekeeping gene. Quantification was performed in a StepOne™ Real-Time PCR System (Thermo Fisher Scientific, Waltham, Massachusetts, U.S.A) using 45 ng of total cDNA, 1 µl of the Taqman™ Probe, and 10 µl of Taqman® Master Mix in a total volume of 20 µl. Each quantitative RT-PCR was incubated at 50 °C for 2 min, then at 95 °C for 10 min with 40 cycles of denaturation at 90 °C, and annealing/extension at 60 °C for 60 s. Each gene was analyzed separately and ran by triplicate in all samples. The average CT threshold calculated for each sample was used to relatively quantify the *EPC1* gene expression using the $2^{-\Delta\Delta CT}$ method expressed as Fold-Change (FC) (Livak & Schmittgen, 2001).

The miRNAs target identification analysis and their pathways

The gene targets of the miRNAs miR-23b-3p, and miR381-3p were identified *in silico* using several bioinformatic databases, that included predicted and experimentally validated targets. For predicted targets, the databases DIANA-microT-CDS (Reczko *et al.*, 2012; Paraskevopoulou *et al.*, 2013), EMMo (<https://mirz.unibas.ch/ELMMo3/index.php>), MicroCosm (<http://multimir.ucdenver.edu/>), miRanda (<http://mirdb.org/>), miRDB (<http://mirdb.org/>), PicTar (<https://pictar.mdc-berlin.de/>), PITA (Segal Lab of Computational Biology, https://genie.weizmann.ac.il/pubs/mir07/mir07_prediction.html), and TargetScanHuman (http://www.targetscan.org/vert_72/) were used. Additionally, the validated targets were searched in the miRecords (<http://c1.accurascience.com/miRecords/>), miRTarBase (Chou *et al.*, 2018), and TarBase (Karagkouni *et al.*, 2018). For each miRNA, we selected only those target genes which were present in at least three or more databases (Script in Supplemental Data). Moreover, to identify the biological pathways where these gene targets participate, we analyzed them further with the Gene Set Enrichment Analysis (GSEA) from WEB-based Gene Set Analysis Toolkit (WebGestalt, <http://www.webgestalt.org/>). Only those biological pathways with a False Discovery Rate (FDR) less than 0.05 were considered.

Statistical analysis

The presence or absence of morphological changes through the PMI in rats was evaluated with the Multiple Correspondence Analysis. The FC of each miRNA was compared among the PMIs with the non-parametric Kruskal Wallis and the Mann U Whitney test. Using the Cohen's d calculation and expecting a large effect size ($d = 0.8$), we expected a statistical power of 0.8 with the sample size of each group in the present study (Lakens, 2013). The dependence and association of the morphological changes with the PMI were evaluated with the Pearson's Chi-squared test and Cochran-Armitage test, respectively. To explore whether there is an association between the post-mortem interval and the expression of miR-381-3p and miR-23b-3p a Spearman Rho correlation was calculated. A Mixed Effect

Model was calculated considering the FC, the morphological changes of brain liquefaction and cerebral edema with PMI, as an independent variable ($y = X\beta + Z\gamma + \varepsilon$; where: y is the response vector of all the observations; X is a fixed effects design matrix; β is a fixed effects vector; Z is a random effects design matrix; γ is a random effects vector; and ε is the observation error vector) in the “lmerTest” package with the active option of the REML (Restricted Maximum Likelihood). All statistics were performed with the R-project software (<https://www.r-project.org/>). The dataset and scripts can be found in github (https://github.com/nshuerta-ForenseUNAM/Dysregulation_miRNA).

RESULTS

Morphological changes are heterogenous at different post-mortem intervals in rats

Internal and external physical changes were evaluated at different post-mortem intervals in 25 rats. The external physical changes evaluated included *algor mortis* (AM), *livor mortis* (LM), *rigor mortis* upper body (RMU), *rigor mortis* lower body (RML), drying (DR), generalized edema (ED), hair loss (HL), abdomen green discoloration (AGD) and abdominal distention (AD). All but RML, ED and AGD, appeared after the first 3 h of PMI (see Table 1). On the other hand, the AGD was not observed until the 12 h of PMI. In the case of *rigor mortis*, the RMU and the RML was only seen from 3 to 6 h-PMI and 6 to 12 h-PMI, respectively.

All animals were dissected to evaluate the following macroscopic characteristics: brain liquefaction (BL), brain edema (BE), discoloration of liver (DL), loss of liver consistency (LLC), muscle *livor mortis* (MML), bowel swelling (BS), ascites (AS), and loss of muscle consistency (LMC). As in the external characteristics, all these changes but for AS and LMC were gradually seen after 3 h of PMI. Interestingly, AS and LMC did not appear until 24 h-PMI and were present in 60 and 80% of the analyzed animals, respectively.

These morphological changes were evaluated in a Multiple Correspondence Analysis (MCA) in order to see how these characteristics group through the PMI (See Fig. 1A). The MCA plot captured at least the 74.2% of the data and, as it was expected, the morphological characteristics of the 0 h-PMI and the 24 h-PMI were located opposite from each other. Also, there were PMIs that clustered into three groups because they shared some morphological characteristics among them (See Fig. 1B). The first group included 0 and 3 h-PMI, the second the 6 and 12 h-PMI, and the third the 24 h-PMI. Group I is consistent with the few morphological changes present within the first 3 h of PMI, while group III is where all the early PMI physical characteristics have been established. However, in group II, there were characteristics that were present or absent in both, the 6 and 12 h-PMI, which did not allow to differentiate them in the MCA. These data suggest that the estimate of PMI using morphological changes could be more precise between 0 to 3 h-PMI and at 24 h-PMI of death.

Table 1 Presence of the external and internal macroscopic morphological characteristics in rats at different post-mortem intervals.

Morphological changes	Frequency %				
	0 h-PMI	3 h-PMI	6 h-PMI	12 h-PMI	24 h-PMI
External					
<i>Algor mortis</i> (AM)	0	100	100	100	100
<i>Livor mortis</i> (LM)	0	100	100	100	100
<i>Rigor mortis</i> upper body (RMU)	0	100	100	0	0
<i>Rigor mortis</i> lower body (RML)	0	0	100	100	0
Drying (DR)	0	100	100	100	100
Generalized Edema (ED)	0	0	100	100	100
Hair loss (HL)	0	100	100	100	100
Abdomen green discoloration (AGD)	0	0	0	40	100
Abdominal distention (AD)	0	100	100	100	100
Internal					
Brain liquefaction (BL)	0	40	60	100	100
Brain edema (BE)	0	20	100	100	100
Discoloration of liver (DL)	0	60	80	100	100
Loss liver consistency (LLC)	0	20	60	80	100
<i>Livor mortis</i> muscle (LMM)	0	60	60	100	100
Bowel swelling (BS)	0	20	100	100	100
Ascites (AS)	0	0	0	0	60
Loss muscle consistency (LMC)	0	0	0	0	80

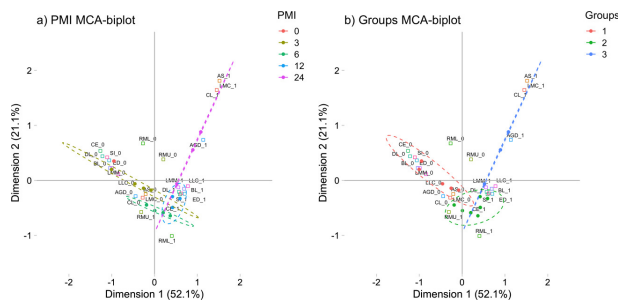


Figure 1 Multiple correspondence analysis (MCA) between the early post-mortem interval and the presence of morphological changes in rats. (A) MCA of the analyzed PMIs (0, 3, 6, 12 and 24 h) and the presence of internal and external morphological changes. (B) MCA of the PMIs groups I (0 and 3 h), II (6 and 12 h) and III (24 h), and the presence of internal and external morphological changes. Both plots represented the greatest cumulative variability and could capture at least the 74.2 % of the data. Abbreviations of the morphological characteristics are shown in Table 1. Dots represent each rat, while squares are the dichotomic presence of morphological changes (0: absence, 1: presence). The dashed line ellipses shown the distribution of the rats throughout the PMI.

Full-size [DOI: 10.7717/peerj.11102/fig-1](https://doi.org/10.7717/peerj.11102/fig-1)

miR-381-3p and miR-23b-3p showed gene expression imbalances throughout different PMIs in rats

The gene expression of miR-381-3p, miR-23b-3p, and miR-144-3p was analyzed using qRT-PCR in skeletal muscle of rats exposed to the aforementioned PMIs (see material and methods). Interestingly, miR-381-3p was found upregulated at the 24 h-PMI group of rats compared to the 0 h-PMI control (FC = 1.02 vs. FC = 1.96; $p = 0.0079$, Mann U Whitney test; Fig. 2A). When the FC of miR-381-3p was analyzed at different PMIs, the gene expression of this miRNA had a J-shape curve (see Fig. 2A). First, within the three hours of PMI, the expression of miR-381-3p was downregulated (FC = 0.73), compared to controls, and this difference was statistically significant ($p = 0.0317$, Mann U Whitney test; Fig. 2A). In fact, the difference in the miR-381-3p gene expression was more evident when comparing the 3hr-PMI with the 24 h-PMI ($p = 0.0079$, Mann U Whitney test). Nevertheless, after the 3 h-PMI, the expression of this miRNA gradually increased from 6 h of PMI to 24 h of PMI interval (see Fig. 2A). As it was expected, the difference in the gene expression between 3 h-PMI and 12 h-PMI was statistically significant ($p = 0.032$, Mann U Whitney test).

Contrary to miR-381-3p, the gene expression of miR-23b-3p decreased as the PMI increases to 24 h. The gene expression of miR-23b-3p was downregulated at 24 h-PMI compared to 0 h-PMI, and this difference was statistically significant (FC = 1.22 vs. FC = 0.13; $p = 0.0079$, Mann U Whitney test; Fig. 2B). Interestingly, when the FC of miR-23b-3p was analyzed by the PMIs, the expression of this miRNA decreased from the 3 h-PMI to the 24 h-PMI (see Fig. 2B). There were significant differences comparing 3 h-PMI vs 24 h-PMI ($p = 0.0079$, Mann U Whitney test), 6 h-PMI vs. 24 h-PMI ($p = 0.0079$, Mann U Whitney test) and 12 h-PMI vs. 24 h-PMI ($p = 0.0079$, Mann U Whitney test).

Finally, although the FC of miR-114-3p decreased from 0 h-PMI to 6 h-PMI, these differences were not significant ($p > 0.05$, Mann U Whitney test; see Fig. 2C). In fact, the FC remained unchanged in the following two post-mortem intervals. These results suggest that there is a dysregulation in gene expression of miR-381-3p and miR-23b-3p as the time of post-mortem interval increases in rats.

Biological process related to miR-381-3p and miR-23b-3p

Using different miRNAs bioinformatic databases (see material and methods), we identified the target genes of miR-381-3p and miR-23b-3p. A total of 2122 and 2076 genes were found to be regulated by miR-381-3p and miR-23b-3p, respectively (Table S1). With each set of genes, a Gene Ontology enrichment analysis was performed to find the main biological processes where they participate (see material and methods). In the case of miR-381-3p, a total of ten biological processes were found to be regulated by this miRNA (see Fig. 3A). Interestingly, some of these biological processes are related to RNA processing as transcription, synthesis and metabolism. Other processes involved with this miRNA, are the positive regulations of gene expression.

On the other hand, ten biological processes were associated with miR-23b-3p, which were different compared with the target genes of miR-381-3p (see Fig. 3B). For instance, the two most enriched biological processes were those related to hypoxia response and

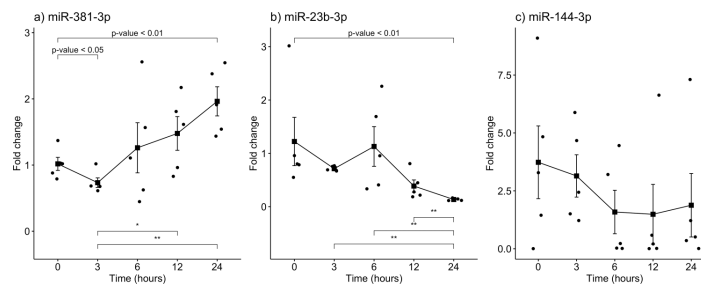


Figure 2 Gene expression analysis of miRNAs miR-381-3p, miR-23b-3p and miR-144-3p in rat skeletal muscle throughout the early different post-mortem interval. The Fold-Change (FC) of miRNAs (A). miR-381-3p (B). miR-23b-3p and (C). miR-144-3p was analyzed in rats skeletal muscle at 0, 3, 6, 12 and 24 hours of PMI using quantitative RT-qPCR. The Fold Change of each miRNA was calculated with the $2^{-\Delta\Delta CT}$ method using miR-361-5p as internal control. The black squares represent the mean of the FC from each group, the whisker corresponds to the 95% confidence interval and the dots are the jittered FC of each sample. Comparisons between the PMI were done with the Mann *U*-Whitney test. * *p*-value < 0.05, ** *p*-value < 0.01.

Full-size [DOI: 10.7717/peerj.11102/fig-2](https://doi.org/10.7717/peerj.11102/fig-2)

oxygen levels. On the other hand, there were processes related to the development of the central nervous system. Interestingly, other complex cellular pathways were implicated with this miRNA as positive regulation of signaling, phosphorylation and cell location. Although none of the biological processes where this miRNA participated are related to apoptosis and inflammation, it seems that their function in PMI would be related to the decomposition process of the body.

Gene expression analysis of *EPC1*

From the target gene list that is regulated by miR-381-3p, *EPC1* was selected for gene expression analyses with qRT-PCR in the same samples used for miRNAs analyses. Despite not seeing a trend as with miR-381-3p, there was a downregulation of *EPC1* gene expression at 3 h-PMI (FC = 1.04 vs. FC = 0.58; *p* = 0.05, Mann *U* Whitney test) and 12 h-PMI (FC = 1.04 vs. FC = 0.57; *p* = 0.01, Mann *U* Whitney test) compared to the control group of 0 h-PMI. These differences were statistically significant (see Fig. 4). Also, there was a slight increase in the expression of *EPC1* gene at 6 h-PMI and at 24 h-PMI compared to 0 h-PMI, though this was not significant. These results indicate that *EPC1* is down regulated or has no change in its expression at different post-mortem intervals.

Estimation of PMI analyzing gene expression of miR-381-3p

A Spearman Rho correlation was calculated with the FC of miR-381-3p from 3 h-PMI to 24 h-PMI, showing a value of $r = 1$ (*p* = 0.037). Since a descriptive pattern and association were observed in some variables, we considered that a model could give certainty that effects (fixed or random) affect the fold change of miR-381-3p. To evaluate this, a mixed effect model was calculated considering the FC (dependent variable), the morphological changes, and PMI as independent variables (see material and methods). From the morphological

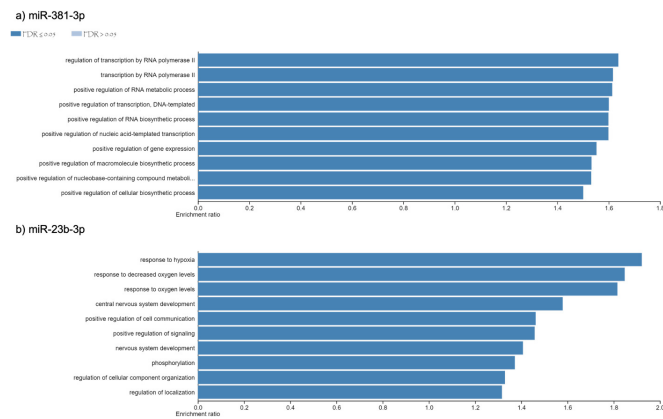


Figure 3 Gene Ontology enrichment analysis. The main biological pathways where the target genes of miRNAs (A) miR-381-3p and (B) miR-23b-3p participate are shown. The x-axis correspond to the enrichment ratio and all the biological pathways have a False Discovery rate less than 0.05.

Full-size [DOI: 10.7717/peerj.11102/fig-3](https://doi.org/10.7717/peerj.11102/fig-3)

changes analyzed, only the presence of brain liquefaction and brain edema were significantly associated with the FC ($p < 0.01$). An approach to estimate the FC according to PMI of miR-381-3p was done with this model. First, the FC values with respect to change of time (PMI) and the presence or absence of brain liquefaction and brain edema were estimated. Through this model, it is possible to indirectly calculate the PMI, comparing the real FC, with the calculated confidence interval of the estimated FC. The mean FC estimated for 0 h-PMI was 1.01 ± 0 (95% CI [1.01–1.01]), 3 h-PMI to 0.73 ± 0.04 (95% CI [0.69–0.77]), 6 h-PMI to 1.26 ± 0.64 (95% CI [0.62–1.90]), 12 h-PMI to 1.47 ± 0 (95% CI [1.47–1.47]), and 24 h-PMI to 1.96 ± 0 (95% CI [1.96–1.96]), respectively. It is important that there be no variability in the PMIs of 0, 12 and 24 h, in the estimated values for the FC, so the value in both limits is the same as the mean. According to our results, although the FC of miR-381-3p could be a good predictor of the 0, 3, 12 and 24 h-PMI, the high variability observed at 6 h-PMI hinders the estimation of an accurate interval of PMI according to FC. Albeit the Spearman Rho correlation was negatively significant to the FC of miR-23b-3p according to PMI ($r = -0.9$, $p < 0.05$), there was no significance in the PMI and morphological variables when the mixed effects model was calculated (data not shown).

DISCUSSION

In the present work we found a gene expression dysregulation of miRNAs miR-381-3p and miR-23b-3p in skeletal muscle tissue of rats exposed to different post-mortem intervals compared to the control group. The miR-23b-3p gene expression decreased from 3 to 24 h of PMI. On the contrary, the gene expression of miR-381-3p increased, with a

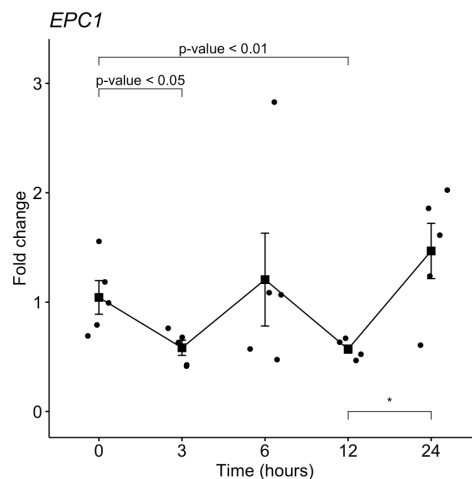


Figure 4 Gene expression analysis of *EPC1* gene in rat skeletal muscle at early post-mortem interval. The Fold-Change (FC) of *EPC1* was analyzed in rats skeletal muscle at 3, 6, 12 and 24 hours of PMI relatively to the 0 h-PMI group, using quantitative RT-qPCR. The Fold Change was calculated with the $2^{-\Delta\Delta CT}$ method using as internal control. The black squares represent the mean of the FC from each group, the whisker corresponds to the 95% confidence interval and the dots are the jittered FC of each sample. Comparisons between the PMI were done with the Mann *U*-Whitney test. * *p*-value < 0.05, ** *p*-value < 0.01.

Full-size [DOI: 10.7717/peerj.11102/fig-4](https://doi.org/10.7717/peerj.11102/fig-4)

J-shape curve, as the PMI increased. These two miRNAs regulate the expression of genes which participate in different processes as hypoxia or oxygen depletion sensing, and RNA transcription. Moreover, the gene expression of *EPC1*, which is a gene target of miR-381-3p, was found downregulated or with no change at early PMI, compared to the 0-PMI. Using a mixed effect model, the Fold-change of miR-381-3p could be predicted at 0, 3, 12 and 24 h of PMI.

The presence of several miRNAs in various tissues has been described through the PMI in humans and in rats (Lv *et al.*, 2017; Tu *et al.*, 2019). However, the analyzed gene expression of some miRNAs has been mainly focused in finding control genes potentially useful for PMI calculation based on gene expression analysis in death bodies. For instance, the gene expression of miR-9 and miR-125b barely fluctuates throughout the different PMI analyzed in spleen (Lv *et al.*, 2014). Nevertheless, within the first 24 h of PMI, an upregulation or downregulation of some miRNAs has also been found (Lv *et al.*, 2014). In the rat's brain, a slight downregulation of miR-16 was found throughout the 24 h of PMI (Nagy *et al.*, 2015). On the contrary, miR-124a, miR-205, and miR-21 were found upregulated within the first 24 h of PMI in brain and skin (Nagy *et al.*, 2015; Ibrahim *et al.*, 2019). These studies and our results suggest that some miRNAs could be actively involved

in the decomposition process, possibly regulating the expression of other genes, rather than being inert molecules which heavily resist degradation.

After the death of an individual, the autolysis process is seen as a necessary step to achieve body decomposition, and it occurs nearly immediately after the death of the individual (Zapico, Menéndez & Núñez, 2014). Nevertheless, more than the liberation of enzymes and proteasomal degradation, the autolysis process is a complex process, where a struggle between survival and pro-apoptical signals takes place (Sanoudou et al., 2004). On the other hand, it has been reported that several genes, some of them related to cell survival, are dysregulated in the PMI, and could last for several days (Sanoudou et al., 2004; Zhu et al., 2017; Ferreira et al., 2018). Thus, it is possible that those genes transcriptionally active favor the body decomposition activating pathways such as apoptosis (Zapico, Menéndez & Núñez, 2014). This can also be seen in the biological pathways where the gene targets of the altered miRNAs found in our study participate. Each miRNA regulates different processes that could be related to the autolysis process such as RNA transcription or oxygen levels sensing.

In humans, the miR-381 has been considered as a tumor suppressor in prostate and non-small cell lung cancer inhibiting cell proliferation, invasion and migration through inhibition of nuclear factor- κ B signaling (Formosa et al., 2014; Huang et al., 2018). Regarding the PMI, the increase of this miRNA expression could be as a mechanism for promoting apoptosis related to oxidative stress produced by the hypoxia. Another mechanism where miR-381 could participate in PMI is the inflammation inhibition in the autolysis process (Chen et al., 2018a). Interestingly, we found a downregulation of *EPC1* gene at 3 h-PMI and 12 h-PMI compared to the control group of 0-PMI, and no change at 6 and 24 of PMI. The enhancer of polycomb homolog 1 (*EPC1*) gene codes for a protein member of the polycomb group (PcG) family and is gene target of miR-381 (Kozomara, Birgaoanu & Griffiths-Jones, 2019). The coded product of *EPC1* is a part of the NuA4 (Nucleosome Acetyltransferase of H)/TIP60 (Tat Interacting Protein 60) acetyltransferase complex, which participates in several processes to repair DNA double strand breaks (DBSs) and apoptosis (Zhang et al., 2020). Also, it has been reported that *EPC1* acts as an oncogene in some types of cancer, such as acute myeloid leukemia (AML), since its suppression triggered apoptosis in cell lines (Huang et al., 2014). Our results suggest that one of the mechanisms in of miR-381 that may promote apoptosis could be by down-regulation of *EPC1*, although these results should be confirmed in further works to understand these mechanisms in the PMI.

Contrary to miR-381, the miR-23b-3p showed a gradual reduction of its expression throughout the analyzed PMIs. The miR-23b-3p has been considered as an onco-miR in several types of cancers, such as gastric or breast cancer (Chen et al., 2012; Hu et al., 2017). Also, it has been found in osteosarcoma that miR-23b-3p promotes cell proliferation, while inhibiting oxidative phosphorylation increasing the lactate levels in these cells (Zhu, Li & Ma, 2019). Nonetheless, it is important to emphasize that these results were found in cancer, which could differ from PMI, where the metabolism of the cell is strictly anaerobic (Donaldson & Lamont, 2015). The proliferation mediated by miR-23b-3p is due to activation of TGF- β signaling by inhibition of *TGIF1* (Barbollat-Boutrand et al., 2017).

Also, miR-23b-3p regulates many genes which participate in processes related to oxygen consumption. The participation of this miRNA in the PMI could be in the regulation of the expression of genes related to the response of lower levels of oxygen, which is expected due to the oxygen deprivation in the dead body. For instance, it has been found in mice, that in the first 24 h of PMI, there is an upregulation of hypoxia-related gene transcripts as *Degs2* (Pozhitkov et al., 2017). Although we could not discard that the downregulation found on miR-23b-3p at the PMI is due to a higher degradation rate compared to other miRNAs at PMI, its function seems to be closely related with oxygen deprivation present at PMI.

Several works have used the C_T obtained from some genes to estimate the PMI through univariate or multivariate linear regression analyses with high coefficient of determination (Li et al., 2014; Lv et al., 2014; Tu et al., 2019). In our study we used the FC, which relatively estimates the change in expression compared to a control group. From the three miRNAs that we analyzed, the only significant model to estimate the FC was miR-381-3p with a good coefficient of determination ($r^2 = 0.91$). Except for the 6 h-PMI, we were able to estimate the FC according to the 3, 12 and 24 h of PMI. This could be due to a high variability of miR-381-3p expression found at 6 h-PMI, that may be related to individual differences in the autolysis process at this PMI. Interestingly, this variability was also seen in the physical characteristics of the rats at this PMI, which was corroborated in the Multiple Correspondence Analysis. One explanation for this variability is that, at this PMI, there is a heterogeneity in rat's body decomposition; thus, we found rats that presented morphological changes above or below the 6 h mark.

Although we found differences in the gene expression of miR-381-3p and miR-23b-3p in rat skeletal muscle throughout the post-mortem interval, it is important to mention the limitations of the present study. For instance, the sample size from each group in the present study is limited and the findings should be taken as exploratory. Also, it is possible that the analyzed PMIs could not fully reflect the main biological processes occurring in the early post-mortem interval, so further studies involving more PMIs would be required to better define these processes. Since the PMI is a complex biological process, it is probable that there are other miRNAs interacting with other genes in this process. Finally, the conditions of the experiments were performed in an animal model by controlling the environmental conditions, such as temperature and humidity, which can differ drastically from real forensic scenarios. For this reason, we cannot discard that the expression of these miRNAs could vary across different environmental conditions.

CONCLUSIONS

The gene expression dysregulation of miR-381-3p and miR-23b-3p found in rat muscle at early post-mortem intervals, suggest that these miRNAs participate in the autolysis process. The targets of these miRNAs are involved in pathways related to hypoxia, apoptosis and RNA metabolism. The *EPC1* gene target of miR-381-3p was found downregulated or with no change at an early post-mortem interval. Although miR-381-3p gene expression could be a promising biomarker for post-mortem interval estimation, further studies will be required to refine these predictions.

ACKNOWLEDGEMENTS

This study was part of the dissertation to obtain the Ms C. degree of Vanessa Martínez Rivera at the Posgrado de Maestría en Ciencias Biológicas, Universidad Nacional Autónoma de México (UNAM).

ADDITIONAL INFORMATION AND DECLARATIONS

Funding

This work was supported by the National Autonomous University of Mexico (UNAM), PAPIIT grant number IA204420. The funders had no role in study design, data collection and analysis, decision to publish, or preparation of the manuscript.

Grant Disclosures

The following grant information was disclosed by the authors:
National Autonomous University of Mexico (UNAM).
PAPIIT: IA204420.

Competing Interests

The authors declare there are no competing interests.

Author Contributions

- Vanessa Martínez-Rivera performed the experiments, analyzed the data, prepared figures and/or tables, authored or reviewed drafts of the paper, and approved the final draft.
- Christian A. Cárdenas-Monroy, Oliver Millan-Catalan and Jessica González-Corona performed the experiments, prepared figures and/or tables, and approved the final draft.
- N. Sofia Huerta-Pacheco and Antonio Martínez-Gutiérrez analyzed the data, prepared figures and/or tables, and approved the final draft.
- Alexa Villavicencio-Queijeiro performed the experiments, authored or reviewed drafts of the paper, and approved the final draft.
- Carlos Pedraza-Lara performed the experiments, prepared figures and/or tables, authored or reviewed drafts of the paper, and approved the final draft.
- Alfredo Hidalgo-Miranda analyzed the data, authored or reviewed drafts of the paper, and approved the final draft.
- María Elena Bravo-Gómez and Carlos Pérez-Plasencia analyzed the data, prepared figures and/or tables, authored or reviewed drafts of the paper, and approved the final draft.
- Mariano Guardado-Estrada conceived and designed the experiments, analyzed the data, prepared figures and/or tables, authored or reviewed drafts of the paper, and approved the final draft.

Animal Ethics

The following information was supplied relating to ethical approvals (i.e., approving body and any reference numbers):

The committee for the care and use of laboratory animals (CICUAL) of the Faculty of Medicine from the National Autonomous University of Mexico (UNAM) with approval number 027-CIC-2018.

Ethics

The following information was supplied relating to ethical approvals (i.e., approving body and any reference numbers):

The local ethic and scientific committee of the Faculty of Medicine from the National Autonomous University of Mexico (UNAM) approved this research (approval number 102-2018).

Data Availability

The following information was supplied regarding data availability:

The script used to select the targets of the analyzed miRNAs and the dataset and scripts used for the miRNAs analysis are available at GitHub: https://github.com/nshuerta-ForensUNAM/Dysregulation_miRNA.

Supplemental Information

Supplemental information for this article can be found online at <http://dx.doi.org/10.7717/peerj.11102#supplemental-information>.

REFERENCES

- Ansari N, Menon SK. 2017.** Determination of time since death using vitreous humor tryptophan. *Journal of Forensic Sciences* 62:1351–1356 DOI 10.1111/1556-4029.13430.
- Barbollat-Boutrand L, Joly-Tonetti N, Dos Santos M, Metral E, Boher A, Masse I, Berthier-Vergnes O, Bertolino P, Damour O, Lamartine J. 2017.** MicroRNA-23b-3p regulates human keratinocyte differentiation through repression of TGIF1 and activation of the TGF- β -SMAD2 signalling pathway. *Experimental Dermatology* 26:51–57 DOI 10.1111/exd.13119.
- Brooks JW. 2016.** Postmortem changes in animal carcasses and estimation of the postmortem interval. *Veterinary Pathology* 53:929–940 DOI 10.1177/0300985816629720.
- Chen L, Han L, Zhang K, Shi Z, Zhang J, Zhang A, Wang Y, Song Y, Li Y, Jiang T, Pu P, Jiang C, Kang C. 2012.** VHL regulates the effects of miR-23b on glioma survival and invasion via suppression of HIF-1 α /VEGF and β -catenin/Tcf-4 signaling. *Neuro-Oncology* 14:1026–1036 DOI 10.1093/neuonc/nos122.
- Chen WC, Luo J, Cao XQ, Cheng XG, He DW. 2018a.** Overexpression of miR-381-3p promotes the recovery of spinal cord injury. *European Review for Medical and Pharmacological Sciences* 22:5429–5437 DOI 10.26355/eurrev_201809_15802.
- Chen G, Ma Y, Jiang Z, Feng Y, Han Y, Tang Y, Zhang J, Ni H, Li X, Li N. 2018b.** Lico A causes ER stress and apoptosis via up-regulating miR-144-3p in human lung cancer cell line H292. *Frontiers in Pharmacology* 9:837 DOI 10.3389/fphar.2018.00837.

- Chou C-H, Shrestha S, Yang C-D, Chang N-W, Lin Y-L, Liao K-W, Huang W-C, Sun T-H, Tu S-J, Lee W-H, Chiew M-Y, Tai C-S, Wei T-Y, Tsai T-R, Huang H-T, Wang C-Y, Wu H-Y, Ho S-Y, Chen P-R, Chuang C-H, Hsieh P-J, Wu Y-S, Chen W-L, Li M-J, Wu Y-C, Huang X-Y, Ng FL, Buddhakosai W, Huang P-C, Lan K-C, Huang C-Y, Weng S-L, Cheng Y-N, Liang C, Hsu W-L, Huang H-D. 2018. miRTarBase update 2018: a resource for experimentally validated microRNA-target interactions. *Nucleic Acids Research* 46:D296–D302 DOI 10.1093/nar/gkx1067.
- Della Bella E, Stoddart MJ. 2019. Cell detachment rapidly induces changes in noncoding RNA expression in human mesenchymal stromal cells. *BioTechniques* 67:286–293 DOI 10.2144/btn-2019-0038.
- Dix J. 1999. *Time of Death, Decomposition and Identification: An Atlas*. (1st ed.). Boca Raton: CRC Press DOI 10.4324/9780367806422.
- Donaldson AE, Lamont IL. 2015. Metabolomics of post-mortem blood: identifying potential markers of post-mortem interval. *Metabolomics* 11:237–245 DOI 10.1007/s11306-014-0691-5.
- Ferreira PG, Muñoz Aguirre M, Reverter F, Godinho CPSá, Sousa A, Amadoz A, Sodaei R, Hidalgo MR, Pervouchine D, Carbonell-Caballero J, Nurtdinov R, Breschi A, Amador R, Oliveira P, Çubuk C, Curado J, Aguet F, Oliveira C, Dopazo J, Sammeth M, Ardlie KG, Guigó R. 2018. The effects of death and post-mortem cold ischemia on human tissue transcriptomes. *Nature Communications* 9:490 DOI 10.1038/s41467-017-02772-x.
- Formosa A, Markert EK, Lena AM, Italiano D, Finazzi-Agro' E, Levine AJ, Bernardini S, Garabadgiu AV, Melino G, Candi E. 2014. MicroRNAs, miR-154, miR-299-5p, miR-376a, miR-376c, miR-377, miR-381, miR-487b, miR-485-3p, miR-495 and miR-654-3p, mapped to the 14q32.31 locus, regulate proliferation, apoptosis, migration and invasion in metastatic prostate cancer cells. *Oncogene* 33:5173–5182 DOI 10.1038/onc.2013.451.
- Hu X, Wang Y, Liang H, Fan Q, Zhu R, Cui J, Zhang W, Zen K, Zhang C-Y, Hou D, Zhou Z, Chen X. 2017. miR-23a/b promote tumor growth and suppress apoptosis by targeting PDCD4 in gastric cancer. *Cell Death & Disease* 8:e3059–e3059 DOI 10.1038/cddis.2017.447.
- Huang X, Spencer GJ, Lynch JT, Ciceri F, Somerville TDD, Somerville TCP. 2014. Enhancers of Polycomb EPC1 and EPC2 sustain the oncogenic potential of MLL leukemia stem cells. *Leukemia* 28:1081–1091 DOI 10.1038/leu.2013.316.
- Huang R, Zheng Y, Zhao J, Chun X. 2018. microRNA-381 suppresses the growth and increases cisplatin sensitivity in non-small cell lung cancer cells through inhibition of nuclear factor- κ B signaling. *Biomedicine & Pharmacotherapy* 98:538–544 DOI 10.1016/j.biopha.2017.12.092.
- Ibrahim SF, Ali MM, Basyouni H, Rashed LA, Amer EAE, El-Kareem DAbd. 2019. Histological and miRNAs postmortem changes in incisional wound. *Egyptian Journal of Forensic Sciences* 9:37 DOI 10.1186/s41935-019-0141-7.

- Itani M, Yamamoto Y, Doi Y, Miyaishi S. 2011.** Quantitative analysis of DNA degradation in the dead body. *Acta medica Okayama* **65**:299–306
DOI [10.18926/AMO/47011](https://doi.org/10.18926/AMO/47011).
- Jiang X, Yu M, Zhu T, Lou L, Chen X, Li Q, Wei D, Sun R. 2020.** Kcnq1ot1/miR-381-3p/ETS2 axis regulates inflammation in mouse models of acute respiratory distress syndrome. *Molecular Therapy—Nucleic Acids* **19**:179–189
DOI [10.1016/j.omtn.2019.10.036](https://doi.org/10.1016/j.omtn.2019.10.036).
- Karagkouni D, Paraskevopoulou MD, Chatzopoulos S, Vlachos IS, Tastsoglou S, Kanellos I, Papadimitriou D, Kavakiotis I, Maniou S, Skoufos G, Vergoulis T, Dalamagas T, Hatzigeorgiou AG. 2018.** DIANA-TarBase v8: a decade-long collection of experimentally supported miRNA–gene interactions. *Nucleic Acids Research* **46**:D239–D245 DOI [10.1093/nar/gkx1141](https://doi.org/10.1093/nar/gkx1141).
- Koppelkamm A, Vennemann B, Lutz-Bonengel S, Fracasso T, Vennemann M. 2011.** RNA integrity in post-mortem samples: influencing parameters and implications on RT-qPCR assays. *International Journal of Legal Medicine* **125**:573–580
DOI [10.1007/s00414-011-0578-1](https://doi.org/10.1007/s00414-011-0578-1).
- Kozomara A, Birgaoanu M, Griffiths-Jones S. 2019.** miRBase: from microRNA sequences to function. *Nucleic Acids Research* **47**:D155–D162
DOI [10.1093/nar/gky1141](https://doi.org/10.1093/nar/gky1141).
- Lakens D. 2013.** Calculating and reporting effect sizes to facilitate cumulative science: a practical primer for *t*-tests and ANOVAs. *Frontiers in psychology* **4**:863
DOI [10.3389/fpsyg.2013.00863](https://doi.org/10.3389/fpsyg.2013.00863).
- Lee Goff M. 2009.** Early post-mortem changes and stages of decomposition in exposed cadavers. *Experimental and Applied Acarology* **49**:21–36
DOI [10.1007/s10493-009-9284-9](https://doi.org/10.1007/s10493-009-9284-9).
- Li W-C, Ma K-J, Lv Y-H, Zhang P, Pan H, Zhang H, Wang H-J, Ma D, Chen L. 2014.** Postmortem interval determination using 18S-rRNA and microRNA. *Science & Justice* **54**:307–310 DOI [10.1016/j.scijus.2014.03.001](https://doi.org/10.1016/j.scijus.2014.03.001).
- Livak KJ, Schmittgen TD. 2001.** Analysis of relative gene expression data using real-time quantitative PCR and the $2^{-\Delta\Delta CT}$ method. *Methods* **25**:402–408
DOI [10.1006/meth.2001.1262](https://doi.org/10.1006/meth.2001.1262).
- Lv Y-H, Ma J-L, Pan H, Zeng Y, Tao L, Zhang H, Li W-C, Ma K-J, Chen L. 2017.** Estimation of the human postmortem interval using an established rat mathematical model and multi-RNA markers. *Forensic Science, Medicine, and Pathology* **13**:20–27
DOI [10.1007/s12024-016-9827-4](https://doi.org/10.1007/s12024-016-9827-4).
- Lv Y, Ma K, Zhang H, He M, Zhang P, Shen Y, Jiang N, Ma D, Chen L. 2014.** A time course study demonstrating mRNA, microRNA, 18S rRNA, and U6 snRNA changes to estimate PMI in deceased rat's spleen. *Journal of Forensic Sciences* **59**:1286–1294
DOI [10.1111/1556-4029.12447](https://doi.org/10.1111/1556-4029.12447).
- Madea B. 2016.** Methods for determining time of death. *Forensic Science, Medicine, and Pathology* **12**:451–485 DOI [10.1007/s12024-016-9776-y](https://doi.org/10.1007/s12024-016-9776-y).
- Madea B, Käferstein H, Hermann N, Sticht G. 1994.** Hypoxanthine in vitreous humor and cerebrospinal fluid—a marker of postmortem interval and prolonged (vital)

- hypoxia? Remarks also on hypoxanthine in SIDS. *Forensic Science International* 65:19–31 DOI 10.1016/0379-0738(94)90296-8.
- Madea B, Kreuser C, Banaschak S. 2001. Postmortem biochemical examination of synovial fluid—a preliminary study. *Forensic Science International* 118:29–35 DOI 10.1016/S0379-0738(00)00372-8.
- Maile AE, Inoue CG, Barksdale LE, Carter DO. 2017. Toward a universal equation to estimate postmortem interval. *Forensic Science International* 272:150–153 DOI 10.1016/j.forsciint.2017.01.013.
- Muñoz Barús JI, Suárez-Peñaranda JM, Otero XL, Rodríguez-Calvo MS, Costas E, Miguéns X, Concheiro L. 2002. Improved estimation of postmortem interval based on differential behaviour of vitreous potassium and hypoxanthine in death by hanging. *Forensic Science International* 125:67–74 DOI 10.1016/S0379-0738(01)00616-8.
- Na J-Y. 2020. Estimation of the post-mortem interval using microRNA in the bones. *Journal of Forensic and Legal Medicine* 75:102049 DOI 10.1016/j.jflm.2020.102049.
- Nagy C, Maheu M, Lopez JP, Vaillancourt K, Cruceanu C, Gross JA, Arnovitz M, Mechawar N, Turecki G. 2015. Effects of postmortem interval on biomolecule integrity in the brain. *Journal of Neuropathology & Experimental Neurology* 74:459–469 DOI 10.1097/NEN.0000000000000190.
- Paraskevopoulou MD, Georgakilas G, Kostoulas N, Vlachos IS, Vergoulis T, Reczko M, Filippidis C, Dalamagas T, Hatzigeorgiou AG. 2013. DIANA-microT web server v5.0: service integration into miRNA functional analysis workflows. *Nucleic Acids Research* 41:W169–W173 DOI 10.1093/nar/gkt393.
- Pozhitkov AE, Neme R, Domazet-Lošo T, Leroux BG, Soni S, Tautz D, Noble PA. 2017. Tracing the dynamics of gene transcripts after organismal death. *Open Biology* 7:160267 DOI 10.1098/rsob.160267.
- Reczko M, Maragkakis M, Alexiou P, Grosse I, Hatzigeorgiou AG. 2012. Functional microRNA targets in protein coding sequences. *Bioinformatics* 28:771–776 DOI 10.1093/bioinformatics/bts043.
- Sanoudou D, Kang PB, Haslett JN, Han M, Kunkel LM, Beggs AH. 2004. Transcriptional profile of postmortem skeletal muscle. *Physiological Genomics* 16:222–228 DOI 10.1152/physiolgenomics.00137.2003.
- Tomita Y, Nihira M, Ohno Y, Sato S. 2004. Ultrastructural changes during in situ early postmortem autolysis in kidney, pancreas, liver, heart and skeletal muscle of rats. *Legal Medicine* 6:25–31 DOI 10.1016/j.legalmed.2003.09.001.
- Tu C, Du T, Ye X, Shao C, Xie J, Shen Y. 2019. Using miRNAs and circRNAs to estimate PMI in advanced stage. *Legal Medicine* 38:51–57 DOI 10.1016/j.legalmed.2019.04.002.
- Vishnoi A, Rani S. 2017. MiRNA biogenesis and regulation of diseases: an overview. In: *Methods in molecular biology*. vol. 1509. New York: Humana Press DOI 10.1007/978-1-4939-6524-3_1.
- Wang H, Mao J, Li Y, Luo H, Wu J, Liao M, Liang W, Zhang L. 2013. 5 miRNA expression analyze in post-mortem interval (PMI) within 48 h. *Forensic Science International* 4:e190–e191 DOI 10.1016/j.fsigs.2013.10.098.

- Zapico CS, Menéndez ST, Núñez P. 2014.** Cell death proteins as markers of early postmortem interval. *Cellular and Molecular Life Sciences* **71**:2957–2962 DOI [10.1007/s00018-013-1531-x](https://doi.org/10.1007/s00018-013-1531-x).
- Zhang H, Devoucoux M, Song X, Li L, Ayaz G, Cheng H, Tempel W, Dong C, Loppnau P, Côté J, Min J. 2020.** Structural basis for EPC1-mediated recruitment of MBTD1 into the NuA4/TIP60 acetyltransferase complex. *Cell Reports* **30**:3996–4002.e4 DOI [10.1016/j.celrep.2020.03.003](https://doi.org/10.1016/j.celrep.2020.03.003).
- Zhou W, Xu J, Wang C, Shi D, Yan Q. 2019.** miR-23b-3p regulates apoptosis and autophagy via suppressing SIRT1 in lens epithelial cells. *Journal of Cellular Biochemistry* **120**:19635–19646 DOI [10.1002/jcb.29270](https://doi.org/10.1002/jcb.29270).
- Zhu R, Li X, Ma Y. 2019.** miR-23b-3p suppressing PGC1 α promotes proliferation through reprogramming metabolism in osteosarcoma. *Cell Death & Disease* **10**:381 DOI [10.1038/s41419-019-1614-1](https://doi.org/10.1038/s41419-019-1614-1).
- Zhu Y, Wang L, Yin Y, Yang E. 2017.** Systematic analysis of gene expression patterns associated with postmortem interval in human tissues. *Scientific Reports* **7**:5435 DOI [10.1038/s41598-017-05882-0](https://doi.org/10.1038/s41598-017-05882-0).
- Zilg B, Bernard S, Alkass K, Berg S, Druid H. 2015.** A new model for the estimation of time of death from vitreous potassium levels corrected for age and temperature. *Forensic Science International* **254**:158–166 DOI [10.1016/j.forsciint.2015.07.020](https://doi.org/10.1016/j.forsciint.2015.07.020).

- 8.4. Figueroa-Gonzalez G., Carrillo-Hernandez, J.,...,Martinez-Gutierrez, Antonio-D., et al. Negative regulation of serine threonine kinase 11 (Stk11) through mir-100 in head and neck cancer. *Genes*. 2020

Article

Negative Regulation of Serine Threonine Kinase 11 (STK11) through miR-100 in Head and Neck Cancer

Gabriela Figueroa-González ^{1,2,†}, José F. Carrillo-Hernández ^{2,†}, Itzel Perez-Rodriguez ², David Cantú de León ², Alma D. Campos-Parra ², Antonio D. Martínez-Gutiérrez ², Jossimar Coronel-Hernández ², Verónica García-Castillo ³, César López-Camarillo ⁴, Oscar Peralta-Zaragoza ⁵, Nadia J. Jacobo-Herrera ⁶, Mariano Guardado-Estrada ⁷ and Carlos Pérez-Plasencia ^{2,3,*}

¹ Unidad Multidisciplinaria de Investigación Experimental Zaragoza (UMIEZ), Facultad de Estudios Superiores Zaragoza, Universidad Nacional Autónoma de México, Mexico City 09230, Mexico; gabufg@gmail.com

² Unidad de Investigación Biomédica en Cáncer, Laboratorio de Genómica, Instituto Nacional de Cancerología, Mexico City 14080, Mexico; josejosecarr@gmail.com (J.F.C.-H.); perez.itzel3e@gmail.com (I.P.-R.); dfcantu@gmail.com (D.C.d.L.); adcamposparra@gmail.com (A.D.C.-P.); maga94@comunidad.unam.mx (A.D.M.-G.); jossithunders@gmail.com (J.C.-H.)

³ Unidad de Investigación Biomédica en Cáncer, Laboratorio de Genómica del Cáncer, Facultad de Estudios Superiores Iztacala, Universidad Nacional Autónoma de México, Tlalnepantla 54090, Edo.Mex, Mexico; veronica_garcia_367@hotmail.com

⁴ Posgrado en Ciencias Genómicas, Universidad Autónoma de la Ciudad de México, Mexico City 09790, Mexico; genomicas@yahoo.com.mx

⁵ Dirección de Infecciones Crónicas y Cáncer, Centro de Investigación Sobre Enfermedades Infecciosas, Instituto Nacional de Salud Pública, Cuernavaca 62100, Morelos, Mexico; operalta@insp.mx

⁶ Unidad de Bioquímica, Instituto Nacional de Nutrición y Ciencias Médicas, Salvador Zubirán, Mexico City 14000, Mexico; nadia.jacobo@gmail.com

⁷ Laboratorio de Genética, Licenciatura en Ciencia Forense, Facultad de Medicina, Universidad Nacional Autónoma de México, Mexico City 04360, Mexico; mguardado@cienciaforense.facmed.unam.mx

* Correspondence: carlos.pplas@gmail.com; Tel.: +52-55-5628-0400

† Both authors contributed equally to this work.

Received: 2 July 2020; Accepted: 25 August 2020; Published: 8 September 2020



Abstract: Background: Serine Threonine Kinase 11 (STK11), also known as LKB1, is a tumor suppressor gene that regulates several biological processes such as apoptosis, energetic metabolism, proliferation, invasion, and migration. During malignant progression, different types of cancer inhibit STK11 function by mutation or epigenetic inactivation. In Head and Neck Cancer, it is unclear what mechanism is involved in decreasing STK11 levels. Thus, the present work aims to determine whether STK11 expression might be regulated through epigenetic or post-translational mechanisms. Methods: Expression levels and methylation status for STK11 were analyzed in 59 cases of head and neck cancer and 10 healthy tissue counterparts. Afterward, we sought to identify candidate miRNAs exerting post-transcriptional regulation of STK11. Then, we assessed a luciferase gene reporter assay to know if miRNAs directly target STK11 mRNA. The expression levels of the clinical significance of miR-100-3p, -5p, and STK11 in 495 HNC specimens obtained from the TCGA database were further analyzed. Finally, the Kaplan–Meier method was used to estimate the prognostic significance of the miRNAs for Overall Survival, and survival curves were compared through the log-rank test. Results: STK11 was under-expressed, and its promoter region was demethylated or partially methylated. miR-17-5p, miR-106a-5p, miR-100-3p, and miR-100-5p could be negative regulators of STK11. Our experimental data suggested evidence that miR-100-3p and -5p were over-expressed in analyzed tumor patient samples. Luciferase gene reporter assay experiments showed that miR-100-3p targets and down-regulates STK11 mRNA directly. With respect to overall survival, STK11 expression level was significant for predicting clinical outcomes. Conclusion: This is,

to our knowledge, the first report of miR-100-3p targeting STK11 in HNC. Together, these findings may support the importance of regulation of STK11 through post-transcriptional regulation in HNC and the possible contribution to the carcinogenesis process in this neoplasia.

Keywords: microRNA; mir-100; *STK11*; promoter methylation; head and neck cancer

1. Introduction

Head and Neck cancer (HNC) is the sixth most common cancer worldwide, and approximately 200,000 annual deaths are attributed to this type of cancer [1]. Head and neck squamous cell carcinoma comprises more than 95% of all HNC [2]. In addition, HNC is a heterogeneous disease affecting different anatomical areas such as oral cavity, oropharynx, hypopharynx and larynx [3]. It has been established that tobacco, alcohol, and their synergistic effect are strong risk factors for HNC development [4,5]; nevertheless, the presence of high-risk human papillomaviruses (HPVs) has also been reported, and they are considered to be etiological agents for some of these cancers [6].

As previously mentioned, this malignancy is determined by several alterations and risk factors, which in combination lead to greater tumor heterogeneity and thus pose a complex challenge for treatment [7]. There are molecular markers, such as HPV-positivity, that could indicate increased sensitivity to some chemotherapeutics such as roscovitine [8]. Despite this, it is of great interest in the research and clinical fields to fully understand the molecular events that generate this carcinogenic process and to clearly identify the key genes at the center of its regulation; this knowledge is imperative in the quest for novel therapeutic approaches and therapies.

Liver Kinase B1, LKB1 (coded by *STK11* gene), is a tumor suppressor gene that regulates several biological pathways such as p53-dependent apoptosis, energetic metabolism, fatty acid biosynthesis, proliferation, and cell cycle polarity [9–12]. Moreover, LKB1 phosphorylates and activates AMP-activated protein kinase (AMPK). The LKB1/AMPK pathway negatively regulates cancer cell proliferation and metabolism, and is also involved in tumor invasion and migration, as an important carcinoma progression hallmark [13]. Human *STK11* gene is located on chromosome 19p13.3 [14]; loss-of-function mutations in its coding sequence have been found in lung [15,16], breast [17,18], cervical [15], pancreatic and biliary carcinomas [15,19,20], and also in testicular cancer, malignant melanoma [21,22], hepatocellular carcinoma [23], and HNC [24]. Recent reports suggest that *STK11* might play an important role in tumor cell proliferation and invasion capacity through regulation of p53 and p21/WAF1 expression [25]. Hence, *STK11* could control the regulation of important hallmarks of cancer such as cellular energetics and cell proliferation, among others.

The function of LKB1 is regulated by diverse mechanisms in different types of tumors, with loss of heterozygosity LOH [26], somatic mutations that inactivate the function of the protein (for an extensive review [27]), and hyper-methylation in the promoter region of the gene [28,29] having been observed. Regarding the negative regulation exerted by microRNAs on *STK11* expression in human cancers, it has been reported that miR-199a, miR-17 and miR-155 might regulate *STK11* expression in cervical cancer [30–32]; in pancreatic cancer miR-7 represses autophagy via directly targeting LKB1 [33]. Remarkably, despite the role that *STK11* plays in regulating various hallmarks of cancer there is little information on the inhibition afforded by microRNAs. In the present study, we investigate the epigenetic and post-transcriptional mechanisms involved in controlling the expression of *STK11* in HNC. To our knowledge, this is the first report suggesting evidence that downregulation of *STK11* in HNC is not attributable to gene promoter methylation, but to post-transcriptional regulation in which miR-100-3p had a negative regulation on LKB1 mRNA level through the union to its 3' UTR region. Finally, data obtained from the TCGA expression database showed a significant correlation between *STK11* expression and overall survival in HNC.

2. Materials and Methods

2.1. Clinical Samples

Our study included 59 patients prospectively enrolled in the National Cancer Institute of Mexico (Instituto Nacional de Cancerología, INCan) tumor bank protocol. All patients signed informed consent; the protocol No. 014/003/CCI was approved by the Institutional Ethics Committee (CEI/892) following the Declaration of Helsinki. Immediately after surgical excision, tumor biopsies were split into two pieces, one for pathological confirmation of at least 80% of tumor cells and the other for nucleic acid isolation (RNA and DNA). Biopsies for nucleic acid isolation were frozen in liquid nitrogen until DNA and RNA extraction. Eligibility criteria were (1) patients with a confirmed pathological diagnosis of head and neck cancer stages II to IV; (2) histology of squamous cell carcinoma; (3) no previous oncological treatment. Normal samples were obtained from non-pathological adjacent tissue.

2.2. Nucleic Acid Isolation and Assessment

Tissues were homogenized using GREEN Bead Lysis (Bullet Blender-Next Advance, Troy, NY, USA) in the MagNA Lyser Instrument (Roche Diagnostics, Basilea, Suiza). DNA isolation was done with QiAmp DNA Blood MiniKit (Qiagen, Hilden, Germany). RNA was isolated using TRizol Reagent (Ambion, Austin, TX, USA) according to the manufacturer's instructions. Samples were stored at -80°C until used. To determine specimen adequacy for PCR amplification, human β -globin was employed as an internal control.

2.3. HPV Detection and Genotyping

HPV detection and genotyping were performed as previously described by Sotlar et al. [34] with little modification. First PCR was performed with 100 ng of DNA as a template and using the PCR Master Mix (Thermo Scientific, Waltham, MA, USA) in a total volume of 20 μL . Reactions (GP-E6/E7) were subjected to one 95°C for 3 min, then 40 cycles of 95°C for 30 s, 38°C for 1 min and 72°C for 30 s, followed by 72°C for 10 min in an Arktik PCR machine (ThermoFisher, Waltham, MA, USA). Nested PCR containing 1.5 μL of first PCR product reaction was performed with the same PCR Master Mix. Two primer cocktails were used for genotyping: cocktail 1 for HPV-16, -18, -31, -59, and -45; and cocktail 2 for HPV-33, -6/11, -58, -52, and -56. Reactions were subjected to the following amplification conditions: 95°C for 3 min, then 38 cycles of 95°C for 30 s, 56°C for 30 s, 72°C for 30 s, followed by 72°C for 4 min. DNA isolated from SiHa cell line was used as an internal control for primer cocktail 1, as it contained integrated human papillomavirus type 16 genome; and 5 pg of HPV-33 plasmid was used as a control for primer cocktail 2. β -globin was used as a housekeeping gene: (forward 5'-GGTTGGCCAATCTACTCCCAGG-3' reverse 5'-TGGTCTCCTTAAACCTGTCTTG-3') with the following conditions: 95°C for 3 min, then 35 cycles of 95°C for 30 s, 59°C for 30 s, 72°C for 30 s, followed by 72°C for 10 min. Amplicons obtained from all PCRs protocols were subjected to 2% agarose gel electrophoresis along with positive and negative controls and 100 bp DNA ladder, stained with ethidium bromide. Images were processed using Gel Doc RZ Imager (BioRad, Hercules, CA, USA). Sequences of all the type-specific nested PCR primers are shown in Table 1.

Table 1. Sequences of type-specific nested PCR primers.

Primer/Cocktail	HPV Genotype	Amplicon (bp)	Sequence (5'-3')
GP-E7-5B			CTG AGC TGT CAR NTA AIT GCT CA
GP-E6-3F		630	GGG W GK KAC TGA AAT CGG T
GP-E7-6B			TCC TCT GAG TYG YCP AAT TGC TC

Table 1. Cont.

Primer/Cocktail	HPV Genotype	Amplicon (bp)	Sequence (5'-3')
Cocktail I	16	457	Forward CAC AGT TATGCA CAG AGC TGC Reverse CAT ATA TTC ATG CAA TGT AGG TGT A
	18	322	Forward CAC TTC ACT GCA AGA CAT AGA Reverse GTT GTG AAA TCGTCGTTT TTC A
	31	263	Forward GAA ATT GCA TGA ACT AAG CTC G Reverse CAC ATA TAC CTT TGTTTG TCA A
	59	215	Forward CAA AGG GGA ACT GCA AGA AAG Reverse TAT AAC AGC GTA TCA GCA GC
	45	151	Forward GTG GAA AAG TGC ATT ACA GG Reverse ACC TCT GTG GGT CCC AAT GT
Cocktail II	33	398	Forward ACT ATA CAC AAC ATT GAA CTA Reverse GTT TTT ACA CGT CAC AGT GCA
	6/11	334	Forward TGC AAG AAT GCA CTG ACC AC Reverse TGC ATG TTG TCC AGC AGT GT
	58	274	Forward GTA AAG TGT GCT TAC GAT TGC Reverse GTTGTTACA GGT TAC ACT TGT
	52	229	Forward TAA GGC TCG AGT GTG TGC AG Reverse CTAATA GTT ATT TCA CTT AAT GGT

2.4. Bisulfite Conversion and STK11 Gene Methylation

Primer sequences for methylation-specific PCR (MSP) of STK11 were designed using the MethPrimer Software 2.0 (<http://www.urogene.org/cgi-bin/methprimer/methprimer.cgi>) [35]. The CpG island enriched DNA sequence near the STK11 promoter was obtained using the GenomeBrowser island prediction function (chr19:1205041-1207555); the DNA sequence was uploaded to the MethPrimer program in order to obtain MSP primers. Finally, we chose a primer set that covered a 180 pb region near to the STK11 promoter. For bisulfite conversion, 500 ng of DNA were treated with EZ DNA Methylation-Direct Kit (Zymo Research, Irvine, CA, USA). Then, 20 ng of the converted DNA were used for methylation-specific PCR and performed by using the STK11 methylated (forward 5'-CGA GTT TTA TCG AGG TTA TAG TCG T-3', reverse 5'-GTT AAT TAA ACC TAC CAT CCC CG-3') and unmethylated (forward 5'-TGA GTT TTA TTG AGG TTA TAG TTG T-3', reverse 5'-ATT AAT TAA ACC TAC CAT CCC CAA C-3') primer set. Human methylated and non-methylated DNA sets were used as positive and negative control respectively (Zymo Research, Irvine, CA, USA). The MSP reactions were performed using the Zymo Taq DNA Polymerase Kit (Zymo Research, Irvine, CA, USA)

with the following amplification conditions: 95 °C for 10 min, then 40 cycles of 95 °C for 30 s, 60 °C for 35 s, 72 °C for 35 s, followed by 72 °C for 7 min in an Arktik PCR machine (ThermoFisher, Waltham, MA, USA). PCR products were analyzed by 2% agarose gel electrophoresis, stained with ethidium bromide, and documented using Gel Doc RZ Imager (BioRad, Hercules, CA USA).

2.5. Real-Time PCR Analysis

STK11 mRNA expression complementary DNA (cDNA) was obtained using High-Capacity cDNA Reverse Transcription kit (Applied Biosystems, Foster City, CA, USA) and assessed by real-time PCR with a qPCR Master Mix (Thermo Fisher, CA, USA) following the manufacturer's instructions. The sequence of primers was as follows: for STK11, Forward 5'-ACG GTG CCC GGA CAG G-3', reverse 5'-CTG TGC CGT TCA TAC ACA CG-3'; and for β -actin, Forward 5'-ATG ACT TAG TTG CGT TAC ACC CT-3', Reverse 5'-TGC TCG CTC CAA CCG ACT G-3'. Triplicate RT was performed for each assay; data for mRNA expression were normalized with a β -actin housekeeping gene. The comparative $\Delta\Delta C_t$ method was used to quantify gene expression, and the relative quantification was calculated as $2^{-\Delta\Delta C_t}$. To measure expression levels of STK11, 36 tumor and 10 normal adjacent samples were used.

MiRNA target prediction was assessed using miRWalk 2.0 (<http://zmf.umm.uni-heidelberg.de/mirwalk2> [36]), and RNAhybrid 2.2 (<http://bibiserv.techfak.uni-bielefeld.de/rnahybrid> [37]), where we found that miR-17-5p, miR-100-3p, miR-100-5p, and miR-106a-5p had putative target regions in the STK11 3'UTR. Relative expressions of mature sequences of miR-17-5p, miR-100-3p, miR-100-5p, and miR-106a-5p were quantified by using the TaqMan Universal Master Mix II kit and the appropriate miRNA TaqMan probes (Applied Biosystems, Foster City, CA, USA). Briefly, cDNA was generated from 100 ng total RNA with the TaqMan Micro-RNA Reverse Transcription Kit (Applied Biosystems) in a 15 μ L volume; qPCR was performed using 1 μ L cDNA and the miRNAs taqman probes (Applied Biosystems). Amplification conditions were 10 min at 95 °C, followed by 40 cycles of 95 °C for 15 s, 68 °C for 60 s. Triplicate RT was performed for each assay; relative expression data was calculated through the $2^{-\Delta\Delta C_t}$ method (Applied Biosystems) and normalized relative to U6 snRNA. To measure expression levels of the above-mentioned miRNAs, 20 tumor samples and 10 healthy controls were used.

2.6. Cell Culture and Transfection

Hela cell line (ATCC, CCL-2) was used as a model of interaction between STK11 mRNA 3' UTR and putative microRNAs and was maintained following ATCC recommendations.

All plasmids and microRNA mimics used for this study were transfected using Plus Reagent-supplemented Lipofectamine 2000 transfection reagent (Invitrogen, Carlsbad, CA, USA), following the manufacturer's protocol.

2.7. Luciferase Reporter Assay

Reporter plasmids were constructed by ligation of synthetic oligonucleotide duplexes (IDT, San Jose, CA, USA) containing putative miR-100-5p and miR-100-3p target regions in the STK11 3'UTR, obtained from RNAhybrid 2.2, into the pMIR-REPORT System (Ambion, Austin, CA, USA) to form a DNA duplex with overhanging SpeI and HindIII half sites in the 5' and 3' ends, respectively, which was cloned into the appropriately digested pMIR-REPORT plasmid. This construct was co-transfected with miR-100-5p and miR-100-3p mirVana miRNA mimic (Applied Biosystems, Foster City, CA, USA) and the pMIR-REPORT and renilla Control Plasmid (Ambion, Austin, TX, USA) into HeLa cells. Luciferase activity was analyzed using the Dual-Luciferase Reporter Assay System (Promega, Madison, WI, USA) 48 h after transfection, in a GloMax 96 Microplate Luminometer (Promega). Luciferase activity was normalized to β -gal activity for each transfected well; each experiment was performed in triplicate. As negative controls we employed a miRNA random sequence (scrambled) and mutated sequences of

STK11 (three nucleotides changed). Three independent experiments were performed, and the data are presented as the mean \pm SD.

2.8. Patient Survival Analysis of STK11, miR-100-3p, and miR-100-5p

To know the clinical significance of STK11, miR-100-3p, and -5p expression levels, the TCGA database was analyzed. The expression data of 495 HNSC specimens were obtained, normalized, and log2 transformed. Finally, Cox regression analysis and the Kaplan–Meier method were used to estimate the prognostic significance of the miRNAs for overall survival, and survival curves were compared through the log-rank test. The median value of each RNA expression was defined as a cut-off value between high expression and low expression. Statistical significance was defined as $p < 0.05$.

2.9. Statistical Analysis

All values are expressed as the mean \pm SD. Statistical analysis between normal and tumor samples were performed with a two-tailed Student's *t*-test. Regarding clinical samples, a two-way ANOVA of the clinicopathologic data was performed using SPSS Statistics v. 22.0 followed by Tukey's multiple comparison test. The clinical characteristics used in the ANOVA were MSP status, anatomic region, and clinical stage. Correlation analyses were performed using the Spearman correlation. *p*-Value < 0.05 was considered as significant.

3. Results

3.1. STK11 mRNA is Down-Regulated in HNC

The studied population consisted of HNC tumors from 59 patients (Table 2 summarizes clinicopathologic and data from patients) of INCan, Mexico. Patient ages ranged from 28 to 88 years (median 65 years). According to this study, 58% of patients ($n = 35$) have a history of alcoholic habit and cigarette smoking; smokers were defined by those subjects who consumed more than 15 cigarettes a day for a period of time ≥ 15 years; while alcoholism was defined as consumers of ≥ 4 whiskey equivalents daily (30 cc for each equivalent) for ≥ 15 years. Primary tumor was located in the lip and oral cavity ($n = 50$, 84.7%), pharynx ($n = 7$, 11.9%), larynx ($n = 1$, 1.7%) and nasal cavity ($n = 1$, 1.7%). Almost ninety percent of patients (54/59) presented advanced stages III or IV of HNC, whereas 5/59 patients (~9%) presented early stages (II). Patient gender distribution was male (41/59), and 32% were female (19/59). The histology of all samples was squamous cell carcinoma. The presence of high-risk HPV-16 was detected in 4/59 (6.8%) samples by multiplex-PCR; these four samples (2-IVA and 2-IVC) were used in all experiments. Interestingly, other HPV genotypes analyzed were negative in all samples (HPV-16, -18, -31, -59, -45, 33, -11, -58, -52, and -56).

Table 2. Clinicopathologic characteristics of patients.

Clinical Parameters	Patients $n = 59$ (100%)	STK11 Promoter Methylation $n = 59$	STK11 Expression $n = 36$	miRNA Expression $n = 20$
Gender				
Male	40 (67.8%)			
Female	19 (32.2%)			
Age				
<50	10 (16.9%)			
≥ 50	49 (83.1%)			
Clinical stage				
II	5 (8.5%)	5 (8.5%)	4 (11.1%)	2 (10%)
III	11 (18.6%)	11, 3a (18.6%)	6, 3a (16.7%)	4, 3a (20%)
IVA	28 (47.5%)	28, 6a (47.5%)	15, 6a (41.7%)	8, 6a (40%)
IVB	10 (16.9%)	10 (16.9%)	8 (22.2%)	4 (20%)
IVC	5 (8.5%)	5, 1a (8.5%)	3, 1a (8.3%)	2, 1a (10%)

Table 2. Cont.

Clinical Parameters	Patients <i>n</i> = 59 (100%)	<i>STK11</i> Promoter Methylation <i>n</i> = 59	<i>STK11</i> Expression <i>n</i> = 36	miRNA Expression <i>n</i> = 20
Anatomic region				
Lip and oral cavity	50 (84.7%)			
Larynx	1 (1.7%)			
Pharynx	7 (11.9%)			
Nasal cavity	1 (1.7%)			
Histologic grade				
Low	10 (16.9%)			
Moderate	48 (81.4%)			
High	1 (1.7%)			
High-risk HPV				
16	4 (6.8%)			
Negative for HPV	55 (93.2%)			
Smoking Habit				
Positive	34 (57.6%)			
Negative	25 (42.4%)			
Alcoholism				
Positive	34 (57.6%)			
Negative	25 (42.4%)			
Tumor size				
>5 cm	29 (49.2%)			
<5 cm	30 (50.8%)			

a Number of matched healthy adjacent tissue used as control.

To determine the expression level of *STK11* in samples, a qRT-PCR analysis was performed using 36 HNC tumors and 10 non-pathological controls (adjacent healthy tissue). Interestingly, the *STK11* expression level diminished ~95% in HNC tumors samples analyzed compared to samples obtained from adjacent healthy tissue (Figure 1). Four tumor samples from stage II (early stage), and six and twenty-six HNC tumors classified as III and IV stages (advanced stages), respectively, were analyzed to quantify *STK11* expression level (Figure 1a). Accordingly, the expression level was significantly reduced in all analyzed stages compared to normal tissue. While analyzing matched samples of adjacent healthy tissue and tumor counterparts, the same pattern of subexpression of *STK11* is observed (Figure 1b).

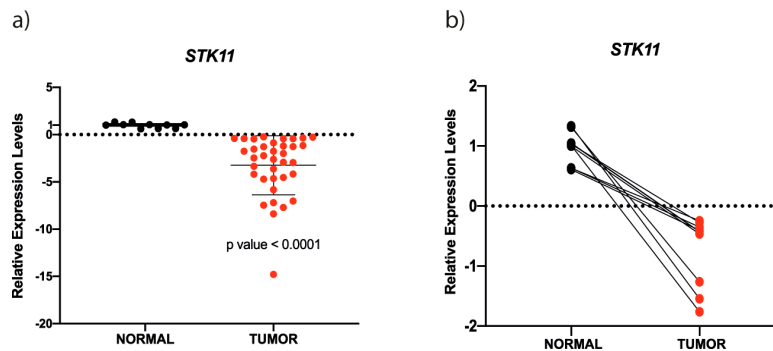


Figure 1. *STK11* is down-expressed in HNC samples. (a) Expression levels of *STK11* determined by qRT-PCR in HNC samples (red circles) and healthy tissue samples (black circles). *STK11* was 5-fold down-expressed in HNC tumors compared to control tissue. The statistically significant difference is indicated by *p*-values (*p*-value < 0.0001). (b) Matched expression of healthy adjacent tissue and its tumor counterpart.

3.2. STK11 Promoter Methylation Status

As inactivation of tumor suppressor genes can occur via promoter methylation, we assessed the status of the STK11 promoter methylation in HNC samples through MSP. Accordingly, the STK11 promoter was found to be demethylated or partially methylated in the majority of tumor samples (Figure 2); only two tumor tissues were found to be methylated. These results suggested that a post-transcriptional mechanism could negatively regulate STK11 expression. Next, we performed an ANOVA between the STK11 expression and the MSP status, clinical stages and histological grade. As expected, we observed significant differences between the STK11 promoter methylation status and the expression of STK11 (Figure 2c), although no significant difference was found in the STK11 expression level in early or advanced stages of HNC tumors, their histological grade nor between the anatomic region (Supplementary Table S1), suggesting that the down-regulation of STK11 occurs since early stages and is maintained during the progression of the disease.

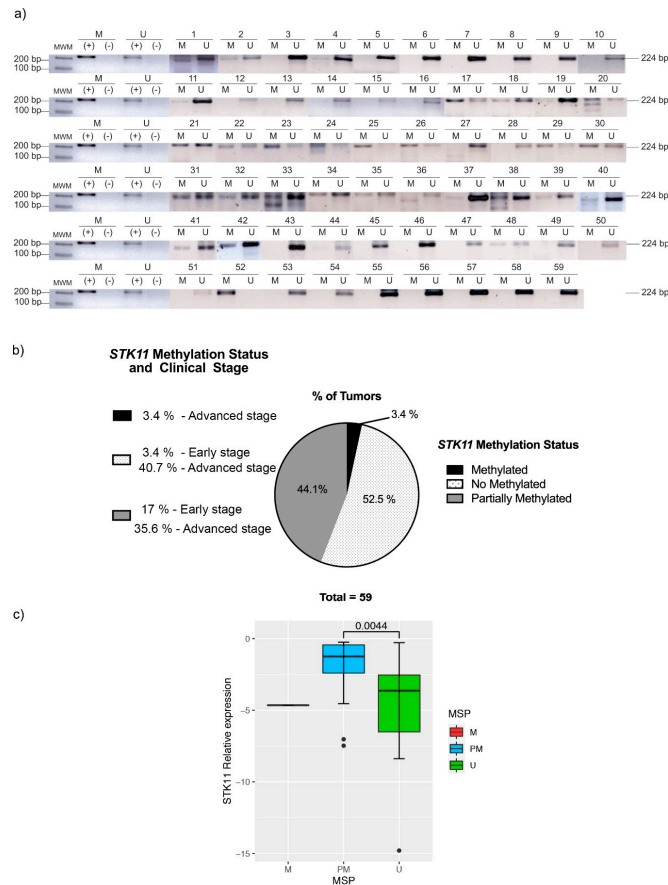


Figure 2. Methylation status of *STK11* assessed by MSP-PCR in patients with HNC. (a) End-point PCR of each sample, and (b) the proportion of methylated versus non-methylated and partially methylated samples. M: methylated, U: unmethylated, (-): negative control, (+): positive control, as well as the clinical stage per group. (c) Boxplot of the relative expression of *STK11* between the MSP groups.

3.3. miR-100-3p Interacts with STK11 mRNA

It has been established that there are miRNAs that down-regulate virtually every expressed gene by means of post-transcriptional regulation. We searched public databases for microRNAs that could interact with the 3'-UTR of STK11; thereby, we found that miR-17-5p, miR-106a-5p and miR-100-3p and -5p might be implicated in STK11 down-regulation in HNC, since STK11 could be a putative target. Then, we assessed expression levels of those miRNAs in tissue samples from HNC patients and found no variation in miR-17-5p and miR-106a-5p (Figure 3a,b) between tumor samples and their healthy counterparts. However, the overexpression of miR-100-5p and miR-100-3p was observed in the same samples (Figure 3c,d). The same was observed when the expression of each miRNA was analyzed among adjacent normal tissues matched with tumor tissues (Figure 4). Similarly to STK11, we observed no difference in the expression of the miRNAs when comparing the clinical stage (early vs. advanced) and their histological grade (0–4); this suggests that their up-regulation is maintained during the progression of the disease (Supplementary Table S1).

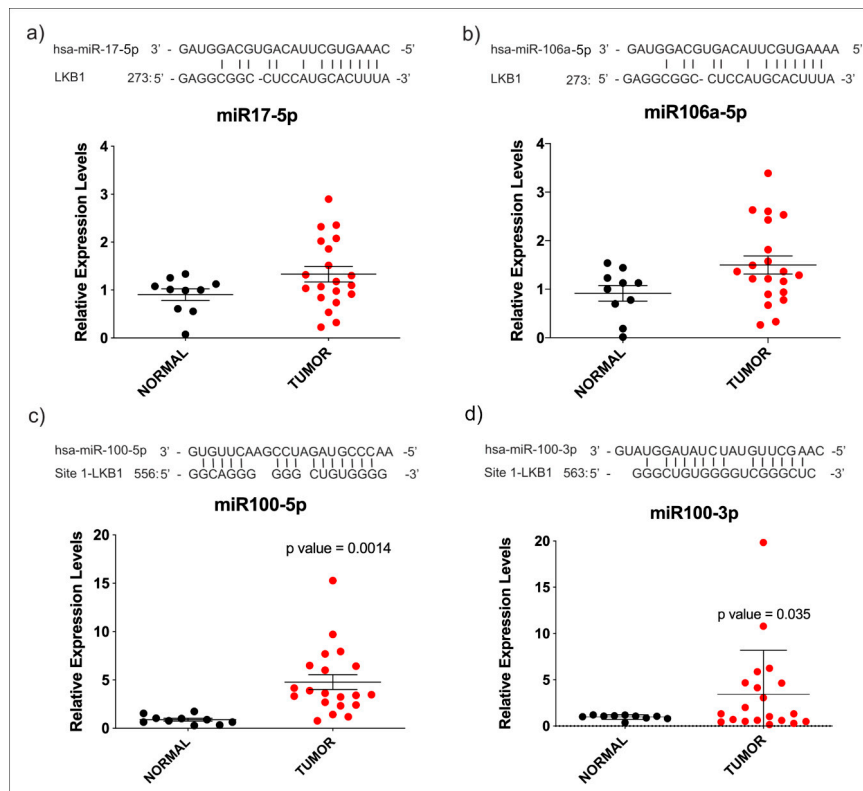


Figure 3. miRNAs relative expression in HNC patients. Relative expression of miR-17-5p (a), miR-106a-5p (b), miR-100-5p (c) and miR-100-3p (d) in HNC samples versus normal adjacent tissue. Seed regions of 3'-UTR of *STK11* are depicted for each miRNA (upper sequence). The statistically significant difference is indicated by *p*-values.

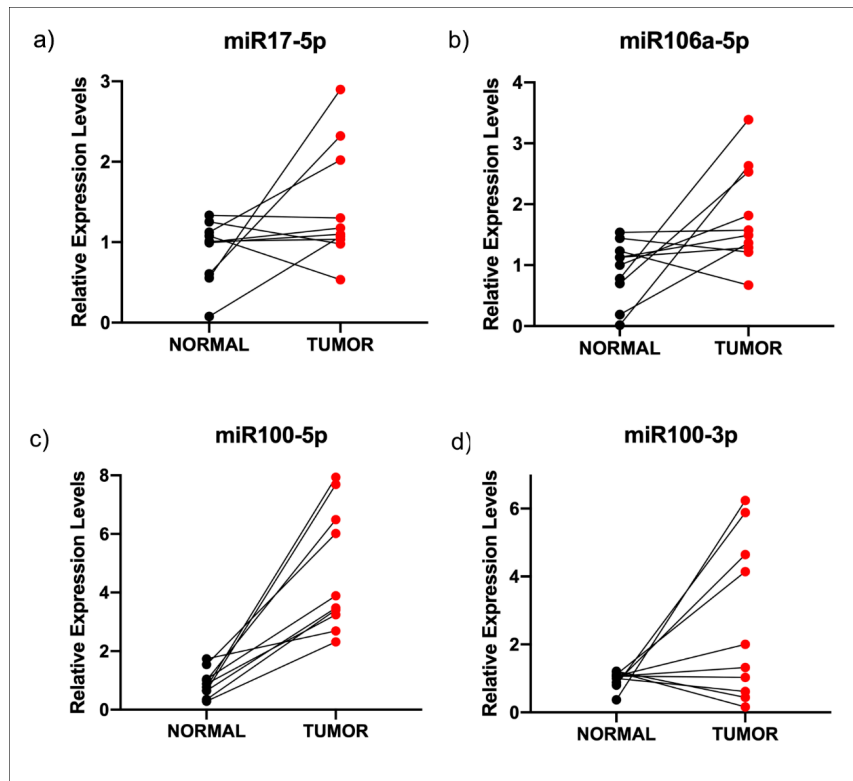


Figure 4. Relative expression of miRNAs in ten matched normal and carcinoma samples. Relative expression of miR-17-5p (a), miR-106a-5p (b), miR-100-5p (c) and miR-100-3p (d). As observed, only miR100-3p and -5p were overexpressed in tumor samples.

Therefore, to confirm whether miR-100-5p and miR-100-3p exerted a direct regulation on mRNA of STK11, we performed a Luciferase reporter assay in HeLa cells transfected with the miR-100-5p and miR-100-3p mimics. As shown in Figure 5, luciferase activity decreased significantly after the transfection of the mimic in just one of the interacting regions (miR-100-3p), with it being the most efficient interaction site at decreasing luciferase levels. These experiments confirm the predicted binding of miR-100-3p with the 3'-UTR of STK11. Additionally, the experiment was performed using a mutant interaction site with three changes in the seed sequence (Figure 5). The observed rescue of the luciferase emission confirmed the specificity of the miR-100-3p and STK11 3'-UTR interaction. Moreover, we correlated the expression of STK11 and the two strands of miR-100 (Figure 5b,c). In this analysis, we observed a significant negative correlation between STK11 and miR-100-5p, which is in agreement with our hypothesis. Then, we assessed the clinical relevance of these molecules using data from the TCGA Head and Neck project [38,39]. The Kaplan–Meier analysis showed that only STK11 expression levels were significantly associated with the clinical outcome (Figure 6) and that its expression was highly heterogeneous in normal vs. tumor samples, although these differences were not significant while miR-100-3p and -5p showed no association with the clinical outcome.

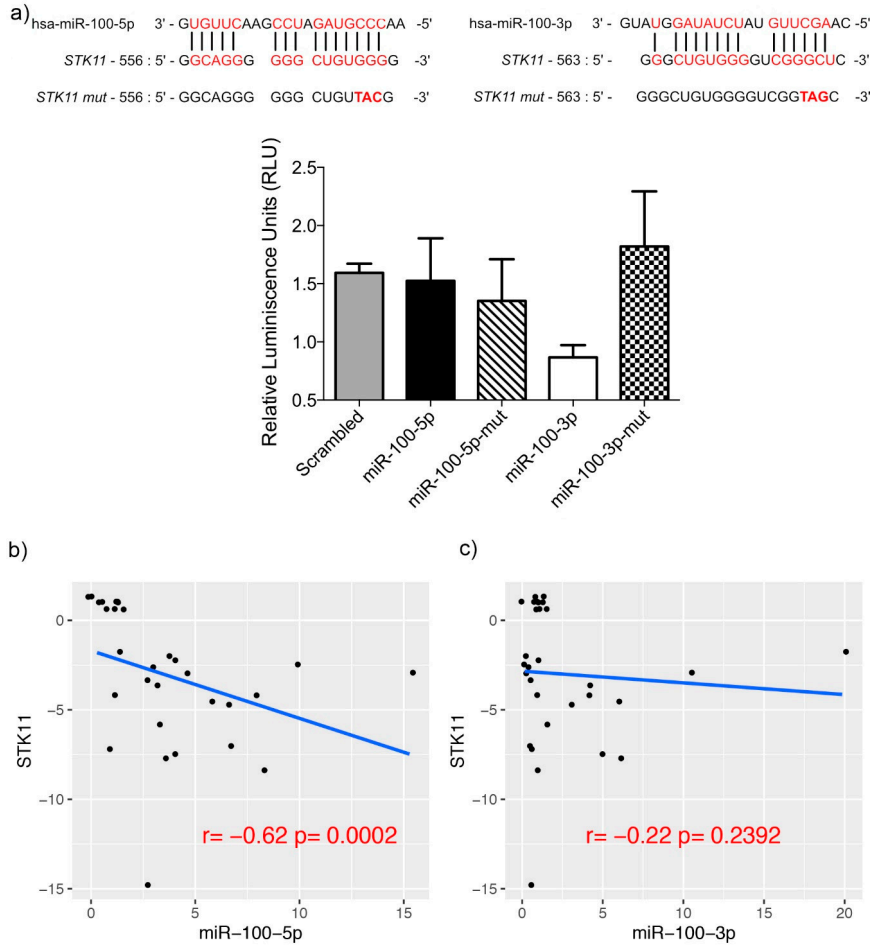


Figure 5. Dual-light Luciferase Assay. (a) Luciferase assay and constructions with the interaction of *STK11* and its mutated region with miR-100-5p and miR-100-3p. (b,c) Correlation between the expression of matched tumor samples of *STK11* and miR-100-5p and miR-100-3p, respectively.

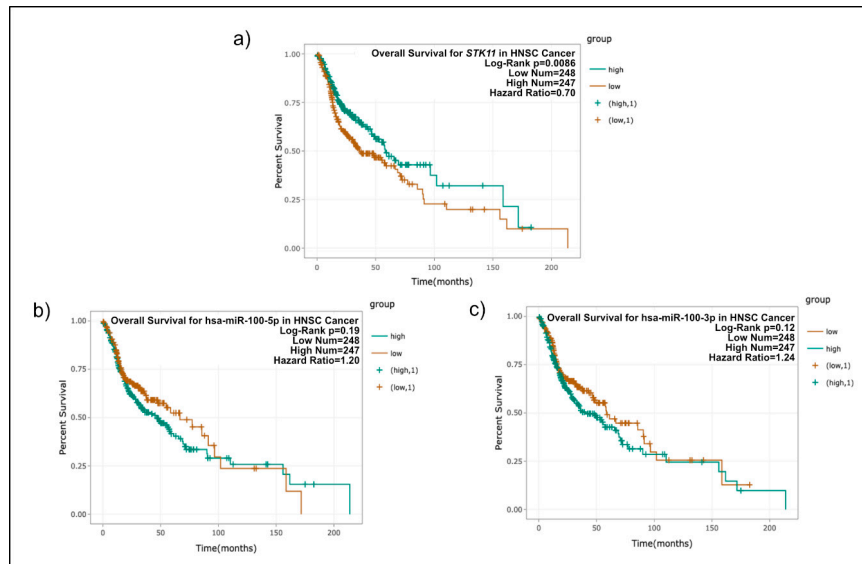


Figure 6. Overall survival TCGA analysis of (a) *STK11*, (b) miR-100-5p, and (c) miR-100-3p in head and neck cancer. The expression values of genes from RNA-seq data were scaled with $\log_2(\text{FPKM} + 0.01)$.

4. Discussion

While previous epidemiological studies have reported that HPV is found in HNC tumors [6,40–45], our data showed little evidence that HPV is etiologically linked to this kind of carcinoma, probably because most of our cases correspond to oral cavity carcinoma. We found HPV in 6.8% of the tumor samples, and all of them corresponded to the IV-A to IV-C clinical stage. These findings are statistically consistent with those reported by Gillison and colleagues [46] in HPV-infected HNC patients.

Worldwide, common high-risk HPVs are HPV-16, -18, -66, and -51, among others [46], and according to our data, HPV-16 was found in four HNC samples. Even though HPV-18 is also very common in cervical cancer, our HNC results correlate with a previous systematic review where authors explain the rare presence of HPV-18, aside from other oncogenic HPVs [47]. In the present study, by means of two primer cocktails, different HPV genotypes were analyzed (cocktail 1 for HPV-16, -18, -31, -59, and -45, and cocktail 2 for HPV-33, -6/11, -58, -52, and -56). Although the number of cases included in the present study was not sufficient to make epidemiological conjectures about the presence of HPV in oral cavity cancer in the Mexican population, the low frequency of viral infection could shed some light on the involvement of additional etiological factors in the development of this type of tumor, aside from the fact that the most frequent primary origin in our series was the oral cavity. More studies involving a broader patient cohort will be needed in order to determine the HPV distribution in HNC tumors in Mexico.

It has been recently shown that *STK11* is a tumor suppressor gene associated with Peutz-Jeghers syndrome, which is a multiple-cancer susceptible disease characterized by inactivation of *LKB1* [48]. Somatic loss of function *STK11* mutations has been found in several cancer types. Additionally, *STK11* is downregulated in tumor cells, and this behavior is thought to be part of the tumorigenesis processes and the higher rate of cell proliferation [49,50]. *STK11* exerts its functions by phosphorylating and activating AMPK; then, *LKB1*/AMPK controls and restrains cell metabolism and proliferation through the inhibition of biosynthetic pathways such as lipid, glycogen, and rRNA biosynthesis. *LKB1*/AMPK pathway can also inhibit cell proliferation through the inactivation of the mTOR pathway;

hence, activation of AMPK by LKB1 suppresses cell growth and proliferation when energy and nutrient levels are limited [51].

In the present study, we showed a down-regulation of STK11 expression in HNC tumors, compared to their normal counterparts. Then, we searched for a mechanism that could explain the decrease in the levels of STK11 expression in tumor biopsies. The methylation of CpG islands in promoter regions drives the inactivation of gene expression in different tumor suppressor genes. We were not able to find a correlation between methylation and expression levels of STK11 in tumor samples through our MSP methylation status analysis. Since no significant statistical difference or relation between STK11 expression, methylation status, and clinicopathological features was found in our study, it can be assumed that STK11 downregulation is not the result of promoter methylation. Nonetheless, the methylation status of the STK11 promoter region may be associated with a decrease in expression levels observed in tumor samples; it would be necessary to analyze the entire region that covers 2500 pb. Moreover, although MSP is the most common technique used for DNA methylation assays, it should take into consideration for further experiments the use of a quantitative approach [52].

It has been shown that in a broad range of tumor types, methylation status might change compared to non-cancerous tissues [51,53], and that it can be used as a potential diagnostic tool. Some evidence notes the difference between methylation status in cancer vs. healthy tissues, such as the case of hepatocellular carcinoma (HCC) and the frequently methylated 3OST2 gene. Interestingly, the authors also reported that STK11 was rarely methylated in HCC samples [54] and, according to our results, the tendency of STK11 to be unmethylated or partially methylated was retained in HNC tumors. Concordantly, Ekizoglu and colleagues demonstrated that STK11 promoter is partially methylated in HNC; their study showed no significant difference between normal and tumor tissues [50]. In this context, our results also showed that the methylation status was independent of HPV presence. Although previous reports have assessed genome-wide methylation and expression differences in HPV (+) or HPV (−) HNC, finding that promoter hypermethylation is widely recognized as an HNC progression mechanism [50], we report here that the methylation status for the promoter of STK11 gene is not related to the HPV presence or clinical stage. Further studies are necessary to determine the involved mechanism in STK11 demethylation in HNC, as well as the point at which this mechanism is consistent between HPV (+) and HPV (−) tumors. Interestingly, HPV-positive HNC had a different miRNA profile in comparison to HPV-negative HNC [55].

As these results suggested that a post-transcriptional mechanism instead of methylation status negatively regulated expression of STK11, we searched for putative miRNAs regulating 3' UTR of STK11. We found that miR-100-3p was able to regulate STK11 and that it was overexpressed in tumor samples, this means that the more miR-100-3p is present, the lower expression of STK11 will be, as can be appreciated in Figure 5.

miR-100 is deregulated in several cancer types and acts as a tumor suppressor, as is the case of oral cancer [56], epithelial ovarian cancer [57], bladder cancer [58], and hepatocellular carcinoma [59], among others, but to our knowledge, this is the first report showing STK11 is negatively regulated by miR-100-3p in human cancer. Interestingly, miR-100 was found to decrease its expression in patient biopsies obtained from oral cavity tumors (OSCC) and cell lines derived from these cancers. It is possible that the experimental design could induce the observed differences in miR-100 expression levels. In our study, we compared tumor tissue versus adjacent normal tissue, while the study by Henson et al. made use of primary cultures of keratinocytes obtained from the oral cavity of healthy subjects as controls [56]. The experimental variability induced by culture conditions should be analyzed in more detail. Specifically, we found that STK11 under-expression in HNC could be caused by direct interaction with miR-100-3p but there should be other mechanisms including different microRNAs explaining reduction of mRNA levels in HNC.

5. Conclusions

STK11 is a multifunctional gene associated with several types of cancer, including HNC. We report that in HNC, STK11 is downregulated regardless of tumor stage or HPV presence (6.8% of total tumors), although miR-100-3p shows marginal expression in the TCGA database; we found that the reduction in expression levels of STK11 could be explained in part by the negative regulation exerted by miR-100-3p. Finally, our data established miR-100-3p to be a bona fide negative regulator of STK11, and a potential role for miR-100-3p as an oncomiR in this type of cancer via the inactivation of tumor suppressor STK11 can be proposed, although further assays may be necessary. To our knowledge, this is the first report of an oncogenic role of miR-100-3p.

Supplementary Materials: The following are available online at <http://www.mdpi.com/2073-4425/11/9/1058/s1>, Table S1: Multivariate analysis of clinical parameters.

Author Contributions: G.F.-G., N.J.J.-H., J.F.C.-H. and C.P.-P. were involved in designing the study, drafting the manuscript and collection of data; J.F.C.-H., M.G.-E., and G.F.-G. were enrolled in the collection of biopsies of patients and data analysis; I.P.-R., A.D.C.-P., A.D.M.-G., V.G.-C., and J.F.C.-H. participated in the analysis and interpretation of data; D.C.d.L., C.L.-C., J.C.-H., and O.P.-Z. were responsible for in vitro analysis and interpretation of data. All authors have disclosed no potential conflicts of interest, and have read the journal's policy on conflicts of interest and the authorship agreement. All authors have read and agreed to the published version of the manuscript.

Funding: This research was funded by INCAN research funds and by UNAM PAPIIT-IN231420.

Conflicts of Interest: The authors declare no conflict of interest.

References

1. Ferlay, J.; Shin, H.-R.; Bray, F.; Forman, D.; Mathers, C.; Parkin, D.M. Estimates of worldwide burden of cancer in 2008: GLOBOCAN 2008. *Int. J. Cancer* **2010**, *127*, 2893–2917. [[CrossRef](#)] [[PubMed](#)]
2. Jemal, A.; Siegel, R.; Ward, E.; Murray, T.; Xu, J.; Smigal, C.; Thun, M.J. Cancer statistics, 2006. *CA Cancer J. Clin.* **2006**, *56*, 106–130. [[CrossRef](#)] [[PubMed](#)]
3. Leemans, C.R.; Braakhuis, B.J.M.; Brakenhoff, R.H. The molecular biology of head and neck cancer. *Nat. Rev. Cancer* **2011**, *11*, 9–22. [[CrossRef](#)]
4. Jethwa, A.R.; Khariwala, S.S. Tobacco-related carcinogenesis in head and neck cancer. *Cancer Metastasis Rev.* **2017**, *36*, 411–423. [[CrossRef](#)]
5. Ragin, C.C.R.; Modugno, F.; Gollin, S.M. The epidemiology and risk factors of head and neck cancer: A focus on human papillomavirus. *J. Dent. Res.* **2007**, *86*, 104–114. [[CrossRef](#)]
6. Gillison, M.L.; Koch, W.M.; Capone, R.B.; Spafford, M.; Westra, W.H.; Wu, L.; Zahurak, M.L.; Daniel, R.W.; Viglione, M.; Symer, D.E.; et al. Evidence for a causal association between human papillomavirus and a subset of head and neck cancers. *J. Natl. Cancer Inst.* **2000**, *92*, 709–720. [[CrossRef](#)]
7. Puram, S.V.; Rocco, J.W. Molecular aspects of head and neck cancer therapy. *Hematol. Oncol. Clin. N. Am.* **2015**, *29*, 971–992. [[CrossRef](#)]
8. Gary, C.; Hajek, M.; Biktasova, A.; Bellinger, G.; Yarbrough, W.G.; Issaeva, N. Selective antitumor activity of roscovitine in head and neck cancer. *Oncotarget* **2016**, *7*, 38598–38611. [[CrossRef](#)]
9. Karuman, P.; Gozani, O.; Odze, R.D.; Zhou, X.C.; Zhu, H.; Shaw, R.; Brien, T.P.; Bozzuto, C.D.; Ooi, D.; Cantley, L.C.; et al. The Peutz-Jegher gene product LKB1 is a mediator of p53-dependent cell death. *Mol. Cell* **2001**, *7*, 1307–1319. [[CrossRef](#)]
10. Hawley, S.A.; Boudeau, J.; Reid, J.L.; Mustard, K.J.; Udd, L.; Makela, T.P.; Alessi, D.R.; Hardie, D.G. Complexes between the LKB1 tumor suppressor, STRAD α/β and MO25 α/β are upstream kinases in the AMP-activated protein kinase cascade. *J. Biol.* **2003**, *2*, 28. [[CrossRef](#)]
11. Thomson, D.M.; Brown, J.D.; Fillmore, N.; Condon, B.M.; Kim, H.-J.; Barrow, J.R.; Winder, W.W. LKB1 and the regulation of malonyl-CoA and fatty acid oxidation in muscle. *Am. J. Physiol. Endocrinol. Metab.* **2007**, *293*, E1572–E1579. [[CrossRef](#)] [[PubMed](#)]
12. Tiainen, M.; Ylikorkkala, A.; Makela, T.P. Growth suppression by Lkb1 is mediated by a G(1) cell cycle arrest. *Proc. Natl. Acad. Sci. USA* **1999**, *96*, 9248–9251. [[CrossRef](#)] [[PubMed](#)]

13. Li, N.; Huang, D.; Lu, N.; Luo, L. Role of the LKB1/AMPK pathway in tumor invasion and metastasis of cancer cells (Review). *Oncol. Rep.* **2015**, *34*, 2821–2826. [[CrossRef](#)] [[PubMed](#)]
14. Mehenni, H.; Gehrig, C.; Nezu, J.; Oku, A.; Shimane, M.; Rossier, C.; Guex, N.; Blouin, J.L.; Scott, H.S.; Antonarakis, S.E. Loss of LKB1 kinase activity in Peutz-Jeghers syndrome, and evidence for allelic and locus heterogeneity. *Am. J. Hum. Genet.* **1998**, *63*, 1641–1650. [[CrossRef](#)]
15. Avizienyte, E.; Loukola, A.; Roth, S.; Hemminki, A.; Tarkkanen, M.; Salovaara, R.; Arola, J.; Butzow, R.; Husgafvel-Pursiainen, K.; Kokkola, A.; et al. LKB1 somatic mutations in sporadic tumors. *Am. J. Pathol.* **1999**, *154*, 677–681. [[CrossRef](#)]
16. Sanchez-Cespedes, M.; Parrella, P.; Esteller, M.; Nomoto, S.; Trink, B.; Engles, J.M.; Westra, W.H.; Herman, J.G.; Sidransky, D. Inactivation of LKB1/STK11 is a common event in adenocarcinomas of the lung. *Cancer Res.* **2002**, *62*, 3659–3662.
17. Bignell, G.R.; Barfoot, R.; Seal, S.; Collins, N.; Warren, W.; Stratton, M.R. Low frequency of somatic mutations in the LKB1/Peutz-Jeghers syndrome gene in sporadic breast cancer. *Cancer Res.* **1998**, *58*, 1384–1386.
18. Nakanishi, C.; Yamaguchi, T.; Iijima, T.; Saji, S.; Toi, M.; Mori, T.; Miyaki, M. Germline mutation of the LKB1/STK11 gene with loss of the normal allele in an aggressive breast cancer of Peutz-Jeghers syndrome. *Oncology* **2004**, *67*, 476–479. [[CrossRef](#)]
19. Petersen, G.M. Familial pancreatic cancer. *Semin. Oncol.* **2016**, *43*, 548–553. [[CrossRef](#)]
20. Su, G.H.; Hruban, R.H.; Bansal, R.K.; Bova, G.S.; Tang, D.J.; Shekher, M.C.; Westerman, A.M.; Entius, M.M.; Goggins, M.; Yeo, C.J.; et al. Germline and somatic mutations of the STK11/LKB1 Peutz-Jeghers gene in pancreatic and biliary cancers. *Am. J. Pathol.* **1999**, *154*, 1835–1840. [[CrossRef](#)]
21. Guldberg, P.; thor Straten, P.; Ahrenkiel, V.; Seremet, T.; Kirkin, A.F.; Zeuthen, J. Somatic mutation of the Peutz-Jeghers syndrome gene, LKB1/STK11, in malignant melanoma. *Oncogene* **1999**, *18*, 1777–1780. [[CrossRef](#)] [[PubMed](#)]
22. Rowan, A.; Bataille, V.; MacKie, R.; Healy, E.; Bicknell, D.; Bodmer, W.; Tomlinson, I. Somatic mutations in the Peutz-Jeghers (LKB1/STK11) gene in sporadic malignant melanomas. *J. Investig. Dermatol.* **1999**, *112*, 509–511. [[CrossRef](#)] [[PubMed](#)]
23. Kim, C.J.; Cho, Y.G.; Park, J.Y.; Kim, T.Y.; Lee, J.H.; Kim, H.S.; Lee, J.W.; Song, Y.H.; Nam, S.W.; Lee, S.H.; et al. Genetic analysis of the LKB1/STK11 gene in hepatocellular carcinomas. *Eur. J. Cancer* **2004**, *40*, 136–141. [[CrossRef](#)]
24. Qiu, W.; Schonleben, F.; Thaker, H.M.; Goggins, M.; Su, G.H. A novel mutation of STK11/LKB1 gene leads to the loss of cell growth inhibition in head and neck squamous cell carcinoma. *Oncogene* **2006**, *25*, 2937–2942. [[CrossRef](#)] [[PubMed](#)]
25. Zeng, P.-Y.; Berger, S.L. LKB1 is recruited to the p21/WAF1 promoter by p53 to mediate transcriptional activation. *Cancer Res.* **2006**, *66*, 10701–10708. [[CrossRef](#)] [[PubMed](#)]
26. Lee, S.M.; Choi, J.E.; Na, Y.K.; Lee, E.J.; Lee, W.K.; Choi, Y.Y.; Yoon, G.S.; Jeon, H.-S.; Kim, D.S.; Park, J.Y. Genetic and epigenetic alterations of the LKB1 gene and their associations with mutations in TP53 and EGFR pathway genes in Korean non-small cell lung cancers. *Lung Cancer* **2013**, *81*, 194–199. [[CrossRef](#)]
27. Kullmann, L.; Krahn, M.P. Controlling the master-upstream regulation of the tumor suppressor LKB1. *Oncogene* **2018**, *37*, 3045–3057. [[CrossRef](#)]
28. Zheng, F.; Yuan, X.; Chen, E.; Ye, Y.; Li, X.; Dai, Y. Methylation of STK11 promoter is a risk factor for tumor stage and survival in clear cell renal cell carcinoma. *Oncol. Lett.* **2017**, *14*, 3065–3070. [[CrossRef](#)]
29. Trojan, J.; Brieger, A.; Raedle, J.; Esteller, M.; Zeuzem, S. 5'-CpG island methylation of the LKB1/STK11 promoter and allelic loss at chromosome 19p13.3 in sporadic colorectal cancer. *Gut* **2000**, *47*, 272–276. [[CrossRef](#)]
30. Lee, C.G.; Kim, Y.W.; Kim, E.H.; Meng, Z.; Huang, W.; Hwang, S.J.; Kim, S.G. Farnesoid X receptor protects hepatocytes from injury by repressing miR-199a-3p, which increases levels of LKB1. *Gastroenterology* **2012**, *142*, 1206–1217.e7. [[CrossRef](#)]
31. Chen, H.; Untiveros, G.M.; McKee, L.A.K.; Perez, J.; Li, J.; Antin, P.B.; Konhilas, J.P. Micro-RNA-195 and -451 regulate the LKB1/AMPK signaling axis by targeting MO25. *PLoS ONE* **2012**, *7*, e41574. [[CrossRef](#)] [[PubMed](#)]
32. Lao, G.; Liu, P.; Wu, Q.; Zhang, W.; Liu, Y.; Yang, L.; Ma, C. Mir-155 promotes cervical cancer cell proliferation through suppression of its target gene LKB1. *Tumour. Biol.* **2014**, *35*, 11933–11938. [[CrossRef](#)] [[PubMed](#)]

33. Gu, D.-N.; Jiang, M.-J.; Mei, Z.; Dai, J.-J.; Dai, C.-Y.; Fang, C.; Huang, Q.; Tian, L. microRNA-7 impairs autophagy-derived pools of glucose to suppress pancreatic cancer progression. *Cancer Lett.* **2017**, *400*, 69–78. [[CrossRef](#)]
34. Sotlar, K.; Diemer, D.; Dethleffs, A.; Hack, Y.; Stubner, A.; Vollmer, N.; Menton, S.; Menton, M.; Dietz, K.; Wallwiener, D.; et al. Detection and typing of human papillomavirus by e6 nested multiplex PCR. *J. Clin. Microbiol.* **2004**, *42*, 3176–3184. [[CrossRef](#)] [[PubMed](#)]
35. Li, L.-C.; Dahiya, R. MethPrimer: Designing primers for methylation PCRs. *Bioinformatics* **2002**, *18*, 1427–1431. [[CrossRef](#)]
36. Dweep, H.; Gretz, N. MiRWalk2.0: A comprehensive atlas of microRNA-target interactions. *Nat. Methods* **2015**, *12*, 697. [[CrossRef](#)]
37. Krü, J.; Rehmsmeier, M. RNAhybrid: Microrna target prediction easy, fast and flexible. *Nucleic Acids Res.* **2006**. [[CrossRef](#)]
38. Lawrence, M.S.; Sougnez, C.; Lichtenstein, L.; Cibulskis, K.; Lander, E.; Gabriel, S.B.; Getz, G.; Ally, A.; Balasundaram, M.; Birol, I.; et al. Comprehensive genomic characterization of head and neck squamous cell carcinomas. *Nature* **2015**, *517*, 576–582. [[CrossRef](#)]
39. Colaprico, A.; Silva, T.C.; Olsen, C.; Garofano, L.; Cava, C.; Garolini, D.; Sabedot, T.S.; Malta, T.M.; Pagnotta, S.M.; Castiglioni, I.; et al. TCGAAbiolinks: An R/Bioconductor package for integrative analysis of TCGA data. *Nucleic Acids Res.* **2015**, *44*, 71. [[CrossRef](#)]
40. Walboomers, J.M.; Jacobs, M.V.; Manos, M.M.; Bosch, F.X.; Kummer, J.A.; Shah, K.V.; Snijders, P.J.; Peto, J.; Meijer, C.J.; Munoz, N. Human papillomavirus is a necessary cause of invasive cervical cancer worldwide. *J. Pathol.* **1999**, *189*, 12–19. [[CrossRef](#)]
41. Khode, S.R.; Dwivedi, R.C.; Rhys-Evans, P.; Kazi, R. Exploring the link between human papilloma virus and oral and oropharyngeal cancers. *J. Cancer Res. Ther.* **2014**, *10*, 492–498. [[CrossRef](#)] [[PubMed](#)]
42. Paz, I.B.; Cook, N.; Odom-Maryon, T.; Xie, Y.; Wilczynski, S.P. Human papillomavirus (HPV) in head and neck cancer. An association of HPV 16 with squamous cell carcinoma of Waldeyer’s tonsillar ring. *Cancer* **1997**, *79*, 595–604. [[CrossRef](#)]
43. Haraf, D.J.; Nodzenski, E.; Brachman, D.; Mick, R.; Montag, A.; Graves, D.; Vokes, E.E.; Weichselbaum, R.R. Human papilloma virus and p53 in head and neck cancer: Clinical correlates and survival. *Clin. Cancer Res.* **1996**, *2*, 755–762. [[PubMed](#)]
44. Schwartz, S.M.; Daling, J.R.; Doody, D.R.; Wipf, G.C.; Carter, J.J.; Madeleine, M.M.; Mao, E.J.; Fitzgibbons, E.D.; Huang, S.; Beckmann, A.M.; et al. Oral cancer risk in relation to sexual history and evidence of human papillomavirus infection. *J. Natl. Cancer Inst.* **1998**, *90*, 1626–1636. [[CrossRef](#)]
45. Fouret, P.; Monceaux, G.; Temam, S.; Lacourreye, L.; St Guily, J.L. Human papillomavirus in head and neck squamous cell carcinomas in nonsmokers. *Arch. Otolaryngol. Head Neck Surg.* **1997**, *123*, 513–516. [[CrossRef](#)]
46. Gillison, M.L.; Castellsague, X.; Chaturvedi, A.; Goodman, M.T.; Snijders, P.; Tommasino, M.; Arbyn, M.; Franceschi, S. Eurogin Roadmap: Comparative epidemiology of HPV infection and associated cancers of the head and neck and cervix. *Int. J. Cancer* **2014**, *134*, 497–507. [[CrossRef](#)]
47. Kreimer, A.R.; Clifford, G.M.; Boyle, P.; Franceschi, S. Human papillomavirus types in head and neck squamous cell carcinomas worldwide: A systematic review. *Cancer Epidemiol. Biomark. Prev.* **2005**, *14*, 467–475. [[CrossRef](#)]
48. Resta, N.; Pierannunzio, D.; Lenato, G.M.; Stella, A.; Capocaccia, R.; Bagnulo, R.; Lastella, P.; Susca, F.C.; Bozzao, C.; Loconte, D.C.; et al. Cancer risk associated with STK11/LKB1 germline mutations in Peutz-Jeghers syndrome patients: Results of an Italian multicenter study. *Dig. Liver Dis.* **2013**, *45*, 606–611. [[CrossRef](#)]
49. Rowan, A.; Churchman, M.; Jefferey, R.; Hanby, A.; Poulson, R.; Tomlinson, I. In situ analysis of LKB1/STK11 mRNA expression in human normal tissues and tumours. *J. Pathol.* **2000**, *192*, 203–206. [[CrossRef](#)]
50. Ekizoglu, S.; Dalay, N.; Karaman, E.; Akdeniz, D.; Ozaydin, A.; Buyru, N. LKB1 downregulation may be independent of promoter methylation or FOXO3 expression in head and neck cancer. *Transl. Res.* **2013**, *162*, 122–129. [[CrossRef](#)]
51. Dai, W.; Teodoridis, J.M.; Zeller, C.; Graham, J.; Hersey, J.; Flanagan, J.M.; Stronach, E.; Millan, D.W.; Siddiqui, N.; Paul, J.; et al. Systematic CpG islands methylation profiling of genes in the wnt pathway in epithelial ovarian cancer identifies biomarkers of progression-free survival. *Clin. Cancer Res.* **2011**, *17*, 4052–4062. [[CrossRef](#)] [[PubMed](#)]

52. Claus, R.; Wilop, S.; Hielscher, T.; Sonnet, M.; Dahl, E.; Galm, O.; Jost, E.; Plass, C. A systematic comparison of quantitative high-resolution DNA methylation analysis and methylation-specific PCR. *Epigenetics* **2012**, *7*, 772–780. [[CrossRef](#)] [[PubMed](#)]
53. Summers, T.; Langan, R.C.; Nissan, A.; Brucher, B.L.D.M.; Bilchik, A.J.; Protic, M.; Daumer, M.; Avital, I.; Stojadinovic, A. Serum-based DNA methylation biomarkers in colorectal cancer: Potential for screening and early detection. *J. Cancer* **2013**, *4*, 210–216. [[CrossRef](#)] [[PubMed](#)]
54. Chen, H.; Zhang, T.; Sheng, Y.; Zhang, C.; Peng, Y.; Wang, X.; Zhang, C. Methylation Profiling of Multiple Tumor Suppressor Genes in Hepatocellular Carcinoma and the Epigenetic Mechanism of 3OST2 Regulation. *J. Cancer* **2015**, *6*, 740–749. [[CrossRef](#)] [[PubMed](#)]
55. Sartor, M.A.; Dolinoy, D.C.; Jones, T.R.; Colacino, J.A.; Prince, M.E.P.; Carey, T.E.; Rozek, L.S. Genome-wide methylation and expression differences in HPV(+) and HPV(-) squamous cell carcinoma cell lines are consistent with divergent mechanisms of carcinogenesis. *Epigenetics* **2011**, *6*, 777–787. [[CrossRef](#)]
56. Henson, B.J.; Bhattacharjee, S.; O'Dee, D.M.; Feingold, E.; Gollin, S.M. Decreased expression of miR-125b and miR-100 in oral cancer cells contributes to malignancy. *Genes Chromosomes Cancer* **2009**, *48*, 569–582. [[CrossRef](#)]
57. Peng, D.-X.; Luo, M.; Qiu, L.-W.; He, Y.-L.; Wang, X.-F. Prognostic implications of microRNA-100 and its functional roles in human epithelial ovarian cancer. *Oncol. Rep.* **2012**, *27*, 1238–1244. [[CrossRef](#)]
58. Xu, C.; Zeng, Q.; Xu, W.; Jiao, L.; Chen, Y.; Zhang, Z.; Wu, C.; Jin, T.; Pan, A.; Wei, R.; et al. miRNA-100 inhibits human bladder urothelial carcinogenesis by directly targeting mTOR. *Mol. Cancer Ther.* **2013**, *12*, 207–219. [[CrossRef](#)]
59. Ge, Y.-Y.; Shi, Q.; Zheng, Z.-Y.; Gong, J.; Zeng, C.; Yang, J.; Zhuang, S.-M. MicroRNA-100 promotes the autophagy of hepatocellular carcinoma cells by inhibiting the expression of mTOR and IGF-1R. *Oncotarget* **2014**, *5*, 6218–6228. [[CrossRef](#)]



© 2020 by the authors. Licensee MDPI, Basel, Switzerland. This article is an open access article distributed under the terms and conditions of the Creative Commons Attribution (CC BY) license (<http://creativecommons.org/licenses/by/4.0/>).


- 8.5. Coronel-Hernandez J., Lopez-Urrutia, E.,...,Martinez-Gutierrez, Antonio-D.,, et al. Cell migration and proliferation are regulated by miR-26a in colorectal cancer via the PTEN–AKT axis. *Cancer Cell International*. 2019

PRIMARY RESEARCH

Open Access



Cell migration and proliferation are regulated by miR-26a in colorectal cancer via the PTEN–AKT axis

Jossimar Coronel-Hernández^{1,7†}, Eduardo López-Urrutia^{1†}, Carlos Contreras-Romero¹, Izamary Delgado-Waldo¹, Gabriela Figueroa-González², Alma D. Campos-Parra², Rebeca Salgado-García², Antonio Martínez-Gutierrez², Miguel Rodríguez-Morales², Nadia Jacobo-Herrera³, Luis Ignacio Terrazas⁴, Abraham Silva-Carmona⁵, César López-Camarillo⁶ and Carlos Pérez-Plasencia^{1,2*} 

Abstract

Background: Invasion and metastasis are determinant events in the prognosis of Colorectal cancer (CRC), a common neoplasm worldwide. An important factor for metastasis is the acquired capacity of the cell to proliferate and invade adjacent tissues. In this paper, we explored the role of micro-RNA-26a in the regulation of proliferation and migration in CRC-derived cells through the negative regulation of PTEN, a key negative regulator of the AKT pathway.

Methods: Expression levels of PTEN and miR-26a were surveyed in normal and CRC-derived cell lines; paraffin embedded human tissues, TCGA CRC expression data and a Balb/c mice orthotopic induced CRC model. CRC was induced by an initial intraperitoneal dose of the colonic carcinogen Azoxymethane followed by inflammatory promoter Dextran Sulfate Sodium Salt. Luciferase assays provide information about miR-26a–PTEN 3'UTR interaction. Proliferation and migration by real time cell analysis and wound-healing functional analyses were performed to assess the participation of miR-26a on important hallmarks of CRC and its regulation on the PTEN gene.

Results: We observed a negative correlation between PTEN and miR-26a expression in cell lines, human tissues, TCGA data, and tissues derived from the CRC mouse model. Moreover, we showed that negative regulation of PTEN exerted by miR-26a affected AKT phosphorylation levels directly. Functional assays showed that miR-26a directly down-regulates PTEN, and that miR-26a over-expressing cells had higher proliferation and migration rates.

Conclusions: All this data proposes an important role of miR-26a as an oncomir in the progression and invasion of CRC. Our data suggested that miR-26a could be used as a biomarker of tumor development in CRC patients, however more studies must be conducted to establish its clinical role.

Keywords: MicroRNA, miR-26a, PTEN, AKT, Colorectal cancer, Animal model for carcinogenesis

*Correspondence: carlos.pplas@gmail.com

[†]Jossimar Coronel-Hernández and Eduardo López-Urrutia contributed equally to this work

²Laboratorio de Genómica, Instituto Nacional de Cancerología, Av. San Fernando No 22, Col. Sección XVI, Tlalpan, Zip code 14080 Mexico City, DF, Mexico

Full list of author information is available at the end of the article



Background

Colorectal cancer (CRC) is the third most common neoplasm and the fourth cause of cancer-related death worldwide in both sexes. Invasion and metastasis are determinant events in the prognosis of CRC. An important factor for metastasis is the acquired capacity of the cell to proliferate and invade adjacent tissues. One of the most relevant signaling pathways regulating cell proliferation, survival, angiogenesis, and metastasis is PI3K/AKT; which is negatively regulated by the tumor suppressor Phosphatase and Tensin homolog (PTEN) [1]. Loss of PTEN function occurs in several types of cancer—including CRC—through various genetic mechanisms such as point mutations or allelic loss of chromosome 10q2; however, biallelic inactivation of this site has not been demonstrated. Finally, methylation of the PTEN promoter has been reported to be associated in high microsatellite instability in 19% of colorectal cancers [2] and the PTEN messenger has been demonstrated to be targeted by microRNA regulation [3].

Micro-RNAs (miRNAs) are non-coding short RNAs that modulate gene expression by inducing mRNA degradation or translational repression [4]. They perform this function by binding to the 3' UTR of their target mRNA through complete or partial base complementarity, thus they are capable of pleiotropic effects [5, 6]. Deregulation of the expression patterns of several microRNAs has been implicated in establishment and progression of many types of cancer. Particularly, mir-26a has been associated to development of glioblastoma [7], cholangiocarcinoma [8] and ovarian cancer [9] and thus labeled as an oncomir in those cancers; however, mir-26a has also been classified as tumor suppressor in pancreatic cancer [10], hepatocellular carcinoma [11] and nasopharyngeal carcinoma [12].

In CRC, mir-26a is significantly upregulated [13], but the function and clinical relevance of this miRNA in CRC is still partially understood. Our group has recently found that in CRC Rb1 gene is a target of mir-26a [14], but this is still far from the complete picture, as a single miRNA has been observed to target several genes. For example, mir-182-5p targets three genes involved in DNA repair [15], and drives metastasis of primary sarcomas [16]. On the other hand, various miRNAs can target the same gene, yielding similar effects in spite of being different regulators; hence, overexpression of both mir-130a [17] and mir-23a [18] enhance migration, invasion and the epithelial-mesenchymal transition (EMT) in osteosarcoma cells through direct PTEN regulation.

The aim of present study was to further explore the participation of mir-26a in CRC development, through the analysis of the relationship between mir-26a expression and PTEN. We found that mir-26a does regulate

PTEN, abrogating its expression both in CRC-derived cell lines and in a mouse model that closely resembles colitis-mediated CRC. Moreover, over-expression of mir-26a mimic increases the phosphorylation levels of AKT T-308 that is the active form of AKT and triggers cell migration, proliferation among other hallmarks of cancer. Our findings suggest that mir-26a is indeed a key regulator of colorectal carcinogenesis since it targets at least two important tumor suppressor genes Rb and PTEN; thus, mir-26a is also a promising molecular biomarker involved in the progression of colon carcinogenesis process.

Methods

Patient samples

Twenty CRC paraffin-embedded tissue samples staged locally advanced; ten Crohn's disease paraffin-embedded tissue samples and 13 healthy tissues from colorectal were obtained by colonoscopy without macro and microscopic lesions from Instituto Nacional de Cancerología—National Cancer Institute, Mexico pathology registry, present investigation was approved by ethics committee (approval number INCAN/CI/826/17). None of the authors had access to potentially identifying information from the donors of the paraffin-embedded samples.

Tissue expression for in silico meta-analysis

Mature Mir-26a (RefSeq MI0000083) and mRNA PTEN (NM_001304717) expression data were obtained from The Cancer Genome Atlas in different stages of 424 (75 Stage I, 304 Stage II-III and 45 Stage IV) Colorectal Cancer samples and were normalized with *deSeq2* (Bioconductor Package; data were compared with 41 healthy tissues. To assess the protein expression of PTEN; antibody-based proteomic data was obtained from The Human Protein Atlas [19]; staining intensity was compared between all the available healthy and cancer tissue data (2 and 13, respectively) from the PTEN entry. mir26a is encoded in two *loci*; mir-26a1 is localized in chromosome 3 within the CTDSPL gene and mir-26a2 is in chromosome 12 within the CTDSP2 gene.

Cell culture and transfection

CRC-derived HCT116 cells (ATCC CCL-247) were cultured in RPMI medium supplemented with 10% (v/v) fetal bovine serum and maintained (FBS) at 37 °C with 5% CO₂. CRC-derived SW480 (ATCC CCL-228), SW620 (ATCC CCL-227) and non-tumoral immortalized epithelial CRL1790 colon cells obtained from ATCC were cultured in DMEM F12 medium supplemented with 10% (v/v) fetal bovine serum and maintained at 37 °C with 5% CO₂.

All employed plasmids were transfected using Lipofectamine 2000 transfection agent (Invitrogen), following the manufacturer's protocol. Mirvana Micro-RNA mimics and inhibitors (Ambion) were transfected using the siPORT NeoFX transfection agent (Life Technologies) following the manufacturer's protocol. Unless otherwise indicated, RNA and protein expression was analyzed 24 h post-transfection.

CRC mouse model

Twelve female Balb/c mice (Harlan Laboratories, México) aged 6 weeks used in this study were maintained at Facultad de Estudios Superiores Iztacala Animal Facility according to the institutional animal care guidelines (number of protocol FES-2016-1423). Animals were housed in plastic cages (6 mice/cage) with drinking water and pelleted basal diet ad libitum under controlled humidity ($50 \pm 10\%$), light (12/12 h light/dark cycles) and temperature ($23 \pm 2^\circ\text{C}$). CRC was induced by an initial intraperitoneal dose of the colonic carcinogen Azoxymethane (AOM) followed by three Dextran Sulfate Sodium Salt (DSS) 7d-long, ad libitum administrations during the second, 5th and 8 weeks of treatment. This mouse model was thoroughly described in a previous paper from our group [20].

Three randomly chosen mice were euthanized after each DSS dose for mRNA and protein analysis, so as to have three biological replicates of every mRNA or protein expression measurements. Large bowels were flushed with saline and excised. Inflammation-related cancer development was confirmed by histological analysis.

RNA expression analysis

Large bowel parts of each experimental group mice were homogenized by triplicate in a Bullet Blender (Next Advance) following the manufacturer's protocol for intestinal tissue. Total RNA was isolated from the homogenized samples or from cultured cells (CRL1790, HCT116, SW480 or SW620) grown to approximately 80–85% confluence, using the TRIzol reagent (Invitrogen) following the manufacturer's protocol. miRNAs were isolated from tissue blocks using the miRNeasy FFPE kit (Qiagen) following the manufacturer's recommendations.

Mature miR-26a and the PTEN messenger were detected in the murine model samples by RT-PCR using a Roche Light Cycler 2.0. For miR-26a, cDNA was generated from 100 ng total RNA with the TaqMan Micro-RNA Reverse Transcription Kit (Applied Biosystems) in a 15 μL volume; qPCR was performed using 1 μL cDNA and the miR-26a taqman probe (Applied Biosystems). Amplification conditions were 10 min at 95°C , followed by 40 cycles of 95°C for 15 s, 68°C for 60 s. For PTEN mRNA detection, we used Titan One

RT-PCR kit (Roche) supplemented with SybrGreen and the following primers: Fw AGGCACAAGAGGCC TAGAT, Rv AACTGAGGATTGCAAGTTCG. cDNA was synthesized at 50°C for 30 min, immediately followed by denaturation at 94°C for 2 min, 40 cycles of 94°C for 10 s, primer-dependent annealing temperature for 30 s and 68°C for 45 s, and a final extension at 68°C for 7 min.

MiR-26a and the PTEN messenger were detected in cultured cells and tissue block samples by RT-PCR using the Bio-Rad CFX 96 Touch and the miR-26a taqman probe (Applied Biosystems) or the SYBR Select Master Mix for CFX (Applied Biosystems). Amplification conditions for miR-26a were as mentioned above. For PTEN mRNA detection, cDNA was synthesized from 2 μg total RNA using the High-Capacity cDNA Reverse Transcription Kit (Roche); a twentieth of this reaction was used for qPCR. Amplification conditions were 2 min at 95°C for initial denaturation, followed by 40 cycles of 95°C for 15 s, primer-dependent annealing temperature for 15 s and 72°C for 60 s.

Relative expression data was calculated through the $\Delta\Delta\text{Ct}$ method (Applied Biosystems) and normalized relative to U6 snRNA or GAPDH mRNA accordingly.

Protein expression analysis

Protein extracts from large bowel parts of each experimental mouse group or from cultured cells was obtained by homogenization in RIPA buffer (SantaCruz Biotechnology); a Bullet Blender (Next Advance) and stainless-steel beads was used for bowel tissues. Protein extract was cleared by centrifugation at 12,000 rpm for 20 min.

For immunodetection, 50 μg total protein from tumor tissue or cultured cells were mixed with Laemmli sample buffer, boiled, separated in 12% or 15% SDS-PAGE and transferred onto a Hybond-P PVDF membrane (Amersham-GE Healthcare). Membranes were probed overnight using a 1:500 (v/v) dilution of the anti-PTEN (Sc-7974) and AKT total (Sc-H-136) (Santa Cruz Biotechnologies, CA, USA) and phosphorylated (AKT-phospho-T308, Ab-38449) (Abcam, Cambridge, UK); for detection, 1:2500 (v/v) dilutions of HRP anti-rabbit or anti-mouse conjugate antibodies (SantaCruz Biotechnology) were used. Finally, using the SuperSignal West-Femto chemiluminescent substrate (Thermo Scientific), the membranes were scanned in the C-Digit blot scanner (Li-Cor) and the images were analyzed for densitometry in the associated ImageStudio software (LiCor). Membranes were stripped and re-probed for detection of actin (anti-actin, Sc-47778) as a loading control. A representative image from three independent experiments is shown.

Luciferase reporter assays

Reporter plasmids were constructed by ligation of synthetic oligonucleotide duplexes (IDT) containing putative miR-26a target regions in the PTEN 3'UTR: 5'-CTA GTT AAC TGT TAG GGA ATT TTA CTT GAA A -3' and 5'-AGC TTT TCA AGT AAA ATT CCC TAA CAG TTA A -3', obtained from microRNA.org [21] to form a DNA duplex with overhanging SpeI and HindIII half sites in the 5' and 3' ends respectively, which was cloned into the appropriately digested pMIR-REPORT plasmid (Ambion). This construct was co-transfected with miR-26a mirVana miRNA mimic (Applied Biosystems) and the pMIR-REPORT β -gal Control Plasmid (Ambion) into HCT116 cells. Luciferase activity was analyzed using the Dual-Luciferase Reporter Assay System (Promega) 48 h after transfection, in a GloMax 96 Microplate Luminometer (Promega). Luciferase activity was normalized to β -gal activity for each transfected well; each experiment was performed in triplicate.

Real-time analysis of cell proliferation and migration

The xCELLingence real-time cell analyzer (RTCA) instrument was used with E-plates to analyze proliferation and with CIM-plates (ACEA, Biosciences) to monitor migration of cells transfected with miR-26 mimic and inhibitor. For proliferation assays, HCT116 cells were cultured and transfected in 6 well-plates (5 \times 105 cells per well) with 10% FBS-supplemented medium at 37 °C for 24 h, after that cells were trypsinized and counted by Neubauer chamber. We plated 1 \times 104 cells per E-plate well with 10% FBS-supplemented in 150 μ L/well. The RTCA recorded cell index values over 24 h by 15 min-intervals. For migration assays, 1 \times 104 cells per well were cultured in 150 μ L without FBS-avoiding therefore, cell proliferation- in the upper CIM-plate chamber while 160 μ L/well of 10% FBS-supplemented medium was added as a chemoattractant to the lower chamber. The cell index values recorded by 15 min-intervals over 24 h. These experiments were performed by triplicate.

Wound healing assay

A wound healing assay was performed to assess migration. HCT116 cells were seeded into 6 well-plates (4 \times 105 cells per well) and were maintained with 2% FBS-supplemented medium to avoid cell proliferation at 37 °C for 24 h. These cells were transfected with miR-26a mimic, anti-miR26a or controls using Lipofectamine 2000 as transfection reagent for 6 h. Afterwards, the medium was removed and replaced with freshly-changed medium 2% FBS-supplemented medium, and a wound was

performed with a sterile 200 μ L pipette tip in each well. Cells were monitored every 24 h for 72 h.

Statistical analysis

All values are expressed as the mean \pm SEM. Data were analyzed in the Prism 5.0 (GraphPad) software using a one-way ANOVA analysis followed by Tukey's Multiple Comparison Test.

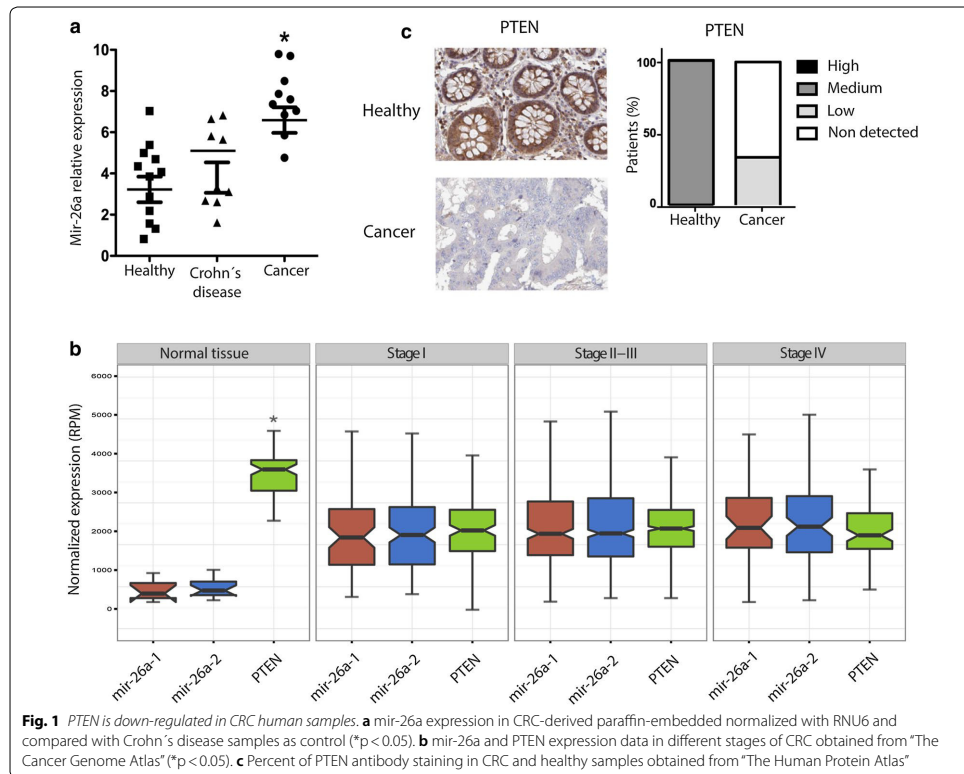
Results

PTEN and mir-26a expression are inversely correlated in human CRC samples

We measured mir-26a expression in CRC-derived paraffin-embedded tissue samples and found heterogeneous expression of this microRNA. The average mir-26a tumor expression was significantly higher than that found in both Crohn's disease and healthy tissue samples suggesting that mir-26a was overexpressed in CRC tissue samples (Fig. 1a). To verify whether this pattern was consistent in a broader sample, we used data from a third source—The Cancer Genome Atlas—and analyzed expression levels of PTEN and mir26a in 41 normal samples: 75 Stage I, 304 Stage II-III and 45 Stage IV (Fig. 1b). The data showed that mir-26a was significantly upregulated in tumors compared to normal tissues; although there was no significant difference between expression in different CRC stages. Correspondingly, PTEN was downregulated in tumors, further confirming the inverse correlation between mir-26a and PTEN that we had observed in paraffin embedded tissues samples results. Respecting to PTEN protein levels in situ we performed an in silico analysis sourcing data from the Human Protein Atlas database and compared the protein expression levels of PTEN in 2 healthy and 13 CRC samples. Immunohistochemistry data showed positive PTEN staining in all healthy samples, but none in CRC samples, indicating that loss of PTEN expression has an inverse correlation with mir-26a overexpression in CRC samples (Fig. 1c; compare to 1a and b).

PTEN is downregulated in CRC-derived cell lines

We measured the expression of mir-26a and PTEN in HCT116, SW480 and SW620, corresponding to stages I, III and metastatic respectively by qRT-PCR; CRL1790 non-tumoral colon cells were used as control. As shown in Fig. 2a, we found a slight increase in the expression level of mir-26a in HCT116; however, in SW480 and SW620 cell lines we observed a high expression of this microRNA, four- and seven-fold respectively. We consistently found an inverse correlation between mRNA PTEN and miR-26a levels: relative expression of PTEN was significantly decreased in every CRC cell line. Nevertheless, PTEN mRNA levels were diminished in HCT116



and this cell line did not have changes in mir-26a expression, suggesting there is another mechanism that regulates PTEN levels in HCT116 or Stage 1 of CRC. In all cell lines tested and mouse healthy tissue, PTEN protein levels were concordant to RNA levels. Besides, PTEN protein detection reflected an inverse correlation with miR-26a levels (Fig. 2b). Together, these results showed that both mRNA and protein levels of PTEN are down-regulated and correlate with mir-26a overexpression in CRC-derived cell lines suggesting a possible regulation of this miRNA.

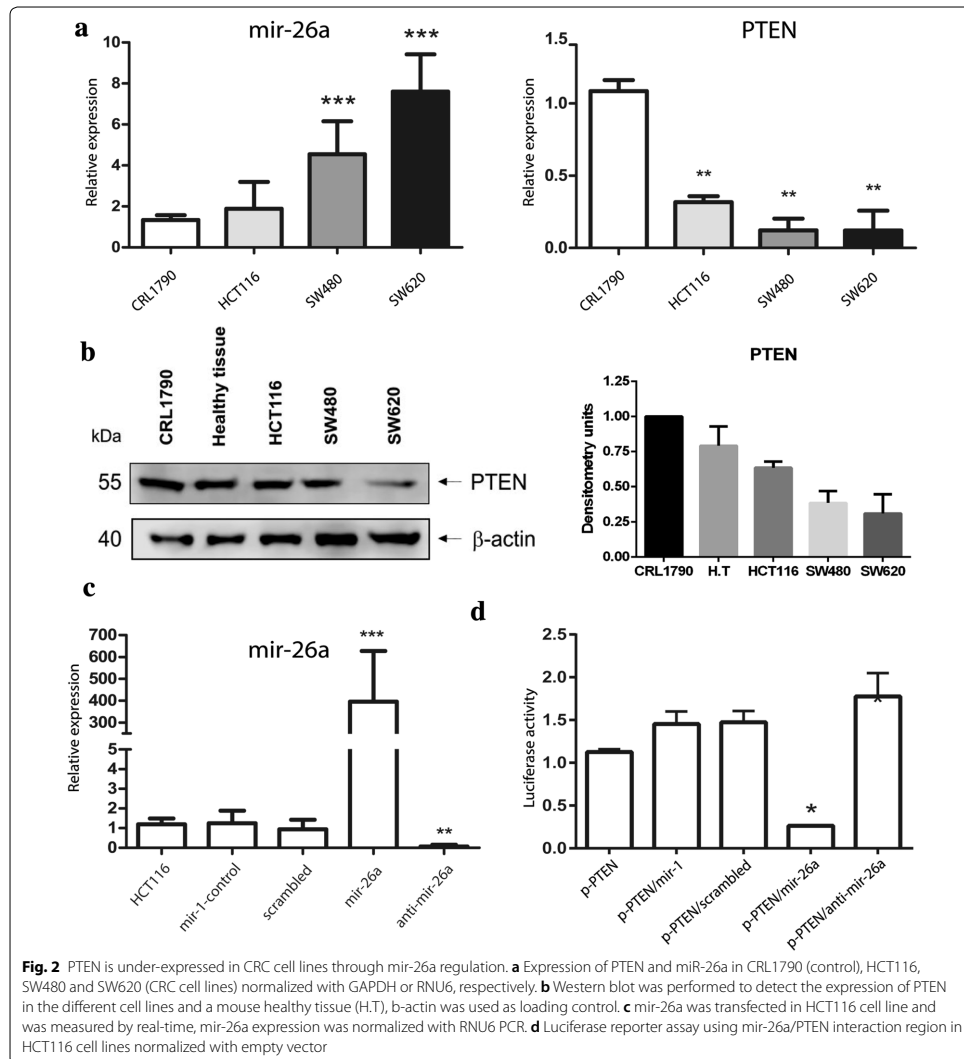
mir-26a directly inhibited PTEN expression through 3' UTR interaction

To confirm whether mir-26a directly regulates the PTEN mRNA, we used a reporter construct harboring the 3' UTR specific binding site sourced from Targetscan bioinformatics algorithm (microRNA.org) downstream from the Luciferase gene to form p-Luc-PTEN. From

the previously assayed cell lines, HCT116 showed better transfection capability and the lowest endogenous mir-26a expression, so we employed them to assess the negative regulation of PTEN exerted by mir-26a. HCT116 cells were transfected with mir-26a mimic; then the expression level of miR-26 was measured by qRT-PCR to standardize transfection conditions (Fig. 2c); later, we co-transfected p-Luc-PTEN with mir-26a for 48 h, which resulted in 74% reduction in luciferase levels compared to empty vector. These findings indicated that mir-26a could bind the 3' UTR of the PTEN mRNA (Fig. 2d).

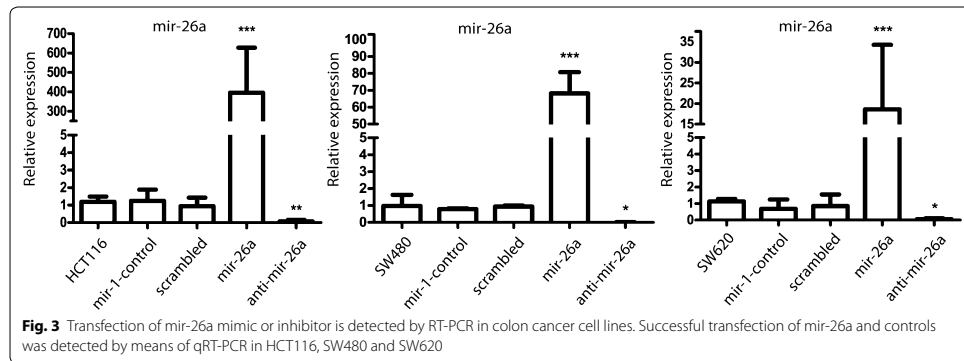
mir-26a regulates PTEN expression in a CRC-derived cell line

To clarify the effect of mir-26a on PTEN expression, mir-26a was overexpressed or repressed in HCT116, SW480 and SW620 CRC cell lines by transfection with a mir-26a mimic or inhibitor. qRT-PCR detection of miR-26a in these cells and the corresponding controls,



confirmed successful transfection (Fig. 3). We observed a better transfection capability in HCT116 and SW480 cell lines, so we chose them for following experiments. PTEN mRNA was measured by qRT-PCR and it was decreased by miR-26a over-expression in both cell lines

(Fig. 4a); however, a slight increase was observed with anti-miR-26 in HCT116, whereas a substantial increase was found in SW480. Finally, the same results were observed at the protein level in PTEN, while AKT did not show evident changes at protein level; however, we observed a direct correlation between mir-26a expression and p-AKT (Thr308)—the active state of AKT—in



both cell lines (Fig. 4b), indicating that mir-26a affects PTEN expression and AKT activity in CRC cells.

mir-26a regulates proliferation and migration in HCT116 cells

PTEN is involved in the negative regulation of AKT activation, which affects cell proliferation and migration among other crucial hallmarks of cancer. We used the xCELLingence RTCA system to measure cell proliferation and migration in each group. As expected, mir-26a overexpression increased slightly cell proliferation, on the other hand, the mir-26a downregulation, significantly decreased the proliferation rate by >50% compared to untransfected HCT116 cells indicating that mir-26a does not increase proliferation but its presence is pivotal to keep it (Fig. 5a). Next, we examined the role of mir-26a in CRC cell migration using the xCELLingence CIM plate and wound healing assays. We observed that cell migration was significantly increased after transfection with mir-26a mimic in both experiments (33%) compared to their respective controls (Fig. 5b, c). These observations suggest that mir-26a plays an important role in the proliferation maintenance and promote migration process in CRC.

mir-26a is overexpressed in AOM/DSS-induced CRC mouse model

We established a CRC mouse model to study miR-26a and PTEN expression in different stages of CRC development. All experimental groups received a single dose of Azoxymethane (AOM) and three Dextran Sulfate Sodium (DSS), every third week to generate progressive tumor development. The mean weight of the three animals in each group decreased with each DSS administration and the presence of tumors was detected after the third DSS administration (Fig. 6a). Histological analysis

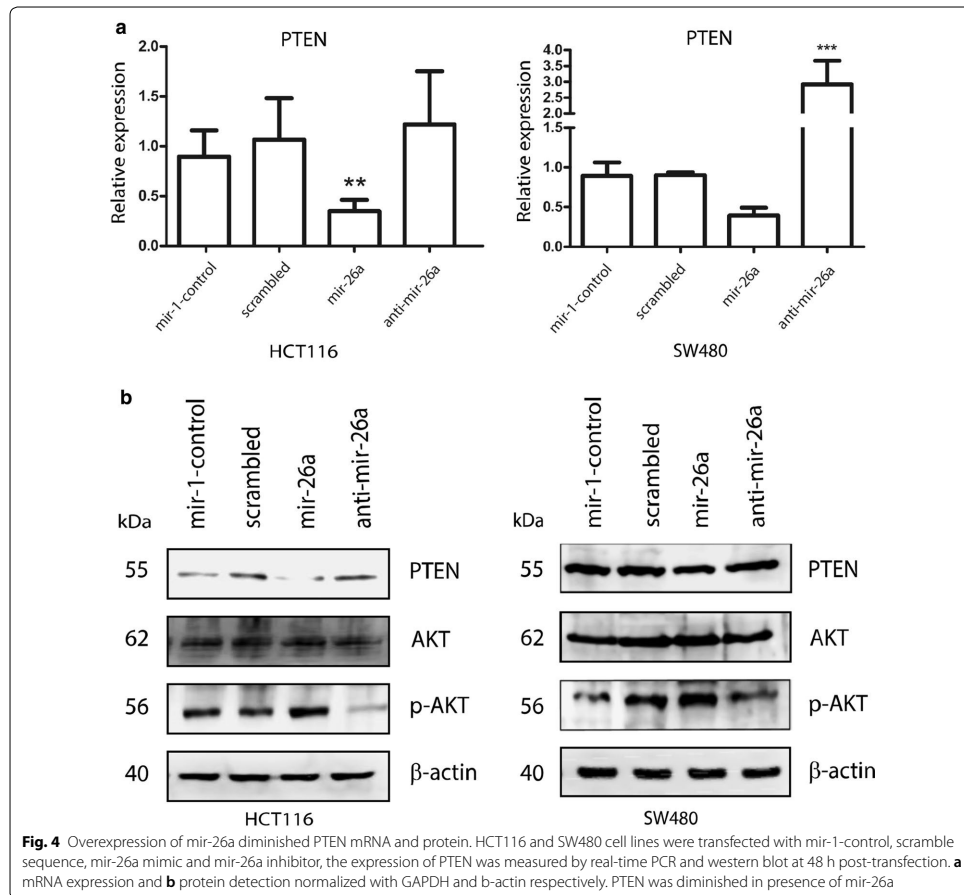
confirmed these results, revealing a generalized loss of epithelial morphology throughout the DSS cycles. After the second DSS administration, we observed chronic intestinal inflammation and slight crypt distortion with epithelial hyperplasia and after the third DSS dose, formation of adenomas composed of tubular and villous structures lined by epithelium with high grade of dysplasia (Fig. 6b). A thorough analysis of this tumors was published in a recent study from our group [20].

Expression of miR-26a and the PTEN messenger were measured after each DSS administration and we found that miR-26a expression levels remained unchanged in first DSS cycle, showed slight increase in second DSS cycle, and increased sixfold by the final DSS cycle (Fig. 6c). PTEN mRNA expression showed a gradual decrease from the first DSS cycle to the third one, in which it was undetectable (Fig. 6d). These results revealed an inverse correlation between miR-26a expression and PTEN mRNA. Conversely, the PTEN protein remained unchanged after the first and second DSS cycles and decreased only slightly after the third DSS cycle. The downstream effector regulated by PTEN activity, AKT, showed a gradual increase expression at the protein level from the first DSS cycle to the end of mouse model, suggesting that a slight decrease in PTEN allows an increase in the expression of AKT in vivo (Fig. 6e). We concluded that miR-26a targets the PTEN mRNA causing its degradation in our mouse CRC model.

Overall, our data showed that mir-26a had a key role CRC development, since it downregulated PTEN and thus enhanced cell proliferation and migration.

Discussion

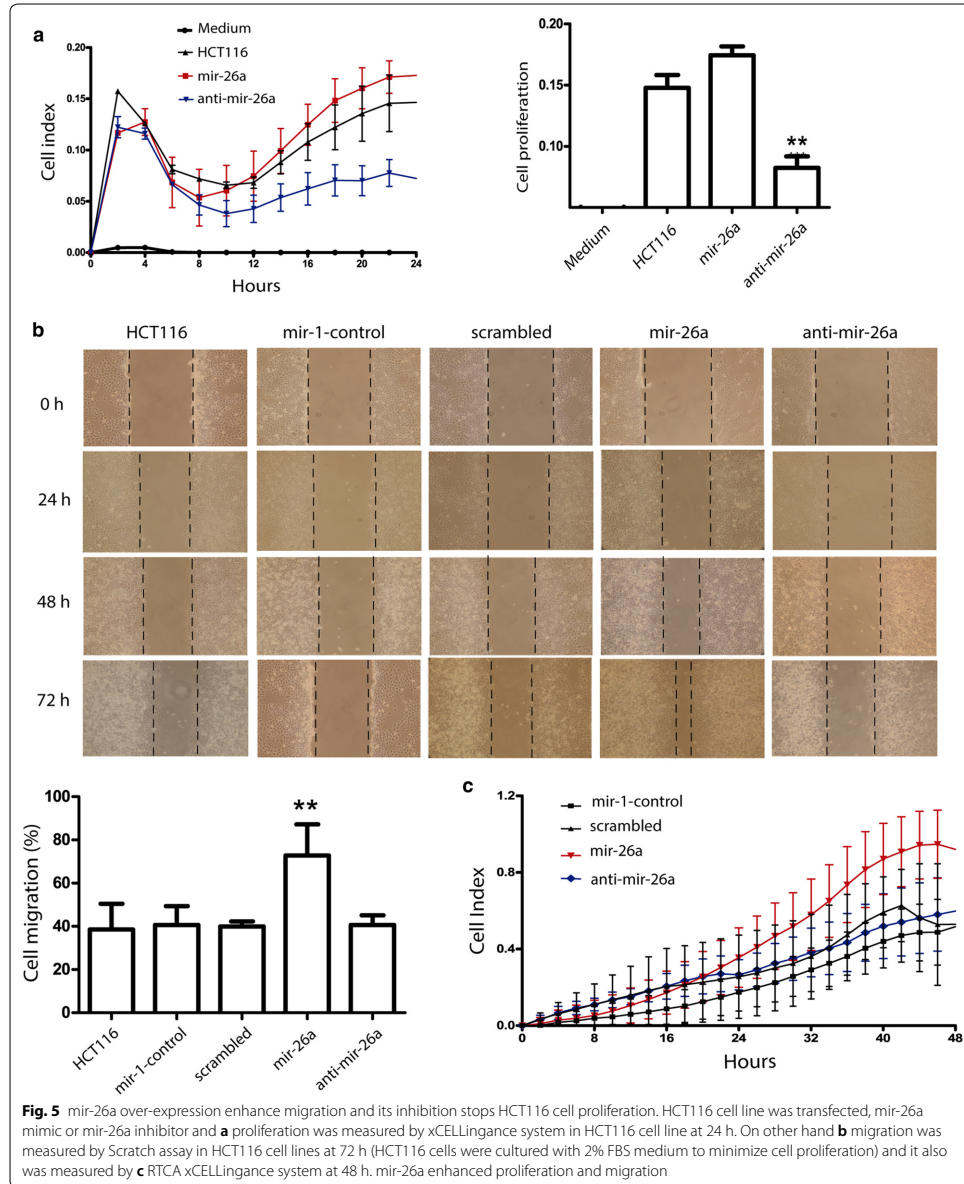
In this study, we found that mir-26a was overexpressed in CRC tissues, CRC-derived cell lines, and in samples listed in the TCGA database; furthermore, we found

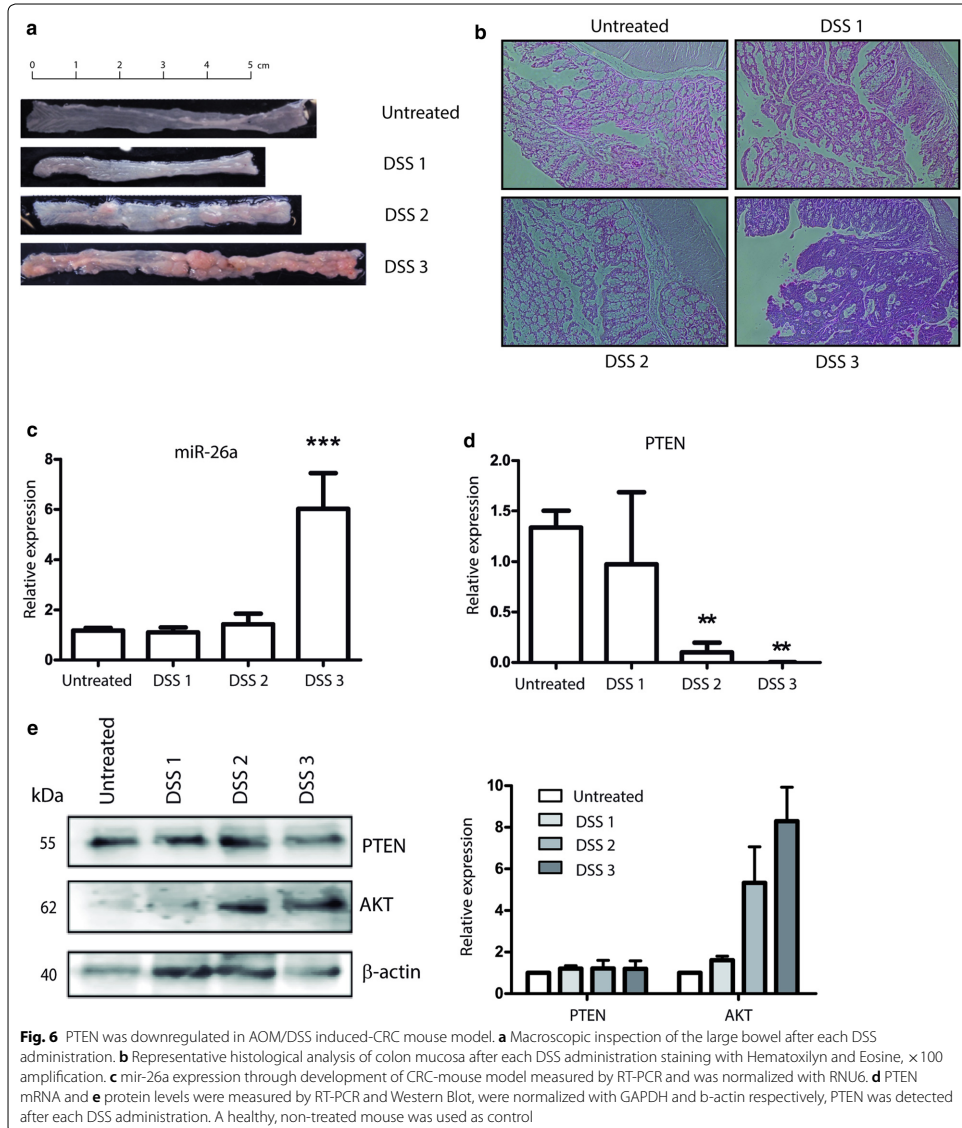


that mir-26a also was overexpressed in a CRC mouse model and that, when overexpressed in CRC-derive cell lines, it maintains proliferation and enhance migration via direct regulation of PTEN; moreover, mir-26a affected phosphorylation levels of AKT that is an effector of PTEN-PI3K pathway (Fig. 7). The importance of negative regulation of PTEN exerted by miR-26 resides in its phosphatase activity, thus its absence would mean more phosphorylation of its targets [22]. We were able to show (Fig. 4b) that pAKT level is increased when cells were treated with the miR-26 mimetic (i.e. lower PTEN levels lead to lowered phosphatase activity which leads to higher detection of pAKT) and decreased when

miR-26 was abolished with the anti-miRNA (i.e. higher PTEN levels lead to increased phosphatase activity leading to lower pAKT detection). Neither mir-26a or PTEN is known to affect AKT expression, therefore its levels remained expectedly unchanged.

PTEN has important role as a negative regulator of survival signaling and metastasis. Several studies have demonstrated that loss of PTEN expression contribute to CRC development and is associated with the migration aggressive capacity [23]. Correspondingly, the PI3K-AKT pathway, which is negatively regulated by PTEN is hyperactive in several cancers [24]. Loss of PTEN function has been characterized in tumors such as glioblastoma,





endometrial cancer, non-small cell lung cancer and colorectal cancer among others [25]; yet, the mechanisms that lead to it are still controversial. Recently, Lin and colleagues [26] successfully identified mechanisms such as

point mutations and promoter hypermethylation in CRC patient samples with loss of PTEN expression, but failed to identify a mechanism for more than 50% of them. Another study showed that hypermethylation of PTEN

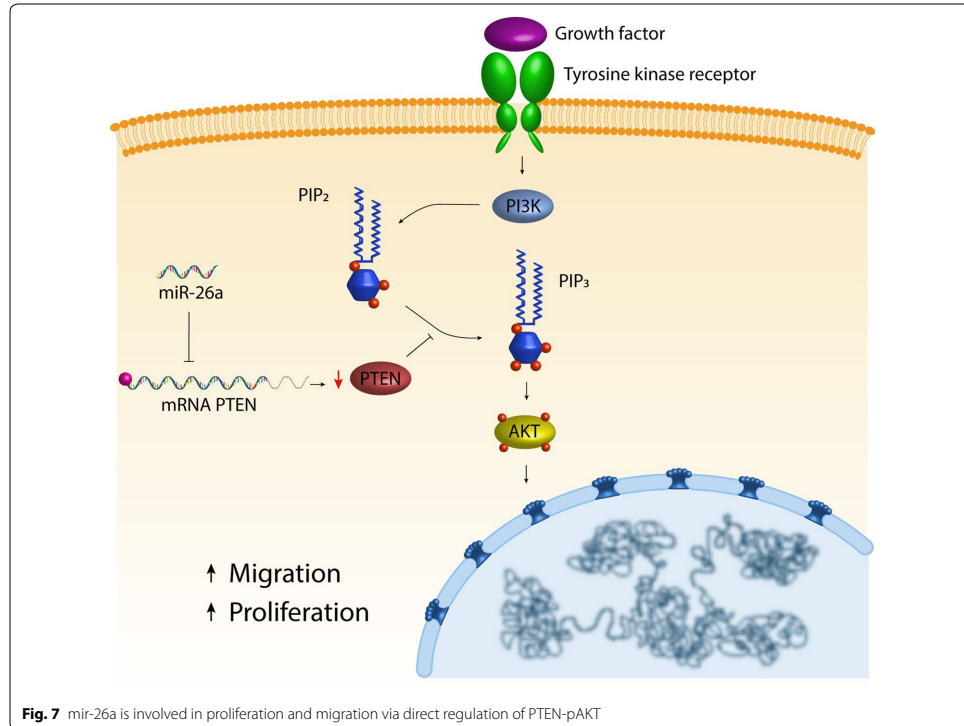


Fig. 7 miR-26a is involved in proliferation and migration via direct regulation of PTEN-pAKT

promotor occurs only in around 20% of colorectal tumors [2] indicating that other epigenetic mechanisms involved in the negative regulation of PTEN are unclear. Concurrently, several groups have found that the PTEN mRNA is subject to tight miRNA regulation, for instance, it is downregulated by miR-4534 in prostate cancer [27], and miR-29a in breast cancer [28]. Huse and colleagues were able to show that miR-26 targets and induces the degradation of PTEN in high grade glioma tumors [7] and Liu in 2012 demonstrated that miR-26a overexpression enhances migration and invasion process through wound healing and invasion chamber assays respectively, in lung cancer cells by targeting PTEN [29]. But the evidence from lung and colorectal cancer is most interesting: In lung cancer, PTEN is downregulated also by miR-21 [30], miR-205 [31], and miR-92a [32]; while in colorectal cancer, it is regulated by miR-21 [33], miR-92a [34] and miR-106b [35]. To our knowledge, we show for the first-time a negative regulation of PTEN exerted by miR-26a in colorectal cancer.

We found the lowest mRNA and protein expression in SW620 cell line, compared to the other lines used in this study. Interestingly, there was an inverse correlation as this same cell line showed the highest miR-26a levels. HCT116 cell line represents a primary tumor in early stage, in this cell line we did not observe a correlation between miR-26a and PTEN, suggesting another mechanism on PTEN regulation. There are other miRNAs that only are transcribed in primary stages, such as miR-32, miR-200c and miR-221/222. These miRNAs are highly expressed in HCT116, HT-29 [36] and Dukes' A CRC samples (where HT-29 cells and Dukes' A samples represent a primary tumor stage) and downregulated in SW480, SW620 and Dukes' D CRC samples. Therefore, PTEN is regulated by these miRNAs and their overexpression is caused by oncogenic K-RAS mutation, a key event in early CRC development [37]. On the other hand in the cell lines SW480 and SW620 which represent the most advanced stage our data suggested that the miR-26a-PTEN regulation takes place in that stage. This fact could explain the variations in the PTEN

expression after mimic and inhibitor transfection in these lines [38]. Our findings complement this data, proving that PTEN is regulated by miR-26a as well. So, thus far, nine different miRNAs have been found to regulate PTEN in CRC: miR-21, miR-92a, miR-106b, miR-32, miR-200c, miR-221/222 and miR-26a. This highlights the importance of PTEN downregulation as a means to achieve cell over-proliferation, and constitutes a plausible candidate for the missing mechanism in the aforementioned work [26].

Chronic inflammatory process is a key event in colorectal CRC development, due to activated inflammatory cells produce reactive oxygen species and reactive nitrogen intermediates which be able to induce DNA damage and mutations. Also, in CRC has been observed immune cells enhance cytokine production and growth factors, causing oxidative damage and epigenetic silencing of tumor suppressor genes [39]. In our results, we noticed that miR-26a expression is slightly higher in Cronh's disease than healthy tissue, however this result is not statistically significant. Moreover, levels of miR-26a has been found overexpressed in inactive colonic mucosa of patients with ulcerative colitis and Cronh's disease and it has been considered as a crucial player in these diseases and miR-26 can be used as good diagnostic biomarker [40].

Besides, miR-26a is an important pro-oncogenic regulator on its own, its downregulation impacts several processes that promote the establishment of tumoral phenotype, such as cell proliferation, cellular senescence, cell migration and metastasis [41]. Particularly in CRC, it has been reported to target PDHX [42], Rb1 [14], and, as per the data that we present in this work, PTEN. It has also been demonstrated that PTEN downregulation enhances epithelial-mesenchymal transition by a direct Wnt/B-catenin pathway activation in CRC [43]. Strikingly, GSK3-B—a negative key regulator of this pathway—is also a miR-26a target [8]. Mir-26a has been described as a crucial factor in the regulation of cell death, having a dual function showing a tissue-specific function. In human oral cancer cells, metformin treatment trigger miR-26a overexpression resulting in apoptosis induction [44]. Another study showed this miRNA have a protective role in ethanol-induced acute liver injury through enhancing autophagy by means of regulating DUSP4 and DSP5, two MAPKs inhibitors [45]. Moreover, in our results downregulation of miR-26a significantly reduced cell proliferation, it could be due to lack of miR-26a induces cell death. In hepatocellular carcinoma, overexpression of miR-26a/b inhibits autophagy induced by doxorubicin treatment through regulate ULK1 expression and also induces apoptosis to enhance cell chemosensitivity; On the other hand, low level of

mir-26a confers chemoresistance via autophagy induction when cells were treated with doxorubicin [46]. To our knowledge the role of miR-26 related to cell death or cell cycle arrest in CRC deserves new studies, but this growing body of evidence shows how important a regulator is miR-26a in colorectal cancer development: so far it is known to play a role in cancer cell metabolism, cell migration, and cell proliferation. Then, the question arises as to whether there are more miR-26a targets and how they interact with each other toward the generation and/or maintenance of the tumoral phenotype in CRC.

Conclusions

Overall our data suggested that mir-26a could be used as a biomarker of tumor development in CRC patients, however more studies must be conducted to establish its clinical role. Future studies will both validate these interactions in patient cohorts to establish miR-26a as a CRC diagnostic marker, and probably find further miR-26a targets to elucidate a complete picture of the miR-26a regulation network that drives CRC development.

Authors' contributions

Conceptualization, J.C.-H., E.L.-U., C.P.-P., Methodology, J.C.-H., E.L.-U.; Software, A.M.-G.; Validation, M.R.-M., A.C.-P.; Investigation, J.C.-H., E.L.-U., C.C.-R., I.D.-W., G.F.-G., A.C.-P., R.S.-G.; Writing-Original Draft Preparation, J.C.-H., E.L.-U., C.P.-P.; Writing-Review & Editing, J.C.-H., E.L.-U., C.P.-P.; Supervision, N.J.-H., L.I.-T., A.S.-C., C.L.-C.; Project Administration, C.P.-P.; Funding Acquisition, E.L.-U., C.P.-P. All authors read and approved the final manuscript.

Author details

¹ Laboratorio de Genómica Funcional, Unidad de Biomedicina, FES-IZTACALA, UNAM, Tlalnepantla, Mexico. ² Laboratorio de Genómica, Instituto Nacional de Cancerología, Av. San Fernando No 22, Col. Sección XVI, Tlalpan, Zip code 14080 Mexico City, DF, Mexico. ³ Unidad de Bioquímica, Instituto de Ciencias Médicas y Nutrición, Salvador Zubirán, Tlalpan, Mexico City, DF, Mexico. ⁴ Laboratorio de Inmunología de Parásitos, Unidad de Biomedicina, FES-IZTACALA, UNAM, Tlalnepantla, Mexico. ⁵ Laboratorio de Genética, Genómica y Bioinformática, Hospital Infantil de México, Mexico City, Mexico. ⁶ Posgrado en Ciencias Genómicas, Universidad Autónoma de la Ciudad de México, Mexico City, Mexico. ⁷ Programa de Doctorado en Ciencias Biomédicas, Universidad Nacional Autónoma de México, Mexico City, Mexico.

Acknowledgements

J. Coronel-Hernández is a doctoral student from Programa de Doctorado en Ciencias Biomédicas, Universidad Nacional Autónoma de México (UNAM) and received fellowship 402278 from CONACYT.

Competing interests

All authors declare that they have no competing interests.

Availability of data and materials

The datasets analysed during the current study are available from the publicly available The Cancer Genome Atlas and Protein Atlas repositories <https://cancergenome.nih.gov>; <https://www.proteinatlas.org>. All other data generated or analysed during this study are included in this published article.

Animal ethics Committee

All procedures performed in studies involving animals were in accordance with the ethical standards of the Facultad de Estudios Superiores Iztacala-UNAM. Twelve female Balb/c mice (Harlan Laboratories, México) aged 6 weeks used in this study were maintained at Facultad de Estudios Superiores Iztacala

Animal Facility according to the institutional animal care guidelines (Number of Approval FES-2016-1423).

Consent for publication

Not applicable.

Ethics approval and consent to participate

All procedures performed in studies involving human samples were in accordance with the ethical standards of the Instituto Nacional de Cancerología (National Cancer Institute, Mexico) and with the 1964 Helsinki declaration and its later amendments or comparable ethical standards. Present investigation was approved by ethics committee (Approval Number INCAN/CI/826/17). None of the authors had access to potentially identifying information from the donors of the paraffin-embedded samples.

Funding

This work was partially funded by PAPCA (Programa de Apoyo a los Profesores de Carrera) program, FES Iztacala-UNAM PAPCA-2014-6. The funders had no role in study design, data collection and analysis, decision to publish, or preparation of the manuscript.

Publisher's Note

Springer Nature remains neutral with regard to jurisdictional claims in published maps and institutional affiliations.

Received: 28 November 2018 Accepted: 23 March 2019

Published online: 02 April 2019

References

- Keniry M, Parsons R. The role of PTEN signaling perturbations in cancer and in targeted therapy. *Oncogene*. 2008;27(41):5477–85. <http://www.nature.com/articles/onc2008248>.
- Goel A, Arnold CN, Niedzwiecki D, Carethers JM, Dowell JM, Wasserman L, et al. Frequent inactivation of PTEN by promoter hypermethylation in microsatellite instability-high sporadic colorectal cancers. *Cancer Res*. 2004;64(214):3014–21.
- Molinari F, Frattini M. Functions and regulation of the PTEN gene in colorectal cancer. *Front Oncol*. 2013;3(January):326. <https://doi.org/10.3389/fonc.2013.00326/abstract>.
- Bartel DP, Lee R, Feinbaum R. MicroRNAs: genomics, biogenesis, mechanism, and function. *Cell*. 2004;116:281–97.
- Hayes J, Peruzzi PP, Lawler S. MicroRNAs in cancer: biomarkers, functions and therapy. *Trends Mol Med*. 2014;20(8):460–9. <https://doi.org/10.1016/j.molmed.2014.06.005>.
- Liu J, Zheng M, Tang Y, Liang X, Yang Q. microRNAs, an active and versatile group in cancers. *Int J Oral Sci*. 2011;3(4):165–75. <http://www.natur.e.com/jjos/journal/v3/n4/abs/jjos201123a.html>.
- Huse JT, Brennan C, Hambardzumyan D, Wee B, Pena J, Rouhanifard SH, et al. The PTEN-regulating microRNA miR-26a is amplified in high-grade glioma and facilitates gliomagenesis in vivo. *Genes Dev*. 2009;23(11):1327–37.
- Zhang J, Han C, Wu T. MicroRNA-26a promotes cholangiocarcinoma growth by activating β -catenin. *Gastroenterology*. 2012;143(1):1–19.
- Shen W, Song M, Liu J, Qiu G, Li T, Hu Y, et al. MiR-26a promotes ovarian cancer proliferation and tumorigenesis. *PLoS ONE*. 2014;9(1):e86871.
- Batchu RB, Gruzdyn OV, Qazi AM, Kaur J, Mahmud EM, Weaver DW, et al. Enhanced phosphorylation of p53 by microRNA-26a leading to growth inhibition of pancreatic cancer. *Surgery*. 2015;158(4):981–7. <https://doi.org/10.1016/j.surg.2015.05.019>.
- Chai ZT, Kong J, Zhu XD, Zhang YY, Lu L, Zhou JM, et al. MicroRNA-26a inhibits angiogenesis by down-regulating VEGFA through the PI3K2a/Akt/HIF-1 α pathway in hepatocellular carcinoma. *PLoS ONE*. 2013;8(10):1–12.
- Lu J, He ML, Wang L, Chen Y, Liu X, Dong Q, et al. MiR-26a inhibits cell growth and tumorigenesis of nasopharyngeal carcinoma through repression of EZH2. *Cancer Res*. 2011;71(1):225–33.
- Yang L, Belaguli N, Berger DH. MicroRNA and colorectal cancer. *World J Surg*. 2009;33(4):638–46. <https://doi.org/10.1007/s00268-008-9865-5>.
- López-Urrutia E, Coronel-Hernández J, García-Castillo V, Contreras-Romero C, Martínez-Gutiérrez A, Estrada-Galicia D, et al. MiR-26a downregulates retinoblastoma in colorectal cancer. *Tumor Biol*. 2017;39(4):101042831769594. <https://doi.org/10.1177/1010428317695945>.
- Krishnan K, Steptoe AL, Martin HC, Wani S, Nones K, Vlassov A, et al. MicroRNA-182-5p targets a network of genes involved in DNA repair. *RNA*. 2013;19:230–42.
- Sachdeva M, Mito JK, Lee CL, Zhang M, Li Z, Dodd RD, et al. MicroRNA-182 drives metastasis of primary sarcomas by targeting multiple genes. *J Clin Invest*. 2014;124(10):4305–19.
- Chen J, Yan D, Wu W, Zhu J, Ye W, Shu Q. MicroRNA-130a promotes the metastasis and epithelial-mesenchymal transition of osteosarcoma by targeting PTEN. *Oncol Rep*. 2016;35(6):3285–92. <https://doi.org/10.3892/or.2016.4719>.
- Tian K, Di R, Wang L. MicroRNA-23a enhances migration and invasion through PTEN in osteosarcoma. *Cancer Gene Ther*. 2015;22(7):351–9. <https://doi.org/10.1038/cgt.2015.27>.
- Uhlen M, Fagerberg L, Hallstrom BM, Lindskog C, Oksvold P, Mardinoglu A, et al. Tissue-based map of the human proteome. *Science*. 2015;347(6220):1260419. <https://doi.org/10.1126/science.1260419>.
- Figueroa-gonzález G, García-castillo V, Coronel-hernández J, León-cabrera S, Arias-romero LE, Terrazas LI, et al. Anti-inflammatory and antitumor activity of a triple therapy for a colitis-related colorectal cancer. *J Cancer*. 2016;7:1632.
- Betel D, Wilson M, Gabow A, Marks DS, Sander C. The microRNA.org resource: targets and expression. *Nucleic Acids Res*. 2007;36(Database):D149–53. <https://academic.oup.com/nar/article-lookup/doi/10.1093/nar/gkm995>.
- Lee Y-R, Ming C. The functions and regulation of the PTEN tumour suppressor: new modes and prospects. *Science*. 2017;355(6320):64–7. <https://doi.org/10.1038/s41580-018-0015-0>.
- Sawai H, Yasuda A, Ochi N, Ma J, Matsuo Y, Wakasugi T, et al. Loss of PTEN expression is associated with colorectal cancer liver metastasis and poor patient survival. *BMC Gastroenterol*. 2008;8:56. <http://www.pubmedcentral.nih.gov/articlerender.fcgi?artid=2611992&ool=pmc&rendertype=abstract>.
- Carracedo A, Pandolfi PP. The PTEN–PI3K pathway: of feedbacks and cross-talks. *Oncogene*. 2008;27(41):5527–41. <http://www.nature.com/articles/onc2008247>.
- Parsons R. Human cancer, PTEN and the PI-3 kinase pathway. *Semin Cell Dev Biol*. 2004;15(2):171–6.
- Lin P-C, Lin J-K, Lin H-H, Lan Y-T, Lin C-C, Yang S-H, et al. A comprehensive analysis of phosphatase and tensin homolog deleted on chromosome 10 (PTEN) loss in colorectal cancer. *World J Surg Oncol*. 2015;13:186.
- Nip H, Dar AA, Saini S, Colden M, Varahram S, Chowdhary H, et al. Oncogenic microRNA-4534 regulates PTEN pathway in prostate cancer. *Oncotarget*. 2016; 7(42):68371–84. <http://www.oncotarget.com/fulltext/12031>.
- Shen H, Li L, Yang S, Wang D, Zhong S, Zhao J, et al. MicroRNA-29a contributes to drug-resistance of breast cancer cells to adriamycin through PTEN/AKT/GSK3 β signaling pathway. *Gene*. 2016;593(1):84–90.
- Liu B, Wu X, Liu B, Wang C, Liu Y, Zhou Q, et al. MiR-26a enhances metastasis potential of lung cancer cells via AKT pathway by targeting PTEN. *Biochim Biophys Acta Mol Basis Dis*. 2012;1822(11):1692–704.
- Zhang J, Wang J, Zhao F, Liu Q, Jiang K, Yang G. MicroRNA-21 (miR-21) represses tumor suppressor PTEN and promotes growth and invasion in non-small cell lung cancer (NSCLC). *Clin Chim Acta*. 2010;411(11–12):846–52.
- Bai J, Zhu X, Ma J, Wang W. miR-205 regulates A549 cells proliferation by targeting PTEN. *Int J Clin Exp Pathol*. 2015;8(2):1175–83.
- Ren P, Gong F, Zhang Y, Jiang J, Zhang H. MicroRNA-92a promotes growth, metastasis, and chemoresistance in non-small cell lung cancer cells by targeting PTEN. *Tumor Biol*. 2016;37(3):3215–25. <https://doi.org/10.1007/s13277-015-4150-3>.
- Yang Y, Yang JJ, Tao H, Jin W. MicroRNA-21 controls hTERT via PTEN in human colorectal cancer cell proliferation. *J Physiol Biochem*. 2015;71(1):59–68.
- Ke T-W, Wei P-L, Yeh K-T, Chen W-T, Cheng Y-W. MiR-a promotes cell metastasis of colorectal cancer through PTEN-mediated PI3K/AKT pathway. *Ann Surg Oncol*. 2015;22(8):2649–55.

35. Zheng L, Zhang Y, Liu Y, Zhou M, Lu Y, Yuan L, et al. miR-106b induces cell radioresistance via the PTEN/PI3K/AKT pathways and p21 in colorectal cancer. *J Transl Med*. 2015;13(1):252.
36. Wu W, Yang J, Feng X, Wang H, Ye S, Yang P, et al. MicroRNA-32 (miR-32) regulates phosphatase and tensin homologue (PTEN) expression and promotes growth, migration, and invasion in colorectal carcinoma cells. *Mol Cancer*. 2013;32:1–11.
37. Tsunoda T, Takashima Y, Yoshida Y, Doi K, Tanaka Y, Fujimoto T, et al. Oncogenic KRAS regulates miR-200c and miR-221/222 in a 3D-specific manner in colorectal cancer cells. *Anticancer Res*. 2011;31(7):2453–9.
38. Ahmed D, Eide PW, Eilertsen IA, Danielsen SA, Eknæs M, Hektoen M, et al. Epigenetic and genetic features of 24 colon cancer cell lines. *Oncogenesis*. 2013;2:0424.
39. Terzi J, Grivennikov S, Karin E, Karin M. Inflammation and colon cancer. *Gastroenterology*. 2010;138(6):2101–14.
40. Balzola F, Bernstein C, Ho GT, Lees C. Identification of restricted subsets of mature microRNA abnormally expressed in inactive colonic mucosa of patients with inflammatory bowel disease: commentary. *Inflamm Bowel Dis Monit*. 2011;11(3):126–7.
41. Chen J, Zhang K, Xu Y, Gao Y, Li C, Wang R, et al. The role of microRNA-26a in human cancer progression and clinical application. *Tumor Biol*. 2016;1:1–14. <https://doi.org/10.1007/s13277-016-5017-y>.
42. Chen B, Liu Y, Jin X, Lu W, Liu J, Xia Z, et al. MicroRNA-26a regulates glucose metabolism by direct targeting PDHX in colorectal cancer cells. *BMC Cancer*. 2014;14(1):443.
43. Kariagina A, Aupperlee MD, Haslam SZ. PTEN loss induces epithelial–mesenchymal transition in human colon cancer cells. 2010;18(1):11–33.
44. Wang F, Xu J, Liu H, Liu Z, Xia F. Metformin induces apoptosis by microRNA-26a-mediated downregulation of myeloid cell leukaemia-1 in human oral cancer cells. *Mol Med Rep*. 2016;13(6):4671–6.
45. Han W, Fu X, Xie J, Meng Z, Gu Y, Wang X, et al. miR-26a enhances autophagy to protect against ethanol-induced acute liver injury. *J Mol Med*. 2015;93(9):1045–55.
46. Jin F, Wang Y, Li M, Zhu Y, Liang H, Wang C, et al. MiR-26 enhances chemosensitivity and promotes apoptosis of hepatocellular carcinoma cells through inhibiting autophagy. *Cell Death Dis*. 2017;8(1):e2540. <https://doi.org/10.1038/cddis.2016.461>.

Ready to submit your research? Choose BMC and benefit from:

- fast, convenient online submission
- thorough peer review by experienced researchers in your field
- rapid publication on acceptance
- support for research data, including large and complex data types
- gold Open Access which fosters wider collaboration and increased citations
- maximum visibility for your research: over 100M website views per year

At BMC, research is always in progress.

Learn more biomedcentral.com/submissions



8.6. LOPEZ-URRUTIA, E.,CORONEL-HERNANDEZ J.,.....,MARTINEZ-GUTIERREZ, ANTONIO-D., ET AL. MIR-26A DOWNREGULATES RETINOBLASTOMA IN COLORECTAL CANCER. TUMOR BIOLOGY. 2017

8.6. Lopez-Urrutia, E.,Coronel-Hernandez J.,.....,Martinez-Gutierrez, Antonio-D., et al. MiR-26a downregulates retinoblastoma in colorectal cancer. Tumor Biology. 2017

MiR-26a downregulates retinoblastoma in colorectal cancer

Tumor Biology
April 2017: 1–9
© The Author(s) 2017
Reprints and permissions:
sagepub.co.uk/journalsPermissions.nav
DOI: 10.1177/1010428317695945
journals.sagepub.com/home/tub
SAGE

Eduardo López-Urrutia¹, Jossimar Coronel-Hernández¹,
Verónica García-Castillo¹, Carlos Contreras-Romero¹,
Antonio Martínez-Gutierrez¹, Diana Estrada-Galicia¹, Luis Ignacio
Terrazas², César López-Camarillo³, Hector Maldonado-Martínez⁴,
Nadia Jacobo-Herrera⁵ and Carlos Pérez-Plasencia^{1,6}

Abstract

MicroRNAs are non-coding short RNAs that target the 3' untranslated region of messenger RNAs (mRNAs) and lead to their degradation or to translational repression. Several microRNAs have been designated as oncomirs, owing to their regulating tumor suppressor genes. Interestingly, a few of them have been found to target multiple genes whose simultaneous suppression contributes to the development of a tumoral phenotype. Here, we have showed that miR-26a is overexpressed in colorectal cancer data obtained from TCGA Research Network and in human colon cancer pathological specimens; moreover, an orthotopic in vivo model of colon cancer showed overexpression of miR-26a, while *Rb1* expression inversely correlated to miR-26a in TCGA Research Network data, pathological samples, and the in vivo model. Then, by means of luciferase assay, we demonstrated that miR-26a targets the 3' untranslated region of *Rb1* mRNA directly. This is, to our knowledge, the first report of miR-26a targeting *Rb1* in colon cancer. The results of this study suggested that miR-26a could serve as a progression biomarker in colorectal cancer. Further validation studies are still needed to confirm our findings.

Keywords

microRNA-26, colorectal cancer, retinoblastome protein

Date received: 4 October 2016; accepted: 23 December 2016

Introduction

MicroRNAs (miRNAs) are non-coding short RNAs that target the 3' untranslated region (3'UTR) of mRNAs and lead to their degradation or to translational repression;¹ despite their relatively recent discovery, they are widely recognized as important post-transcriptional regulators. They exert their functions by binding to the 3'UTR of their target mRNA through complete or partial base complementarity and thus are rather promiscuous and capable of pleiotropic effects (extensively reviewed in Liu et al.² and Hayes et al.³). Several miRNAs have been designated as oncomirs, owing to their regulating tumor suppressor genes. Interestingly, a few of them have been found to target multiple genes whose simultaneous suppression contributes to the development of a tumoral phenotype.⁴ For instance, miR-182-5p targets *BRCA1*, *RGS17*, and *FOXO3*, three genes involved in DNA repair,⁵ and drives metastasis

¹Laboratorio de Genómica Funcional, Unidad de Biomedicina, Facultad de Estudios Superiores (FES) Iztacala, Universidad Nacional Autónoma de México (UNAM), Tlalnepantla, México

²Laboratorio de Inmunología, Facultad de Estudios Superiores (FES) Iztacala, Universidad Nacional Autónoma de México (UNAM), Tlalnepantla, México

³Posgrado en Ciencias Genómicas, Universidad Autónoma de la Ciudad de México, Mexico City, Mexico

⁴Dirección de Patología, Instituto Nacional de Cancerología, Tlalpan, México

⁵Unidad de Bioquímica, Instituto Nacional De Ciencias Médicas Y Nutrición Salvador Zubirán, Tlalpan, Mexico

⁶Laboratorio de Genómica, Instituto Nacional de Cancerología, Tlalpan, México

Corresponding author:

Carlos Pérez-Plasencia, Laboratorio de Genómica, Instituto Nacional de Cancerología, Av. San Fernando No 22, Col. Sección XVI, Tlalpan 14080, México.

Email: carlos.pplas@gmail.com



Creative Commons Non Commercial CC-BY-NC: This article is distributed under the terms of the Creative Commons Attribution-NonCommercial 3.0 License (<http://www.creativecommons.org/licenses/by-nc/3.0/>) which permits non-commercial use, reproduction and distribution of the work without further permission provided the original work is attributed as specified on the SAGE and Open Access pages (<https://us.sagepub.com/en-us/nam/open-access-at-sage>).

of primary sarcomas by targeting genes such as *Rsu1*, *Mtss1*, *Pail1*, and *Timp1*, implicated in cytoskeleton remodeling and cell migration.⁶

Deep understanding of these genetic regulation networks is remarkably important in complex diseases such as colorectal cancer (CRC)—the world's fourth most deadly cancer, which takes almost 700,000 lives every year⁷—so as to gain insight into their multifactorial origin, development, and response to treatment. Among several miRNAs upregulated in CRC,⁸ miR-26a is particularly interesting. Besides established roles as a gene expression modulator in smooth cell function,⁹ pancreatic cell differentiation,¹⁰ and even miRNA biogenesis,¹¹ published evidence show that miR-26 plays a significant role in cancer development. However significant, the role that miR-26a plays in carcinogenesis seems highly context-dependent based on the current evidence: it has been demonstrated that its overexpression promotes cholangiocarcinoma by targeting *GSK3A*¹² and glioma by targeting *PTEN*;¹³ on the other hand, it has been found to be underexpressed in miRNA profiles of renal cell carcinoma¹⁴ and liver cancer¹⁵ and to drive esophageal adenocarcinoma development by targeting *Rb1*.¹⁶ These data show that the particular function of miR-26a in CRC development cannot be inferred, but must be analyzed directly. Currently, it is known that it targets *PDHX* and modifies glucose metabolism,¹⁷ but whether it actually targets known CRC-related genes such as *PTEN*, *GSK3A*, and *Rb1* in CRC development remains to be explored; in this article, we do so with the miR-26a *Rb1* interaction.

The retinoblastoma (Rb1) protein is one of the first described tumor suppressors,¹⁸ and its loss of function is considered one of the hallmarks of cancer.¹⁹ Although Rb1 has a well-described role in carcinogenesis,²⁰ its role in CRC is less clear. Its expression is heterogeneous in CRC samples,^{21,22} so it cannot be considered a bona fide molecular marker for this neoplasm,²³ but recent works have demonstrated that the lack or inactivation of Rb1 can drive colorectal tumor development.^{24,25} So we find it reasonable to infer that Rb1 downregulation is not only a consequence of overall gene dysregulation in CRC, but also an important element in its development. Such downregulation is, evidently, part of a tightly controlled network in which miRNAs may play an important role due to their negative regulator nature.

We have successfully applied the model of chronic inflammation-associated CRC²⁶ to analyze molecular events involved in colon carcinogenesis. Thus, BALB/c mice were induced to develop—through carcinogen azoxymethane (AOM) followed by three cycles of dextran sulfate sodium—an orthotopic colon tumor. Here, we have showed that miR-26a is overexpressed in both tumor murine samples and human pathological specimens; meanwhile, *Rb1* expression inversely correlated to miR-26a. Then, we demonstrated that miR-26a targets the 3' UTR of

Rb1 mRNA directly. This is, to our knowledge, the first report of miR-26a targeting *Rb1* in colon cancer.

Material and methods

Patient samples

Twenty CRC paraffin-embedded tissue samples staged locally advanced and, for comparison with neoplasia-free tissues, 10 Crohn's disease paraffin-embedded tissue samples were obtained from INCAN (Instituto Nacional de Cancerología—National Cancer Institute, Mexico) pathology registry.

CRC mouse model

Twelve female BALB/c mice (Harlan Laboratories) aged 6 weeks were used in this study. They were maintained at Facultad de Estudios Superiores Iztacala Animal Facility according to the institutional animal care guidelines. All animals were housed in plastic cages (3 mice/cage) with drinking water and pelleted basal diet ad libitum under controlled humidity ($50 \pm 10\%$), light (12/12 h light/dark cycles), and temperature ($23 \pm 2^\circ\text{C}$). They were quarantined for the first 7 days and then randomized by body weight into an experimental ($n=6$) and one control ($n=3$) group. Both groups were administered a single intraperitoneal injection (12.5 mg/kg body weight) of a colonic carcinogen AOM from Sigma-Aldrich. One week after the injection, animals were subjected to three Dextran Sulfate Sodium Salt (DSS) cycles for colitis induction. Each DSS cycle consisted of a week-long administration of reagent-grade DSS with a molecular weight of 36,000–50,000 (MP Biomedicals), dissolved in the drinking water at a concentration of 2% (w/v), followed by 2 weeks without treatment.

Three mice were euthanized after each DSS dose so as to monitor mRNA and protein expression throughout cancer development. After euthanasia, large bowels were flushed with saline and excised. Inflammation-related cancer development was confirmed by histological analysis as previously reported.²⁶

Cell culture and transfection

CRC-derived HCT116 cells (ATCC CCL-247) were cultured in Roswell Park Memorial Institute medium (RPMI medium) supplemented with 10% (v/v) fetal bovine serum and maintained at 37°C with 5% CO_2 . CRC-derived SW620 (ATCC CCL-227) and normal colon-derived CRL1790 (ATCC CRL1790) cells were cultured in Dulbecco's Modified Eagle Medium/Nutrient Mixture F-12 (DMEM/F12) medium supplemented with 10% (v/v) fetal bovine serum and maintained at 37°C with 5% CO_2 .

All plasmids used for this study were transfected using Lipofectamine 2000 transfection agent (Invitrogen), following the manufacturer's protocol. MicroRNA mimics and inhibitors were transfected using the siPORT NeoFX transfection agent (Life Technologies) following the manufacturer's protocol. For functional assays, we transfected an miR-26a mimic or an miR-26a anti-miRNA, as well as an unrelated miRNA (miR-1) or a scrambled 20-nt sequence as control (all of them purchased from Ambion).

RNA expression analysis

MiRNAs were isolated from paraffin-embedded tissue samples using the miRNeasy FFPE kit (Qiagen) following the manufacturer's recommendations. Large bowel parts of each experimental group mice were homogenized by triplicate in a Bullet Blender (Next Advance) following the manufacturer's protocol for intestinal tissue. Total RNA was isolated from the homogenized samples or from cultured cells (CRL1790, HCT116, or SW620 grown to approximately 80%–85% confluence), using the TRIzol reagent (Invitrogen) following the manufacturer's protocol.

Quantitative reverse transcription polymerase chain reaction (RT-PCR) was performed in the murine model samples using a Roche Light Cycler 2.0. MiR-26a and its putative target genes were detected in tissue samples using the TaqMan Universal Master Mix II kit and the miR-26a TaqMan probe (Applied Biosystems) or the Titan One RT-PCR kit (Roche) supplemented with SYBR Green and the corresponding primers (primer information available upon request). Amplification conditions were as follows: for miR-26a, complementary DNA (cDNA) was generated from 100 ng total RNA with the TaqMan MicroRNA Reverse Transcription Kit (Applied Biosystems) in a 15 μ L volume; quantitative polymerase chain reaction (qPCR) was performed using a microliter, denatured for 10 min at 95°C, followed by 40 cycles of 95°C for 15 s, 68°C for 60 s. For mRNA detection, we used the Titan One RT-PCR kit (Roche) supplemented with SYBR Green. cDNA was synthesized at 50°C for 30 min, immediately followed by denaturation at 94°C for 2 min, 40 cycles of 94°C for 10 s, primer-dependent annealing temperature for 30 s and 68°C for 45 s, and a final extension at 68°C for 7 min.

MiR-26a or the *Rbl* messenger was detected in cultured cells and paraffin-embedded tissue samples using the Bio-Rad CFX 96 Touch and the miR-26a TaqMan probe (Applied Biosystems) or the SYBR Select Master Mix for CFX (Applied Biosystems). Amplification conditions for miR-26a were as mentioned above. For mRNA detection, cDNA was synthesized from 2 μ g total RNA using the High-Capacity cDNA Reverse Transcription Kit (Roche); one-twentieth of this reaction was used for qPCR. Amplification conditions were 2 min at 95°C for initial denaturation, followed by 40 cycles of 95°C for 15 s, primer-dependent annealing temperature for 15 s, and 72°C for 60 s.

Relative expression data were calculated through the $\Delta\Delta C_t$ method (Applied Biosystems), normalized relative to U6 snRNA (small nuclear RNA) or glyceraldehyde 3-phosphate dehydrogenase (GAPDH) mRNA accordingly.

Protein expression analysis

Protein extracts from large bowel parts of each experimental mouse group of cultured cells were obtained by homogenization in radioimmunoprecipitation assay buffer (RIPA buffer; Santa Cruz Biotechnology); a Bullet Blender (Next Advance) and stainless steel beads were used for bowel tissues. Protein extract was cleared by centrifugation at 12,000 rpm for 20 min.

For immunodetection, 50 μ g total protein from tumor tissue or cultured cells was mixed with Laemmli sample buffer, boiled, separated in 12% or 15% sodium dodecyl sulfate polyacrylamide gel electrophoresis (SDS-PAGE), and transferred onto a Hybond-P polyvinylidene difluoride (PVDF) membrane (Amersham-GE Healthcare). Membranes were probed overnight using a 1:500 (v/v) dilution of anti-Rbl (Sc-50); for detection, 1:2500 (v/v) dilutions of horseradish peroxidase (HRP)-conjugated anti-rabbit or anti-mouse antibodies (Santa Cruz Biotechnology) were used. Finally, using the SuperSignal West Femto chemiluminescent substrate (Thermo Scientific), the membranes were scanned in the C-Digit blot scanner (Li-Cor), and the images were analyzed for densitometry in the associated ImageStudio software (Li-Cor). Membranes were stripped and re-probed for detection of actin (anti-actin, Sc-47778) as a loading control. A representative image from three independent experiments is shown.

Luciferase reporter assays

Reporter plasmids were constructed by ligation of synthetic oligonucleotide duplexes (IDT) containing putative miR-26a target regions in the *Rbl* 3'UTR, 5'-CTA GTT AAG TAC CCA TGT AGT ACT TGA AA-3' and 5'-AGC TTT TCA AGT ACT ACA TGG GTA CTT AA-3', obtained from microRNA.org,²⁷ into the pMIR-REPORT plasmid (Ambion). This construct was co-transfected with miR-26a mirVana miRNA mimic (Applied Biosystems) and the pMIR-REPORT β -gal Control Plasmid (Ambion) into HCT116 cells. Luciferase activity was analyzed using the Dual-Luciferase Reporter Assay System (Promega) 48 h after transfection in a GloMax 96 Microplate Luminometer (Promega). Luciferase activity was normalized to β -gal activity for each transfected well; each experiment was performed in triplicate.

Tissue expression meta-analysis

Antibody-based proteomic data of 3 normal colon tissue and 11 CRC samples were obtained from The Human Protein

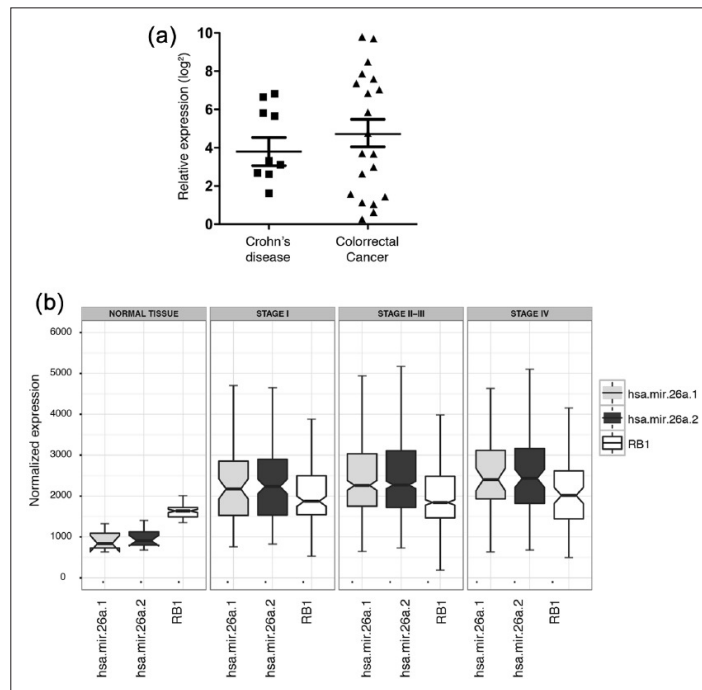


Figure 1. MiR-26a overexpression in CRC. (a) Detection of miR-26a in 20 CRC and 10 Crohn's disease samples normalized by RNU6 expression; higher miR-26a levels were found in CRC samples. (b) Meta-analysis of miR-26a1, MiR-26a2, and *Rb1* expression values from 42 normal colon samples and 76, 305, and 46 colorectal tumors of stages I, II–III, and IV; miR-26a expression was lower than that of *Rb1* in normal tissue and higher in CRC samples.

Atlas.²⁸ Antibody staining intensity was compared between healthy and cancer tissues from the *Rb1* entry.

MiR-26a1, MiR-26a2, and *Rb1* expression values from 42 normal colon samples and 76, 305, and 46 colorectal tumors of stages I, II–III, and IV, respectively, were downloaded from TCGA Research Network RNAseq V2 (cancergenome.nih.gov; 29) and graphed as normalized total counts.

Statistical analysis

All values are expressed as the mean \pm standard error of the mean (SEM). Data were analyzed in the Prism 5.0 (GraphPad) software using a one-way analysis of variance (ANOVA) followed by Tukey's multiple comparison test.

Results

MiR-26a overexpression in tissue samples

We assessed miR-26a expression in CRC-derived paraffin-embedded tissue samples and found wide variation in

expression levels; however, the maximum expression values were higher than those observed in the Crohn's disease tissue samples that we analyzed as neoplasia-free controls due to the difficulties of obtaining healthy tissue biopsies (Figure 1(a)). Analysis of data sourced from the TCGA Research Network²⁹ yielded consistent results: miR-26a was overexpressed in CRC samples relative to normal colon tissues. Interestingly, we found that *Rb1* was expressed at a higher level than miR-26a in CRC, as opposed to normal tissue, where its expression was higher (Figure 1(b)). Previous studies have already described miR-26a overexpression in Crohn's disease,³⁰ so we reasoned that the overall tendency to a higher expression of miR-26 in CRC compared to normal tissue and the pre-malignant Crohn's disease merited further investigation.

AOM/DSS-induced CRC mouse model

We established a CRC model suitable for miR-26a expression studies. All experimental groups received a single dose of a colonic genotoxic carcinogen (AOM) and

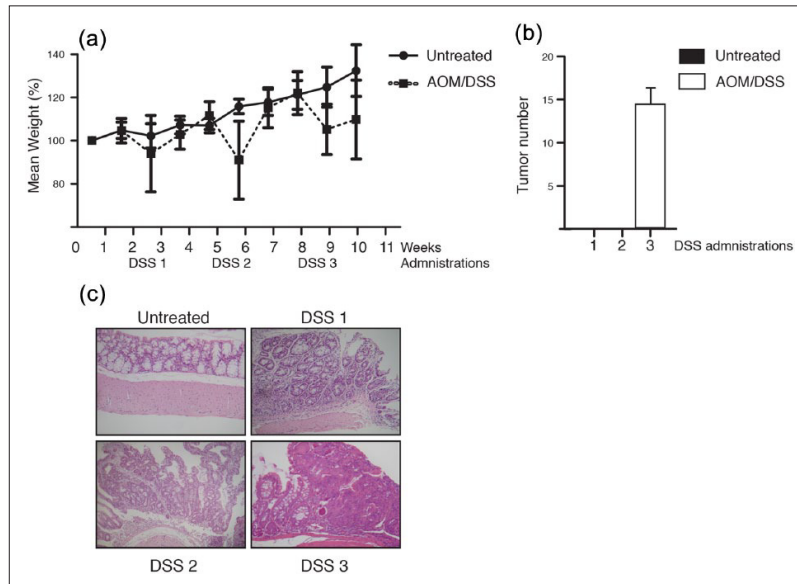


Figure 2. AOM/DSS-derived CRC mouse model. (a) Mean weight increment of the mice subject to the AOM/DSS treatment. (b) Average tumor number observed after each DSS administration. (c) Representative histological analysis of the large bowel during the progression of the model.

repeated exposure to a colitis inductor (DSS), which caused the tumor development. The mean weight of the animals decreased with each DSS administration (Figure 2(a)), and tumors were observed after the third one (DSS 3, Figure 2(b)). Histological analysis confirmed these results, revealing a generalized loss of epithelial morphology throughout the DSS cycles. After the second DSS administration, we observed 1C chronic intestinal inflammation and slight crypt distortion with epithelial hyperplasia, and after the third DSS dose, formation of adenomas composed of tubular and villous structures lined by epithelium with high grade of dysplasia was observed (Figure 2(c)). In-depth analysis of these tumors was published recently in another article from our group.²⁶

Mir-26a targets and Rb1 mRNA in an AOM/DSS-induced CRC mouse model

Expression analysis for miR-26a and the *Rb1* messenger was performed after each DSS administration. The results are shown in Figure 2: miR-26a expression levels remained unchanged after the first DSS cycle, showed a modest increase after DSS 2, and increased around sixfold after DSS 3 (Figure 3(a)). This increase corresponded to previous findings about an augmented miR-26a expression in CRC. We next assessed *Rb1* mRNA level at the same time points

(Figure 3(b)). *Rb1* mRNA showed a different pattern was slightly upregulated after DSS1, and its detection levels considerably diminished until the third DSS. These results showed consistency between the detection of miR-26a expression and its target *Rb1* mRNA, as the latter diminished clearly as miR-26a presence increased. Conversely, the Rb1 protein showed a modest increase through DSS 1 and 2 and only a slight but reproducible decrease after DSS 3 (Figure 3(c) and (d)). We concluded that miR-26a targets the *Rb1* mRNA causing its degradation in mouse CRC model. The discrepancy between the mRNAs and its protein product suggested further regulation of the Rb1 expression, likely a shift in translation efficiency.

Mir-26a interacts directly with the Rb1 mRNA 3' UTR

In order to confirm whether miR-26a exerted a direct regulation on the *Rb1* messenger, we performed luciferase reporter assays in HCT116 cells transfected with an miR-26a mimic or the corresponding anti-miRNA. Figure 4(a) shows miR-26a presence in HCT116 cells transfected with the miR-26a mimic compared to its endogenous expression. Luciferase expression decreased significantly regardless of the full-length *Rb1* 3' UTR (Figure 4(b)) or only the miR-26a interaction region (Figure 4(c)),

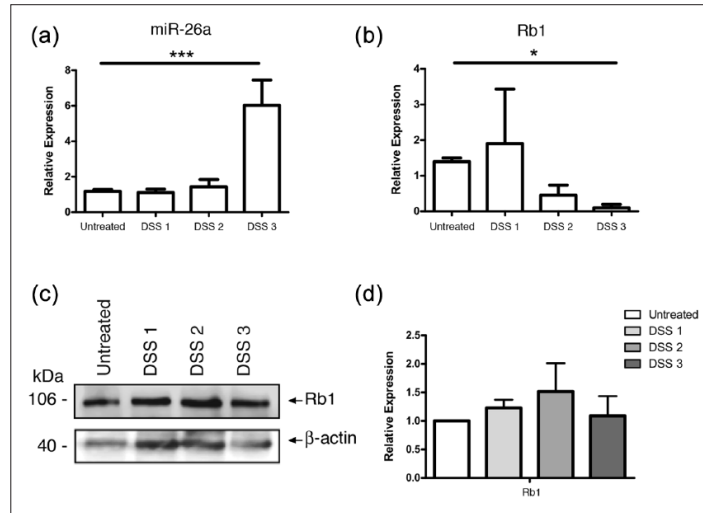


Figure 3. MiR-26a targets the Rb1 mRNA in an AOM/DSS-derived CRC mouse model. (a) MiR-26a and (b) Rb1 mRNA expression after each DSS administration, relative to the expression in untreated mice. (c) Representative image and (d) average densitometric values of Rb1 immunodetection after each DSS administration; β -actin was detected as a loading control and was used to normalize densitometric data.

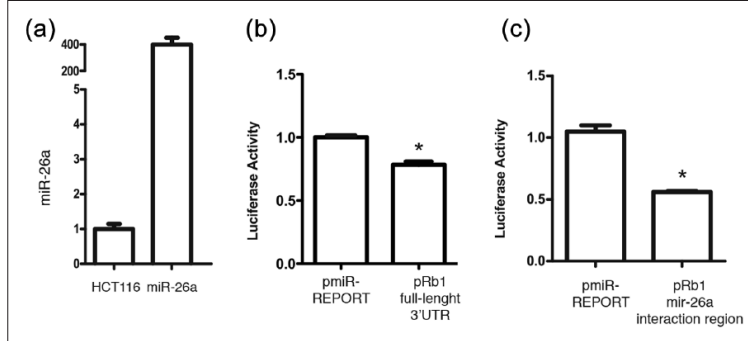


Figure 4. MiR-26a directly targets the Rb1 3' UTR. (a) MiR-26a expression in HCT116 cells transfected with an miR-26a mimic normalized to endogenous miR-26a expression in untransfected cells. (b and c) Luciferase reporter assay using the full-length Rb1 3' UTR and the miR-26a interaction region, respectively. Each experiment was performed in triplicate, and the mean values were normalized to the empty vector (pMIR-REPORT) luciferase activity.

confirming the predicted binding of miR-26a to the *Rb1* mRNA²⁷ in contrast to the context of the complete untranslated region.

CRC samples show decreased Rb1 expression

The miR-26a/*Rb1* regulation envisioned by our experiments would only be relevant if patient samples showed

evidences of it, so we turned to The Human Protein Atlas³¹ as a means to assess Rb1 expression in a broad range of normal and cancer tissues. We found high Rb1 expression levels in 100% of the healthy colon tissues present in The Human Protein Atlas database and, in contrast, in only 60% of cancer tissue. Rb1 was present in the remaining cancer samples at either medium levels or below the detection limit (Figure 5). This evidence supports our previous

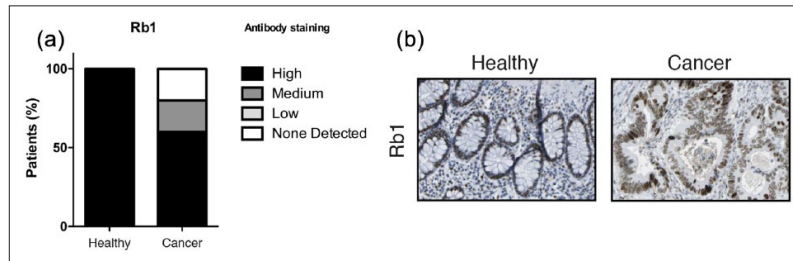


Figure 5. Rb1 underexpression in The Human Protein Atlas data set. (a) Antibody staining values found in healthy and cancer tissue samples. (b) Representative image of Rb1 immunohistochemical analysis showing reduced staining in cancer tissue.

findings, as Rb1 expression is decreased in 40% of the cancer samples.

Mir-26a regulates Rb1 in CRC-derived cell lines

We next set out to investigate whether the regulation exerted by miR-26a on the *Rb1* messenger was reproducible in human cells. First, we surveyed the expression of *Rb1* at the mRNA and protein levels in CRC-derived cell lines and the CRL1790 normal colon cell line. Consistent with expression data from normal and cancer tissues, *Rb1* expression was significantly lower in both HCT116 and SW620 cells (Figure 6(a) and (b)). When transfected with an miR-26a mimic, Rb1 expression in HCT116 cells decreased dramatically. This decrease was not observed in cells transfected with miR-1 (an unrelated control) or with a scrambled miRNA sequence; however, Rb1 expression was rescued by transfection of anti-miR-26a (Figure 6(c) and (d)). These results indicated that miR-26a downregulates the *Rb1* mRNA in the context of CRC.

Discussion

Taken together, our results show that miR-26a is an important regulator in CRC; it targets the *Rb1* messenger directly in a CRC mouse model and in CRC-derived cell lines, and decreases its protein levels.

Mir-26 is dysregulated in several cancer types: it plays tumor suppressor role in some of them such as prostate cancer and melanoma, although it is considered oncogenic in others such as cholangiocarcinoma and CRC.³² Most interesting in this regard is the work by Zhang et al.,¹⁶ which shows that miR-26a acts as a tumor suppressor in esophageal cancer by downregulating *Rb1*, while in this work, we confirmed its function as a regulator of the *Rb1* messenger but described a novel oncogenic role in CRC. This apparent discrepancy renders miRNA regulation even more astonishing, as it suggests that a given miRNA-mRNA interaction is not oncogenic or tumor suppressing per se, but can have either outcome depending on the

context. The evidence that we present here, together with the targeting of *PDHX*,¹⁷ highlights the importance of this miRNA as an oncogenic regulator in CRC.

The role of Rb1 in colorectal carcinogenesis remains controversial, as it does not show a constant dysregulation pattern among CRC samples. Palmqvist et al.³³ and Cui et al.,³⁴ among others, have found that Rb1 expression is important for CRC development, while works from Kucherlapati et al.³⁵ and Parisi et al.²⁵ show that it is the Rb1 suppression that drives colorectal tumorigenesis. This apparent discrepancy is consistent with our analysis of The Human Protein Atlas data set, where we found Rb1 in varying degrees of underexpression in about half of the tumor samples. These two tumor groups (Rb1 overexpression and suppression) have been distinguished before,³⁶ so we find it reasonable to assume that the underlying regulation network can lead to CRC development either through Rb1 over- or underexpression. Our data showed that both the colorectal tumors in our murine model and the CRC-derived cell lines that we assayed display Rb1 underexpression and thus resemble this sort of tumors.

Therefore, we propose that miR-26a modulates cell proliferation through Rb1 downregulation in CRC, due to its role in cell cycle regulation. And this function, together with the previously observed regulation of glucose metabolism through PDHX targeting,¹⁷ accentuates the importance of miR-26a as a multifunctional regulator in colorectal carcinogenesis.

On the other hand, Rb1 is regulated by miR-106a as well,³⁶ and this article appoints miR-26a as a second regulator of this tumor suppressor gene. Several studies are necessary to completely grasp complex regulation networks. In this one, we contribute to this understanding by reporting for the first time that the Rb1 underexpression in CRC is caused by direct interaction with miR-26a. Further studies will undoubtedly show a wider perspective of the regulation network that controls CRC development. Further validation studies employing larger number of pathological samples could help to support the utility of miR-26a as diagnostic molecular marker.

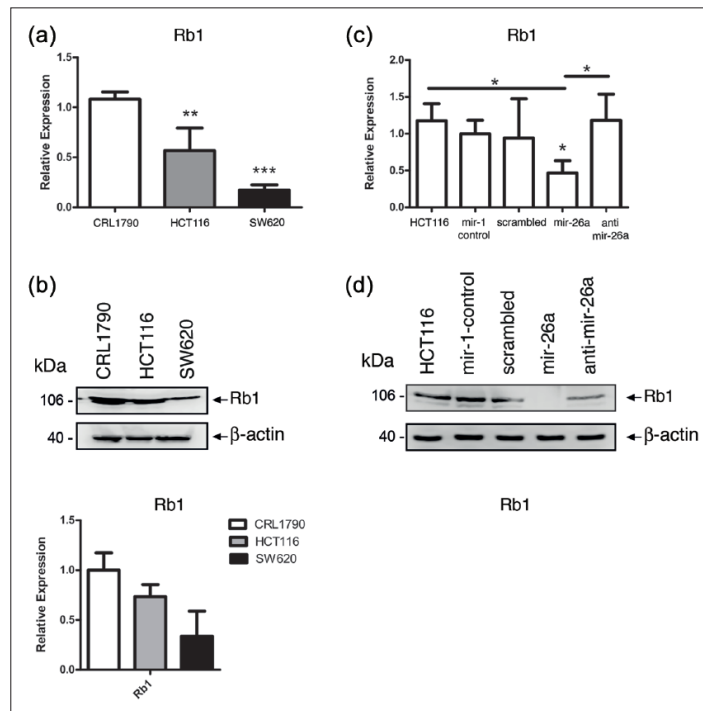


Figure 6. MiR-26a regulation over Rb1 in CRC-derived cells. (a) MiR-26a expression in HCT116 and SW620 CRC-derived cell lines relative to the CRL1790 non-tumorigenic colonic cells. (b) Representative image and average densitometric values of Rb1 immunodetection in CRC-derived cells; β -actin was detected as a loading control and was used to normalize densitometric data. (c) mRNA and (d) protein Rb1 expression in HCT116 cells transfected with an unrelated miRNA (miR-1), a scrambled 20-nt sequence, an miR-26a mimic or an miR-26a anti-miRNA normalized to untreated cells. Rb1 was downregulated only by the miR-26a mimic.

Acknowledgements

E.L.-U. and J.C.-H. contributed equally to this work.

Declaration of conflicting interests

The author(s) declared no potential conflicts of interest with respect to the research, authorship, and/or publication of this article.

Funding

The author(s) disclosed receipt of the following financial support for the research, authorship, and/or publication of this article: This work was partially funded by PAPCA (Programa de Apoyo a los Profesores de Carrera) 2014 program, FES Iztacala-UNAM.

References

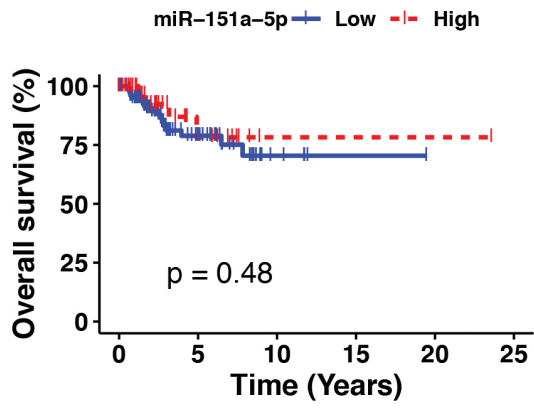
- Bartel DP. MicroRNAs: genomics, biogenesis, mechanism, and function. *Cell* 2004; 116: 281–297.
- Liu J, Zheng M, Tang YL, et al. MicroRNAs, an active and versatile group in cancers. *Int J Oral Sci* 2011; 3: 165–175.
- Hayes J, Peruzzi PP and Lawler S. MicroRNAs in cancer: biomarkers, functions and therapy. *Trends Mol Med* 2014; 20: 460–469.
- Di Leva G, Garofalo M and Croce CM. MicroRNAs in cancer. *Annu Rev Pathol* 2014; 9: 287–314.
- Krishnan K, Steptoe AL, Martin HC, et al. MicroRNA-182-5p targets a network of genes involved in DNA repair. *RNA* 2013; 19: 230–242.
- Sachdeva M, Mito JK, Lee C-L, et al. MicroRNA-182 drives metastasis of primary sarcomas by targeting multiple genes. *J Clin Invest* 2014; 124: 4305–4319.
- Ferlay J, Soerjomataram I, Dikshit R, et al. Cancer incidence and mortality worldwide: sources, methods and major patterns in GLOBOCAN 2012. *Int J Cancer* 2015; 136(5): E359–E386.
- Yang L, Belaguli N and Berger DH. MicroRNA and colorectal cancer. *World J Surg* 2009; 33: 638–646.

9. Leeper NJ, Raiesdana A, Kojima Y, et al. MicroRNA-26a is a novel regulator of vascular smooth muscle cell function. *J Cell Physiol* 2011; 226: 1035–1043.
10. Fu X, Jin L, Wang X, et al. MicroRNA-26a targets ten eleven translocation enzymes and is regulated during pancreatic cell differentiation. *Proc Natl Acad Sci U S A* 2013; 110(44): 17892–17897.
11. Fu X, Meng Z, Liang W, et al. MiR-26a enhances miRNA biogenesis by targeting Lin28B and Zcchc11 to suppress tumor growth and metastasis. *Oncogene* 2014; 33: 4296–4306.
12. Zhang J, Han C and Wu T. MicroRNA-26a promotes cholangiocarcinoma growth by activating β -catenin. *Gastroenterology* 2012; 143: 246–248.
13. Huse JT, Brennan C, Hambarzumyan D, et al. The PTEN-regulating microRNA miR-26a is amplified in high-grade glioma and facilitates gliomagenesis in vivo. *Genes Dev* 2009; 23: 1327–1337.
14. Heinzelmann J, Henning B, Sanjmyatav J, et al. Specific miRNA signatures are associated with metastasis and poor prognosis in clear cell renal cell carcinoma. *World J Urol* 2011; 29: 367–373.
15. Ji J, Shi J, Budhu A, et al. MicroRNA expression, survival, and response to interferon in liver cancer. *N Engl J Med* 2009; 361: 1437–1447.
16. Zhang Y-F, Zhang A-R, Zhang B-C, et al. MiR-26a regulates cell cycle and anoikis of human esophageal adenocarcinoma cells through Rb1-E2F1 signaling pathway. *Mol Biol Rep* 2013; 40: 1711–1720.
17. Chen B, Liu Y, Jin X, et al. MicroRNA-26a regulates glucose metabolism by direct targeting PDHX in colorectal cancer cells. *BMC Cancer* 2014; 14: 443.
18. Friend SH, Bernards R, Rogelj S, et al. A human DNA segment with properties of the gene that predisposes to retinoblastoma and osteosarcoma. *Nature* 1986; 323: 643–646.
19. Hanahan D and Weinberg RA. The hallmarks of cancer. *Cell* 2000; 100: 57–70.
20. Williams JP, Stewart T, Li B, et al. The retinoblastoma protein is required for Ras-induced oncogenic transformation. *Mol Cell Biol* 2006; 26: 1170–1182.
21. Ali AA, Marcus JN, Harvey JP, et al. RB1 protein in normal and malignant human colorectal tissue and colon cancer cell lines. *FASEB J* 1993; 7: 931–937.
22. Ayhan S, Isisag A, Saruc M, et al. The role of pRB, p16 and cyclinD1 in colonic carcinogenesis. *Hepatogastroenterology* 2010; 57: 251–256.
23. Poller DN, Baxter KJ and Shepherd NA. p53 and Rb1 protein expression: are they prognostically useful in colorectal cancer? *Br J Cancer* 1997; 75: 87–93.
24. Kucherlapati MH, Yang K, Fan K, et al. Loss of *Rb1* in the gastrointestinal tract of *Apc*^{1638N} mice promotes tumors of the cecum and proximal colon. *Proc Natl Acad Sci U S A* 2008; 105: 15493–15498.
25. Parisi T, Bronson RT and Lees JA. Inactivation of the retinoblastoma gene yields a mouse model of malignant colorectal cancer. *Oncogene* 2015; 34: 5890–5899.
26. Figueroa-González G, Garcia-Castillo V, Coronel-Hernández J, et al. Anti-inflammatory and antitumor activity of a triple therapy for a colitis-related colorectal cancer. *J Cancer* 2016; 7: 1632–1644.
27. Betel D, Wilson M, Gabow A, et al. The microRNA.org resource: targets and expression. *Nucleic Acids Res* 2008; 36: D149–D153.
28. Uhlen M, Fagerberg L, Hallstrom BM, et al. Tissue-based map of the human proteome. *Science* 2015; 347(6220): 1260419.
29. Cancer Genome Atlas Research Network, Weinstein JN, Collisson EA, et al. The Cancer Genome Atlas Pan-Cancer analysis project. *Nat Genet* 2013; 45: 1113–1120.
30. Fasseu M, Tréton X, Guichard C, et al. Identification of restricted subsets of mature microRNA abnormally expressed in inactive colonic mucosa of patients with inflammatory bowel disease. *PLoS ONE* 2010; 5: e13160.
31. Uhlen M, Oksvold P, Fagerberg L, et al. Towards a knowledge-based Human Protein Atlas. *Nat Biotechnol* 2010; 28: 1248–1250.
32. Chen J, Zhang K, Xu Y, et al. The role of microRNA-26a in human cancer progression and clinical application. *Tumour Biol* 2016; 37: 7095–7108.
33. Palmqvist R, Stenling R and Öberg Å. Expression of cyclin D1 and retinoblastoma protein in colorectal cancer. *Eur J Cancer* 1998; 34: 1575–1581.
34. Cui X, Shirai Y, Wakai T, et al. Aberrant expression of pRB and p16^{INK4a}, alone or in combination, indicates poor outcome after resection in patients with colorectal carcinoma. *Hum Pathol* 2004; 35: 1189–1195.
35. Kucherlapati MH, Nguyen AA, Bronson RT, et al. Inactivation of conditional Rb by Villin-Cre leads to aggressive tumors outside the gastrointestinal tract. *Cancer Res* 2006; 66: 3576–3583.
36. Catela Ivkovic T, Aralica G, Cacev T, et al. MiR-106a overexpression and pRB downregulation in sporadic colorectal cancer. *Exp Mol Pathol* 2013; 94: 148–154.

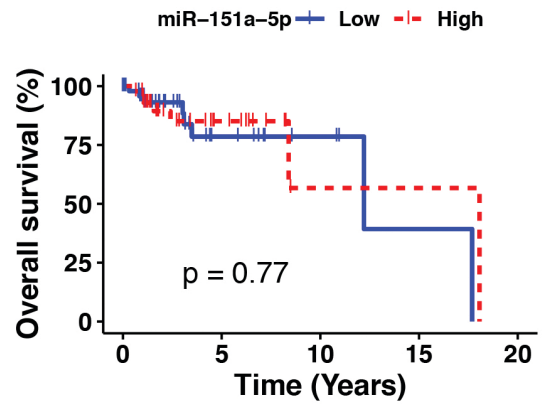
Figuras suplementarias

9.1. Figura suplementaria 1

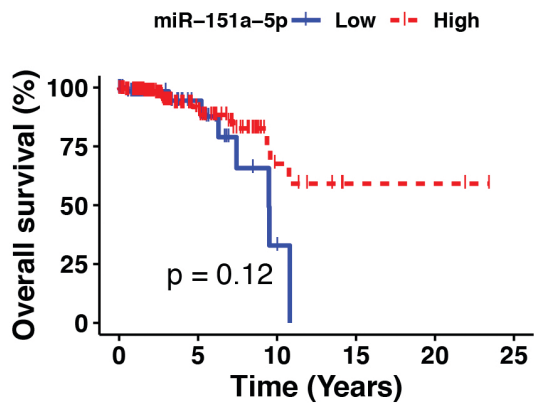
Basal subtype



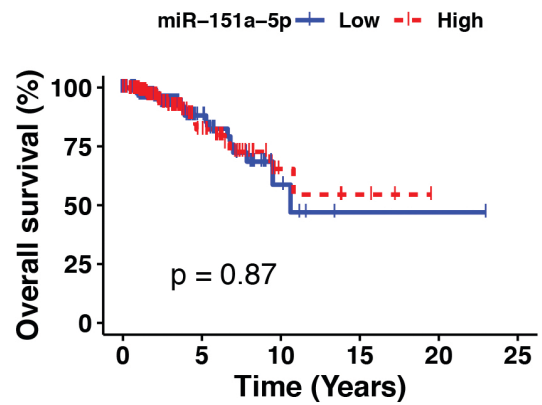
Her2 subtype



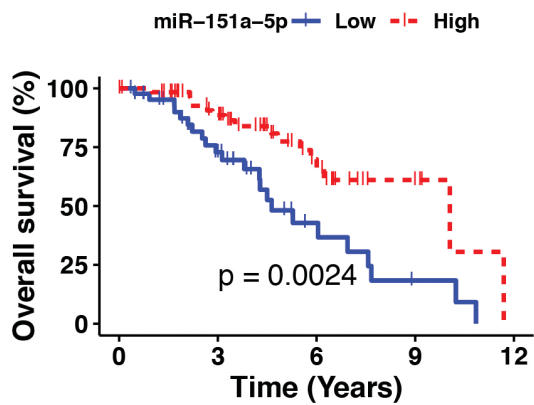
LumA subtype



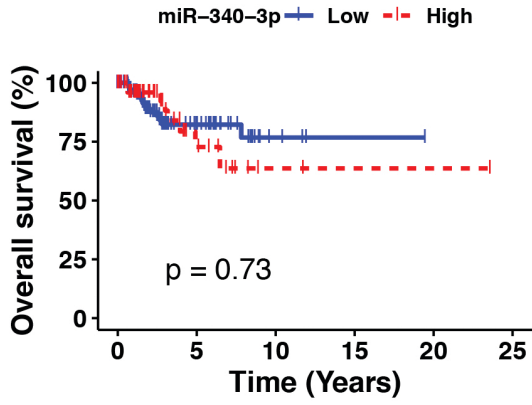
LumB subtype



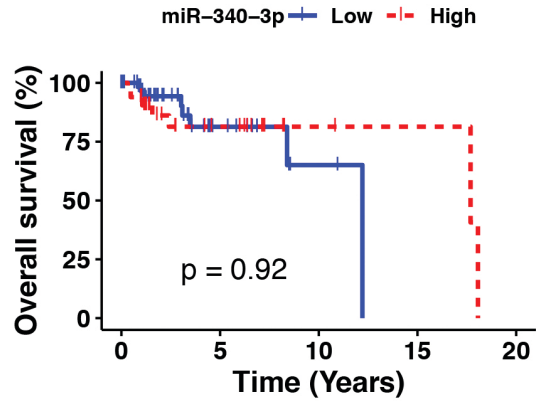
Normal subtype



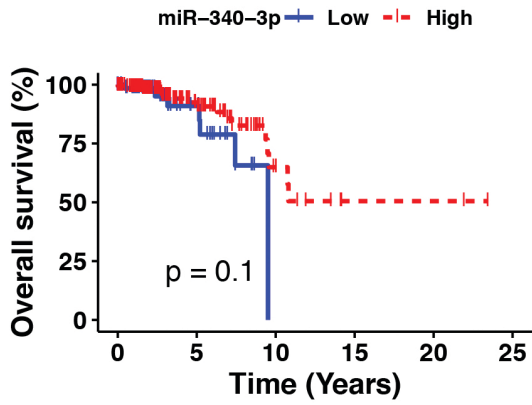
Basal subtype



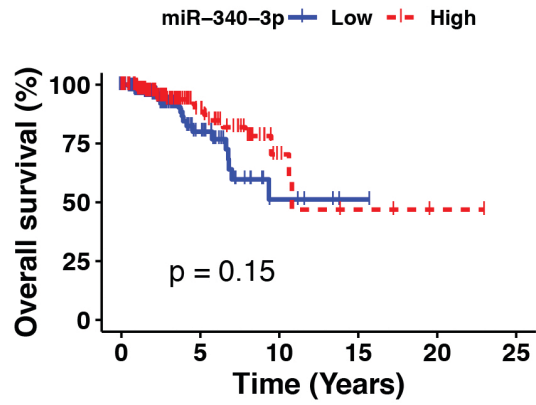
Her2 subtype



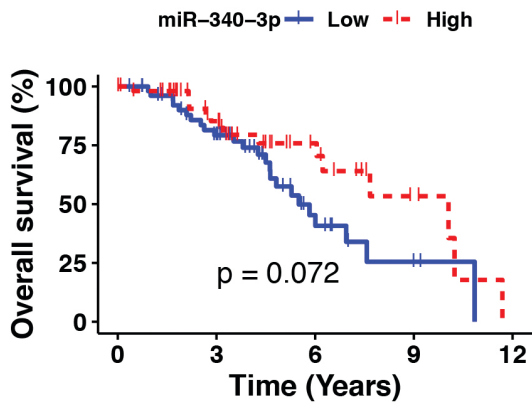
LumA subtype



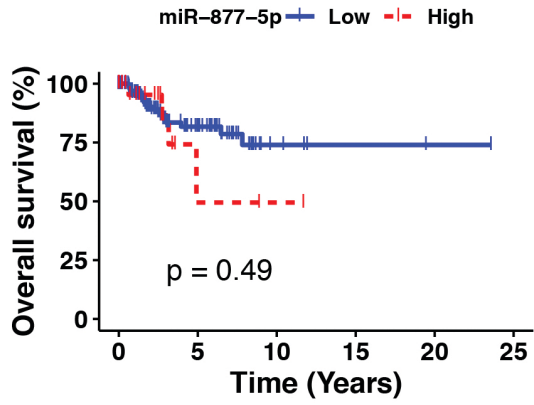
LumB subtype



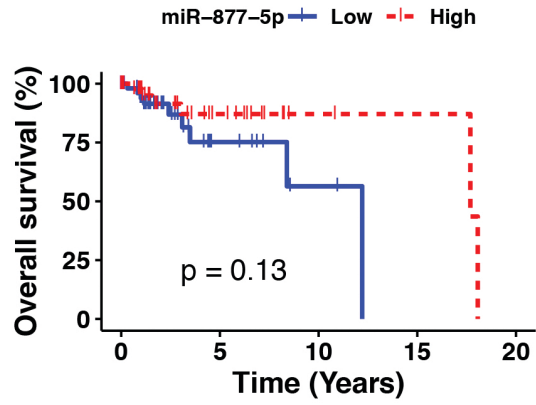
Normal subtype



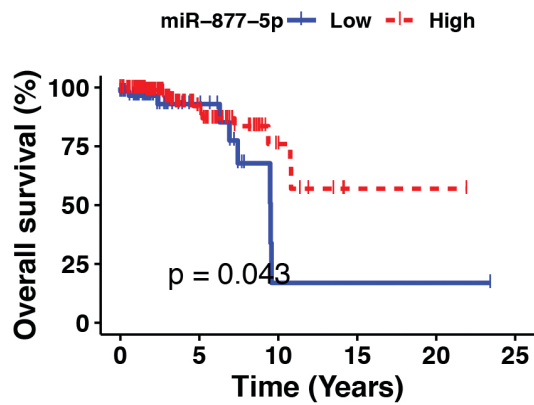
Basal subtype



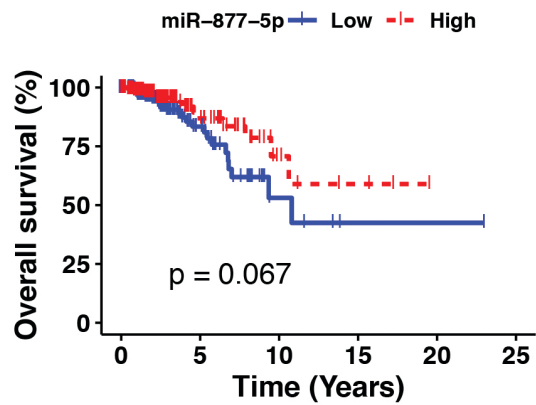
Her2 subtype



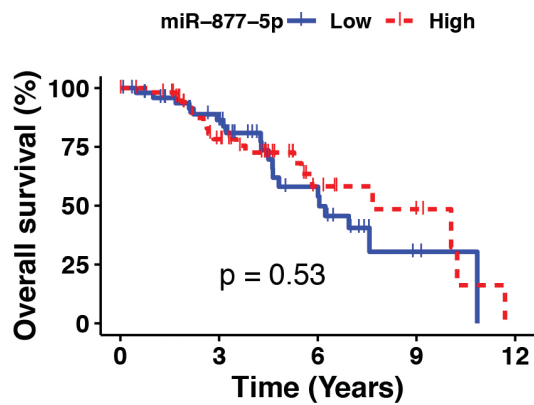
LumA subtype



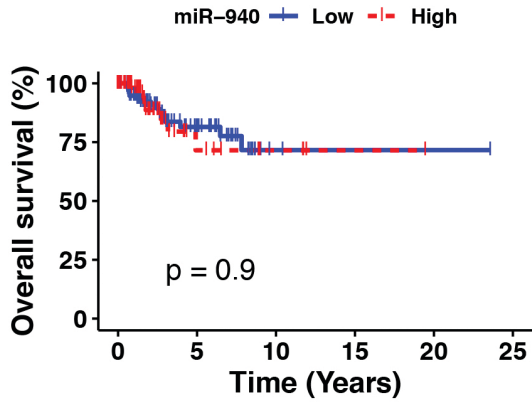
LumB subtype



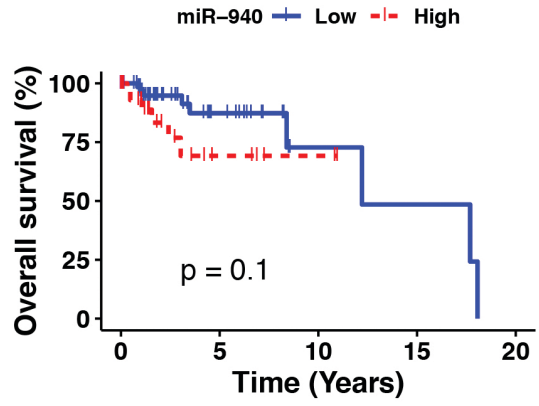
Normal subtype



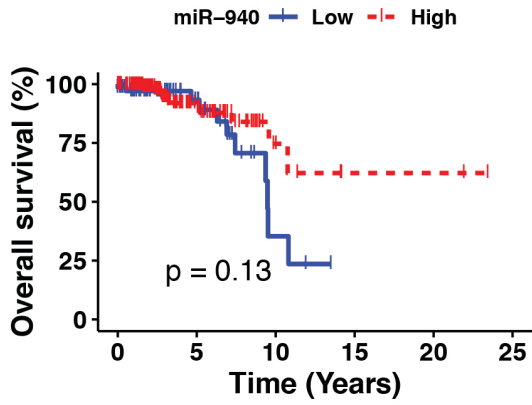
Basal subtype



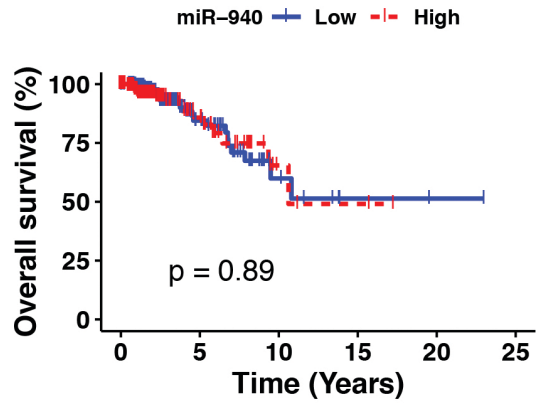
Her2 subtype



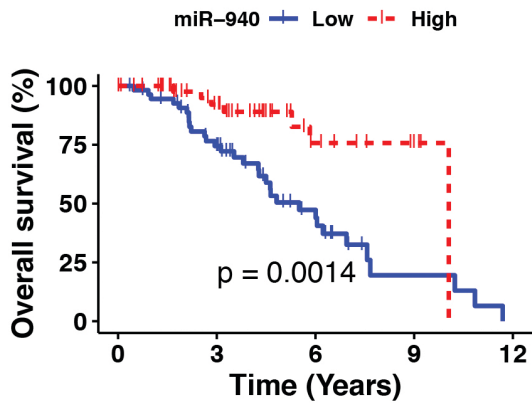
LumA subtype



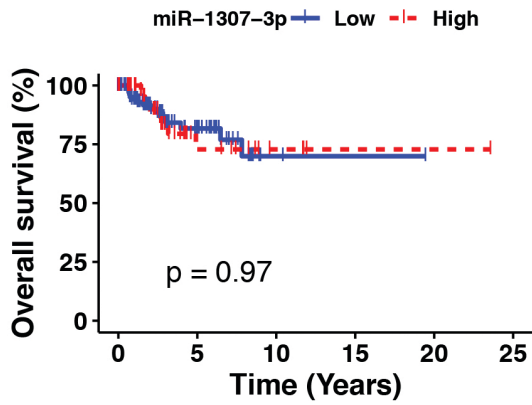
LumB subtype



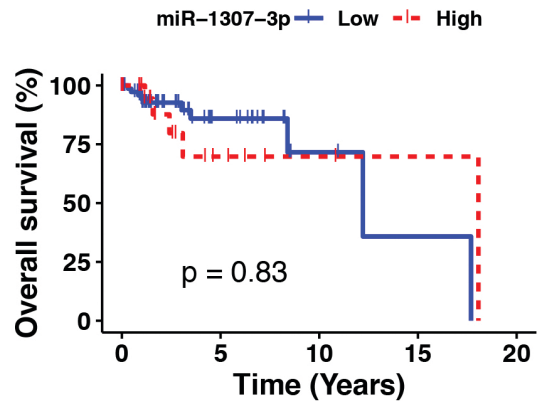
Normal subtype



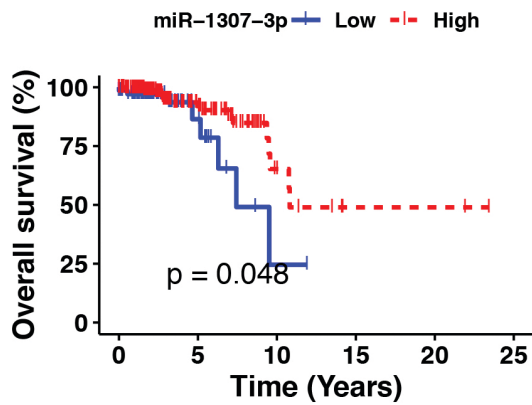
Basal subtype



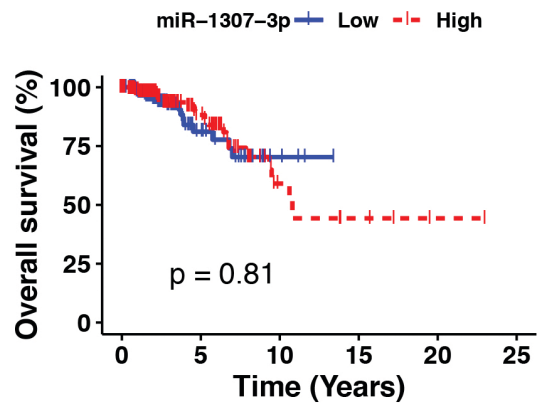
Her2 subtype



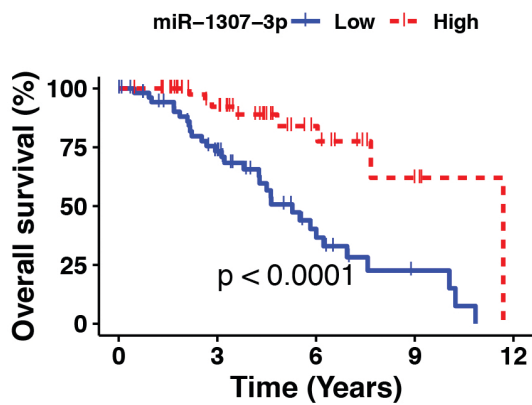
LumA subtype



LumB subtype



Normal subtype



Bibliografía

- [1] R. Bast, D. Kufe, and E. Frei, *Holland-Frei Cancer Medicine*, 5th ed., J. Holland, Ed. Wiley, 2006. [1](#), [5](#), [6](#)
- [2] D. Hanahan and R. a. Weinberg, “Hallmarks of cancer: The next generation,” *Cell*, vol. 144, no. 5, pp. 646–674, 2011. [Online]. Available: <http://dx.doi.org/10.1016/j.cell.2011.02.013> [1](#), [2](#)
- [3] F. Bray, J. Ferlay, I. Soerjomataram, R. L. Siegel, L. A. Torre, and A. Jemal, “Global cancer statistics 2018: GLOBOCAN estimates of incidence and mortality worldwide for 36 cancers in 185 countries,” *CA: A Cancer Journal for Clinicians*, vol. 68, no. 6, pp. 394–424, nov 2018. [Online]. Available: <http://doi.wiley.com/10.3322/caac.21492> [2](#)
- [4] A. Gomez-Herrera and A. Meneses-Garcia, *Manual de oncología y procedimientos medico quirurgicos*, 6th ed. McGraw-Hill, 2016. [2](#), [4](#)
- [5] N. Harbeck, F. Penault-Llorca, J. Cortes, M. Gnant, N. Houssami, P. Poortmans, K. Ruddy, J. Tsang, and F. Cardoso, “Breast cancer,” *Nature Reviews Disease Primers*, vol. 5, no. 1, dec 2019. [3](#), [4](#)
- [6] C. M. Perou, T. Sørile, M. B. Eisen, M. Van De Rijn, S. S. Jeffrey, C. A. Rens, J. R. Pollack, D. T. Ross, H. Johnsen, L. A. Akslen, Ø. Fluge, A. Pergammenschlkov, C. Williams, S. X. Zhu, P. E. Lønning, A. L. Børresen-

BIBLIOGRAFÍA

- Dale, P. O. Brown, and D. Botstein, “Molecular portraits of human breast tumours,” *Nature*, vol. 406, no. 6797, pp. 747–752, aug 2000. [Online]. Available: <https://www.nature.com/articles/35021093> 3
- [7] P. S. Bernard, J. S. Parker, M. Mullins, M. C. Cheung, S. Leung, D. Voduc, T. Vickery, S. Davies, C. Fauron, X. He, Z. Hu, J. F. Quackenbush, I. J. Stijleman, J. Palazzo, J. S. Matron, A. B. Nobel, E. Mardis, T. O. Nielsen, M. J. Ellis, and C. M. Perou, “Supervised risk predictor of breast cancer based on intrinsic subtypes,” *Journal of Clinical Oncology*, vol. 27, no. 8, pp. 1160–1167, mar 2009. 3
- [8] A. E. Giuliano, J. L. Connolly, S. B. Edge, E. A. Mittendorf, H. S. Rugo, L. J. Solin, D. L. Weaver, D. J. Winchester, and G. N. Hortobagyi, “Breast Cancer-Major changes in the American Joint Committee on Cancer eighth edition cancer staging manual,” *CA: A Cancer Journal for Clinicians*, vol. 67, no. 4, pp. 290–303, jul 2017. [Online]. Available: <https://acsjournals.onlinelibrary.wiley.com/doi/full/10.3322/caac.21393><https://acsjournals.onlinelibrary.wiley.com/doi/abs/10.3322/caac.21393><https://acsjournals.onlinelibrary.wiley.com/doi/10.3322/caac.21393> 4
- [9] C. J. Conti, “Mechanisms of Tumor Progression,” *Comprehensive Toxicology, Second Edition*, vol. 14, pp. 335–347, jan 2010. [Online]. Available: <https://www.sciencedirect.com/science/article/pii/B9780080468846014172> 5
- [10] C. Richard Boland, “Non-coding RNA: It’s Not Junk,” pp. 1107–1109, may 2017. [Online]. Available: <https://link.springer.com/article/10.1007/s10620-017-4506-1> 7
- [11] L. F. R. Gebert and I. J. MacRae, “Regulation of microRNA function in animals,” *Nature Reviews Molecular Cell Biology*, p. 1, aug 2018. [Online]. Available: <http://www.nature.com/articles/s41580-018-0045-7> 7
- [12] L. Wu, J. Fan, and J. G. Belasco, “MicroRNAs direct rapid deadenylation of

-
- mRNA,” *Proceedings of the National Academy of Sciences of the United States of America*, vol. 103, no. 11, pp. 4034–4039, mar 2006. [Online]. Available: <https://pubmed.ncbi.nlm.nih.gov/16495412/> 8
- [13] S. Lin and R. I. Gregory, “MicroRNA biogenesis pathways in cancer,” *Nature Reviews Cancer*, vol. 15, no. 6, pp. 321–333, may 2015. [Online]. Available: <http://www.nature.com/doifinder/10.1038/nrc3932> 8
- [14] S. Vasudevan, “Posttranscriptional Upregulation by MicroRNAs,” *Wiley Interdisciplinary Reviews: RNA*, vol. 3, no. 3, pp. 311–330, may 2012. [Online]. Available: <http://doi.wiley.com/10.1002/wrna.121> 8, 9, 30
- [15] U. A. Ørom, F. C. Nielsen, and A. H. Lund, “MicroRNA-10a Binds the 5UTR of Ribosomal Protein mRNAs and Enhances Their Translation,” *Molecular Cell*, vol. 30, no. 4, pp. 460–471, may 2008. [Online]. Available: <https://linkinghub.elsevier.com/retrieve/pii/S1097276508003286> 8, 9, 30
- [16] A. A. Caudy, M. Myers, G. J. Hannon, and S. M. Hammond, “Fragile X-related protein and VIG associate with the RNA interference machinery,” *Genes and Development*, vol. 16, no. 19, pp. 2491–2496, oct 2002. [Online]. Available: [/pmc/articles/PMC187452/](https://pmc/articles/PMC187452/)[/pmc/articles/PMC187452/?report=abstract](https://pmc/articles/PMC187452/?report=abstract)<https://www.ncbi.nlm.nih.gov/pmc/articles/PMC187452/> 9
- [17] P. Jin, D. C. Zarnescu, S. Ceman, M. Nakamoto, J. Mowrey, T. A. Jongens, D. L. Nelson, K. Moses, and S. T. Warren, “Biochemical and genetic interaction between the fragile X mental retardation protein and the microRNA pathway,” *Nature Neuroscience*, vol. 7, no. 2, pp. 113–117, feb 2004. [Online]. Available: <https://www.nature.com/articles/nn1174> 9
- [18] S. Vasudevan and J. A. Steitz, “AU-Rich-Element-Mediated Upregulation of Translation by FXR1 and Argonaute 2,” *Cell*, vol. 128, no. 6, pp. 1105–1118, mar 2007. [Online]. Available: <https://pubmed.ncbi.nlm.nih.gov/17382880/> 9
-

BIBLIOGRAFÍA

- [19] S. Vasudevan, Y. Tong, and J. A. Steitz, “Switching from Repression to Activation: MicroRNAs Can Up-Regulate Translation,” *Science*, vol. 318, no. 5858, pp. 1931–1934, dec 2007. [Online]. Available: <http://www.ncbi.nlm.nih.gov/pubmed/18048652><http://www.sciencemag.org/cgi/doi/10.1126/science.1149460> 9
- [20] A. J. Murphy, P. M. Guyre, and P. A. Pioli, “Estradiol Suppresses NF- κ B Activation through Coordinated Regulation of let-7a and miR-125b in Primary Human Macrophages,” *The Journal of Immunology*, vol. 184, no. 9, pp. 5029–5037, may 2010. [Online]. Available: <https://pubmed.ncbi.nlm.nih.gov/20351193/> 9
- [21] X. Zhang, X. Zuo, B. Yang, Z. Li, Y. Xue, Y. Zhou, J. Huang, X. Zhao, J. Zhou, Y. Yan, H. Zhang, P. Guo, H. Sun, L. Guo, Y. Zhang, and X. D. Fu, “MicroRNA directly enhances mitochondrial translation during muscle differentiation,” *Cell*, vol. 158, no. 3, pp. 607–619, jul 2014. [Online]. Available: <https://pubmed.ncbi.nlm.nih.gov/25083871/> 9
- [22] F. Ma, X. Liu, D. Li, P. Wang, N. Li, L. Lu, and X. Cao, “MicroRNA-4661 Upregulates IL-10 Expression in TLR-Triggered Macrophages by Antagonizing RNA-Binding Protein Tristetraprolin-Mediated IL-10 mRNA Degradation,” *The Journal of Immunology*, vol. 184, no. 11, pp. 6053–6059, jun 2010. [Online]. Available: <https://pubmed.ncbi.nlm.nih.gov/20410487/> 9
- [23] T. Ghosh, K. Soni, V. Scaria, M. Halimani, C. Bhattacharjee, and B. Pillai, “MicroRNA-mediated up-regulation of an alternatively polyadenylated variant of the mouse cytoplasmic β -actin gene,” *Nucleic Acids Research*, vol. 36, no. 19, pp. 6318–6332, 2008. [Online]. Available: <https://pubmed.ncbi.nlm.nih.gov/18835850/> 9
- [24] K. R. Cordes, N. T. Sheehy, M. P. White, E. C. Berry, S. U. Morton, A. N. Muth, T. H. Lee, J. M. Miano, K. N. Ivey, and D. Srivastava, “MiR-145 and miR-143 regulate smooth muscle cell fate and plasticity,”

- Nature*, vol. 460, no. 7256, pp. 705–710, aug 2009. [Online]. Available: <https://www.nature.com/articles/nature08195> 9
- [25] J. Guo, J. Lv, M. Liu, and H. Tang, “MiR-346 Up-regulates Argonaute 2 (AGO2) protein expression to augment the activity of other MicroRNAs (miRNAs) and contributes to cervical cancer cell malignancy,” *Journal of Biological Chemistry*, vol. 290, no. 51, pp. 30342–30350, dec 2015. [Online]. Available: <https://pubmed.ncbi.nlm.nih.gov/26518874/> 9
- [26] N. P. Tsai, Y. L. Lin, and L. N. Wei, “MicroRNA mir-346 targets the 5-untranslated region of receptor-interacting protein 140 (RIP140) mRNA and up-regulates its protein expression,” *Biochemical Journal*, vol. 424, no. 3, pp. 411–418, dec 2009. [Online]. Available: <https://pubmed.ncbi.nlm.nih.gov/19780716/> 9
- [27] M. Liu, A. Roth, M. Yu, R. Morris, F. Bersani, M. N. Rivera, J. Lu, T. Shioda, S. Vasudevan, S. Ramaswamy, S. Maheswaran, S. Diederichs, and D. A. Haber, “The IGF2 intronic miR-483 selectively enhances transcription from IGF2 fetal promoters and enhances tumorigenesis,” *Genes and Development*, vol. 27, no. 23, pp. 2543–2548, dec 2013. [Online]. Available: <https://pubmed.ncbi.nlm.nih.gov/24298054/> 9
- [28] J. I. Henke, D. Goergen, J. Zheng, Y. Song, C. G. Schüttler, C. Fehr, C. Jünemann, and M. Niepmann, “microRNA-122 stimulates translation of hepatitis C virus RNA,” *EMBO Journal*, vol. 27, no. 24, pp. 3300–3310, dec 2008. [Online]. Available: <https://pubmed.ncbi.nlm.nih.gov/19020517/> 9
- [29] V. Huang, R. F. Place, V. Portnoy, J. Wang, Z. Qi, Z. Jia, A. Yu, M. Shuman, J. Yu, and L. C. Li, “Upregulation of Cyclin B1 by miRNA and its implications in cancer,” *Nucleic Acids Research*, vol. 40, no. 4, pp. 1695–1707, feb 2012. [Online]. Available: <https://pubmed.ncbi.nlm.nih.gov/22053081/> 9

BIBLIOGRAFÍA

- [30] R. F. Place, L. C. Li, D. Pookot, E. J. Noonan, and R. Dahiya, “MicroRNA-373 induces expression of genes with complementary promoter sequences,” *Proceedings of the National Academy of Sciences of the United States of America*, vol. 105, no. 5, pp. 1608–1613, feb 2008. [Online]. Available: <https://pubmed.ncbi.nlm.nih.gov/18227514/> 9
- [31] M. Xiao, J. Li, W. Li, Y. Wang, F. Wu, Y. Xi, L. Zhang, C. Ding, H. Luo, Y. Li, L. Peng, L. Zhao, S. Peng, Y. Xiao, S. Dong, J. Cao, and W. Yu, “MicroRNAs activate gene transcription epigenetically as an enhancer trigger,” *RNA Biology*, vol. 14, no. 10, pp. 1326–1334, oct 2017. [Online]. Available: <https://pubmed.ncbi.nlm.nih.gov/26853707/> 9
- [32] M. Williams, Y. Y. Cheng, C. Blenkiron, and G. Reid, “Exploring Mechanisms of MicroRNA Downregulation in Cancer,” *MicroRNA*, vol. 6, no. 1, pp. 2–16, may 2017. [Online]. Available: <http://www.ncbi.nlm.nih.gov/pubmed/27928946http://www.eurekaselect.com/node/148230/article> 10
- [33] E. van Schooneveld, H. Wildiers, I. Vergote, P. B. Vermeulen, L. Y. Dirix, and S. J. Van Laere, “Dysregulation of microRNAs in breast cancer and their potential role as prognostic and predictive biomarkers in patient management.” *Breast cancer research : BCR*, vol. 17, no. 1, p. 21, feb 2015. [Online]. Available: <http://www.ncbi.nlm.nih.gov/pubmed/25849621> 10
- [34] P. Olson, J. Lu, H. Zhang, A. Shai, M. G. Chun, Y. Wang, S. K. Libutti, E. K. Nakakura, T. R. Golub, and D. Hanahan, “MicroRNA dynamics in the stages of tumorigenesis correlate with hallmark capabilities of cancer.” *Genes & development*, vol. 23, no. 18, pp. 2152–65, sep 2009. [Online]. Available: <http://www.ncbi.nlm.nih.gov/pubmed/19759263http://www.pubmedcentral.nih.gov/articlerender.fcgi?artid=PMC2751988> 10
- [35] J. N. Goh, S. Y. Loo, A. Datta, K. S. Siveen, W. N. Yap, W. Cai, E. M. Shin, C. Wang, J. E. Kim, M. Chan, A. M. Dharmarajan, A. S.-G. Lee, P. E.

- Lobie, C. T. Yap, and A. P. Kumar, “microRNAs in breast cancer: regulatory roles governing the hallmarks of cancer,” *Biological Reviews*, vol. 91, no. 2, pp. 409–428, may 2016. [Online]. Available: <http://doi.wiley.com/10.1111/brv.12176> 10
- [36] J. Hayes, P. P. Peruzzi, and S. Lawler, “MicroRNAs in cancer: biomarkers, functions and therapy.” *Trends in molecular medicine*, vol. 20, no. 8, pp. 460–9, aug 2014. [Online]. Available: <http://www.ncbi.nlm.nih.gov/pubmed/25027972> 10
- [37] A. Martinez-Gutierrez, O. Catalan, R. Vazquez-Romo, F. Porras Reyes, A. Alvarado-Miranda, F. Lara Medina, J. Bargallo-Rocha, L. Orozco Moreno, D. Cantu De Leon, L. Herrera, C. Lopez-Camarillo, C. Perez-Plasencia, and A. Campos-Parra, “miRNA profile obtained by next-generation sequencing in metastatic breast cancer patients is able to predict the response to systemic treatments,” *International Journal of Molecular Medicine*, vol. 44, no. 4, pp. 1267–1280, jul 2019. [Online]. Available: <http://www.spandidos-publications.com/10.3892/ijmm.2019.4292> 10
- [38] M. Hemmatzadeh, H. Mohammadi, F. Jadidi-Niaragh, F. Asghari, and M. Yousefi, “The role of oncomirs in the pathogenesis and treatment of breast cancer,” *Biomedicine & Pharmacotherapy*, vol. 78, pp. 129–139, 2016. 10
- [39] C. Caldas and J. D. Brenton, “Sizing up miRNAs as cancer genes,” *Nature Medicine*, vol. 11, no. 7, pp. 712–714, jul 2005. [Online]. Available: <http://www.nature.com/doifinder/10.1038/nm0705-712> 10
- [40] B. Zhang, X. Pan, G. P. Cobb, and T. A. Anderson, “microRNAs as oncogenes and tumor suppressors,” *Developmental Biology*, vol. 302, no. 1, pp. 1–12, 2007. 10
- [41] V. D. Haakensen, V. Nygaard, L. Greger, M. R. Aure, B. Fromm, I. R. Bukholm, T. Lüders, S.-F. Chin, A. Git, C. Caldas, V. N. Kristensen,

BIBLIOGRAFÍA

- A. Brazma, A.-L. Børresen-Dale, E. Hovig, and Å. Helland, “Subtype-specific micro-RNA expression signatures in breast cancer progression,” *International Journal of Cancer*, vol. 139, no. 5, pp. 1117–1128, sep 2016. [Online]. Available: <http://www.ncbi.nlm.nih.gov/pubmed/27082076><http://doi.wiley.com/10.1002/ijc.30142> 10
- [42] J. Chen, Y. Zhi, X. Chang, S. Zhang, and D. Dai, “Expression of ADAMTS1 and Its Correlation with Angiogenesis in Primary Gastric Cancer and Lymph Node Metastasis,” *Digestive Diseases and Sciences*, vol. 58, no. 2, pp. 405–413, feb 2013. [Online]. Available: <http://www.ncbi.nlm.nih.gov/pubmed/23001403><http://link.springer.com/10.1007/s10620-012-2379-x> 10
- [43] H. Dvinge, A. Git, S. Gräf, M. Salmon-Divon, C. Curtis, A. Sottoriva, Y. Zhao, M. Hirst, J. Armisen, E. A. Miska, S.-F. Chin, E. Provenzano, G. Turashvili, A. Green, I. Ellis, S. Aparicio, and C. Caldas, “The shaping and functional consequences of the microRNA landscape in breast cancer,” *Nature*, vol. 497, no. 7449, pp. 378–382, may 2013. [Online]. Available: <http://www.nature.com/doifinder/10.1038/nature12108> 10
- [44] R. Laubenbacher, V. Hower, A. Jarrah, S. V. Torti, V. Shulaev, P. Mendes, F. M. Torti, and S. Akman, “A systems biology view of cancer,” *Biochimica et Biophysica Acta - Reviews on Cancer*, vol. 1796, no. 2, pp. 129–139, dec 2009. [Online]. Available: </pmc/articles/PMC2782452/?report=abstract><https://www.ncbi.nlm.nih.gov/pmc/articles/PMC2782452/> 12
- [45] D. C. Koboldt, R. S. Fulton, M. D. McLellan, H. Schmidt, J. Kalicki-Veizer, J. F. McMichael, L. L. Fulton, D. J. Dooling, L. Ding, E. R. Mardis, R. K. Wilson, A. Ally, M. Balasundaram, Y. S. N. Butterfield, R. Carlsen, C. Carter, A. Chu, E. Chuah, H.-J. E. Chun, R. J. N. Coope, N. Dhalla, R. Guin, C. Hirst, M. Hirst, R. A. Holt, D. Lee, H. I. Li, M. Mayo, R. A. Moore, A. J. Mungall, E. Pleasance, A. Gordon Robertson, J. E. Schein, A. Shafiei, P. Sipahimalani, J. R. Slobodan, D. Stoll, A. Tam, N. Thiessen, R. J. Varhol, N. Wye, T. Zeng, Y. Zhao, I. Birol,

S. J. M. Jones, M. A. Marra, A. D. Cherniack, G. Saksena, R. C. Onofrio, N. H. Pho, S. L. Carter, S. E. Schumacher, B. Tabak, B. Hernandez, J. Gentry, H. Nguyen, A. Crenshaw, K. Ardlie, R. Beroukhim, W. Winckler, G. Getz, S. B. Gabriel, M. Meyerson, L. Chin, P. J. Park, R. Kucherlapati, K. A. Hoadley, J. Todd Auman, C. Fan, Y. J. Turman, Y. Shi, L. Li, M. D. Topal, X. He, H.-H. Chao, A. Prat, G. O. Silva, M. D. Iglesia, W. Zhao, J. Usary, J. S. Berg, M. Adams, J. Booker, J. Wu, A. Gulabani, T. Bodenheimer, A. P. Hoyle, J. V. Simons, M. G. Soloway, L. E. Mose, S. R. Jefferys, S. Balu, J. S. Parker, D. Neil Hayes, C. M. Perou, S. Malik, S. Mahurkar, H. Shen, D. J. Weisenberger, T. Triche Jr, P. H. Lai, M. S. Bootwalla, D. T. Maglinte, B. P. Berman, D. J. Van Den Berg, S. B. Baylin, P. W. Laird, C. J. Creighton, L. A. Donehower, G. Getz, M. Noble, D. Voet, G. Saksena, N. Gehlenborg, D. DiCara, J. Zhang, H. Zhang, C.-J. Wu, S. Yingchun Liu, M. S. Lawrence, L. Zou, A. Sivachenko, P. Lin, P. Stojanov, R. Jing, J. Cho, R. Sinha, R. W. Park, M.-D. Nazaire, J. Robinson, H. Thorvaldsdottir, J. Mesirov, P. J. Park, L. Chin, S. Reynolds, R. B. Kreisberg, B. Bernard, R. Bressler, T. Erkkila, J. Lin, V. Thorsson, W. Zhang, I. Shmulevich, G. Ciriello, N. Weinhold, N. Schultz, J. Gao, E. Cerami, B. Gross, A. Jacobsen, R. Sinha, B. Arman Aksoy, Y. Antipin, B. Reva, R. Shen, B. S. Taylor, M. Ladanyi, C. Sander, P. Anur, P. T. Spellman, Y. Lu, W. Liu, R. R. G. Verhaak, G. B. Mills, R. Akbani, N. Zhang, B. M. Broom, T. D. Casasent, C. Wakefield, A. K. Unruh, K. Baggerly, K. Coombes, J. N. Weinstein, D. Haussler, C. C. Benz, J. M. Stuart, S. C. Benz, J. Zhu, C. C. Szeto, G. K. Scott, C. Yau, E. O. Paull, D. Carlin, C. Wong, A. Sokolov, J. Thusberg, S. Mooney, S. Ng, T. C. Goldstein, K. Ellrott, M. Grifford, C. Wilks, S. Ma, B. Craft, C. Yan, Y. Hu, D. Meerzaman, J. M. Gastier-Foster, J. Bowen, N. C. Ramirez, A. D. Black, R. E. XPATH ERROR: unknown variable "tname"., P. White, E. J. Zmuda, J. Frick, T. M. Lichtenberg, R. Brookens, M. M. George, M. A. Gerken, H. A. Harper, K. M. Leraas, L. J. Wise, T. R. Tabler, C. McAllister, T. Barr, M. Hart-Kothari, K. Tarvin, C. Saller, G. Sandusky, C. Mitchell, M. V. Iacocca,

BIBLIOGRAFÍA

- J. Brown, B. Rabeno, C. Czerwinski, N. Petrelli, O. Dolzhansky, M. Abramov, O. Voronina, O. Potapova, J. R. Marks, W. M. Suchorska, D. Murawa, W. Kycler, M. Ibbs, K. Korski, A. Spychała, P. Murawa, J. J. Brzeziński, H. Perz, R. Łażniak, M. Teresiak, H. Tatka, E. Leporowska, M. Bogusz-Czerniewicz, J. Malicki, A. Mackiewicz, M. Wiznerowicz, X. Van Le, B. Kohl, N. Viet Tien, R. Thorp, N. Van Bang, H. Sussman, B. Duc Phu, R. Hajek, N. Phi Hung, T. Viet The Phuong, H. Quyet Thang, K. Zaki Khan, R. Penny, D. Mallery, E. Curley, C. Shelton, P. Yena, J. N. Ingle, F. J. Couch, W. L. Lingle, T. A. King, A. Maria Gonzalez-Angulo, G. B. Mills, M. D. Dyer, S. Liu, X. Meng, M. Patangan, F. Waldman, H. Stöppler, W. Kimryn Rathmell, L. Thorne, M. Huang, L. Boice, A. Hill, C. Morrison, C. Gaudioso, W. Bshara, K. Daily, S. C. Egea, M. D. Pegram, C. Gomez-Fernandez, R. Dhir, R. Bhargava, A. Brufsky, C. D. Shriver, J. A. Hooke, J. Leigh Campbell, R. J. Mural, H. Hu, S. Somiari, C. Larson, B. Deyarmin, L. Kvecher, A. J. Kovatich, M. J. Ellis, T. A. King, H. Hu, F. J. Couch, R. J. Mural, T. Stricker, K. White, O. Olopade, J. N. Ingle, C. Luo, Y. Chen, J. R. Marks, F. Waldman, M. Wiznerowicz, R. Bose, L.-W. Chang, A. H. Beck, A. Maria Gonzalez-Angulo, T. Pihl, M. Jensen, R. Sfeir, A. Kahn, A. Chu, P. Kothiyal, Z. Wang, E. Snyder, J. Pontius, B. Ayala, M. Backus, J. Walton, J. Baboud, D. Berton, M. Nicholls, D. Srinivasan, R. Raman, S. Girshik, P. Kigonya, S. Alonso, R. Sanbhadti, S. Barletta, D. Pot, M. Sheth, J. A. Demchok, K. R. Mills Shaw, L. Yang, G. Eley, M. L. Ferguson, R. W. Tarnuzzer, J. Zhang, L. A. L. Dillon, K. Buetow, P. Fielding, B. A. Ozenberger, M. S. Guyer, H. J. Sofia, and J. D. Palchik, “Comprehensive molecular portraits of human breast tumours,” *Nature*, vol. 490, no. 7418, pp. 61–70, sep 2012. [Online]. Available: <http://www.nature.com/doifinder/10.1038/nature11412> 12, 17, 22
- [46] A. P. Carroll, G. J. Goodall, and B. Liu, “Understanding principles of miRNA target recognition and function through integrated biological and bioinformatics approaches,” *Wiley Interdisciplinary Reviews: RNA*, vol. 5, no. 3, pp. 361–379,

- may 2014. [Online]. Available: <http://doi.wiley.com/10.1002/wrna.1217> 12
- [47] E. Hernández-Lemus, “Transcriptional Network Structure Assessment Via the Data Processing Inequality,” *International Journal of Biophysics*, vol. 2, no. 2, pp. 18–25, aug 2012. 13, 16
- [48] J. Stelling, U. Sauer, Z. Szallasi, F. J. Doyle, and J. Doyle, “Robustness of cellular functions.” *Cell*, vol. 118, no. 6, pp. 675–85, sep 2004. [Online]. Available: <http://www.ncbi.nlm.nih.gov/pubmed/15369668> 13
- [49] A. Califano and M. J. Alvarez, “The recurrent architecture of tumour initiation, progression and drug sensitivity.” *Nature reviews. Cancer*, vol. 17, no. 2, pp. 116–130, 2017. [Online]. Available: <http://www.ncbi.nlm.nih.gov/pubmed/27977008><http://www.pubmedcentral.nih.gov/articlerender.fcgi?artid=PMC5541669> 13, 14
- [50] I. Dagogo-Jack and A. T. Shaw, “Tumour heterogeneity and resistance to cancer therapies,” pp. 81–94, feb 2018. [Online]. Available: <https://www.nature.com/articles/nrclinonc.2017.166> 13
- [51] S. V. Puram, I. Tirosh, A. S. Parikh, A. P. Patel, K. Yizhak, S. Gillespie, C. Rodman, C. L. Luo, E. A. Mroz, K. S. Emerick, D. G. Deschler, M. A. Varvares, R. Mylvaganam, O. Rozenblatt-Rosen, J. W. Rocco, W. C. Faquin, D. T. Lin, A. Regev, and B. E. Bernstein, “Single-Cell Transcriptomic Analysis of Primary and Metastatic Tumor Ecosystems in Head and Neck Cancer,” *Cell*, vol. 171, no. 7, pp. 1611–1624.e24, dec 2017. 13
- [52] S. F. Roerink, N. Sasaki, H. Lee-Six, M. D. Young, L. B. Alexandrov, S. Behjati, T. J. Mitchell, S. Grossmann, H. Lightfoot, D. A. Egan, A. Pronk, N. Smakman, J. Van Gorp, E. Anderson, S. J. Gamble, C. Alder, M. Van De Wetering, P. J. Campbell, M. R. Stratton, and H. Clevers, “Intra-tumour diversification in colorectal cancer at the single-cell level,”

BIBLIOGRAFÍA

- Nature*, vol. 556, no. 7702, pp. 437–462, apr 2018. [Online]. Available: <https://www.nature.com/articles/s41586-018-0024-3> 13
- [53] A. P. Patel, I. Tirosh, J. J. Trombetta, A. K. Shalek, S. M. Gillespie, H. Wakimoto, D. P. Cahill, B. V. Nahed, W. T. Curry, R. L. Martuza, D. N. Louis, O. Rozenblatt-Rosen, M. L. Suvà, A. Regev, and B. E. Bernstein, “Single-cell RNA-seq highlights intratumoral heterogeneity in primary glioblastoma,” *Science*, vol. 344, no. 6190, pp. 1396–1401, jun 2014. [Online]. Available: <https://science.sciencemag.org/content/344/6190/1396><https://science.sciencemag.org/content/344/6190/1396.abstract> 13
- [54] P. M. Voorhoeve, “MicroRNAs: Oncogenes, tumor suppressors or master regulators of cancer heterogeneity?” *Biochimica et biophysica acta*, vol. 1805, no. 1, pp. 72–86, jan 2010. [Online]. Available: <http://www.ncbi.nlm.nih.gov/pubmed/19747962> 13
- [55] S. Uda, “Application of information theory in systems biology,” *Biophysical Reviews*, vol. 12, no. 2, pp. 377–384, apr 2020. [Online]. Available: <https://doi.org/10.1007/s12551-020-00665-w> 14, 15
- [56] Z.-P. Liu, “Reverse Engineering of Genome-wide Gene Regulatory Networks from Gene Expression Data,” *Current Genomics*, vol. 16, no. 1, pp. 3–22, jan 2015. [Online]. Available: </pmc/articles/PMC4412962/?report=abstract><https://www.ncbi.nlm.nih.gov/pmc/articles/PMC4412962/> 15
- [57] X. Zhang, X. M. Zhao, K. He, L. Lu, Y. Cao, J. Liu, J. K. Hao, Z. P. Liu, and L. Chen, “Inferring gene regulatory networks from gene expression data by path consistency algorithm based on conditional mutual information,” *Bioinformatics*, vol. 28, no. 1, pp. 98–104, jan 2012. [Online]. Available: <https://pubmed.ncbi.nlm.nih.gov/22088843/> 15
- [58] R. Albert, “Scale-free networks in cell biology,” pp. 4947–4957, nov 2005. [Online]. Available: <https://jcs.biologists.org/content/118/21/4947><https://jcs.biologists.org/content/118/21/4947.abstract> 16

-
- [59] A. Lachmann, F. M. Giorgi, G. Lopez, and A. Califano, “ARACNe-AP: gene network reverse engineering through adaptive partitioning inference of mutual information,” *Bioinformatics*, vol. 32, no. 14, pp. 2233–2235, jul 2016. [Online]. Available: <http://www.ncbi.nlm.nih.gov/pubmed/27153652><http://www.pubmedcentral.nih.gov/articlerender.fcgi?artid=PMC4937200><https://academic.oup.com/bioinformatics/article-lookup/doi/10.1093/bioinformatics/btw216> 16, 23, 29
- [60] M. J. Alvarez, Y. Shen, F. M. Giorgi, A. Lachmann, B. B. Ding, B. H. Ye, and A. Califano, “Functional characterization of somatic mutations in cancer using network-based inference of protein activity,” *Nature Genetics*, vol. 48, no. 8, pp. 838–847, aug 2016. [Online]. Available: <http://www.ncbi.nlm.nih.gov/pubmed/27322546><http://www.pubmedcentral.nih.gov/articlerender.fcgi?artid=PMC5040167><http://www.nature.com/articles/ng.3593> 16, 23, 30, 50
- [61] D. Yang, Y. Sun, L. Hu, H. Zheng, P. Ji, C. V. Pecot, Y. Zhao, S. Reynolds, H. Cheng, R. Rupaimoole, D. Cogdell, M. Nykter, R. Broaddus, C. Rodriguez-Aguayo, G. Lopez-Berestein, J. Liu, I. Shmulevich, A. K. Sood, K. Chen, and W. Zhang, “Integrated Analyses Identify a Master MicroRNA Regulatory Network for the Mesenchymal Subtype in Serous Ovarian Cancer,” *Cancer Cell*, vol. 23, no. 2, pp. 186–199, 2013. 17
- [62] L. Cantini, C. Isella, C. Petti, G. Picco, S. Chiola, E. Ficarra, M. Caselle, and E. Medico, “MicroRNA–mRNA interactions underlying colorectal cancer molecular subtypes,” *Nature Communications*, vol. 6, no. 1, p. 8878, dec 2015. [Online]. Available: <http://www.nature.com/articles/ncomms9878> 17
- [63] L. Cantini, G. Bertoli, C. Cava, T. Dubois, A. Zinovyev, M. Caselle, I. Castiglioni, E. Barillot, and L. Martignetti, “Identification of microRNA clusters cooperatively acting on epithelial to mesenchymal transition in triple negative breast cancer,”
-

BIBLIOGRAFÍA

- Nucleic Acids Research*, vol. 47, no. 5, pp. 2205–2215, mar 2019. [Online]. Available: <https://academic.oup.com/nar/article/47/5/2205/5290485> 17
- [64] A. Colaprico, T. C. Silva, C. Olsen, L. Garofano, C. Cava, D. Garolini, T. S. Sabedot, T. M. Malta, S. M. Pagnotta, I. Castiglioni, M. Ceccarelli, G. Bontempi, and H. Noushmehr, “TCGAbiolinks : an R/Bioconductor package for integrative analysis of TCGA data,” *Nucleic Acids Research*, vol. 44, no. 8, pp. e71–e71, may 2016. [Online]. Available: <https://academic.oup.com/nar/article-lookup/doi/10.1093/nar/gkv1507> 22
- [65] M. I. Love, W. Huber, and S. Anders, “Moderated estimation of fold change and dispersion for RNA-seq data with DESeq2,” *Genome Biology*, vol. 15, no. 12, p. 550, dec 2014. [Online]. Available: <http://genomebiology.biomedcentral.com/articles/10.1186/s13059-014-0550-8> 22, 25
- [66] Y. Ru, K. J. Kechris, B. Tabakoff, P. Hoffman, R. A. Radcliffe, R. Bowler, S. Mahaffey, S. Rossi, G. A. Calin, L. Bemis, and D. Theodorescu, “The multiMiR R package and database: integration of microRNA–target interactions along with their disease and drug associations,” *Nucleic Acids Research*, vol. 42, no. 17, pp. e133–e133, sep 2014. [Online]. Available: <http://academic.oup.com/nar/article/42/17/e133/2902504/The-multiMiR-R-package-and-database-integration-of> 23
- [67] C. Lefebvre, P. Rajbhandari, M. J. Alvarez, P. Bandaru, W. K. Lim, M. Sato, K. Wang, P. Sumazin, M. Kustagi, B. C. Bisikirska, K. Basso, P. Beltrao, N. Krogan, J. Gautier, R. Dalla-Favera, and A. Califano, “A human B-cell interactome identifies MYB and FOXM1 as master regulators of proliferation in germinal centers,” *Molecular Systems Biology*, vol. 6, p. 377, jun 2010. [Online]. Available: <http://www.ncbi.nlm.nih.gov/pubmed/20531406><http://www.pubmedcentral.nih.gov/articlerender.fcgi?artid=PMC2913282><http://msb.embopress.org/cgi/doi/10.1038/msb.2010.31> 23, 30
- [68] J. G. Tate, S. Bamford, H. C. Jubb, Z. Sondka, D. M. Beare, N. Bindal, H. Boutse-

-
- lakis, C. G. Cole, C. Creatore, E. Dawson, P. Fish, B. Harsha, C. Hathaway, S. C. Jupe, C. Y. Kok, K. Noble, L. Ponting, C. C. Ramshaw, C. E. Rye, H. E. Speedy, R. Stefancsik, S. L. Thompson, S. Wang, S. Ward, P. J. Campbell, and S. A. Forbes, “COSMIC: The Catalogue Of Somatic Mutations In Cancer,” *Nucleic Acids Research*, vol. 47, no. D1, pp. D941–D947, jan 2019. 24
- [69] Y. Liao, J. Wang, E. J. Jaehnig, Z. Shi, and B. Zhang, “WebGestalt 2019: gene set analysis toolkit with revamped UIs and APIs,” *Nucleic Acids Research*, vol. 47, no. W1, pp. W199–W205, jul 2019. [Online]. Available: <https://academic.oup.com/nar/article/47/W1/W199/5494758> 25
- [70] D. M. A. Gendoo, N. Ratanasirigulchai, M. S. Schröder, L. Paré, J. S. Parker, A. Prat, and B. Haibe-Kains, “Genefu: an R/Bioconductor package for computation of gene expression-based signatures in breast cancer,” *Bioinformatics*, vol. 32, no. 7, pp. 1097–1099, apr 2016. [Online]. Available: <http://www.ncbi.nlm.nih.gov/pubmed/26607490><https://academic.oup.com/bioinformatics/article-lookup/doi/10.1093/bioinformatics/btv693> 25
- [71] M. Uhlen, L. Fagerberg, B. M. Hallstrom, C. Lindskog, P. Oksvold, A. Mardinoglu, A. Sivertsson, C. Kampf, E. Sjostedt, A. Asplund, I. Olsson, K. Edlund, E. Lundberg, S. Navani, C. A.-K. Szigartyo, J. Odeberg, D. Djureinovic, J. O. Takanen, S. Hober, T. Alm, P.-H. Edqvist, H. Berling, H. Tegel, J. Mulder, J. Rockberg, P. Nilsson, J. M. Schwenk, M. Hamsten, K. von Feilitzen, M. Forsberg, L. Persson, F. Johansson, M. Zwahlen, G. von Heijne, J. Nielsen, and F. Ponten, “Tissue-based map of the human proteome,” *Science*, vol. 347, no. 6220, pp. 1 260 419–1 260 419, jan 2015. [Online]. Available: <https://www.sciencemag.org/lookup/doi/10.1126/science.1260419> 27
- [72] A. C. Oliveira, L. A. Bovolenta, P. G. Nachtigall, M. E. Herkenhoff, N. Lemke, and D. Pinhal, “Combining Results from Distinct MicroRNA Target Prediction Tools Enhances the Performance of Analyses.” *Frontiers in genetics*, vol. 8, p. 59,
-

BIBLIOGRAFÍA

2017. [Online]. Available: <http://www.ncbi.nlm.nih.gov/pubmed/28559915><http://www.pubmedcentral.nih.gov/articlerender.fcgi?artid=PMC5432626> 30
- [73] S. L. Cooke, J. C. Pole, S. F. Chin, I. O. Ellis, C. Caldas, and P. A. Edwards, “High-resolution array CGH clarifies events occurring on 8p in carcinogenesis,” *BMC Cancer*, vol. 8, no. 1, p. 288, oct 2008. [Online]. Available: <http://bmccancer.biomedcentral.com/articles/10.1186/1471-2407-8-288> 37, 52
- [74] O. Anczuków, A. Z. Rosenberg, M. Akerman, S. Das, L. Zhan, R. Karni, S. K. Muthuswamy, and A. R. Krainer, “The splicing factor SRSF1 regulates apoptosis and proliferation to promote mammary epithelial cell transformation,” *Nature Structural and Molecular Biology*, vol. 19, no. 2, pp. 220–228, feb 2012. [Online]. Available: <http://www.ncbi.nlm.nih.gov/pubmed/22245967><http://www.pubmedcentral.nih.gov/articlerender.fcgi?artid=PMC3272117> 37
- [75] P. Eroles, A. Bosch, J.érez-Fidalgo@, and A. Lluch, “Molecular biology in breast cancer: Intrinsic subtypes and signaling pathways,” pp. 698–707, oct 2012. 43
- [76] M. Tarabichi, A. Antoniou, M. Saiselet, J. M. Pita, G. Andry, J. E. Dumont, V. Detours, and C. Maenhaut, “Systems biology of cancer: Entropy, disorder, and selection-driven evolution to independence, invasion and ”swarm intelligence ,” *Cancer and Metastasis Reviews*, vol. 32, no. 3-4, pp. 403–421, dec 2013. 49
- [77] M. S. Ebert and P. A. Sharp, “Roles for microRNAs in conferring robustness to biological processes.” *Cell*, vol. 149, no. 3, pp. 515–24, apr 2012. [Online]. Available: <http://www.ncbi.nlm.nih.gov/pubmed/22541426><http://www.pubmedcentral.nih.gov/articlerender.fcgi?artid=PMC3351105> 49
- [78] J. C. Chen, M. J. Alvarez, F. Talos, H. Dhruv, G. E. Rieckhof, A. Iyer, K. L. Diefes, K. Aldape, M. Berens, M. M. Shen, and A. Califano, “Identification of causal genetic drivers of human disease through systems-level analysis of regulatory networks,” *Cell*, vol. 159, no. 2, pp. 402–414, oct 2014. 49

-
- [79] H. Tovar, R. García-Herrera, and J. Espinal-Enríquez, “Transcriptional master regulator analysis in breast cancer genetic networks,” *Computational Biology and Chemistry*, vol. 59, pp. 67–77, dec 2015. [Online]. Available: <https://www.sciencedirect.com/science/article/pii/S1476927115301262> 50
- [80] A. A. Svoronos, D. M. Engelman, and F. J. Slack, “OncomiR or Tumor Suppressor? The Duplicity of MicroRNAs in Cancer,” *Cancer Research*, vol. 76, no. 13, pp. 3666–3670, jul 2016. [Online]. Available: <http://www.ncbi.nlm.nih.gov/pubmed/27325641><http://www.pubmedcentral.nih.gov/articlerender.fcgi?artid=PMC4930690><http://cancerres.aacrjournals.org/lookup/doi/10.1158/0008-5472.CAN-16-0359> 50, 51
- [81] S. Oliveto, M. Mancino, N. Manfrini, and S. Biffo, “Role of microRNAs in translation regulation and cancer.” *World journal of biological chemistry*, vol. 8, no. 1, pp. 45–56, feb 2017. [Online]. Available: <http://www.ncbi.nlm.nih.gov/pubmed/28289518><http://www.pubmedcentral.nih.gov/articlerender.fcgi?artid=PMC5329714> 51
- [82] J. Lee, H. E. Kim, Y.-S. Song, E. Y. Cho, and A. Lee, “miR-106b-5p and miR-17-5p could predict recurrence and progression in breast ductal carcinoma in situ based on the transforming growth factor-beta pathway,” *Breast Cancer Research and Treatment*, vol. 176, no. 1, pp. 119–130, jul 2019. [Online]. Available: <http://www.ncbi.nlm.nih.gov/pubmed/30989460><http://www.pubmedcentral.nih.gov/articlerender.fcgi?artid=PMC6548759><http://link.springer.com/10.1007/s10549-019-05192-1> 51
- [83] W. Xiang, J. He, C. Huang, L. Chen, D. Tao, X. Wu, M. Wang, G. Luo, X. Xiao, F. Zeng, and G. Jiang, “miR-106b-5p targets tumor suppressor gene SETD2 to inactive its function in clear cell renal cell carcinoma,” *Oncotarget*, vol. 6, no. 6, pp. 4066–79, feb 2015. [Online]. Available: <http://www.ncbi.nlm.nih.gov/pubmed/25714014><http://www.pubmedcentral.nih.gov/articlerender.fcgi?artid=PMC4581444>
-

BIBLIOGRAFÍA

- <http://www.pubmedcentral.nih.gov/articlerender.fcgi?artid=PMC4414173>
<http://www.oncotarget.com/fulltext/2926> 51
- [84] H. Gu, S. Gu, X. Zhang, S. Zhang, D. Zhang, J. Lin, S. Hasengbayi, and W. Han, “miR-106b-5p promotes aggressive progression of hepatocellular carcinoma via targeting RUNX3,” *Cancer Medicine*, p. cam4.2511, sep 2019. [Online]. Available: <http://www.ncbi.nlm.nih.gov/pubmed/31503422><https://onlinelibrary.wiley.com/doi/abs/10.1002/cam4.2511> 51
- [85] F. You, H. Luan, D. Sun, T. Cui, P. Ding, H. Tang, and D. Sun, “MiRNA-106a Promotes Breast Cancer Cell Proliferation, Clonogenicity, Migration, and Invasion Through Inhibiting Apoptosis and Chemosensitivity,” *DNA and Cell Biology*, vol. 38, no. 2, pp. 198–207, feb 2019. [Online]. Available: <http://www.ncbi.nlm.nih.gov/pubmed/30570350> 51
- [86] M. Salem, Y. Shan, S. Bernaudo, and C. Peng, “miR-590-3p Targets Cyclin G2 and FOXO3 to Promote Ovarian Cancer Cell Proliferation, Invasion, and Spheroid Formation.” *International journal of molecular sciences*, vol. 20, no. 8, apr 2019. [Online]. Available: <http://www.ncbi.nlm.nih.gov/pubmed/31013711><http://www.pubmedcentral.nih.gov/articlerender.fcgi?artid=PMC6515004> 51
- [87] Z.-Q. Sun, K. Shi, Q.-B. Zhou, X.-Y. Zeng, J. Liu, S.-X. Yang, Q.-S. Wang, Z. Li, G.-X. Wang, J.-M. Song, W.-T. Yuan, and H.-J. Wang, “MiR-590-3p promotes proliferation and metastasis of colorectal cancer via Hippo pathway.” *Oncotarget*, vol. 8, no. 35, pp. 58 061–58 071, aug 2017. [Online]. Available: <http://www.ncbi.nlm.nih.gov/pubmed/28938537><http://www.pubmedcentral.nih.gov/articlerender.fcgi?artid=PMC5601633> 51
- [88] L. Hou, M. Chen, X. Zhao, J. Li, S. Deng, J. Hu, H. Yang, and J. Jiang, “FAT4 functions as a tumor suppressor in triple-negative breast cancer,” *Tumor Biology*, vol. 37, no. 12, pp. 16 337–16 343, dec 2016. 51
- [89] F. Ozdemir, M. Koksall, V. Ozmen, I. Aydin, and N. Buyru, “Mutations and

-
- Krüppel-like factor 6 (KLF6) expression levels in breast cancer,” *Tumor Biology*, vol. 35, no. 6, pp. 5219–5225, 2014. 51
- [90] Y. Gao, H. Li, X. Ma, Y. Fan, D. Ni, Y. Zhang, Q. Huang, K. Liu, X. Li, L. Wang, L. Gu, Y. Yao, Q. Ai, Q. Du, E. Song, and X. Zhang, “KLF6 suppresses metastasis of clear cell renal cell carcinoma via transcriptional repression of E2F1,” *Cancer Research*, vol. 77, no. 2, pp. 330–342, jan 2017. 51
- [91] S. Volinia, M. Galasso, M. E. Sana, T. F. Wise, J. Palatini, K. Huebner, and C. M. Croce, “Breast cancer signatures for invasiveness and prognosis defined by deep sequencing of microRNA,” *Proceedings of the National Academy of Sciences of the United States of America*, vol. 109, no. 8, pp. 3024–3029, feb 2012. 52
- [92] S. Volinia and C. M. Croce, “Prognostic microRNA/mRNA signature from the integrated analysis of patients with invasive breast cancer.” *Proceedings of the National Academy of Sciences of the United States of America*, vol. 110, no. 18, pp. 7413–7, apr 2013. [Online]. Available: <http://www.ncbi.nlm.nih.gov/pubmed/23589849><http://www.pubmedcentral.nih.gov/articlerender.fcgi?artid=PMC3645522> 52
- [93] L. Cascione, P. Gasparini, F. Lovat, S. Carasi, A. Pulvirenti, A. Ferro, H. Alder, G. He, A. Vecchione, C. M. Croce, C. L. Shapiro, and K. Huebner, “Integrated MicroRNA and mRNA Signatures Associated with Survival in Triple Negative Breast Cancer,” *PLoS ONE*, vol. 8, no. 2, p. e55910, feb 2013. [Online]. Available: <https://dx.plos.org/10.1371/journal.pone.0055910> 52
- [94] P. Gasparini, L. Cascione, M. Fassan, F. Lovat, G. Guler, S. Balci, C. Irkkan, C. Morrison, C. M. Croce, C. L. Shapiro, and K. Huebner, “microRNA expression profiling identifies a four microRNA signature as a novel diagnostic and prognostic biomarker in triple negative breast cancers,” *Oncotarget*, vol. 5, no. 5, pp. 1174–1184, 2014. 52
- [95] W.-T. Chen, Y.-J. Yang, Z.-D. Zhang, Q. An, N. Li, W. Liu, and B. Yang,
-